Mechanisms and Plasticity of Cold Sensitivity in Peripheral Neurons

Clare Hannah Munns

University College London

PhD

ProQuest LLC
789 East Eisenhower Parkway
P.O. Box 1346
Ann Arbor, MI 48106-1346

I, Clare Munns, confirm that the work presented in this thesis is my own. Where information has been derived from other sources, I confirm that this has been indicated in the thesis.

Abstract

The aim of this thesis was to characterise the molecular mechanisms involved in cold transduction in peripheral neurons. Members of the transient receptor potential (TRP) family of cation channels are currently recognised as the principal transducers of thermal stimuli in sensory neurons, and two channels, TRPM8 and TRPA1, have been implicated in cold sensation. Ratiometric calcium imaging and quantitative rt-PCR studies revealed that cold sensitivity in sympathetic neurons and in a significant proportion of sensory neurons is independent of TRPM8 and TRPA1 expression, suggesting the presence of a further cold-sensitive ion channel in these cells. Previous studies had suggested that voltage-gated potassium channels may also be important in the regulation of cold transduction. In calcium imaging experiments, pharmacological blockade of potassium channels unmasked a novel cold sensitivity in previously unresponsive populations of sensory and sympathetic neurons. Moreover, the individual potassium channels underlying these effects differ between neuronal populations, as demonstrated by the differing effects of specific potassium channel blockers on sensory and sympathetic neurons. The chemotherapeutic drug oxaliplatin induces an acute cold hypersensitivity in patients, and has been suggested to act on voltage-gated sodium channels. The activation of sodium channels alone did not alter cold sensitivity in sensory neurons, however the application of oxaliplatin to dissociated cells induced a qualitative change in the cold response, with neurons displaying a unique bursting response pattern. Cold-sensitive neurons are dependent on NGF during development, and a further aim of the thesis was to investigate the influence of this growth factor on cold sensitivity in neonatal sensory neurons. NGF induced an up-regulation of cold sensitivity and functional TRP channel expression. In the case of TRPM8, this effect was mediated via the Runx1 transcription factor, which is known to be expressed in NGF-dependent neurons during development.

Acknowledgements

I would like to acknowledge the following people for all their help in the preparation of this thesis: Professor Martin Koltzenburg, who has been my primary supervisor and mentor for the thesis, and who has provided invaluable guidance and support throughout my time as a PhD student; Dr Mona Al-Qatari, who guided me through many of the techniques used in the project, and who was an invaluable source of help and advice; Nisha Vastani, who kindly shared the data from her own project, aspects of which related very closely to my own work; Lindsey Mair, who provided technical support for many of the experiments presented here. Others who have worked in the laboratory during the last three years and contributed to my time as a PhD student include Dr Konrad Maurer, Professor Lorne Mendell, Dr Jens Hjerling-Leffler.

The studies investigating the influence of NGF and Runx1 on cold sensitivity and TRP channel expression in neonatal sensory neurons were done in collaboration with Professor Patrik Ernfors and Dr Dmitry Usoskin, from the Karolinska Institute, Stockholm. Dr Usoskin taught me in vitro electroporation, and Professor Ernfors kindly provided constructs for use in this project. The preliminary experiments which gave rise to this project were done by Dr Jens Hjerling-Leffler.

I am also very grateful to the following for their continued support throughout the last three years: Kevin Munns, Ann Munns, Lisa Munns, Thomas Fournier.

This work was funded by The Wellcome Trust.

Table of Contents

Tables

Word count: 61568

Abbreviations

4-AP	4-aminopyridine
4HNE	α,β-unsaturated aldehyde 4-hydroxy-2-nonenal
α-rec	α-adrenoceptor
BDNF	Brain-derived neurotrophic factor
BK	Bradykinin
BMP	Bone morphogenetic protein
cDNA	Complementary DNA
CGRP	Calcitonin gene-related peptide
CREB	Cyclic AMP response element binding protein
Ct	Cycle threshold
CTB	Cholera toxin B subunit
DAG	Diacylglycerol
DMSO	Dimethyl sulfoxide
dNTP	Deoxyribonucleotide triphosphate
DRG	Dorsal root ganglion
DTX	α-dendrotoxin
E11.5	Embryonic day 11.5
ECF	Extracellular fluid
EDTA	Ethylenediaminetetraacetic acid
fMRI	Functional magnetic resonance imaging
Fura-2 AM	Fura-2 acetoxymethyl
Gab1/2	Grb2-associated binder-1/2
GAPDH	Glyceraldehyde-3-phoshate dehydrogenase
GDNF	Glial cell-derived neurotrophic factor
GEFS+	Generalised epilepsy with febrile seizures plus
GFP	Green fluorescent protein
Grb2	Growth factor receptor-bound protein
HBSS	Hank's balanced salt solution
HTM	High-threshold mechanoreceptor
HPC cells	Heat, pinch, cold cells
HypoKPP	Hypokalemic periodic paralysis
I_A/I_D	A-type transient potassium current

I_{DR}	Delayed rectifier potassium current
IB4	Isolectin B4
IP3	Inositol tris-phosphate
Kv channels	Voltage-gated potassium channels
L5 DRG	Lumbar 5 dorsal root ganglion
LPL	Lysophospholipids
LTM	Low-threshold mechanoreceptor
MAPK	Mitogen-activated protein kinase
Mash1	Mammalian achaete-scute homologue 1
MEK1/2	MAPK/ERK (extracellular signal-regulated) kinase 1/2
mRNA	Messenger RNA
NA	Noradrenaline
Nav channels	Voltage-gated sodium channels
NCC	Neural crest cell
NGF	Nerve growth factor
NGN1	Neurogenin 1
NGN2	Neurogenin 2
NT3	Neurotrophin 3
NT4	Neurotrophin 4
NTC	Non-template control
Oligo(dT)	Oligodeoxythymidylic acid
P0	Postnatal day 0
P0+2	Cells dissociated at P0 and cultured for 2 days
PAM	Potassium-aggravated myotonia
PAR2	Protease-activated receptor 2
PBS	Phosphate-bufferes saline
pCA-eGFP	Plasmid containing enhanced GFP under the control of the chicken β-actin promotor
PDK-1	Phosphatidylinositide-dependent protein kinase
PE	Primary erythromelalgia
PEPD	Paroxysmal extreme pain disorder
PGE_2	Prostaglandin E_2
PI3-K	Phosphatidylinositide 3-kinase
PIP_2	Phosphatidylinositol 4,5-bisphosphate

PIP_3	Phosphatidylinositol 3,4,5-trisphosphate
PKA	Protein kinase A
PKB	Protein kinase B
PKC	Protein kinase C
PLA_2	Phospholipase A_2
PLC	Phospholipase C
PMC	Paramyotonia congenita
rhNGF	Recombinant human NGF
RIN	RNA integrity number
Rsk	Ribosomal protein S6 kinase
RT	Reverse transcriptase / Room temperature
rt-PCR	Real-time polymerase chain reaction
Runx1d	Dominant-negative isoform of Runx1
SCG	Superior cervical ganglion
SEM	Standard error of the mean
Shc	SH2-containing collagen-related protein
SK channels	Small-conductance calcium-activated potassium channels
SMEI	Severe myoclonic epilepsy of infancy
SMP	Sympathetically maintained pain
SNL	Spinal nerve ligation
Sos	Son of sevenless guanine nucleotide exchange factor
Sox10	High-mobility group transcription factor SRY (sex determining region Y) box 10
STD	Standard deviation
TEA	Tetraethylammonium chloride
TG	Trigeminal ganglion
Trk	Receptor tyrosine kinase
TRP	Transient receptor potential
TTXr	Tetrodotoxin-resistant
TTXs	Tetrodotoxin-sensitive
UCHL1	Ubiquitin carboxyl-terminal hydrolase 1
WAS	Windows application system
Z-VAD-(OMe)-FMK	Caspase inhibitor 1

1. Introduction

1.1. Cold sensation

The ability of an organism to sense changes in temperature, be they hot or cold, innocuous or potentially tissue-damaging, is critical for adaptation and survival, and forms an important part of the body's defence mechanism. From psychophysical testing, it has been found that humans are able to differentiate between three types of cold sensation. A change in ambient temperatures of 0.5-2 °C is detected as an innocuous cool sensation, whereas cold pain, which can manifest as a burning or deep aching sensation, is usually recognised at temperatures below 15 °C (Davis and Pope, 2002). It has been noted that pain thresholds can differ, depending on the skin area tested, the rate of cooling applied, the size of the probe used and how subjects are instructed (Harrison and Davis, 1999). Freezing of the skin causes a stinging pain that is qualitatively distinct from cool and cold pain sensations (Beise et al., 1998).

1.2. Sensory neurons

Thermal, chemical and mechanical stimuli are signalled by specialised primary sensory afferents, whose cell bodies are located in the dorsal root (DRG) or trigeminal ganglia (TG) (Meyer et al., 2005). There are three main types of sensory afferent, the Aα/β-, the Aδ- and the C-fibres, which can be differentiated on the basis of their anatomical and functional characteristics (Julius and Basbaum, 2001). Large-diameter Aα/β-fibres are heavily myelinated and have a rapid conduction velocity. They respond to low threshold mechanical stimuli, and detect limb movement and position (proprioception) and tactile stimuli. Whereas Aα/β-fibres are non-nociceptive, a proportion of Aδ- and C-fibres do have the capacity to detect painful stimuli. Medium-diameter, thinly myelinated Aδ-fibres conduct at an intermediate velocity, while C-fibres are unmyelinated and slowly conducting. Both types of fibre are capable of responding to a variety of stimulus modalities. A subpopulation of C-fibres can be excited by noxious thermal, chemical and mechanical stimuli, and are termed polymodal nociceptors (Table 1.1).

Properties of sensory afferents in the adult mouse

	Aα/β-fibres	Aδ-fibres	C-fibres
Cell size	> 50 μm diameter > 1000 μm^2 area	25-50 μm diameter 500-1000 μm^2 area	< 25 μm diameter < 500 μm^2 area
Myelination	Heavily myelinated	Lightly myelinated	Unmyelinated
Conduction velocity	> 10 m/s	1-10 m/s	< 1 m/s
Stimulus modalities	Mechanical (LTM) Proprioception	Mechanical (LTM, HTM) Chemical Thermal	Mechanical (LTM, HTM) Chemical Thermal
Neurotrophic dependence for survival	NT3	NGF NT4	NGF NT3
Runx expression	Runx3		Runx1
Immunocyto-chemical markers	Parvalbumin Neurofilament	Neurofilament CGRP	Peripherin CGRP, Substance P (peptidergic C-fibres)
Vital stains	CTB	CTB	IB4 (non-peptidergic C-fibres)

Table 1.1. A summary of the features of the three main types of sensory afferent in the mouse. Fibres can be differentiated *in vitro* by conduction velocity, cell size, stimulus modalities or their ability to bind cell-specific markers. LTM, low-threshold mechanoreceptor; HTM, high-threshold mechanoreceptor; NT3, neurotrophin-3; NT4, neurotrophin-4; NGF, nerve growth factor; CGRP, calcitonin gene-related peptide; CTB, cholera toxin B subunit; IB4, isolectin B4.

1.2.1. Development of sensory neurons

Sensory neurons develop from neural crest cells (NCCs), which delaminate from the neural tube between embryonic day (E) 8.5 and E10 in the mouse and then migrate along the ventral pathway to form the sensory ganglia. The production of WNT signalling factors in the neural tube, along with the expression of the neurogenin transcription factors, drive NCCs towards the sensory lineage (Marmigere and Ernfors, 2007).

There are three defined waves of sensory neurogenesis, beginning around E9.5. The first is initiated by the expression of neurogenin 2 (NGN2), and gives rise to large-diameter proprioceptive and mechanoreceptive neurons that reside in the ventrolateral DRG. In the adult ganglion, these neurons comprise around 4 % of the total cell population. The second, neurogenin 1 (NGN1)-mediated wave of neurogenesis produces approximately 91 % of the adult sensory neuron population in the form of large- and small-diameter neurons, the majority of which are nociceptive. Finally, neural crest stem cells migrating from the boundary cap, a structure located at the dorsal root entry and motor exit zones between the central and peripheral nervous systems, develop into sensory neurons with mechanosensitive and nociceptive properties (Maro et al., 2004;Hjerling-Leffler et al., 2005) (Figures 1.1 and 1.2). A recent study looking at neural crest cell migration has suggested that the boundary cap cells migrate into the contralateral DRG during the later stages of migration, where they remain multipotent for a time before becoming nociceptors (George et al., 2007).

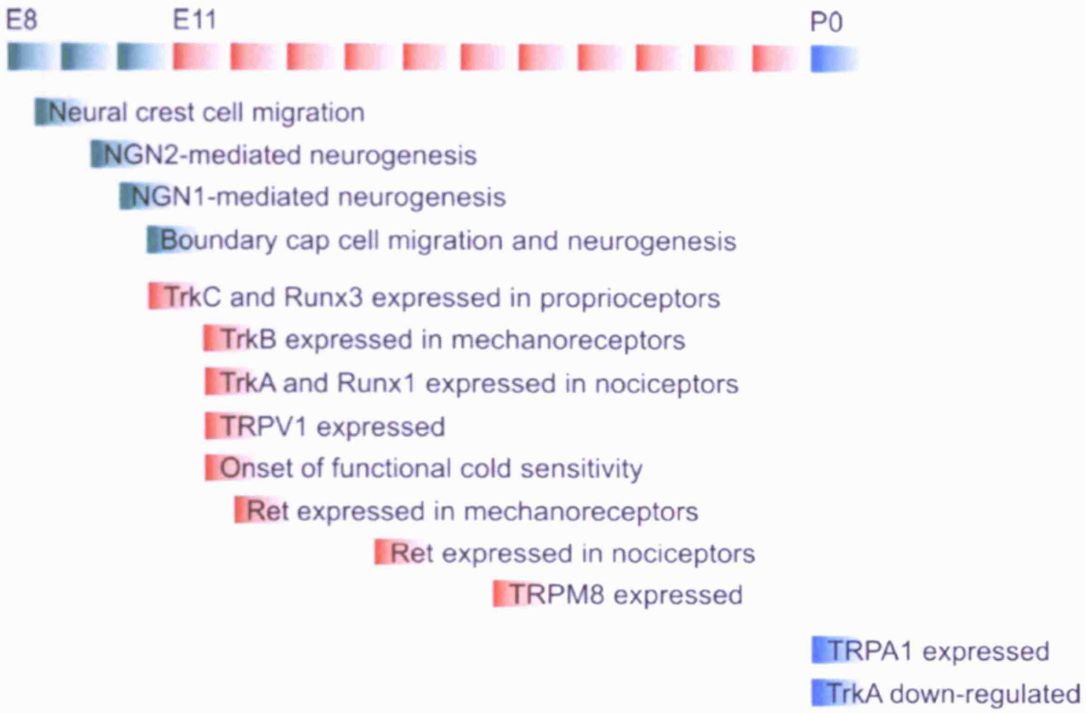

Figure 1.1. Timeline depicting the main events of sensory neuron development. Migration of neural crest cells from the neural tube at E8.5 initiates three waves of neurogenesis, giving rise to cells with proprioceptive, mechanoreceptive and nociceptive properties. Neurotrophic receptors define the different populations between E10.5 and E14.5. TRP channel expression is developmentally regulated throughout embryonic and early postnatal stages.

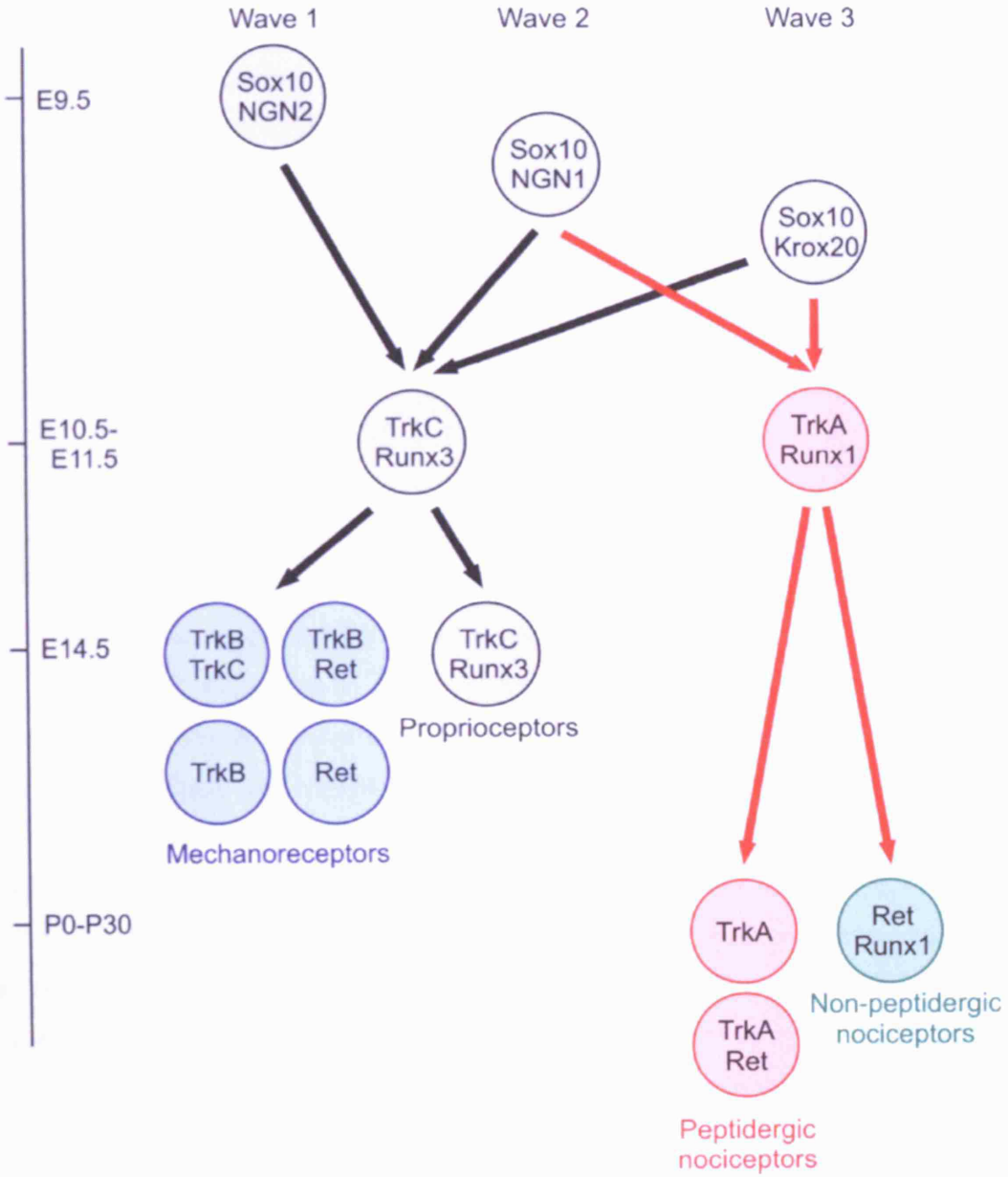

Figure 1.2. Schematic of sensory neuron development. Migratory cells express the high-mobility group transcription factor SRY (sex determining region Y) box 10 (Sox10), which maintains multipotency. NGN2-mediated neurogenesis gives rise to large-diameter proprioceptive and mechanoreceptive cells, while neurons deriving from NGN1-positive cells or boundary cap cells (defined by their expression of Krox20) develop mechanoreceptive and nociceptive phenotypes. In the adult, subpopulations can be defined by neurotrophic dependence and Runx transcription factor expression.

Modified from (Marmigere and Ernfors, 2007).

1.2.2. Neurotrophic dependence of sensory neurons

During development, sensory neurons depend on neurotrophic factors for survival, and different subpopulations can be identified on the basis of receptor tyrosine kinase (Trk) expression (Ernfors, 2001). The large-diameter mechanoreceptive and proprioceptive neurons arising during the first wave of neurogenesis express the TrkB and TrkC receptors, and respond to brain-derived neurotrophic factor (BDNF) and neurotrophin-4 (NT4), or neurotrophin-3 (NT3), respectively. TrkC expression is first detected in DRG neurons at E10.5, and while there is initially a high level of co-expression between TrkC and TrkB, by E12.5 this is significantly reduced (Levanon et al., 2002;Kramer et al., 2006). In addition to the Trk receptors, sensory neurons also express Ret, a co-receptor for the glial cell-derived neurotrophic factor (GDNF) family. A so-called 'early Ret population' appears between E11.5-E12, 80 % of which express TrkB. Again this co-expression does not last, and by E14.5 very few Ret-positive neurons express Trk receptors (Kramer et al., 2006).

At E11.5, TrkA expression is first detected in small-diameter neurons, which are dependent on nerve growth factor (NGF), and by E15, approximately 80 % of cells in the DRG are TrkA-positive (Molliver and Snider, 1997). At E16 TrkA-expressing neurons also start to express the GDNF co-receptor Ret (Luo et al., 2007), the expression of which continues to increase until it reaches adult levels at postnatal day (P) 7 (Molliver et al., 1997). This up-regulation in Ret expression is accompanied by a decrease in TrkA expression, which starts at P1 and continues until P21, at which time only 40 % of neurons remain positive for the NGF receptor (Molliver and Snider, 1997). Recent work has shown that Ret signalling is important in controlling the down-regulation of TrkA (Luo et al., 2007). The switch of neurotrophic dependency from NGF to GDNF in small-diameter neurons signifies the formation of two distinct subpopulations of C-fibres. Ret-positive neurons make up the population of non-peptidergic C-fibres, which are identified *in vitro* by their binding of the isolectin B4 (IB4), whereas TrkA-expressing cells are characterised by their ability to release neuropeptides on activation, such as substance P and calcitonin gene-related peptide (CGRP) (Figures 1.1 and 1.2).

1.2.3. The roles of Runx transcription factors in sensory neurons

Sensory neurons are very heterogeneous, and until recently the mechanisms mediating the development of this neuronal diversity were not known. Progress in this area has been made however with the discovery that sensory neurons express members of the runt-related family of transcription factors (Marmigere and Ernfors, 2007). Three members of this family, Runx1, Runx2 and Runx3, are found in mammals, and two are expressed in sensory neurons. The transcription factors share a homologous DNA-binding domain (the 'Runt' domain), which interacts with its partner protein core binding factor β, and a C-terminal transactivation domain (Bae and Lee, 2006).

The first of the Runx transcription factors to be characterised in sensory neurons was Runx3, which is co-expressed with TrkC in the proprioceptive population, where it acts to repress TrkB expression and promote the proprioceptive phenotype (Levanon et al., 2002;Kramer et al., 2006). In the absence of Runx3, there is a loss of large-diameter neurons in the DRG, along with myelinated axons projecting to the spinal cord and the periphery (Levanon et al., 2002;Inoue et al., 2002). In addition to its survival effects in proprioceptors, Runx3 has also been shown to determine the positioning of axons in the dorso-ventral plane of the spinal cord (Chen et al., 2006a). While Runx3 determines the proprioceptive phenotype, the second of the runt-related transcription factors to be found in sensory neurons, Runx1, is restricted to the nociceptive population (Figure 1.2). Knockdown of Runx1 expression at an early stage of development in the chick leads to significant cell death in the DRG and a loss of TrkA expression (Marmigere et al., 2006), while in the mouse, Runx1 was found to be necessary for the developmental transition from TrkA to Ret expression and suppression of the peptidergic phenotype in favour of a non-peptidergic one (Chen et al., 2006b). Additionally, in the Runx1 knockout animal there was a loss or marked reduction in the expression of a number of ion channels and receptors associated with nociception, including members of the transient receptor potential (TRP) family, Mrgpr G protein-coupled receptors, the ATP-gated P2X3 channel and the tetrodotoxin-resistant sodium channel Nav1.9.

1.2.4. Development of thermal sensation

A recent study investigated the onset of cold sensitivity and temperature-sensitive ion channel expression in neonatal sensory neurons. Members of the TRP family of cation channels are currently recognised as the primary transducers of thermal stimuli in sensory neurons, and two of these channels, TRPM8 and TRPA1, have been implicated in cold transduction (Caterina, 2007). Using a combination of functional imaging and quantitative real-time polymerase chain reaction (rt-PCR) studies, it was shown that DRG neurons develop the ability to respond to cold as early as E11.5 (Hjerling-Leffler et al., 2007). The percentage of cold-sensitive neurons increases between E12.5 and E18.5, at which time approximately 45 % of cells will respond to a decrease in temperature. Cold sensitivity is subsequently down-regulated again, reaching adult levels within the second postnatal week. Interestingly, expression of the two putative cold receptors comes on much later: TRPM8 is first detected at E16.5, while TRPA1 is only expressed postnatally. The founder member of the 'thermoTRP' family, TRPV1, which is sensitive to moderate noxious heat and capsaicin (Caterina et al., 1997), is expressed soon after neurogenesis, with the first functional responses present in neurons at age E11.5 (Figure 1.1).

1.2.5. Cold-sensitive thermoreceptors and nociceptors

A number of neurophysiological studies in primates and rodents have identified three classes of cold-sensitive afferent, the signalling properties of which correspond to the different cold sensations recognised in psychophysical testing. Cooling is signalled by mechanically-insensitive, thinly myelinated Aδ- or unmyelinated C-fibres that respond to small temperature reductions in the innocuous range (termed cold-sensitive thermoreceptors) (LaMotte and Thalhammer, 1982;Kress et al., 1992;Campero et al., 2001), whereas noxious cold stimuli typically excite a subpopulation of mechanosensitive nociceptors (LaMotte and Thalhammer, 1982;Kress et al., 1992). The majority of nociceptive Aδ- and C-fibres will respond to temperatures below freezing (Simone and Kajander, 1996;Simone and Kajander, 1997). Recent *in vitro* and *in vivo* recordings in rodents have found that approximately 20-30 % of unmyelinated and 10 % of myelinated nociceptors respond to noxious cold stimuli, whereas the percentage of cold-sensitive thermoreceptors is around 5 % (Koltzenburg, 2004).

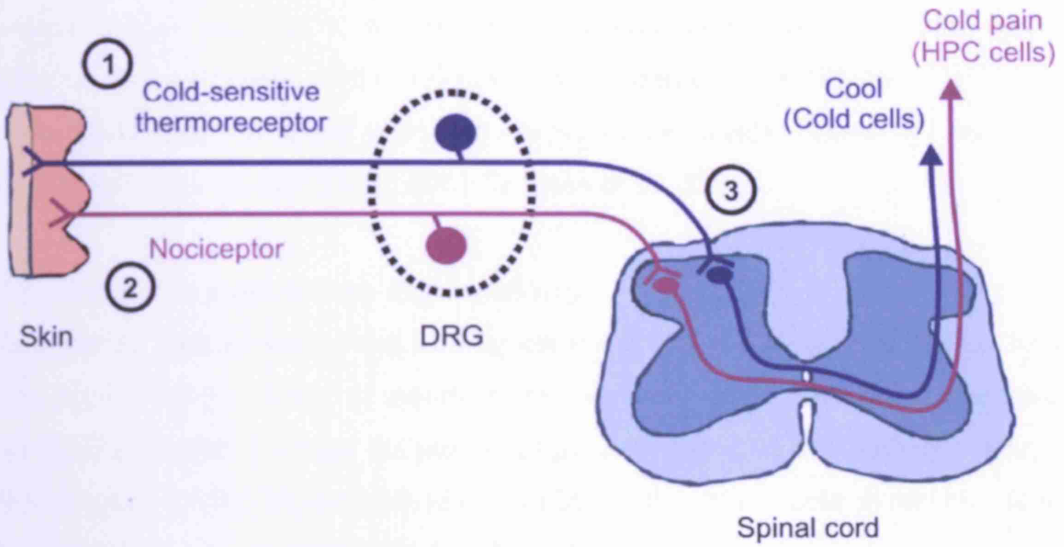

Figure 1.3. Schematic of the innocuous cool and cold pain signalling pathways from the periphery to the central nervous system. Cold-sensitive thermoreceptors detect cool stimuli and synapse onto cold neurons in lamina I of the spinal cord dorsal horn (blue). Cold-sensitive nociceptors detect noxious cold stimuli and synapse onto HPC (heat, pinch, cold) neurons (purple). Freezing temperatures will activate all nociceptive afferents. Input into the pain pathways from nociceptors and HPC cells is inhibited by activation of thermoreceptors and cold cells. Cold hypersensitivity of peripheral origin is hypothesised to develop in three different ways. **1. Central disinhibition**. A reduction in the inhibition exerted by neurons signalling innocuous cold, for example by the thermal grill illusion (simultaneous application of adjacent bars with cool and warm stimuli) or by differential block of cold-sensitive thermoreceptors, will lead to an imbalance in nociceptive and non-nociceptive inputs in spinal cord, thalamus and cortex. Lesions in the central nervous system can also result in such imbalance. **2. Peripheral sensitisation.** Sensitisation of cold-sensitive nociceptors will shift the cold pain threshold to warmer temperatures. **3. Central sensitisation.** Cold-sensitive thermoreceptors will activate central pain-signalling neurons.

In primates cold-sensitive thermoreceptors and nociceptors excite corresponding sets of cold or HPC (heat, pinch, cold) neurons of the superficial dorsal horn, respectively, that project via the lateral quadrant of the spinal cord to the posterior part of the ventral medial nucleus of the thalamus and on to the dorsal insular cortex (Dostrovsky and Craig, 2005) (Figure 1.3). Specifically, fMRI has highlighted activation within the dorsal posterior margin of the insular cortex by innocuous cooling and noxious cold (Craig, 2003;Cattaneo et al., 2007).

1.3. Neuropathic pain and cold hypersensitivity

Neuropathic pain is one of the leading causes of chronic pain. Few studies have investigated the prevalence of painful neuropathy, although peripheral neuropathies are known to affect 2.4 % of the general population, rising to 8 % with age (Martyn and Hughes, 1998). Hypersensitivity to cold, or the 'triple cold syndrome' (cold hyperalgesia, cold hypoaesthesia and cold skin), is a common symptom of neuropathic pain conditions including traumatic nerve injury or polyneuropathy (Ochoa and Yarnitsky, 1994), but the mechanisms underlying its generation are poorly understood (Scadding and Koltzenburg, 2005).

One mechanism, which has been proposed to underlie the triple cold syndrome, is central disinhibition (Ochoa and Yarnitsky, 1994). It is demonstrated by the 'thermal grill illusion', whereby innocuous warm and cool stimuli applied simultaneously to the skin elicit sensations of heat and pain. It was suggested that inhibition normally exerted by cold cells on nociceptive HPC neurons within the spinal cord was reduced in the presence of the warm stimulus, leading to an imbalance of nociceptive and non-nociceptive inputs in the thalamus and cortex (Craig and Bushnell, 1994). Alternatively, specific loss of cold-sensitive thermoreceptors in the periphery would produce the same effect, reducing inhibition in the spinal cord dorsal horn and increasing transmission of nociceptive signals to the central nervous system. In psychophysical testing, subjects often describe a prickling sensation when the skin is rewarmed, which may represent the release of inhibition exerted on nociceptive neurons by cold-sensitive thermoreceptors (Davis, 1998).

Heat hyperalgesia is caused by the sensitisation of peripheral nociceptive afferents (Meyer et al., 2005), and a similar mechanism has been proposed for the development of cold hypersensitivity. In support of this theory, the sensitisation of cold-sensitive

nociceptors by menthol was shown to reduce the cold pain threshold, giving rise to a cold hyperalgesia (Wasner et al., 2004).

Finally, it has been suggested that cold-sensitive thermoreceptors could develop interactions with HPC neurons in the spinal cord dorsal horn, leading to the direct activation of pain pathways, in a process known as central sensitisation (Scadding and Koltzenburg, 2005) (Figure 1.3). This mechanism is thought to be similar to the development of mechanical hyperalgesia, whereby increased nociceptive input to deep dorsal horn neurons also served by Aβ-fibres enhances synaptic efficacy to the extent that innocuous mechanical stimuli will elicit a nociceptive response (Campbell and Meyer, 2006).

Increased growth factor expression following inflammation or nerve lesion is believed to contribute to peripheral and central sensitisation (Heppenstall and Lewin, 2000;Nicol and Vasko, 2007), and is directly implicated in the development of thermal hyperalgesia (Lewin et al., 1993;Koltzenburg et al., 1999). The actions of NGF in sensory neurons in particular have been extensively studied, and its effects have been found to include promoting the expression or post-translational modification of ion channels, and increasing the expression and release of neuropeptides, both at the periphery and in the spinal cord (Nicol and Vasko, 2007). Studies of the L5 spinal nerve ligation (SNL) model in rodents have highlighted the important role of the uninjured L4 afferents in the development of neuropathic pain (Campbell and Meyer, 2006). Consequently, NGF synthesised and released by the injured L5 afferents will be taken up by neighbouring L4 fibres, resulting in modulation of ion channel expression and function within the latter, and subsequent sensitisation. It is by this mechanism that NGF is believed to mediate the onset of cold hyperalgesia following nerve injury (Obata et al., 2006). Incidentally, studies have reported an increase in the percentage of cold-sensitive neurons within the uninjured afferent population following L5 SNL, concluding that an up-regulation in the number of fibres responding to cold would also contribute to cold hypersensitivity (Djouhri et al., 2004;Ji et al., 2007). Furthermore, single unit recordings provided evidence for a phenotypic switch in Aδ- and C-fibres, possibly corresponding to a de novo expression of cold-sensitive receptors in previously insensitive neurons.

1.4. Sympathetic neurons and cold sensation

Cold sensitivity is not restricted to sensory neurons of the dorsal root or trigeminal ganglia. A recent study found that postganglionic sympathetic neurons isolated from the superior cervical ganglion (SCG) also respond *in vitro* to reductions in temperature within both the innocuous and noxious ranges (Smith et al., 2004).

The autonomic nervous system is involved in homeostatic regulation, modulating functions such as heart rate, blood flow, respiration and digestion in response to changes in the external and internal environments. Like sensory neurons, cells of the autonomic lineage, comprising sympathetic and enteric neurons, derive from neural crest cells. Specification to the autonomic lineage is determined by the expression of the proneural gene mammalian achaete-scute homologue 1 (Mash1) in the NCCs, along with high levels of bone morphogenetic protein (BMP) in the dorsal neural tube (Marmigere and Ernfors, 2007). The SCG is one of a number of paravertebral ganglia that develop alongside the vertebral column. Neurons of the SCG receive input from preganglionic efferents originating within the spinal cord, and transmit information to target organs located in the head and thorax (Figure 1.4).

The capacity for sympathetic neurons to be activated by cold could be associated with a temperature-activated axon reflex, resulting in a local release of noradrenaline or ATP. Sympathetic axon reflexes have been described previously for sudomotor neurons and for vasoconstrictor neurons that are activated by orthostatic pressure (Low, 1993).

The cold sensitivity of sympathetic fibres may also contribute to the generation of a condition known as sympathetically maintained pain (SMP) in which cold hypersensitivity is a characteristic symptom (Jänig and Baron, 2003). SMP arises when sensory neurons acquire an abnormal sensitivity to catecholamines. Under these conditions local cold-induced release of noradrenaline might contribute to an abnormal activation of sensory afferents (Figure 1.4). In patients diagnosed with SMP (that is, patients in whom the pain could be relieved by a sympathetic block), injection of noradrenaline or an agonist of the α-adrenoceptor was sufficient to induce pain, and mechanical and cold hyperalgesia (Torebjörk et al., 1995). Furthermore, local release of neurotransmitter in the absence of neural activity has been shown to contribute to tissue inflammation and hyperalgesia (Jänig and Levine, 2005).

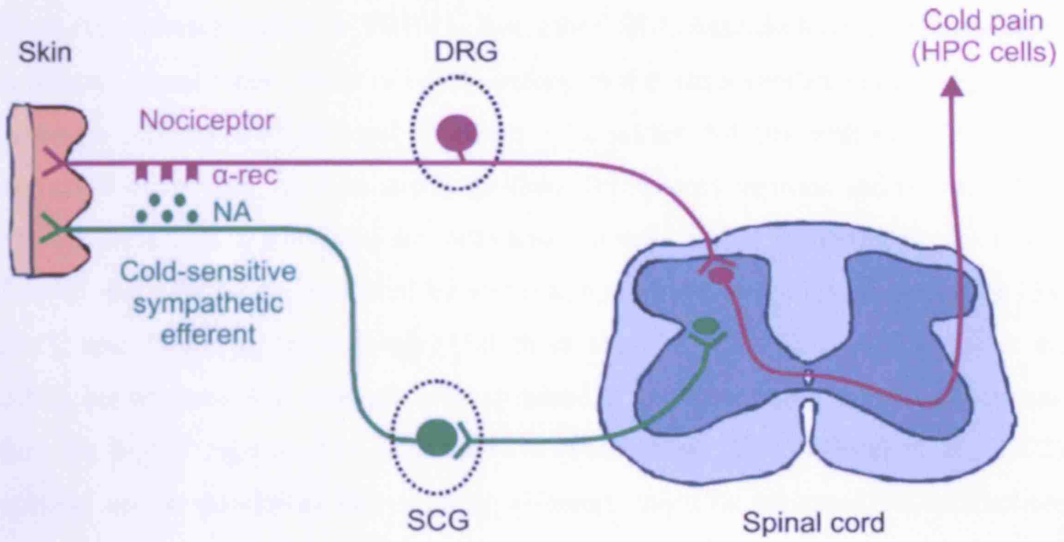

Figure 1.4. Schematic of the sympathetic efferent signalling pathway from the central nervous system to the periphery. Neurons of the SCG receive input from preganglionic efferents originating within the spinal cord, and transmit information to target organs in the head and thorax. Cold-sensitive sympathetic efferents may contribute to sympathetically maintained pain, whereby cold-induced release of noradrenaline (NA) from sympathetic fibres can activate α-adrenoceptors (α-rec) expressed on nociceptive afferents. This will result in the activation of central pain-signalling pathways in the absence of a noxious stimulus.

1.5. TRP channels and thermosensation

The breakthrough in the understanding of the molecular mechanisms underlying thermosensation came with the cloning of a member of the transient receptor potential (TRP) family of ion channels, TRPV1 (Caterina et al., 1997). This channel was initially identified on the basis of its sensitivity to capsaicin, the pungent ingredient of chilli peppers, but was found equally capable of responding to a number of other stimuli, including protons, endogenous lipids, and most interestingly, moderate noxious heat (> 42 °C) (Caterina et al., 1997;Zygmunt et al., 1999;Caterina et al., 2000;Huang et al., 2002). TRPV1 is expressed in 40 % of small-diameter DRG neurons, where it is used as a functional marker for a subpopulation of nociceptive sensory afferents.

Since the characterisation of TRPV1, five other TRP channels have been implicated in thermal transduction, three of which belong to the same vanilloid subfamily as the capsaicin receptor and respond to warm or noxious hot temperatures. TRPV2 is expressed in 16 % of medium and large-diameter sensory neurons and is sensitive to noxious heat with a threshold for activation around 52 °C (Caterina et al., 1999). TRPV3 and TRPV4 are activated by warm temperatures in the innocuous range (34-39 °C and 24-34 °C, respectively) (Smith et al., 2002;Xu et al., 2002;Guler et al., 2002), but whereas both channels are expressed at low levels only in sensory neurons, they are highly expressed in keratinocytes (Peier et al., 2002b;Guler et al., 2002), opening up the possibility that sensory afferents could be activated via interactions with thermally-sensitive skin cells (Caterina, 2007). The other two thermosensitive receptors, TRPM8 and TRPA1, are members of the melastatin and ankyrin subfamilies, respectively, and both have been associated with cold transduction (Figure 1.5).

Mammalian TRP channels are currently divided into seven subfamilies on the basis of amino acid sequence homology: TRPC (classic or canonical), TRPV (vanilloid), TRPM (melastatin), TRPML (mucolipin), TRPP (polycystin), TRPA (ankyrin-like with transmembrane domains 1) and TRPN (NOMP-C, no mechanoreceptor potential-C). Functional TRP channels are believed to exist as homo- or heterotetramers, comprising four subunits with six transmembrane domains and a pore loop region between domains five and six. They are non-specific cation channels, with high permeability for calcium and sodium. Both the amino- and carboxy-terminals are believed to reside intracellularly, and several sites implicated in protein-protein interactions have been identified within the subunit structure. Most TRP channels (except those belonging to the melastatin subfamily) possess a series of ankyrin repeats within the N-terminal domain, while a homologous region of around 25 residues in the C-terminus, termed the TRP domain, is loosely conserved in all TRP subfamilies apart from TRPA and TRPP. Different functions have been assigned to the TRP domain, including tetramerisation in TRPV channels, and activation and desensitisation in TRPM channels (Montell, 2005;Ramsey et al., 2006;Huang et al., 2006).

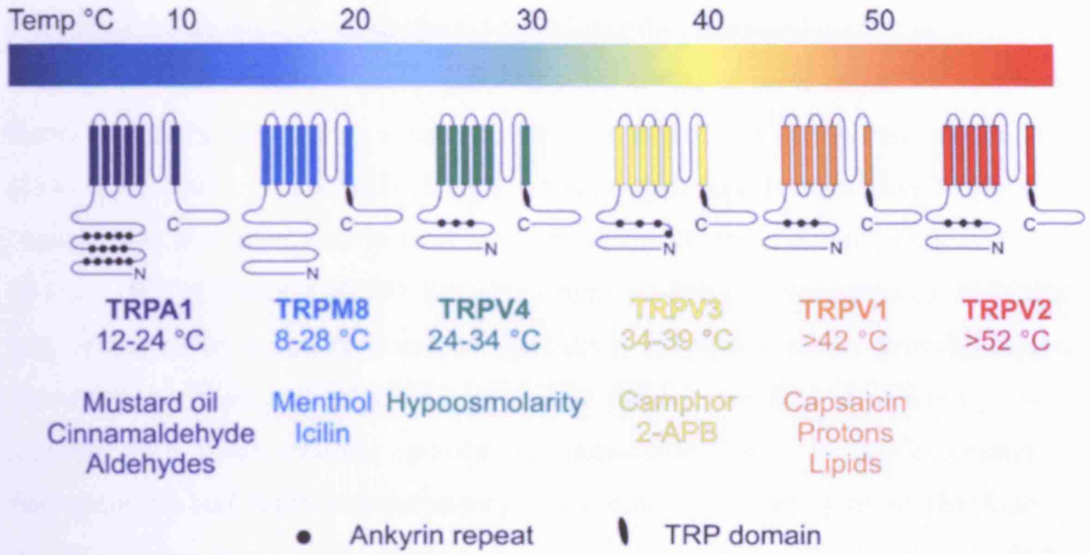

Figure 1.5. Schematic of the six thermosensitive TRP channels, detailing subunit structure, activation threshold and alternative channel agonists.
Modified from (Jordt et al., 2003).

1.5.1. TRPM8

The first cold-sensitive TRP channel to be cloned was TRPM8, which was identified on the basis of its sensitivity to the cooling compound menthol (McKemy et al., 2002) and its sequence similarity to TRPV1 (Peier et al., 2002a). Expression of TRPM8 is first detected at E16.5 in the DRG (Hjerling-Leffler et al., 2007), and is lost with knockdown of the Runx1 transcription factor (Chen et al., 2006b). In the adult, TRPM8 is expressed in small-diameter sensory neurons, comprising around 15 % of the total neuronal population (McKemy et al., 2002;Peier et al., 2002a). TRPM8-expressing fibres terminate in both superficial and deep epidermal layers, and project to laminae I and outer II of the dorsal horn of the spinal cord (Takashima et al., 2007;Dhaka et al., 2008)

1.5.1.1. TRPM8 and cold sensation

TRPM8 is activated by cold and compounds that typically evoke a cooling sensation when applied to the skin, namely menthol, eucalyptol and icilin. The recombinant channel has an activation threshold of around 23 °C, but can be activated by temperatures as low as 8 °C (McKemy et al., 2002;Peier et al., 2002a). Prior to the

cloning of the channel, work on the cold- and menthol-activated current in dissociated sensory neurons revealed many properties in common with intact cold-sensitive thermoreceptors, suggesting a role for this current in innocuous cold transduction (Reid et al., 2002). Accordingly, in one of the original reports describing TRPM8, the channel was not co-expressed with markers of nociceptive neurons, such as CGRP, IB4 and TRPV1 (Peier et al., 2002a), supporting the theory that expression of TRPM8 was restricted to a non-nociceptive population of cold-sensitive thermoreceptors. Since then however, several groups have recorded the existence of menthol-sensitive neurons with characteristics specific to nociceptors, such as the expression of neuropeptides and functional sensitivity to capsaicin, ATP and protons (McKemy et al., 2002;Babes et al., 2004;Okazawa et al., 2004;Xing et al., 2006;Hjerling-Leffler et al., 2007;Takashima et al., 2007). Furthermore, topical application of menthol has been shown to elicit or enhance sensations of pain (Wasner et al., 2004;Namer et al., 2005;Green and Schoen, 2007). Combined with the finding that recombinant TRPM8 is activated by temperatures in the noxious range, there is a strong body of evidence to suggest that TRPM8 may mediate noxious as well as innocuous cold sensation. Indeed, recent behavioural studies in TRPM8 knockout animals demonstrated deficiencies in recognition of innocuous and noxious cold stimuli, and the authors concluded that TRPM8 contributes to the transduction of both cool and painful cold (Dhaka et al., 2007;Colburn et al., 2007;Bautista et al., 2007). The introduction of TRPM8 into cells that have no intrinsic cold sensitivity, such as hippocampal neurons, can cause them to become cold-responsive (de la Pena et al., 2005). Transfected cells had lower activation thresholds than cold-sensitive sensory neurons however, suggesting the presence of additional regulatory mechanisms in the neuronal population.

Associated with its expression in cold-sensitive thermoreceptors, the activation of which inhibits nociceptive input into the central nervous system, TRPM8 has been implicated in the mediation of cold-evoked analgesia. Topical application of the TRPM8 agonist icilin was shown to reduce the thermal and mechanical hyperalgesia induced by chronic constriction of the sciatic nerve, an effect that was abolished by antisense oligonucleotide knockdown of TRPM8 (Proudfoot et al., 2006). In addition, analgesia against formalin-evoked pain provided by exposure to a cold surface was eliminated in TRPM8 knockout animals (Dhaka et al., 2007).

Conversely, TRPM8 has also been implicated in the development of cold hypersensitivity following nerve injury. Alongside the observation that topical application of menthol can produce cold hyperalgesia (Wasner et al., 2004;Namer et al., 2005), several studies have recorded an up-regulation in TRPM8 expression in sensory neurons after nerve injury, with a specific increase noted in the percentage of menthol-sensitive nociceptors (Proudfoot et al., 2006;Frederick et al., 2007;Xing et al., 2007). Furthermore, the TRPM8 knockout mouse did not develop the nerve injury- or inflammation-induced hypersensitivity to acetone normally seen in wild type animals, and it was concluded that TRPM8 is involved in the development of cold allodynia (Colburn et al., 2007).

1.5.1.2. Regulation of TRPM8

The activation of TRPM8 by cooling and menthol is a voltage-dependent process, and like cooling, menthol shifts the voltage dependence of channel activation towards physiological voltages (Voets et al., 2004). This can explain why, in the presence of menthol, neurons become sensitised to cold stimuli and thresholds for the detection of cool or cold pain are shifted towards warmer temperatures (Reid et al., 2002;McKemy et al., 2002;Wasner et al., 2004). On the other hand, identified antagonists of TRPM8, including BCTC, SKF96365 and 1,10-phenanthroline, shift the voltage dependence of activation towards more positive potentials, and the threshold towards colder temperatures, thus desensitising the channel (Malkia et al., 2007).

Recent studies have focussed on elucidating how the subunit structure of TRPM8 relates to its function. The creation of chimeric channels in which the C-terminal region of TRPM8 was replaced with the equivalent region of TRPV1 conferred a heat-sensitive phenotype on the cold receptor (Brauchi et al., 2006), while mutation of positively charged residues in the fourth transmembrane domain (S4) or the linker region between domains four and five (S4-S5 linker) altered the channel's voltage dependence (Voets et al., 2007). A coiled-coil domain located within the C-terminus was found to be required for channel expression and function, and is postulated to promote a tetrameric channel structure (Tsuruda et al., 2006). Finally, residues within the S2 domain and the conserved C-terminal TRP domain have been implicated in the binding of the chemical agonists menthol and icilin (Bandell et al., 2006), while icilin sensitivity is also dependent on residues in the S2-S3 linker and S3 domains (Chuang

et al., 2004). The structural separation of menthol and icilin sensitivity is matched by a difference in the mechanism of channel activation by the two compounds. Whereas responses to icilin and cold can be inhibited by low pH, sensitivity to menthol is unaffected (Andersson et al., 2004). Furthermore, icilin alone provokes only minimal activation of TRPM8, and requires the presence of calcium as a co-agonist so that the channel can fully activate (Chuang et al., 2004).

Studies of TRPM8 in heterologous expression systems and excised cell patches consistently reported lower activation thresholds for the recombinant channel compared to intact neurons (Reid, 2005), suggesting the loss or absence of a regulatory factor in these systems. Subsequent research demonstrated that activity of TRPM8 is modulated by phosphatidylinositol 4,5-bisphosphate (PIP_2) (Liu and Qin, 2005;Rohacs et al., 2005). PIP_2 is required for the cold- and menthol-induced activation of the cloned TRPM8 in heterologous expression systems and can restore channel activity following rundown in excised patches. It achieves this effect by interacting with the TRP domain and maintaining the channel in a phosphorylated state. PIP_2 itself can also activate TRPM8 by the same mechanism as cold and menthol, shifting the voltage dependency to more negative potentials.

In vitro, inflammatory mediators such as bradykinin (BK) and prostaglandin E_2 (PGE_2) have been shown to reduce the response of sensory neurons to cooling and menthol, and shift the threshold for activation to colder temperatures (Linte et al., 2007). This occurs via the activation of protein kinase C (PKC) and protein kinase A (PKA), respectively, both of which have also been shown to reduce menthol and icilin responses in cloned and native channels, most likely via receptor dephosphorylation (Abe et al., 2006;Premkumar et al., 2005;De Petrocellis et al., 2007). Activation of the phospholipase A_2 (PLA_2) mediates the hydrolysis of glycerophospholipids to produce fatty acids and lysophospholipids (LPLs). TRPM8 is differentially regulated by the two products, being inhibited by polyunsaturated fatty acids such as arachidonic acid and activated by LPLs (Andersson et al., 2007). The authors of this report concluded that endogenous modulators such as PIP_2 and LPLs act to raise the threshold for activation, enabling TRPM8 to operate at physiological temperatures.

1.5.2. TRPA1

The second putative cold-sensitive channel TRPA1 is expressed in a sub-population of TRPV1-positive nociceptive afferents (Story et al., 2003;Jordt et al., 2004;Bautista et al., 2005). It was originally shown to be expressed in 4 % of sensory neurons (Story et al., 2003), although more recent studies have suggested expression is much higher, with estimates ranging between 20-60 % (Jordt et al., 2004;Kobayashi et al., 2005;Nagata et al., 2005;Bautista et al., 2005). TRPA1 expression comes on postnatally, with the first functional responses to cinnamaldehyde detected at P0 (Hjerling-Leffler et al., 2007). TRPA1 expression is abolished with the knockdown of the Runx1 transcription factor and the GDNF co-receptor Ret (Chen et al., 2006b;Luo et al., 2007).

1.5.2.1. TRPA1 and cold sensation

When it was first characterised, the recombinant TRPA1 channel was shown to be activated by temperatures in the range of 12-24 °C, and was described as a noxious cold sensor (Story et al., 2003). However a subsequent study failed to replicate this finding and consequently the role of TRPA1 in cold transduction was brought into question (Jordt et al., 2004). Genetic ablation of TRPA1 also failed to resolve the issue of whether the channel functions as a cold receptor in sensory neurons: while one group reported no deficit in cold sensation (Bautista et al., 2006), another recorded reduced sensitivity to noxious cold stimuli in behavioural tests (Kwan et al., 2006). Dissociated sensory neurons with sensitivity to chemical agonists of TRPA1 that did respond to cold displayed slow activation kinetics and a long delay between stimulus onset and channel activation (Bandell et al., 2004), and there is now suggestion that TRPA1 may involved in the signalling of extreme or prolonged stimuli (Reid, 2005), or in the development of cold hypersensitivity following nerve injury and inflammation. A series of studies have demonstrated an up-regulation in TRPA1 expression in neurons exposed to injury or inflammatory mediators, and the alleviation of cold hyperalgesia by antisense oligonucleotide knockdown of the channel (Obata et al., 2005;Katsura et al., 2006;Obata et al., 2006).

As already mentioned, postganglionic sympathetic neurons of the SCG are also excited by cold stimuli (Smith et al., 2004). While these neurons are menthol-insensitive, nested PCR showed that TRPA1 is expressed in the SCG, and it was proposed that cold transduction in sympathetic neurons could be mediated via this

channel. It should be noted that this technique is not quantitative and consequently the exact contribution of TRPA1 to cold sensing in sympathetic neurons is unknown.
Interestingly, two recent papers have highlighted the capacity for TRPA1 to be activated directly by calcium ions, which bind to an EF-hand domain within the N-terminal region of the channel (Zurborg et al., 2007;Doerner et al., 2007). While the cloned receptor was cold-insensitive in the absence of calcium, application of a cold stimulus was found to induce a small increase in basal calcium concentration. These findings have led to the proposal that during a cold stimulus, TRPA1 responds to the cold-induced change in calcium levels rather than the temperature itself.

1.5.2.2. Alternative roles for TRPA1 in sensory transduction

TRPA1 is strongly activated by a number of irritant compounds that elicit burning sensations, including allyl isothiocyanate (mustard oil), cinnamaldehyde, allicin (garlic extract), and the pollutant acrolein (Jordt et al., 2004;Bandell et al., 2004;Macpherson et al., 2005;Bautista et al., 2005;Bautista et al., 2006). More recently, the channel has been shown to be the target for aldehyde compounds, such as formaldehyde and the endogenous α,β-unsaturated aldehyde 4-hydroxy-2-nonenal (4HNE) (McNamara et al., 2007;Trevisani et al., 2007;Macpherson et al., 2007b). 4HNE is produced from the peroxidation of membrane phospholipids in response to tissue injury, inflammation and oxidative stress, and its interaction with TRPA1 suggests a role for the channel in the sensing of chemical tissue damage. Formalin-induced pain responses are abolished with the pharmacological or genetic knockdown of TRPA1 (McNamara et al., 2007;Macpherson et al., 2007b). Many of these compounds, including mustard oil, cinnamaldehyde and formaldehyde, are electrophiles, and activate TRPA1 via covalent modification of cysteine and lysine residues located within the N-terminal region of the channel (Hinman et al., 2006;Macpherson et al., 2007a). Sensitivity to mustard oil is lost in excised cell patches, suggesting that additional cytosolic factors, namely inorganic polyphosphates, are also required to regulate channel activation by pungent compounds (Kim and Cavanaugh, 2007).
Like many TRP channels, TRPA1 can be modulated by the release of inflammatory mediators. Thus, BK was shown to activate the receptor via a phospholipase C (PLC)-mediated signalling cascade (Bandell et al., 2004). Likewise, cleavage of the protease-activated receptor 2 (PAR2) by trypsin, activation of PLC and hydrolysis of

PIP_2 results in the potentiation of responses to cinnamaldehyde and mustard oil (Dai et al., 2007). Arachidonic acid, released by the actions of PLA_2 following inflammation, is converted into prostaglandins, a number of which contain electrophilic moieties, and therefore the means by which to interact with and activate TRPA1 (Taylor-Clark et al., 2008). Inflammation results in the development of hypersensitivity to a number of stimulus modalities, including cold, heat and mechanical. As mentioned above, TRPA1 has been implicated as the main player in the onset of cold hyperalgesia (Obata et al., 2005), and studies of the TRPA1 knockout mouse have shown that this channel is also important in the development of BK-induced thermal and mechanical hyperalgesia (Bautista et al., 2006;Kwan et al., 2006).

1.6. Potassium channels and cold sensation

Besides TRPM8 and TRPA1, voltage-gated potassium and sodium ion channels have also been implicated in the regulation of cold transduction in sensory neurons. In one study, the application of a cold solution to DRG neurons resulted in an increase in the input resistance of the cells, implicating the involvement of a potassium conductance sensitive to changes in temperature (Reid and Flonta, 2001). It was suggested that the cold-induced depolarisation of neurons was caused by the inhibition of a potassium current active at resting membrane potential. Leak potassium currents in sensory neurons are mediated primarily via members of the two-pore domain potassium channel subfamily (Kang and Kim, 2006), some of which have been shown to be temperature-sensitive (Maingret et al., 2000;Kang et al., 2005), and one channel in particular, TREK-1, was implicated in the regulation of cold sensitivity following the demonstration that it could be inhibited by cooling (Maingret et al., 2000). A subsequent study using rt-PCR to investigate transcript expression in cold-sensitive TG neurons however found that TREK-1 was only present in a third of cells displaying a functional cold response (Nealen et al., 2003). Further electrophysiological studies looking at potassium conductance in sensory neurons found that not only was the cold-sensitive background potassium current greater in cold-sensitive neurons, but conversely that cold-insensitive cells expressed higher levels of a transient potassium current, sensitive to the broad spectrum potassium channel blocker 4-aminopyridine (4-AP) (Viana et al., 2002). The properties of this current, named IK_D, led to the proposal that it was acting as an 'excitability brake' in

cold-insensitive neurons, preventing the cells from firing when a cold stimulus was applied. Moreover, the application of 4-AP or another broad spectrum potassium channel antagonist tetraethylammonium (TEA) was found to induce novel cold sensitivity in 30-60 % of previously unresponsive Aδ- and C-neurons (Viana et al., 2002;Cabanes et al., 2003).

1.6.1. Potassium channel expression in sensory neurons

The complexity of voltage-gated potassium channels is reflected in the large number of subfamilies into which the alpha subunits are divided and the different electrophysiological, pharmacological and functional properties that define each group of channels. The ability of 4-AP and TEA to alter cold sensitivity in sensory neurons however implicates two particular groups of potassium channels in the regulation of cold transduction: the A-type (transient) potassium channel (I_A) and the delayed rectifier (I_{DR}).

In addition to maintaining resting membrane potential, the primary role of voltage-gated potassium channels in neurons is to repolarise the membrane following depolarisation and action potential generation, and both I_A and I_{DR} contribute to the latter. Electrophysiologically, I_A is characterised by fast activation and inactivation (although a subset of channels can display slow inactivation and the current is then referred to as I_D), whereas I_{DR} shows fast activation and slow deactivation with a non-inactivating sustained component (Hille, 2001). The two types of current can be further distinguished on the basis of the specific channel isoforms underlying the generation of each, and their sensitivity to pharmacological blockers. In general terms, 4-AP is used to block channels mediating I_A, while TEA is used to inhibit the I_{DR} current, although it should be noted that many voltage-gated potassium channels are sensitive to blockade by both 4-AP and TEA, regardless of the type of current they pass (Table 1.2).

Potassium Channel Isoform	Sensitivity to 4-AP	Sensitivity to TEA
A-type Current (I_A):		
Kv1.4	13 μM	> 100 mM
Kv3.3	1.2 mM	140 μM
Kv3.4		300 μM
Kv4.1	9 mM	> 10 mM
Kv4.2	5 mM	
Kv4.3		
Delayed Rectifier Current (I_{DR}):		
Kv1.1	290 μM	300 μM
Kv1.2	590 μM	560 mM
Kv1.3	195 μM	10 mM
Kv1.5	270 μM	330 mM
Kv1.6	1.5 mM	7 mM
Kv2.1	18 mM	
Kv2.2	1.5 mM	2.6 mM
Kv3.1	29 μM	200 μM
Kv3.2	100 μM	100 μM

Table 1.2. A list of the potassium channel isoforms underlying the A-type (transient) current (I_A) and the delayed rectifier current (I_{DR}), and their sensitivity to the broad spectrum potassium channel blockers 4-AP and TEA. Information was taken from the International Union of Pharmacology Ion Channel Compendium.

Much of the research looking at potassium channel expression in sensory neurons has focussed on the Kv1 subfamily. Consequently, immunohistochemistry has shown that large-diameter neurons express high levels of the Kv1.1 and Kv1.2 channels, while Kv1.4 is the predominant channel in IB4-positive small-diameter neurons (Rasband et al., 2001;Vydyanathan et al., 2005). Indeed whereas whole-cell potassium current in IB4-positive cells is more sensitive to blockade by 4-AP, TEA-sensitive currents are larger in the IB4-negative population. Sensory neurons also express members of the Kv3 and Kv4 subfamilies (Chien et al., 2007). In particular, Kv3.4 is found in 48 %

of all DRG neurons, of which 85 % express markers of nociceptive neurons and 15 % are proprioceptors, while Kv4.3 is restricted to the IB4-positive population, and shows a high level of co-expression with TRPV1.

As well as the 'fast' delayed rectifier channels described above, neurons also possess a slow delayed rectifier current, alternatively called the M-current, which is mediated via members of the Kv7 or KCNQ subfamily (Hille, 2001). Like I_{DR}, this current can be blocked by TEA, at concentrations within the low millimolar range (Passmore et al., 2003). KCNQ channels are activated at relatively negative potentials, and are involved in maintaining resting membrane potential. Information on the role of the M-current in sensory neurons has come from neurophysiological studies carried out in rat myelinated nerve fibres, where it was found to underlie accommodation to subthreshold depolarising stimuli, enhance subexcitability during the recovery cycle following an action potential, and promote adaptation to prolonged stimuli, all of which result in a reduction in neuronal excitability (Schwarz et al., 2006). In the DRG, the M-current was found to be more prevalent among small-diameter neurons, and was mediated through KCNQ2, KCNQ3 and KCNQ5 channels expressed as homo- or heteromultimers (Passmore et al., 2003).

Injury to sensory neurons results in the development of a hyperexcitable state, and it was reasoned that this could be due to up-regulation in sodium channels and/or a down-regulation in potassium channel function. Accordingly, transection of the sciatic nerve did result in a reduction of more than 60 % in I_A and I_{DR} currents in sensory neurons of all sizes (Everill and Kocsis, 1999;Abdulla and Smith, 2001;Yang et al., 2004). Chronic constriction of the DRG was also found to cause a reduction in potassium current, although in this model only the A-current was affected (Tan et al., 2006). Further studies have shown that this reduction in current can be attributed to a down-regulation in the expression of the potassium channels themselves, rather than a loss of function. Several members of the Kv1 subfamily are down-regulated following axotomy (Ishikawa et al., 1999;Rasband et al., 2001;Yang et al., 2004), and spinal nerve ligation results in a 30-50 % reduction in Kv3.4 and Kv4.3 expression in the ligated afferents (Chien et al., 2007). Following the discovery that pharmacological blockade of voltage-gated potassium channels can induce novel cold sensitivity, it is highly possible that injury-induced down-regulation in potassium channel expression could contribute to the development of cold hypersensitivity associated with neuropathic pain.

1.6.2. Potassium channel expression in sympathetic neurons

A systematic investigation into potassium channel expression in sympathetic ganglia in the rat found that several I_A and I_{DR} channel isoforms are expressed in the SCG. Specifically, transcripts were found encoding six members of the Kv1 subfamily, along with Kv2.1, Kv2.2, Kv3.4, Kv4.1 and Kv4.2 (Dixon and McKinnon, 1996). In later studies, the introduction of dominant-negative potassium channel mutants into SCG neurons enabled the identification of the principal channel isoforms underlying the generation of transient and delayed rectifier currents. Thus, the majority of the I_A current is mediated via Kv4.2 and Kv4.3, while the remainder (approximately 25 %) is due to activation of the Kv1.4 channel (Malin and Nerbonne, 2000;Malin and Nerbonne, 2001). Similarly, knockdown of Kv2.1 and Kv2.2 was sufficient to abolish the I_{DR} current in 75 % of cells, and lead to a significant reduction in the remainder (Malin and Nerbonne, 2002). The slow delayed rectifier M-current is particularly prominent in sympathetic neurons, and as in the DRG, is mediated via the KCNQ2, KCNQ3 and KCNQ5 channels (Hadley et al., 2003).

1.7. Sodium channels and cold sensation

There is less evidence supporting a role for sodium channels in the regulation of cold sensitivity than for potassium channels. An early study suggested that cooling could inhibit the Na^+/K^+ ATPase, thereby regulating cold transduction (Pierau et al., 1974), however blockade of the pump with ouabain in a subsequent study failed to elicit action potentials in cold-sensitive sensory neurons and the role of the ATPase in cold signalling was consequently suggested to be a minor one (Reid and Flonta, 2001). Conversely, cold temperatures have been shown to activate members of the DEG/ENaC family of epithelial sodium channels, which are present in DRG, and potentiate responses of other members of the DEG/ENaC family (Askwith et al., 2001;Chraïbi and Horisberger, 2003), and a role for these channels in the modulation of cold sensitivity was strengthened by the finding that amiloride, a blocker of DEG/ENaC channels, inhibited cold responses in TG neurons (Thut et al., 2003).

1.7.1. Voltage-gated sodium channel expression in sensory neurons

Voltage-gated sodium channels are comprised of a large alpha subunit (which contains the ion pore, the voltage sensor, the ion selectivity filter and the region required for fast inactivation, and alone constitutes a functional ion channel),

associated with one or more beta subunits (which target sodium channels to the plasma membrane and modulate their gating properties). Of the ten sodium channel alpha subunits, nine have been detected in sensory neurons, where they are activated by depolarisation of the membrane and are responsible for the generation and conduction of action potentials. Some channels, namely Nav1.7, Nav1.8 and Nav1.9, are associated preferentially with small-diameter nociceptors. Nav1.1 and Nax are expressed predominantly in large-diameter sensory neurons, while Nav1.2 and Nav1.6 are localised to the nodes of Ranvier of myelinated axons in embryonic and adult neurons, respectively. Finally, Nav1.3 and Nav1.5 are present in embryonic DRG, but their expression is down-regulated in the adult (Lai et al., 2004). Sodium channels can also be divided into two groups depending on their sensitivity to the neurotoxin tetrodotoxin (TTX): TTX-sensitive (TTXs) channels can be blocked by concentrations of the toxin in the low nanomolar range, whereas TTX-resistant (TTXr) channels can only be inhibited if the TTX is applied in concentrations greater than 1 μM (Table 1.3).

Like potassium channels, alterations in the expression of voltage-gated sodium channels following nerve injury contribute to the development of neuronal hyperexcitability (Lai et al., 2004;Benarroch, 2007). Sciatic nerve ligation or chronic constriction injury were found to result in a down-regulation in TTXr current and development of a rapidly repriming TTXs current in small-diameter sensory neurons (Cummins and Waxman, 1997;Dib-Hajj et al., 1999), whereas chronic constriction of the DRG caused a hyperpolarising shift in the voltage dependence of activation of TTXs currents (Tan et al., 2006). Accordingly, measurement of sodium channel expression in rat models of nerve injury has demonstrated an up-regulation in the expression of Nav1.3, and a concomitant down-regulation in Nav1.1, Nav1.6, Nav1.7, Nav1.8 and Nav1.9 (Dib-Hajj et al., 1999;Kim et al., 2002). Similarly, changes in sodium channel expression are also observed following inflammation, where the release of neurochemical signals such as PGE_2, serotonin and NGF result in an up-regulation of Nav1.3, Nav1.7, Nav1.8 and Nav1.9 (Black et al., 2004;Benarroch, 2007).

Sodium Channel Alpha Subunit	TTX Sensitivity	Localisation	Clinical Significance
Nav1.1	TTXs	Large-diameter DRG neurons, motor neurons, CNS	Point mutations and deletions cause GEFS+ and SMEI
Nav1.2	TTXs (18 nM)	Embryonic DRG, unmyelinated CNS axons	Point mutations cause GEFS+
Nav1.3	TTXs (15 nM)	Embryonic DRG, CNS	Up-regulated following nerve injury
Nav1.4	TTXs (5 nM)	Skeletal muscle	Point mutations cause hypoKPP, PMC or PAM
Nav1.5	TTXr (1.8 μM)	Embryonic DRG, heart	Point mutations cause long QT syndrome
Nav1.6	TTXs (1 nM)	Nodes of Ranvier in PNS and CNS, motor neurons	Point mutations in mice cause cerebellar ataxia or motor endplate disease
Nav1.7	TTXs (2 nM)	DRG neurons, CNS, sympathetic neurons	Mutations cause PE, PEPD, congenital inability to feel pain
Nav1.8	TTXr (>100 μM)	DRG neurons (80 % small-diameter, 20 % large-diameter)	Up-regulated following inflammation
Nav1.9	TTXr (39 μM)	Small-diameter DRG neurons	Up-regulated following inflammation
Nax		Large-diameter DRG neurons, glia	

Table 1.3. The family of voltage-gated sodium channel alpha subunits, their sensitivity to tetrodotoxin (TTX), tissue distribution and clinical relevance. TTXs, TTX sensitive; TTXr, TTX-resistant; GEFS+, generalised epilepsy with febrile seizures plus; SMEI, severe myoclonic epilepsy of infancy; hypoKPP, hypokalemic periodic paralysis; PMC, paramyotonia congenita; PAM, potassium-aggravated myotonia; PE, primary erythromelalgia; PEPD, paroxysmal extreme pain disorder.

The activity of voltage-gated sodium channels is directly affected by the cold. Several studies have reported a slowing of gating kinetics, a reduction in the peak sodium current, and a shift of voltage-dependent activation and inactivation towards hyperpolarised potentials (Matteson and Armstrong, 1982;Schwarz, 1986;Zimmermann et al., 2007). Recent investigations have shown that the expression of the TTXr channel Nav1.8 in C-fibre nociceptors is essential for the generation of action potentials in cold environments (Zimmermann et al., 2007). Thus, in the presence of TTX, C-fibres became mechanically and electrically insensitive at 30 °C, but responses could be restored on cooling to 10 °C, suggesting the involvement of a TTXr channel. Furthermore, cold-induced action potential generation and behavioural responses to noxious cold stimuli were abolished or severely impaired in the Nav1.8 knockout mouse.

1.7.2. Sodium channel-related disorders and cold sensation

Several disorders associated with mutations in voltage-gated sodium channels have a temperature-dependent feature. For example, mutations of the skeletal muscle sodium channel Nav1.4 can give rise to paramyotonia congenita, characterised by a muscle stiffness triggered by exposure to cold and aggravated by exercise, or hypokalemic periodic paralysis, the symptoms of which (low serum potassium concentration and paralysis) can occasionally be brought on by cold temperatures. Mutations underlying the development of paramyotonia congenita affect primarily sodium channel fast inactivation, causing slowed inactivation kinetics, shifts in the voltage-dependence of inactivation, and increased rate of recovery from inactivation (Fleischhauer et al., 1998;Wu et al., 2001;Bouhours et al., 2003;Mohammadi et al., 2003;Bouhours et al., 2005;Wu et al., 2005). The slowed inactivation and increased rate of recovery result in a larger depolarisation and a shorter refractory period, thus increasing the likelihood of repetitive firing. In a cold environment, the defects in channel inactivation are amplified, and it has been suggested that this additional modulation of sodium channel function is sufficient for neurons to reach the threshold for the onset of myotonia (Fleischhauer et al., 1998;Bouhours et al., 2003;Mohammadi et al., 2003;Bouhours et al., 2005). In the case of hypokalemic periodic paralysis, the mutant channel is activated and inactivated at hyperpolarised potentials relative to the wild type channel in the cold, which in combination with a decrease in serum potassium levels can result in paralysis (Sugiura et al., 2003).

In sensory neurons, gain-of-function mutations in the Nav1.7 sodium channel are associated with two diseases, primary erythromelalgia and paroxysmal extreme pain disorder. Primary erythromelalgia can be either familial or sporadic, and is characterised by a burning pain and redness in the extremities triggered by warmth or exercise. Several mutations in the Nav1.7 channel identified in recent years have been shown to alter sodium channel function in several ways: compared to the wild type Nav1.7, mutant channels display a hyperpolarised shift in the voltage dependence of activation, a depolarised shift in the voltage dependence of inactivation, faster closed-state inactivation, an increased rate of recovery from inactivation, slowed deactivation, and a larger response to slow depolarising stimuli (Cummins et al., 2004;Dib-Hajj et al., 2005;Han et al., 2006;Lampert et al., 2006;Harty et al., 2006). All of these alterations result in increased neuronal excitability, reflected by a depolarised resting membrane potential and a lowered threshold for action potential generation (Harty et al., 2006;Rush et al., 2006). The pain caused by primary erythromelalgia can be relieved by cooling the affected limbs. A recent study found that cooling induced a depolarising shift in the voltage dependence of activation of a mutant channel, partially reversing the hyperpolarisation caused by the presence of the mutation and bringing the threshold for activation closer to that of the wild type channel (Han et al., 2007).

Paroxysmal extreme pain disorder is an autosomal dominant condition in which patients suffer from burning pain in the rectal, ocular and mandibular areas accompanied by autonomic manifestations such as flushing of the skin. Studies of mutations associated with this disease show a depolarised shift in steady-state inactivation and only partial inactivation, leading to persistent sodium currents (Fertleman et al., 2006). Although the onset of symptoms is often unprovoked, similarity between the sodium channel defects seen here and those associated with paramyotonia congenita in Nav1.4 suggest that stimuli such as cold could result in neuronal hyperexcitability.

Oxaliplatin is a chemotherapeutic drug used in the treatment of colorectal, ovarian, breast and lung cancers. Like all platinum-based drugs cumulative doses of oxaliplatin can result in the development of a peripheral sensory neurotoxicity, characterised by paraesthesias, numbness, a loss of vibratory sensation, and a loss of deep tendon reflexes. This form of chronic neuropathy is thought to be caused by the accumulation of platinum-based biotransformation products in the DRG and

peripheral nerves (Luo et al., 1999;Cavaletti et al., 2001). Unlike other platinum-based drugs however, oxaliplatin can also induce an acute sensory neuropathy, which has a very rapid onset and offset, but which can increase in duration and severity with repeated drug administration. Symptoms include paraesthesias and dysaesthesias, often affecting the perioral and laryngo-pharyngeal areas as well as the limbs, muscle spasms and cramps in the limbs, muscle tightness in the throat and jaw, and eye pain. This neuropathy is induced or exacerbated by exposure to cold, and affects over 80 % of patients (Cersosimo, 2005;Pasetto et al., 2006). Recent *in vitro* studies have suggested that the acute oxaliplatin-induced neuropathy could be due to its influence on the function of voltage-gated sodium channels. The application of oxaliplatin to nerve fibres or dissociated sensory neurons has been shown to result in an increased refractory period, a reduction in sodium conductance, a shift in peak activation and inactivation to hyperpolarised potentials, and a slowing of the inactivation kinetics of sodium channels (Adelsberger et al., 2000;Grolleau et al., 2001;Webster et al., 2005;Benoit et al., 2006). There is currently no evidence however demonstrating a direct link between oxaliplatin-induced sodium channel defects and the development of hypersensitivity to cold.

1.8. Aims

The aims of the thesis project were as follows:

1. Evidence supports a role for the two thermosensitive TRP channels TRPM8 and TRPA1 in the detection of innocuous cool and noxious cold in peripheral neurons. The aim of the study was to investigate the precise contribution of these two channels to cold transduction in sensory and sympathetic neurons, correlating functional cold sensitivity with ion channel expression.

2. Previous studies have demonstrated that inhibition of voltage-gated potassium channels can induce novel cold sensitivity in previously insensitive sensory neurons. The aim of the study was to identify potassium channel isoforms contributing to the regulation of cold sensitivity in sensory neurons, and to extend the investigation to see whether similar mechanisms exist in sympathetic neurons.

3. The chemotherapeutic drug oxaliplatin induces an acute sensory neuropathy in patients that is exacerbated by exposure to cold. Oxaliplatin is believed to exert its effects on voltage-gated sodium channels. The aim of this study was to investigate whether the activation of sodium channels or the application of oxaliplatin was sufficient to induce novel cold sensitivity in previously insensitive sensory neurons.

4. The expression of the thermosensitive TRP channels, TRPV1, TRPM8 and TRPA1 is developmentally regulated, but the factors controlling TRP channel expression in sensory neurons are not fully understood. The aim of the study was to investigate whether NGF could modulate functional cold sensitivity and TRP channel expression in neonatal sensory neurons.

5. The transcription factor Runx1 and the GDNF co-receptor Ret have been implicated in the regulation of TRP channel expression in sensory neurons. The aim of the study was to investigate whether NGF could modulate the expression of transcription factors and growth factor receptors in neonatal sensory neurons, and whether Runx1 was involved in the NGF-mediated regulation of cold sensitivity and TRP channel expression.

2. Methods

This chapter provides a general overview of all experimental protocols used during the thesis project. Specific details of individual experiments can be found in the relevant results chapters.

2.1. Animals

Tissue for experiments was obtained from newborn (P0-P5) or adult male (6-8 weeks) C57/B6 mice. The animals were housed in university facilities, on a 12-hour light-dark cycle and with food and water provided ad libitum. All animals were culled humanely according to the Animals (Scientific Procedures) Act 1986.

2.2. Primary tissue culture

2.2.1. Sensory neuron cell culture

Adult male mice were killed by cervical dislocation. The spinal column was removed and bisected along the midline of the ventral and dorsal plates. The spinal cord was carefully removed and DRG from all spinal levels were dissected out into calcium- and magnesium-free Hank's balanced salt solution (HBSS, Table 2.1) (Gibco, UK). The ganglia were incubated in filter-sterilised papain solution (2 mg/ml, Sigma) for 20 minutes at 37 °C, and spun down at 1400 rpm (380 x *g*) for 1 minute. The papain was carefully removed and replaced with collagenase type IV (2 mg/ml, Lorne Laboratories, UK) and dispase type II (2.4 mg/ml, Roche, UK) in HBSS, and the ganglia were incubated for a further 20 minutes. Following centrifugation at 1400 rpm for 1 minute, ganglia were re-suspended in 1 ml HBSS and dissociated mechanically by trituration, using fire-polished, F-12 medium-coated glass pipettes with increasingly narrow bores. Dissociated DRG neurons were spun for 8 minutes at 1400 rpm in a Percoll gradient (Sigma) to remove non-neuronal debris and washed in L-15 medium for 2 minutes at 2300 rpm (1030 x *g*). The neurons were re-suspended in F-12 medium (Table 2.2) (Invitrogen, UK) containing 10 % heat-inactivated horse serum (Invitrogen), 100 U/ml penicillin (Sigma), and 0.1 mg/ml streptomycin (Sigma). The F-12 medium was further supplemented for some experiments with 50 ng/ml recombinant human NGF (rhNGF) (a gift of Genentech Inc., San Francisco, CA, USA). The neurons were plated onto coverslips pre-coated with poly-L-lysine (0.01 %, Autogen Bioclear, UK) and laminin (30 µg/ml, Invitrogen) and placed in 12-

well plates. Cells were allowed to adhere to the coverslips for 2 hours at 37 °C, before being flooded with 1 ml F-12 medium. Neurons were kept at 37 °C under 5 % CO_2 for up to 24 hours. Acute cultures were used within 3-5 hours of plating.

2.2.2. Sympathetic neuron cell culture

Adult male mice were killed by CO_2 inhalation. The trachea was exposed and the SCG lying either side were quickly removed into HBSS. In early experiments looking at the role of TRP channels in cold transduction the SCG were treated in the same way as the adult DRG, using the method outlined above, with the exception that dissociated SCG neurons were not spun through a Percoll gradient. After centrifugation at 2700 rpm (650 x *g*) for 1 minute, the cells were re-suspended in F-12 medium supplemented with 50 ng/ml rhNGF, and plated onto poly-L-lysine and laminin-coated coverslips. Neurons were allowed to adhere to the coverslips for 3 hours before being flooded with 1 ml F-12 medium. SCG neurons were maintained at 37 °C under 5 % CO_2 for up to 5 hours.

During subsequent experiments investigating the role of potassium channels in cold transduction it became necessary to modify the culture protocol in order to increase the yield of viable neurons. Following dissection, the SCG were transferred from HBSS into filter-sterilised papain solution and incubated for 30 minutes at 37 °C. The centrifugation step was omitted, and the ganglia were transferred directly to collagenase and dispase for a further 30 minutes. Ganglia were re-suspended in 300 µl F-12 medium containing 10 % foetal bovine serum, 100 U/ml penicillin, 0.1 mg/ml streptomycin, 50 ng/ml rhNGF and 30 mM D-glucose. Trituration was done in several steps, removing the supernatant to a clean tube regularly and re-suspending the remaining intact ganglia in fresh F-12. The dissociated SCG neurons were not passed through a Percoll gradient, but were spun down at 2500 rpm (550 x *g*) for 2.5 minutes. The neurons were plated onto poly-L-lysine and laminin-coated coverslips, left to settle for 2 hours at 37 °C, and then flooded with 1 ml F-12 medium. Neurons were kept at 37 °C under 5 % CO_2. Acute cultures were used within 3-5 hours of plating.

2.3. In vitro electroporation

DRG neurons from P0 mice were electroporated using the Amaxa Nucleofector according to the manufacturer's instructions (Amaxa, Germany). Dissociated neurons pooled from 2-4 animals were spun down at 2400 rpm (1120 x *g*) for 2 minutes and re-suspended in 100 µl mouse neuron nucleofector solution (Amaxa). 5 µg of a construct containing the Runx1d gene, a dominant-negative form of the Runx1 transcription factor (Marmigere et al., 2006), under the control of the chicken β-actin promotor (pCA-Runx1d) and 5 µg of a green fluorescent protein-coding plasmid (pCA-eGFP, both constructs kindly donated by Prof Patrik Ernfors, Karolinska Institute, Sweden) were added to the cell suspension, and the total volume was transferred into an Amaxa-certified cuvette. Control cultures were mixed with 5 µg pCA-eGFP only. The cuvette was placed into the Nucleofector instrument and the neurons were electroporated using program O-005. The neurons were immediately transferred into 500 µl pre-warmed F-12 medium containing horse serum, penicillin-streptomycin and 100 ng/ml rhNGF. Neurons were spun down at 2000 rpm (780 x *g*) for 2 minutes and re-suspended in F-12 medium for plating. Neurons were maintained at 37 °C under 5 % CO_2 for 5 days. 500 µl of the culture medium was replaced with fresh F-12 every 2-3 days.

Components	Molecular Weight	Concentration mg/L	Molarity mM
Inorganic salts			
Potassium chloride	75	4000	53.33
Potassium phosphate monobasic	136	600	4.41
Sodium chloride	58	80000	1379.31
Sodium phosphate dibasic	268	900	3.36
Other components			
D-glucose	180	10000	55.56

Table 2.1. Media formulation for Hank's Balanced Salt Solution 10X, without calcium, magnesium, phenol red, sodium bicarbonate (Gibco, Cat No. 14185). The final working solution contained 1X HBSS, 5 mM HEPES, and 10 mM D-glucose, pH 7.4.

Components	Molecular Weight	Concentration mg/L	Molarity mM
Amino acids			
Glycine	75	7.5	0.1
L-alanine	89	8.9	0.1
L-arginine hydrochloride	211	211	1
L-asparagine	132	13	0.0985
L-aspartic acid	133	13.3	0.1
L-cysteine hydrochloride	158	36	0.228
L-glutamic acid	147	14.7	0.1
L-glutamine	146	146	1
L-histidine hydrochloride-H_2O	210	21	0.1
L-isoleucine	131	4	0.0305
L-leucine	131	13.1	0.1
L-lysine hydrochloride	183	36.5	0.199
L-methionine	149	4.5	0.0302
L-phenylalanine	165	5	0.0303
L-proline	115	34.5	0.3
L-serine	105	10.5	0.1
L-threonine	119	11.9	0.1
L-tryptophan	204	2.04	0.01
L-tyrosine	181	5.4	0.0298
L-valine	117	11.7	0.1
Vitamins			
Biotin	244	0.0073	0.0000299
Choline chloride	140	14	0.1
D-calcium pantothenate	477	0.5	0.00105
Folic acid	441	1.3	0.00295
I-inositol	180	18	0.1
Niacinamide	122	0.036	0.000295
Pyridoxine hydrochloride	206	0.06	0.000291
Riboflavin	376	0.037	0.0000984
Thiamine hydrochloride	337	0.3	0.000890
Vitamin B-12	1355	1.4	0.00103
Inorganic salts			
Calcium chloride	147	44	0.299
Cupric sulphate	250	0.0025	0.00001
Ferric sulphate	278	0.834	0.003
Magnesium chloride	203	122	0.601
Potassium chloride	75	223.6	2.98
Sodium bicarbonate	84	1176	14
Sodium chloride	58	7599	131.02
Sodium phosphate dibasic	142	142	1
Zinc sulphate	288	0.863	0.003

Other components			
D-glucose (Dextrose)	180	1802	10.01
Hypoxanthine	136	4	0.0294
Linoleic acid	280	0.084	0.0003
Lipoic acid	206	0.21	0.00102
Phenol red	376.4	1.2	0.00319
Putrescine 2HCl	161	0.161	0.001
Sodium pyruvate	110	110	1
Thymidine	242	0.7	0.00289

Table 2.2. Media formulation for F-12 nutrient mixture (Ham) 1X, with L-glutamine (Invitrogen, Cat No. 21765).The final working solution contained 10 % serum, 100 U/ml penicillin, 0.1 mg/ml streptomycin, 50-100 ng/ml rhNGF, and 30 mM D-glucose, as required.

2.4. Ratiometric calcium imaging

Coverslips were incubated for 30 minutes in the calcium-binding dye Fura-2 acetoxymethyl (2 μM Fura-2 AM in 0.1 % DMSO, 0.1 % pluronic acid F-127, both from Invitrogen), followed by 10 minutes in extracellular solution containing isolectin B4-FITC (IB4) (10 μg/ml, Sigma) and cholera toxin B subunit-alexa fluor 594 conjugate (CTB) (1 μg/ml, Invitrogen). In experiments where electroporated neurons were expressing GFP, IB4-FITC was replaced with IB4-TRITC (10 μg/ml, Sigma). The coverslips were positioned on a Zeiss Axiovert 200 inverse microscope (Zeiss, Germany), inside a custom-made recording chamber bathed in room-temperature extracellular fluid (ECF) (145 mM NaCl, 5 mM KCl, 2 mM $CaCl_2$, 1 mM $MgCl_2$, 10 mM D-glucose, 10 mM HEPES, pH 7.4). For experiments requiring calcium-free extracellular solution, magnesium was added to the ECF in place of calcium, along with 1 mM EDTA.

A gravity-driven application system enabled the uniform delivery of different solutions to the cells through an 8-line manifold application system with a common outlet (with an inner diameter ranging between 0.86-1.17 mm, flow rate 3 ml/min). Application of solutions was controlled via the Windows Application System (Dittert et al., 2006) operating a set of two-way valves (General Valve Corporation, Fairfield, NJ, USA). The temperature of the bath was continuously monitored with a PMD1208LS A/D interface and DAQ software (Measurement Computing Corp., Middelboro, MA, USA), at a sampling rate of 10 Hz, with a thermocouple, with a lag

of approximately 25 ms/°C, positioned just outside the field of vision, opposite the stream of the inflow (Figure 2.1). For experiments monitoring cold sensitivity, two of the eight inflows were cooled by a jacket of circulating solution of -5 °C using a thermostat. Two protocols were used to apply a cold stimulus to reach a nadir of approximately 5 °C in the recording chamber. In some experiments stimuli were applied from room temperature (mean baseline temperature 21.6 ± 1.5 °C [standard deviation, STD], n = 253 recordings) and the cold ramp was applied for 20 seconds (mean rate of temperature change 1.4 °C/s). In other experiments the solutions were warmed to 30.7 ± 1.3 °C (n = 19 recordings) by a resistor wire (28 Ω/m, 0.15 mm diameter, Conrad Electronics, UK) wrapped around the common outlet of the manifold, whose current was controlled by a programmable current generator (Current generator DPS-4005PFC, Voltcraft, Germany). In these experiments a cold ramp was applied over a period of 100 seconds (mean rate of temperature change 0.3 °C/s). In early experiments it was noted that condensation would build up on the underside of the recording chamber during application of the cold stimulus. In order to circumvent this problem, humidity levels in the laboratory were kept low and the underside of the chamber was cleaned thoroughly with a household de-icer between each successive recording. In addition, the chamber was fitted with two small platforms on which the coverslip could sit, thus avoiding direct contact between the coverslip and the bottom of the chamber.

Ratiometric images were recorded at 340 and 380 nm excitation (exposure time 50-100 ms), at intervals of 0.3-0.5 seconds for the duration of the cold stimulus and 1-2 seconds thereafter, using a Polychrome IV and an air-cooled CCD Imago Camera (640 x 480 pixel resolution) controlled by TILLvisION software (all from TILL Photonics, Germany). The resulting resolution for temperature measurements during the cold ramps was on average 0.7 or 0.1 °C per ratio when the baseline was set to room temperature or 30 °C, respectively. One field of vision per coverslip was analysed, unless otherwise stated, and only vital neurons that responded to a high (50 mM) potassium stimulus were included in the analysis, which typically comprised more than 90 % of morphologically identified neurons in our culture conditions (Figure 2.1).

Analysis of neuronal responses to applied stimuli was done using the TILLvisION software. Individual neurons were identified from the brightfield image and numbered for analysis. The live fluorescent recordings were converted into images

('ratios') in which the changes in Fura fluorescence in response to increases in intracellular calcium concentration could be visualised. The numbering of the cells was transferred from the brightfield to the ratio image. The software calculated changes in the ratio between the calcium-free and calcium-bound forms of the Fura dye (measured at 380 nm and 340 nm, respectively) over the course of the experiment for each numbered cell, and placed the derived ratio values into an Excel file. During these calculations, ratio values were multiplied by a factor of 1000, and as a consequence, all data presented in the thesis has been converted back to a milliratio (whereby the derived ratio values were divided by 1000). Kinetic traces, in which the ratio was presented as a function of time, were then used to assess peaks in fluorescence, indicative of increases in intracellular calcium concentrations. Each cell was additionally assessed for IB4 and CTB staining using Photoshop (Adobe, San Jose, CA, USA) to overlay brightfield and fluorescent images, and cell area was measured using the Scion Image software (Scion, Frederick, MD, USA) (Figure 2.2). Neurons were considered to be sensitive to a stimulus if there was an increase of > 15 % from baseline in the Fura fluorescence ratio. The baseline was taken as the average ratio value for the 3 seconds preceding the stimulus onset. Activation threshold was measured at the point at which the fluorescence ratio rose above baseline levels. In a number of experiments, a large proportion of cells were observed to respond during the cold stimulus with a small near-linear increase in fluorescence, a phenomenon that has been reported in a previous study of cold sensitivity (Reid et al., 2002). It was suggested that this response reflects the effects that lowering the temperature can have on the properties of the calcium-binding dye itself, and Fura-2 has been shown to display a small increase in fluorescence ratio when the temperature is reduced (Oliver et al., 2000). Another explanation could be the non-specific activation of neurons by very cold temperatures (Simone and Kajander, 1996). Since these responses were generally small and appeared in most cells, they were considered to be non-specific and for the purposes of this study the neurons were classed as cold-insensitive.

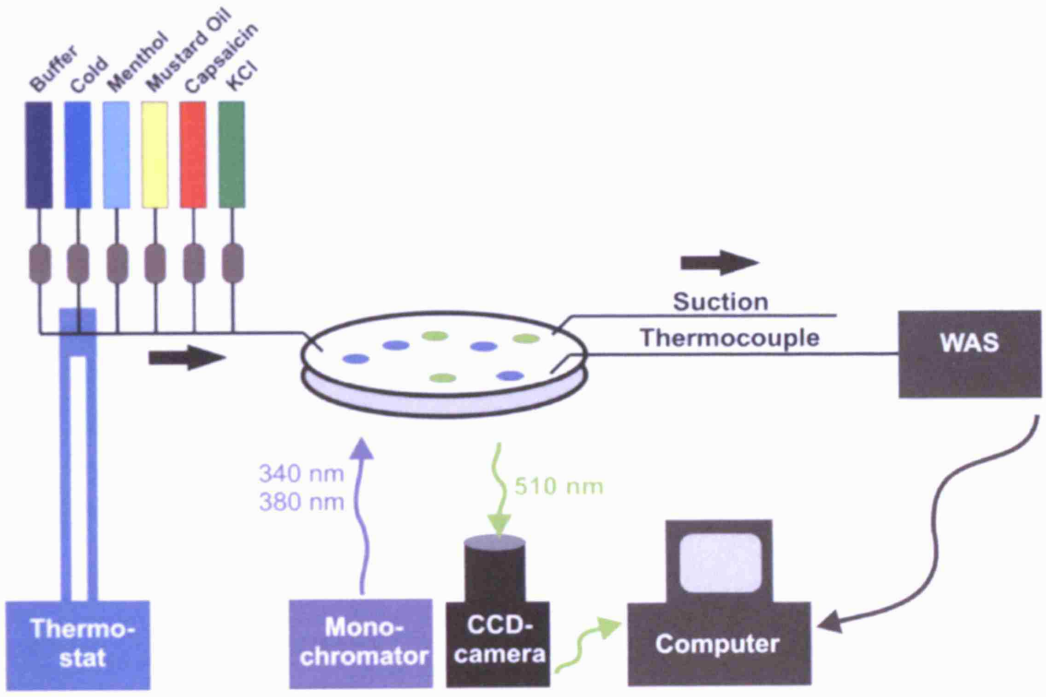

Figure 2.1. Schematic of the set-up used for calcium imaging experiments. Dissociated neurons were loaded with the calcium-binding dye Fura-2 and the coverslip was placed on an inverted microscope. Stimuli were applied to a pre-selected field of cells via a system of two-way valves controlled by the Windows Application System (WAS). The Fura-2 was excited at wavelengths of 340 nm and 380 nm, and emitted light at 510 nm. Images were captured on a CCD camera connected to a PC running the TILLvisION software. Bath temperature was monitored with a thermocouple positioned opposite the inflow and connected via the WAS to a computer running the DAQ software.

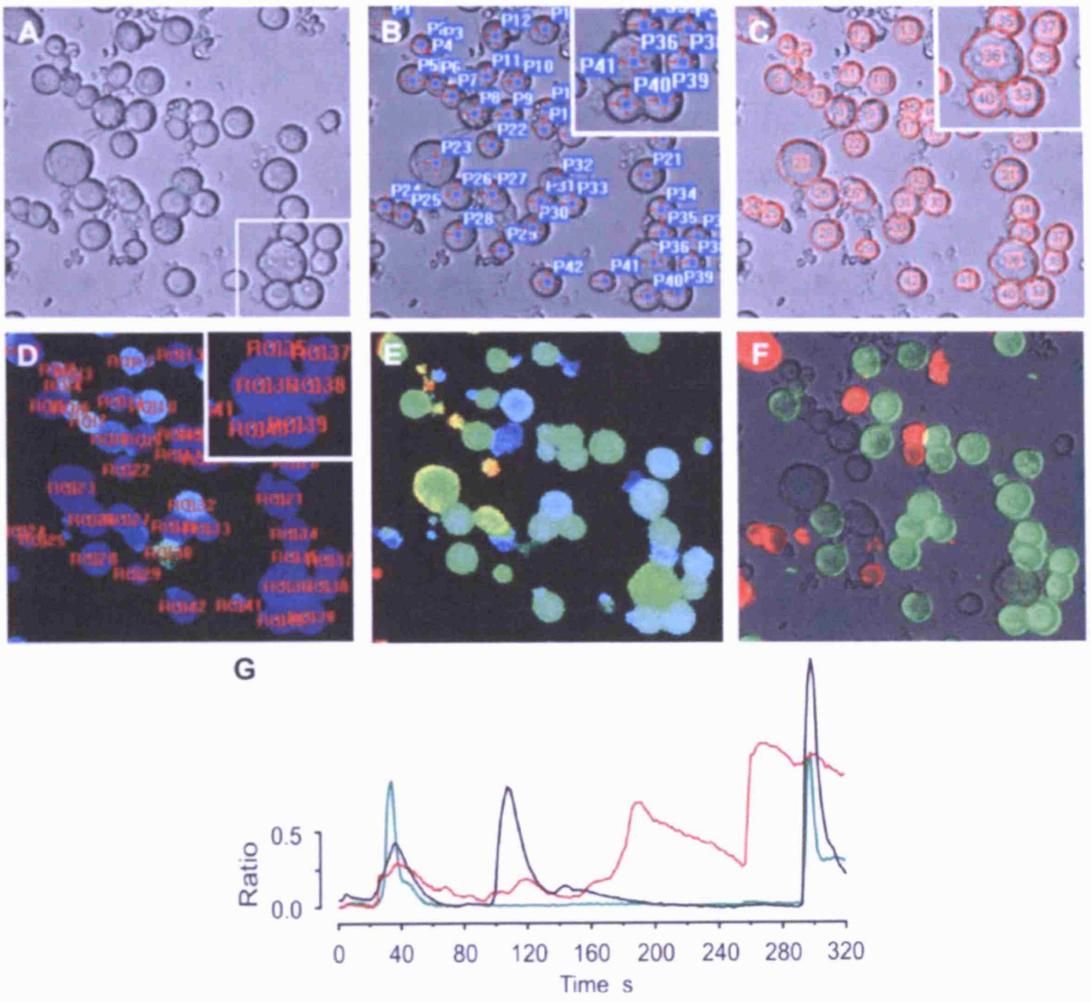

Figure 2.2. Protocol for the analysis of calcium imaging data. (A) Brightfield image of DRG neurons selected for calcium imaging. The boxed area is magnified in images B-D. (B) Morphologically identified neurons were numbered within the TILLvisION program. (C) Cell area of individual neurons was measured by drawing around each cell in Scion Image. (D) Live fluorescent recordings were converted into ratio images, in which increases in intracellular calcium concentration were visualised by an increase in fluorescence (E). (F) Neurons were assessed for IB4 and CTB staining by overlaying the brightfield and fluorescent images in Photoshop. (G) Neuronal responses to applied stimuli were presented as increases in the Fura fluorescent ratio over time. Each trace on the graph represents one cell.

2.5. Quantitative rt-PCR

Freshly triturated adult sensory and sympathetic neurons were spun down and re-suspended in 200 µl cell lysis buffer (Flowgen, UK). Neonatal sensory neurons that had been used for calcium imaging were washed twice in PBS at the end of the experiment and lysed in 100 µl cell lysis buffer directly on the coverslips. Total RNA was extracted from all neurons using the Purescript RNA Purification kit (Flowgen, UK), according to the manufacturer's instructions. For every 100 µl of lysis buffer used, 33 µl protein-DNA precipitation solution were added to the cell lysate which was then incubated on ice for 5 minutes. DNA and protein were removed by centrifugation at 13000 rpm (16060 x *g*) for 4 minutes. The supernatant containing the RNA was mixed with 100 µl isopropanol (Sigma), supplemented with 10 µg glycogen (Flowgen) to improve yield, and spun down at 13000 rpm for 4 minutes. The RNA pellet was washed in 100 µl 70 % ethanol (Sigma) and re-suspended immediately in 5 µl RNAse-free water.

Purified RNA samples were quantified on a NanoDrop 1000 spectrophotometer (NanoDrop Technologies, Wilmington, DE, USA) and RNA quality and integrity was assessed on an Agilent Bioanalyser 2100 (Agilent Technologies Inc., Santa Clara, CA, USA). Where available, the RNA Integrity Number (RIN) was recorded, and was found to be $\geq$ 8 in all cases. RNA with a RIN number greater than 8 is ideal for downstream applications, including real-time PCR (Fleige and Pfaffl, 2006).

RNA samples were DNAse-treated with the Turbo DNA-*free* kit (Ambion, UK). 0.1 volume of DNAse buffer and 1 µl DNAse were added to the RNA solution, which was incubated at 37 °C for 20 minutes. The reaction was stopped with the addition of 2 µl DNAse inactivation reagent. Following centrifugation at 10000 rpm (10000 x *g*) for 2 minutes, the RNA-containing supernatant was recovered. The RNA was reverse transcribed using the iScript cDNA Synthesis kit (Biorad, UK). 10 ng RNA were added to 1 µl RNAse H^+ iScript reverse transcriptase (RT) and 4 µl iScript buffer (containing RNAse inhibitors, and a mix of oligodeoxythymidylic acid (oligo [dT]) and random hexamers), and the volume was made up to 20 µl with RNAse-free water. Reactions were set up with or without the inclusion of the RT. Non-template control reactions contained water in place of the RNA. The PCR reaction was as follows: 5 minutes at 25 °C, 30 minutes at 42 °C, 5 minutes at 85 °C. cDNA samples were diluted 1:2 to give a final concentration of 250 pg/µl.

The cDNA was used for real-time PCR on a Smart Cycler instrument (Cepheid, Sunnyvale, CA, USA), using iQ SYBR green supermix (containing 100 mM KCl, 40 mM Tris-HCl, 0.4 mM each deoxyribonucleotide triphosphate [dNTP], 50 U/ml hot start iTaq DNA polymerase, 6 mM $MgCl_2$, SYBR green I dye, 20 nM fluorescein, pH 8.4) (Biorad), which produces a fluorescent signal when bound to double-stranded DNA. cDNA plus or minus RT was probed using primers specific for housekeeping genes (ubiquitin carboxyl-terminal hydrolase L1 [UCHL1] and glyceraldehyde-3-phosphate dehydrogenase [GAPDH]), TRP ion channels (TRPM8, TRPA1 and TRPV1), voltage-gated potassium channels (Kv1.1, Kv1.2, Kv1.6, Kv3.1, Kv3.2, Kv3.3, Kv3.4), Runx1, TrkA and Ret (Tables 2.3-2.6). All primers were obtained from Operon (Germany), with the exception of primers for Kv3 potassium channels, Runx1, TrkA and Ret, for which pre-designed QuantiTect Primer Assays were used (Qiagen, UK). 250 pg of cDNA were initially added to all PCR reactions, and this was increased to 1.25-3 ng where transcript expression was below the level of detection. PCR runs included non-template control samples to check for contamination and primer dimer formation. Before experiments were carried out, annealing temperature was optimised for every primer pair and serial dilution curves were created. All assays showed a linear correlation between cycle threshold and cDNA concentration. The PCR reaction was as follows: 3 minutes at 95 °C (1 cycle); 15 seconds at 95 °C, 25-30 seconds at 57-64 °C, 30 seconds at 72 °C (50 cycles) (For individual annealing conditions, see Tables 2.3-2.6). A melt curve was run at the end of every reaction (60-95 °C, 0.2 °C/s). Reaction products gave single peaks on melt curve analysis and single bands of expected size on a 2 % agarose gel.

Relative quantification of rt-PCR products was performed using either the total amount of starting RNA or the expression of housekeeping genes, with the ΔΔ method, as a reference (Pfaffl et al., 2002). The ΔΔ method calculates the difference in expression of a target gene within two samples relative to the expression of a reference gene, where expression is based on the cycle threshold (Ct) value. The Ct was taken at the point where the rate of amplification was at its greatest, as determined by the second derivative. Initial quality control experiments were carried out to assess the amount of error introduced into the PCR either by pipetting or by variability between the reaction sites within the Smart Cycler instrument. Eight identical replicates of 250 pg were taken from a single stock solution of DRG cDNA and were probed simultaneously for UCHL1 expression. The intra-sample variability

was found to be very low: the average Ct value was 23.09 (range 22.93 - 23.21), and the coefficient of variance was 0.4 % (standard deviation [0.09] / mean [23.09] x 100).

Gene	Primer Pairs	Annealing Temperature	Amplicon Length
UCHL1	5'TGCTCCTGTTTCCCCTCAC3' 5'AGTTTCCGATGGTCTGCTTC3'	60 °C, 30 s	117 bp
GAPDH	5'ATGTGTCCGTCGTGGATCTGA3' 5'ATGCCTGCTTCACCACCTTCTT3'	60 °C, 30 s	81 bp
TRPM8	5'CTTCCCCTTCGTTGTCTTC3' 5'TGAGTTGTCGTTGGCTTTC3'	57 °C, 30 s	190 bp
TRPA1	5'GCTCATCAAACTCATCATCCA3' 5'TCTGTTCCAGCCTCTCCTTC3'	62 °C, 30 s	107 bp
TRPV1	5'AGGGGAGAAATGAGGGACA3' 5'TACAGCCAGCCAACATCAAC3'	64 °C, 25 s	120 bp

Table 2.3. rt-PCR primers used to probe for expression of the housekeeping genes UCHL1 and GAPDH, and of the thermosensitive TRP channels TRPM8, TRPA1 and TRPV1.

Gene	Primer Pairs	Annealing Temperature	Amplicon Length
Kv1.1	5'ACCCTGGGCACGGAGATAG3' 5'TCTGAACACCCTTACCAAGCG3'	60 °C, 30 s	100 bp
Kv1.2	5'TGGAAACCTTGCCCATCTTCC3' 5'GGAGGTGGACTGCTGGTACCC3'	60 °C, 30 s	100 bp
Kv1.6	5'AAGCAACGAGGGTAGTGGGAC3' 5'CCCAGAGGGAATGCTACCAG3'	60 °C, 30 s	100 bp

Table 2.4. rt-PCR primers used to probe for expression of members of the Kv1 sub-family of voltage-gated potassium channels. The primer sequences were published by (Young et al., 2006).

Gene	Primer Pairs	Annealing Temperature	Amplicon Length
Kv3.1	Quantitect Primer Assay Cat No: QT00290332	60 °C, 30 s	101 bp
Kv3.2	Quantitect Primer Assay Cat No: QT01069838	60 °C, 30 s	150 bp
Kv3.3	Quantitect Primer Assay Cat No: QT00127834	60 °C, 30 s	93 bp
Kv3.4	Quantitect Primer Assay Cat No: QT00125930	60 °C, 30 s	109 bp

Table 2.5. rt-PCR primers used to probe for expression of members of the Kv3 sub-family of voltage-gated potassium channels.

Gene	Primer Pairs	Annealing Temperature	Amplicon Length
Runx1	Quantitect Primer Assay Cat No: QT00100380	60 °C, 30 s	120 bp
TrkA	Quantitect Primer Assay Cat No: QT01046143	60 °C, 30 s	137 bp
Ret	Quantitect Primer Assay Cat No: QT00121583	60 °C, 30 s	78 bp

Table 2.6. rt-PCR primers used to probe for expression of the Runx1 transcription factor, and for the neurotrophic factor receptors TrkA and Ret.

2.6. Statistics

For each set of calcium imaging experiments at least four independent cultures were tested over two experimental days, unless otherwise stated. Each culture usually consisted of several coverslips. The results from the coverslips of one culture were pooled and were used as one data point for subsequent analysis. DRG cultures were obtained from one animal (with the exception of transfected neonatal DRG cultures in which the ganglia from 2-4 animals were pooled), while SCG and TG cultures were obtained from 1-2 animals.

For rt-PCR experiments, at least three independent cDNA samples were assessed for messenger RNA expression. All reactions were run in duplicate and the average Ct value was used as one data point for subsequent analysis. Where RNA was extracted from freshly triturated adult sensory and sympathetic neurons, each sample contained material from 7-10 DRG or 2 SCG, respectively. For neonatal neurons that were plated prior to cell lysis, 1-2 coverslips per culture were processed.

All quantitative comparisons are presented as mean ± standard error of the mean (SEM) unless otherwise stated. For statistical analysis, Student's unpaired *t*-test, Mann-Whitney *U* test, Yates' corrected Chi-squared test, or Fisher's exact test were used (Statistica 6.1, Statsoft, Tulsa, OK, USA).

3. The role of TRP channels in cold transduction

3.1. Background

TRP channels are currently recognised as the principal transducers of thermal stimuli in the peripheral nervous system (Caterina, 2007). While members of the vanilloid subfamily can be activated by heat, two other channels have been implicated in cold transduction. TRPM8 was first described as a cold and menthol receptor expressed in small-diameter sensory neurons, comprising around 15 % of the total neuronal population (McKemy et al., 2002;Peier et al., 2002a). The recombinant TRPM8 channel was found to be activated by temperatures ranging between 8-28 °C, suggesting that it may play a role in the detection of noxious cold as well as innocuous cool stimuli. Functional studies in sensory neurons have reported a significant overlap between menthol and capsaicin sensitivity (McKemy et al., 2002;Babes et al., 2004), a finding that has been both refuted (Peier et al., 2002a) and supported (Okazawa et al., 2004) by in situ hybridisation experiments. Many studies looking at the relationship between cold and menthol sensitivity in sensory neurons were carried out in neurons maintained for several days in the presence of NGF (Reid et al., 2002;Jordt et al., 2004;Okazawa et al., 2004), conditions which have been proven to alter neuronal phenotype (Story et al., 2003).

The second putative cold-sensitive channel, TRPA1, is expressed in a subpopulation of TRPV1-positive nociceptive afferents. It was originally shown to be expressed in 4 % of sensory neurons (Story et al., 2003), although more recent studies have suggested expression is much higher, between 20-60 % (Jordt et al., 2004;Nagata et al., 2005;Bautista et al., 2005). The recombinant channel was shown to be activated by temperatures in the range of 12-24 °C (Story et al., 2003), however another study failed to replicate this finding and consequently the role of TRPA1 in cold transduction was brought into question (Jordt et al., 2004). The channel is strongly activated by a number of irritant compounds that elicit burning sensations, including allyl isothiocyanate (mustard oil), cinnamaldehyde, and allicin (garlic extract) (Jordt et al., 2004;Bandell et al., 2004;Macpherson et al., 2005;Bautista et al., 2005).

Postganglionic sympathetic neurons of the SCG are also excited by cold stimuli (Smith et al., 2004). While these neurons are menthol-insensitive, nested PCR showed that TRPA1 is expressed in the SCG, and it was therefore surmised that cold transduction in sympathetic neurons could be mediated via this channel. However this

technique is not quantitative and as such the exact contribution of TRPA1 to cold sensing in sympathetic neurons is unclear.

3.2. Aims

The aim of this study was to correlate functional cold sensitivity in acutely dissociated peripheral sensory and sympathetic neurons with quantitative ion channel expression, focussing on TRPM8 and TRPA1.

3.3. Methods

This section provides specific information on the experiments carried out in this study. For detailed protocols, please refer to Chapter 2.

3.3.1. Primary tissue culture

DRG and SCG from adult male C57/B6 mice were digested in papain followed by collagenase and dispase, and dissociated mechanically with fire-polished glass pipettes. Neurons were re-suspended in F-12 medium supplemented with 50 ng/ml rhNGF, unless otherwise stated. Neurons were plated onto poly-L-lysine and laminin-coated coverslips and maintained in culture for up to 24 hours. Acutely dissociated neurons were used for imaging experiments within 3-5 hours of plating.

3.3.2. Ratiometric calcium imaging

Neurons were loaded with Fura-2 and vitally stained with IB4-FITC and CTB-Alexa 594. Coverslips were positioned inside a custom-made chamber and solutions were applied to the cells via a gravity-driven application system.

To produce dose-response curves, DRG neurons were stimulated with TRP channel agonists at increasing concentrations. Stock solutions of L-menthol (2 M, Acros Organics, UK), allyl isothiocyanate (mustard oil) (1 M, Sigma, UK), cinnamaldehyde (2 M, Sigma) and camphor (1 M, Sigma) were made up in ethanol and diluted in ECF to the required working concentration on the day of the experiment. When preparing dilutions of camphor, it was discovered that the volume of stock solution added to the ECF had to be less than 1 % of the final volume to prevent precipitation of the camphor out of solution. Menthol, an agonist of TRPM8, was tested at concentrations of 10 μM, 30 μM, 100 μM, 300 μM and 3 mM. Each stimulus was applied for 10 seconds. Two TRPA1 agonists, mustard oil and cinnamaldehyde, were assessed.

Mustard oil was tested at concentrations of 3 μM, 10 μM, 30 μM, 100 μM, 300 μM and 1 mM, while cinnamaldehyde was applied to neurons at concentrations of 10 μM, 30 μM, 100 μM, 300 μM, 1 mM and 3 mM. In both cases, stimuli were applied to cells for 60 seconds. Camphor has been suggested to activate TRPV1 and inhibit TRPA1 (Xu et al., 2005). This compound was tested at concentrations of 1 mM, 3 mM, 10 mM, 30 mM and 100 mM, with each stimulus lasting 60 seconds. Neurons tested with menthol and mustard oil were additionally stimulated with 3 μM capsaicin, in order to functionally identify a subpopulation of nociceptive neurons.

In order to assess the functional contribution of TRP channels to cold sensitivity, acutely dissociated DRG and SCG neurons were stimulated with cold ECF (5 °C), 250 μM menthol (10 second application), 50 μM mustard oil or 100 μM cinnamaldehyde (60 second application), and 1 μM capsaicin (10 second application). Temperature was continuously monitored with a thermocouple positioned just outside the field of vision, opposite the stream of the inflow. In some experiments fast non-linear cold ramps were applied from room temperature. In other experiments the solutions were warmed to approximately 30 °C and a slow linear cold ramp was applied over a period of 100 seconds. Sensory neurons that had been maintained for 24 hours in the presence of 50 ng/ml NGF were analysed using the same imaging protocols, in order to assess changes in cold and TRP channel sensitivity over time in culture.

For calcium-free experiments, calcium was removed from the ECF and replaced with magnesium. In addition, the ECF was supplemented with 1 mM EDTA to ensure complete removal of extracellular calcium ions.

Ratiometric images were recorded at intervals of 0.3-0.5 seconds for the duration of the cold stimulus and 1-2 seconds thereafter, using the TillPhotonics system. One field of vision per coverslip was analysed and only vital neurons that responded to a concentrated (50 mM) potassium stimulus were included in the analysis.

3.3.3. Quantitative rt-PCR

Total RNA was extracted from dissociated DRG and SCG neurons and 10 ng were reverse transcribed into cDNA for use in real-time PCR. cDNA was probed for the expression of the housekeeping genes UCHL1 and GAPDH, and the cold-sensitive TRP channels TRPM8 and TRPA1, using SYBR green dye. All primers had been previously optimised and shown to give a linear correlation between cycle threshold and cDNA concentration in serial dilution experiments. Reaction products gave single peaks on melt curve analysis and single bands of expected size on a 2 % agarose gel. Relative quantification of rt-PCR products was performed, using either the amount of total starting RNA or the expression of housekeeping genes with the $\Delta\Delta$ method as a reference.

3.3.4. Statistics

Calcium imaging experiments were performed on four separate cultures over two experimental days, unless otherwise stated. Each culture usually consisted of several coverslips. The results from the coverslips of one culture were pooled and were used as one data point for subsequent analysis. For rt-PCR experiments, DRG and SCG from four animals each were processed separately for cDNA, and each PCR reaction was run in duplicate. All quantitative comparisons are presented as mean ± SEM. Student's unpaired *t*-test was used for all statistical analyses, with one exception: when comparing rate of onset of the cold response between functionally identified populations, the Mann-Whitney *U* test was used.

3.4. Results

3.4.1. Dose-dependent activation of sensory neurons by TRP channel agonists

Acutely dissociated DRG neurons, cultured without NGF, were assessed for sensitivity to increasing concentrations of the TRPM8 and TRPA1 channel agonists menthol, mustard oil and cinnamaldehyde, and the TRPV1 agonist camphor. From a total of 1101 neurons analysed for sensitivity to menthol, 89 (8 ± 1 %) were sensitive to 3 mM menthol, with an EC_{50} of 125 μM (n = 5) (Figure 3.1). Within the menthol-sensitive population, 44 ± 10 % also responded to 3 μM capsaicin.

1303 neurons were assessed for sensitivity to mustard oil at concentrations ranging between 3-100 μM (n = 6), and a further 676 neurons were tested with concentrations of 30 μM-1 mM (n = 2). 240/676 neurons (36 %) were activated by 1 mM mustard oil, of which 40 % were capsaicin-sensitive and 3 % responded to 300 μM menthol (Figure 3.2). The EC_{50} for mustard oil was 64 μM.

1126 neurons were assessed for sensitivity to concentrations of cinnamaldehyde ranging from 10 μM-1 mM (n = 5), and an additional 631 cells were analysed using concentrations between 100 μM-3 mM (n = 3). 219/631 neurons (41 ± 12 %) were activated by 3 mM cinnamaldehyde, with an EC_{50} of 240 μM (Figure 3.3).

It has previously been reported that 10 mM camphor can elicit currents in capsaicin-sensitive DRG neurons (Xu et al., 2005). However, out of 1098 neurons tested with increasing concentrations of camphor, only 27 (3 ± 1 %) were found to respond (n = 3). Activation of DRG neurons by camphor was not dose-dependent: from the 27 camphor-sensitive neurons, 23 responded at 3 mM but only 2 responded to the highest concentration of 100 mM.

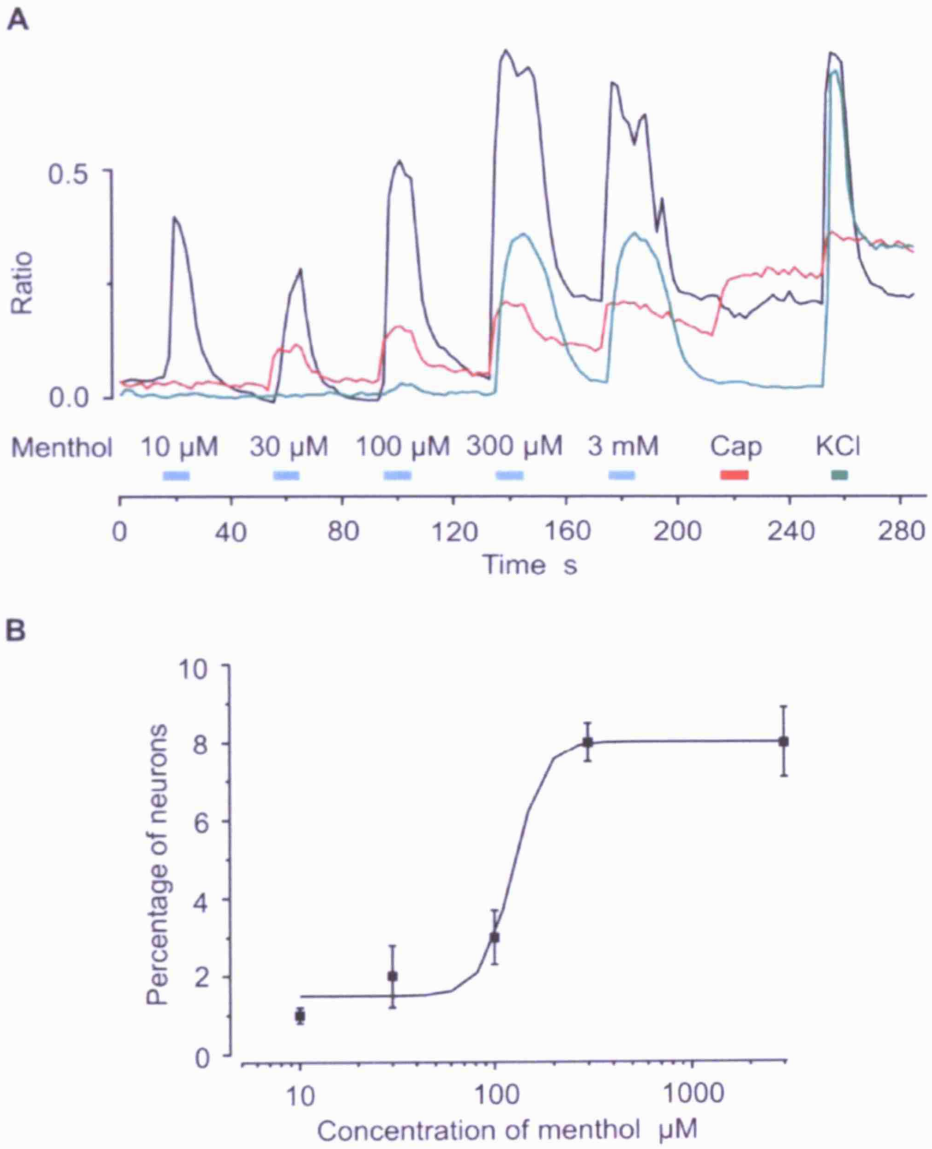

Figure 3.1. (A) Representative kinetic profiles of the responses of three menthol-sensitive DRG neurons. Two cells responded at low menthol concentrations (black and red), while one cell required higher concentrations of menthol to become activated (green). One cell was also capsaicin-sensitive (red). (B) Dose-response curve for menthol in acutely dissociated DRG neurons. $n_{animals} = 5$, $n_{cells} = 1101$. Data are presented as mean percentage of responding neurons ± SEM.

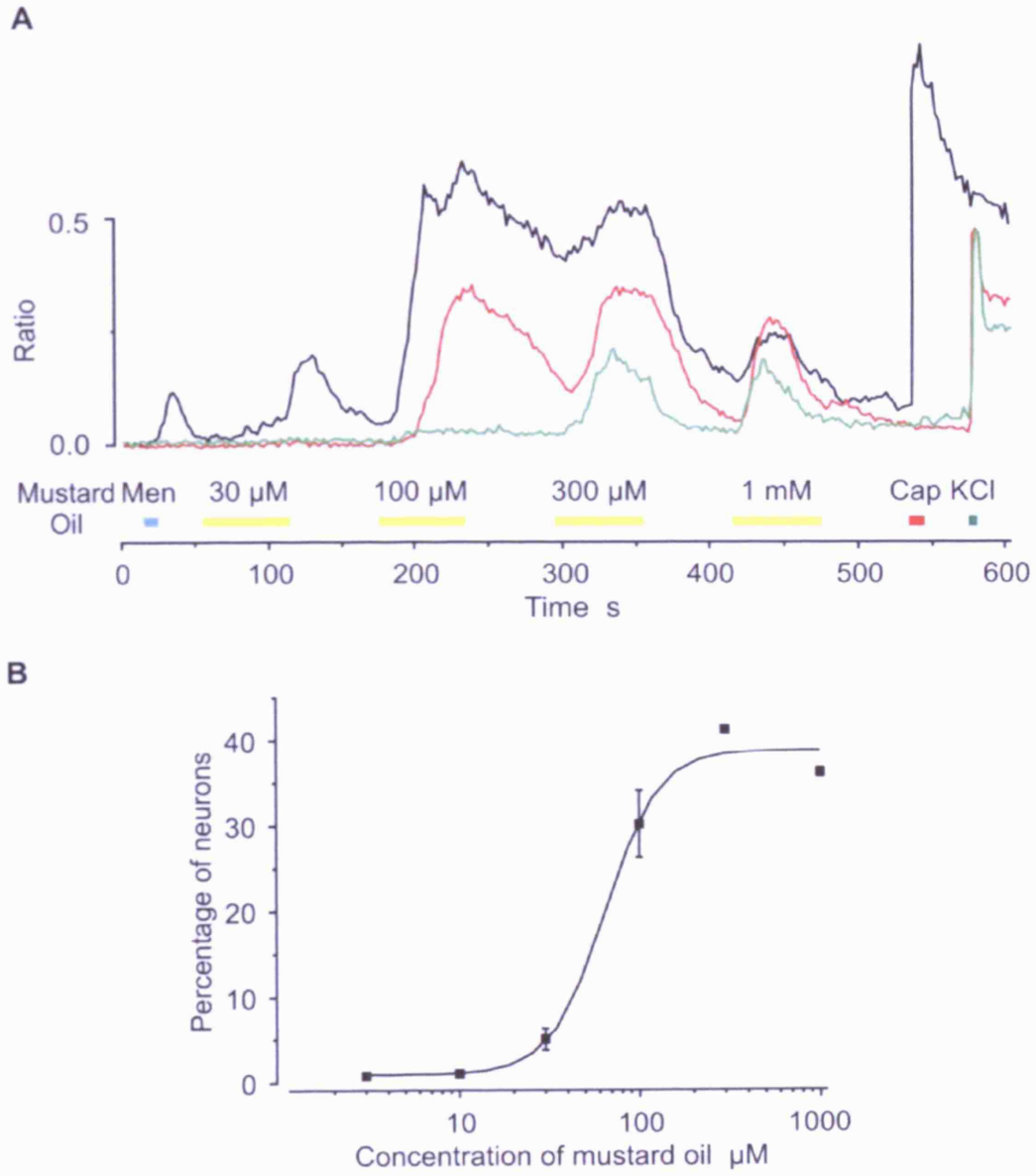

Figure 3.2. (A) Representative kinetic profiles of the responses of three mustard oil-sensitive DRG neurons. The three cells required different concentrations of mustard oil to elicit a response. One cell was also menthol- and capsaicin-sensitive (black). (B) Dose-response curve for mustard oil in acutely dissociated DRG neurons. $n_{animals}$ = 2-6, n_{cells} = 1979. Data are presented as mean percentage of responding neurons ± SEM.

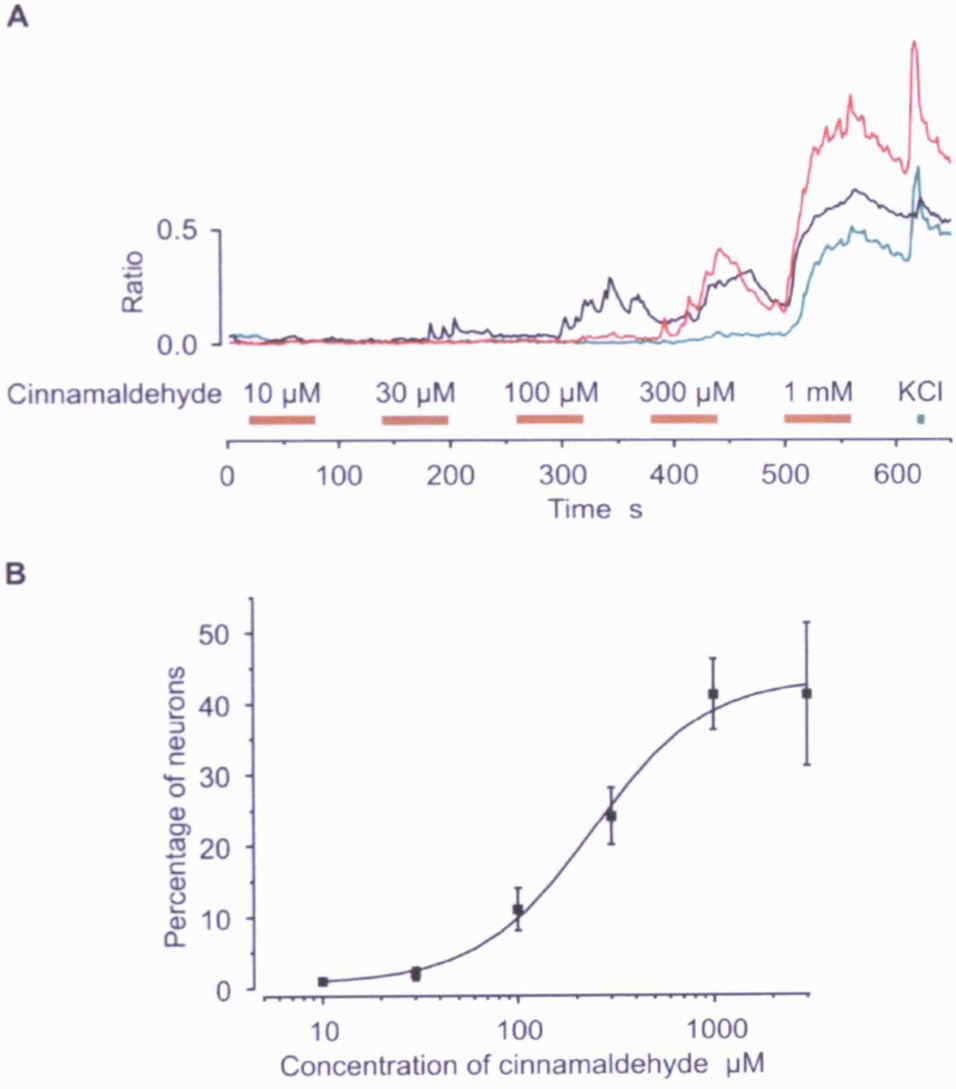

Figure 3.3. (A) Representative kinetic profiles of the responses of three cinnamaldehyde-sensitive DRG neurons. The three cells required different concentrations of cinnamaldehyde to elicit a response. (B) Dose-response curve for cinnamaldehyde in acutely dissociated DRG neurons. $n_{animals}$ = 3-5, n_{cells} = 1757. Data are presented as mean percentage of responding neurons ± SEM.

3.4.2. Many cold-sensitive sensory neurons respond to TRP channel agonists

A total of 2714 acutely dissociated DRG neurons were functionally analysed for responses to cold and TRP channel agonists. This comprised 1462 neurons tested with cold, menthol, mustard oil and capsaicin at room temperature (n = 4); 686 neurons stimulated with cold, menthol, mustard oil and capsaicin at 30 °C (n = 4); and 566 neurons tested with cold, menthol, cinnamaldehyde and capsaicin at 30 °C (n = 4). Of those cells, 500 (17 ± 2 %) were found to be cold-sensitive, 172 (6 ± 1 %) responded to menthol, and 974 (41 ± 4 %) were sensitive to capsaicin. 2148 neurons were tested for sensitivity to mustard oil, and 444 (18 ± 4 %) responded. A second TRPA1-specific agonist, cinnamaldehyde, excited 37/566 (7 ± 4 %) DRG neurons (Figures 3.4 and 3.5).

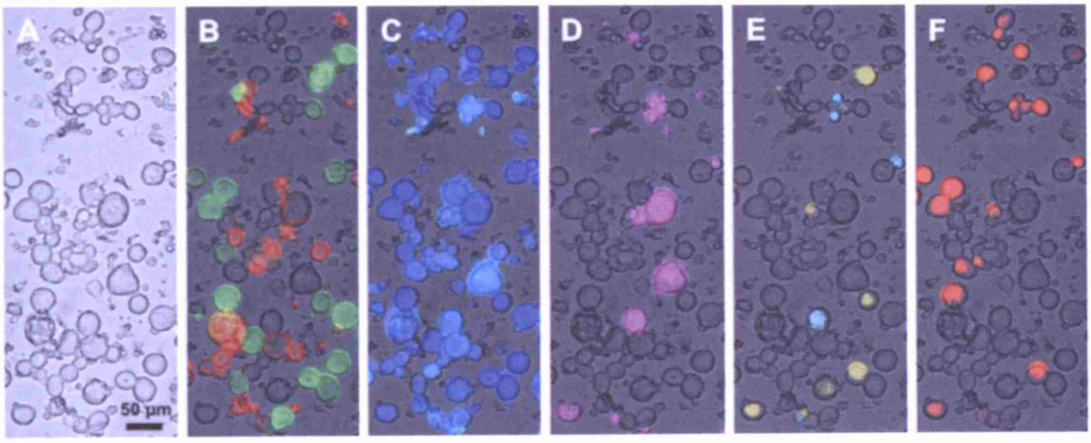

Figure 3.4. Pseudocolour fluorescence images of acutely dissociated DRG neurons. (A) Brightfield image. (B) Overlay of IB4 and CTB staining. (C) Background Fura fluorescence. (D-F) DRG neurons responding to cold and TRP channel agonists are colour-coded. (D) Cold-sensitive neurons. (E) Menthol-sensitive neurons are shown in blue, and mustard oil-sensitive neurons are shown in yellow. Note the lack of overlap between menthol and mustard oil sensitivity. (F) Capsaicin-sensitive neurons.

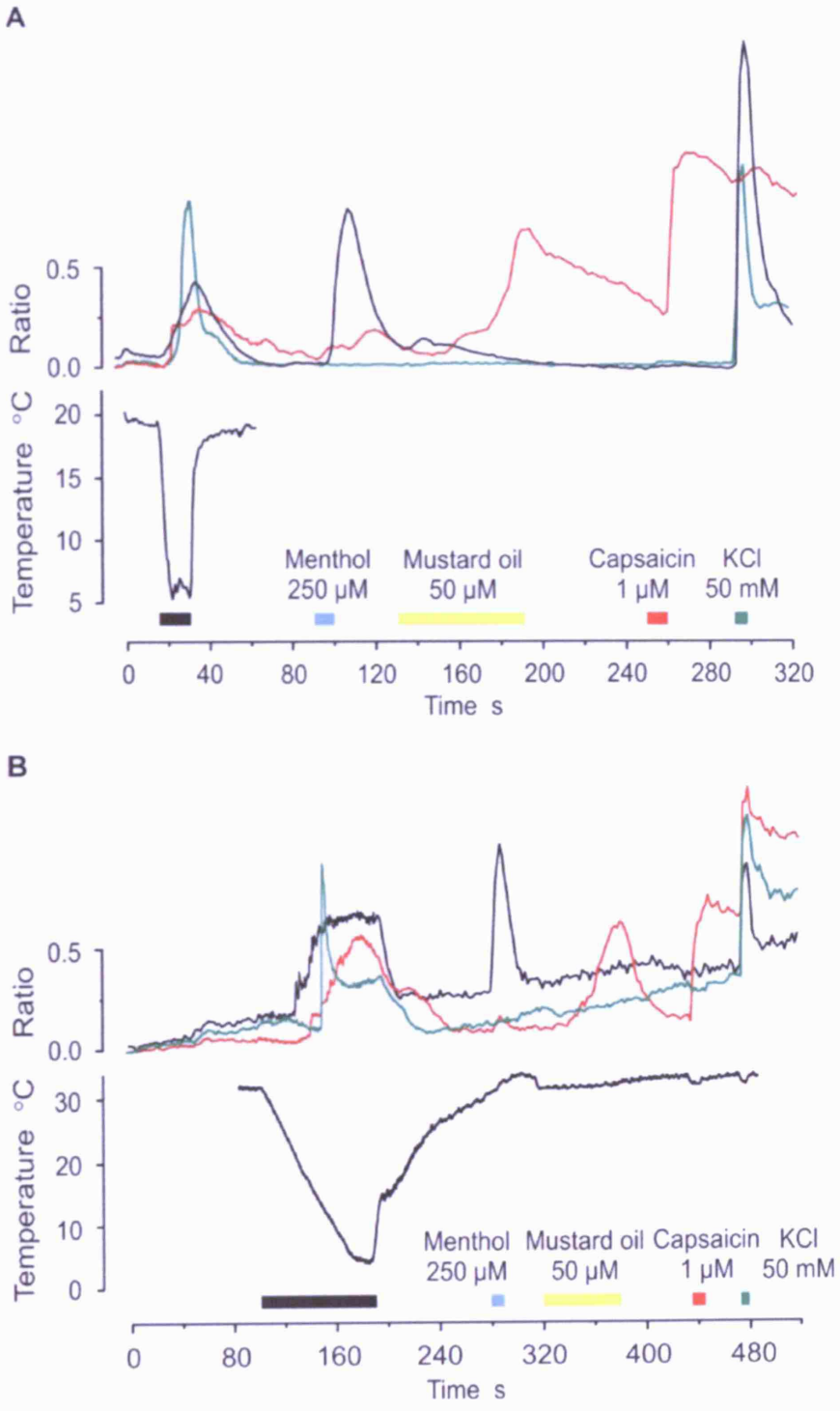

Figure 3.5. Representative kinetic profiles of the responses of three cold-sensitive DRG neurons recorded at room temperature (A) or from a baseline of 30 °C (B). In both cases, one cell also responded to menthol (black), one cell was mustard oil- and capsaicin-sensitive (red), and one cell did not respond to any of the TRP channel agonists (green). All cells responded to the non-specific depolarising stimulus KCl.

Increasing the bath temperature from 20 °C to 30 °C did not affect the number of neurons responding to cold (21 ± 4 % at room temperature versus 15 ± 2 % at 30 °C, $P > 0.1$), menthol (8 ± 1 % at room temperature versus 6 ± 1 % at 30 °C, $P > 0.1$) or mustard oil (20 ± 7 % at room temperature versus 15 ± 6 % at 30 °C, $P > 0.5$), but did lead to a significant increase in the number of capsaicin-sensitive cells (28 ± 9 % at room temperature versus 47 ± 2 % at 30 °C, $P < 0.05$).

The above data were obtained from neurons cultured in NGF. To ensure that the NGF was not affecting sensitivity to any of the stimuli tested, a further 895 DRG neurons were cultured without NGF and analysed for responses to cold and TRP channel agonists ($n = 4$). Of those neurons, 118 (14 ± 3 %) responded to a brief cold stimulus, 66 (9 ± 3 %) were menthol-sensitive, 176 (16 ± 7 %) responded to mustard oil, and 262 (28 ± 4 %) were sensitive to capsaicin. There were no differences in cold or TRP channel sensitivity between DRG neurons cultured with or without NGF (cold: $P > 0.3$; menthol: $P > 0.2$; mustard oil: $P > 0.8$; capsaicin: $P > 0.1$). The following data will include only those responses recorded in NGF-treated neurons, unless otherwise stated.

Cells that responded to menthol or capsaicin did so with a large increase in calcium levels immediately following stimulus application, while responses to mustard oil or cinnamaldehyde were more varied with regard to time of onset and magnitude. Many of the neurons that were sensitive to mustard oil showed a gradual increase and decrease in calcium levels, while others responded sharply or with multiple peaks in calcium concentrations.

In order to examine the distribution of cold sensitivity among sensory neurons, two cell-specific markers, IB4 and CTB, were used to label non-peptidergic C-fibres and presumptive myelinated A-fibres, respectively. Within the population at large, 1094/2714 (39 ± 2 %) neurons labelled with IB4, while 592 (22 ± 2 %) were CTB-positive. Of the cold-sensitive cells, 113/500 (18 ± 3 %) neurons stained for IB4 and 102 (22 ± 3 %) labelled with CTB. The remainder of the cells (63 ± 3 %) did not stain for either marker (Figure 3.6).

The proportion of neurons staining for IB4 and CTB was unaltered by the presence of NGF. In neurons cultured without NGF, 332/895 (36 ± 3 %) neurons were IB4-positive ($P > 0.3$), while 214 (23 ± 2 %) stained for CTB ($P > 0.8$).

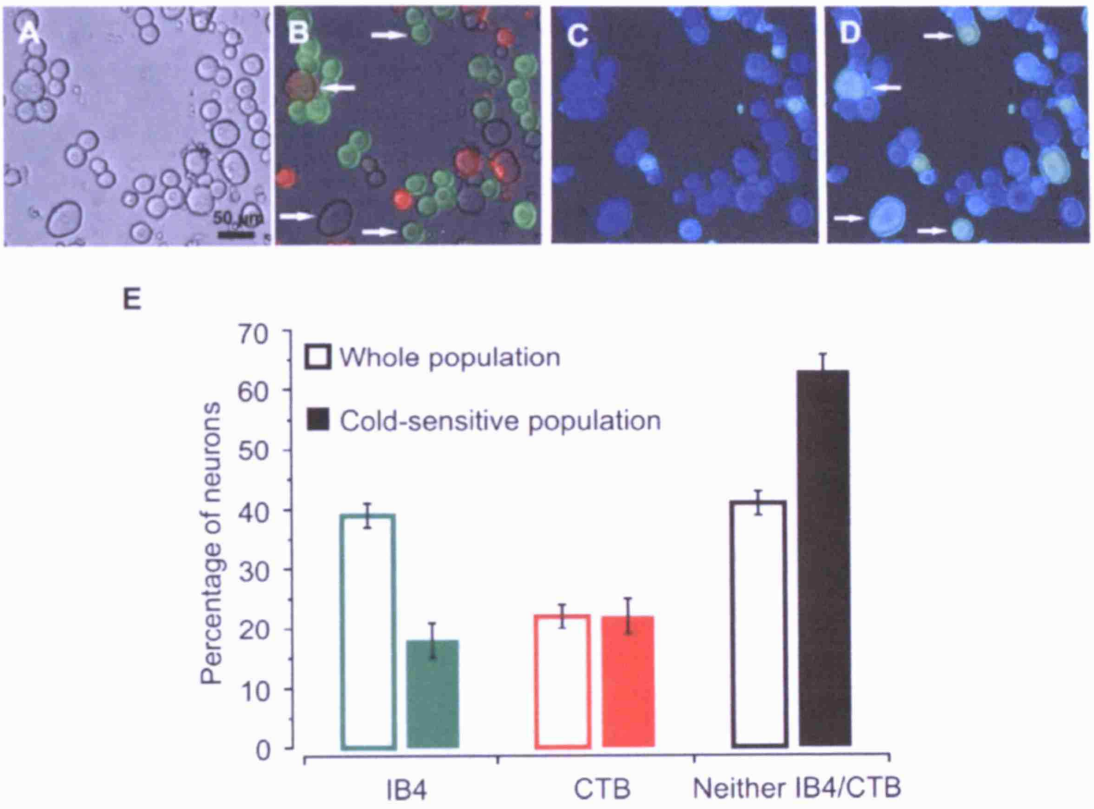

Figure 3.6. Fura fluorescence images of acutely dissociated DRG neurons stained with IB4 and CTB responding to a brief cold stimulus. (A) Brightfield image. (B) Overlay of IB4 and CTB staining. (C) Background Fura fluorescence. (D) DRG neurons responding to cold with an increase in fluorescence, indicative of an increase in intracellular calcium concentration. (E) Cold-sensitive DRG neurons stained for both IB4 and CTB. Whole population: $n_{animals}$ = 12, n_{cells} = 2714; cold-sensitive population: $n_{animals}$ = 12, n_{cells} = 500. Data are presented as mean percentage of labelled neurons ± SEM.

Within the cold-sensitive population of sensory neurons, 150/500 (35 ± 3 %) responded to menthol and 209 (50 ± 5 %) were sensitive to capsaicin. From 415 neurons tested for sensitivity to mustard oil, 85 (18 ± 3 %) responded. Only 5 ± 1 % of cold-sensitive cells responded to both menthol and mustard oil. Interestingly, 27 ± 4 % of the cold-responsive cells did not respond to any of the TRP channel agonists used for this study, while 54 ± 4 % were insensitive to menthol and mustard oil (Figure 3.7).

As observed in the population at large, the percentage of cold-sensitive neurons responding to menthol or mustard oil was not altered when the temperature of the solution was increased from 20 °C to 30 °C (menthol-sensitive neurons: 33 ± 9 % at room temperature versus 37 ± 2 % at 30 °C, $P > 0.5$; mustard oil-sensitive neurons: 20 ± 6 % at room temperature versus 16 ± 3 % at 30 °C, $P > 0.6$). However, the capsaicin-sensitive population was significantly larger at warmer temperatures (37 ± 13 % at room temperature versus 57 ± 2 % at 30 °C, $P < 0.05$).

The presence of NGF also had no effect on the sensitivity of cold-responsive neurons to TRP channel agonists. 50/118 (45 ± 14 %) neurons cultured without NGF were sensitive to menthol ($P > 0.3$), 27 (17 ± 6 %) responded to mustard oil ($P > 0.8$), and 48 (43 ± 3 %) were capsaicin-sensitive ($P > 0.4$).

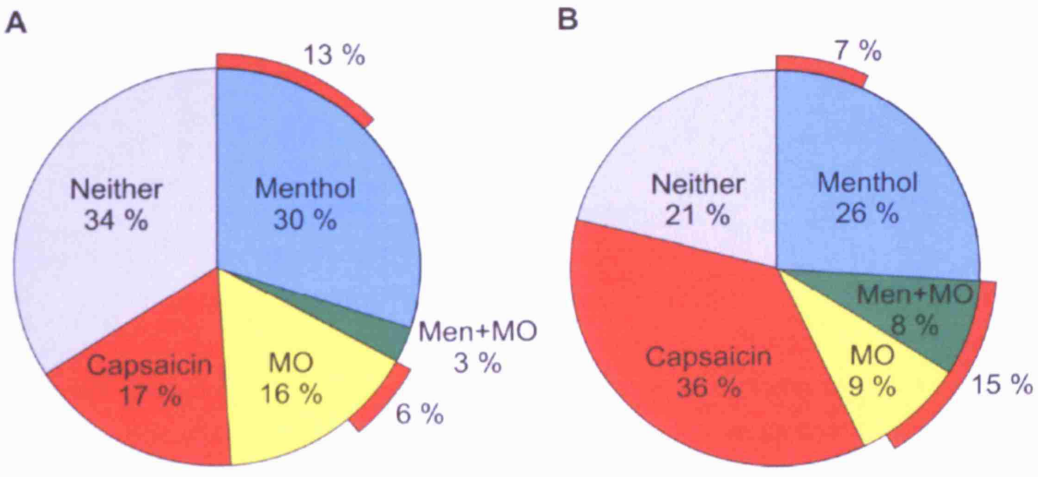

Figure 3.7. Representation of the proportion of cold-sensitive DRG neurons responding to TRP channel agonists. Recordings were made at room temperature (A) or at 30 °C (B). Room temperature: $n_{animals} = 4$, $n_{cells} = 319$; 30 °C: $n_{animals} = 4$, $n_{cells} = 95$. Data are presented as mean percentage of responding neurons.

Cold-sensitive neurons were characterised into two distinct populations according to the profile of the calcium response. One population of cells, defined as fast onset neurons, reached a peak calcium concentration very quickly after activation. In some cells the response plateaued off before calcium levels slowly decreased back to baseline, while in others the response dropped back very quickly to baseline levels. Cells with a slow onset response demonstrated a gradual increase and decrease in calcium concentration over the period of stimulus application (Figure 3.12). The rate of onset was defined as the change in the Fura fluorescence ratio (ΔF) over time. A histogram of response profiles demonstrated a bimodal distribution, with slowly responding neurons defined as having a rate of onset $\leq$ 0.055 ΔF/500 ms (n = 255) while fast responders had a rate of onset > 0.055 ΔF/500 ms (n = 94) (Figure 3.8). There was no difference in menthol sensitivity (25 ± 9 % versus 32 ± 10 %, P > 0.6), mustard oil sensitivity (49 ± 18 % versus 15 ± 6 %, P > 0.1) or capsaicin sensitivity (29 ± 18 % versus 37 ± 11 %, P > 0.7), or in mean temperature threshold (12.3 ± 0.5 °C versus 11.8 ± 0.3 °C, P > 0.4) between fast and slow responders, respectively.

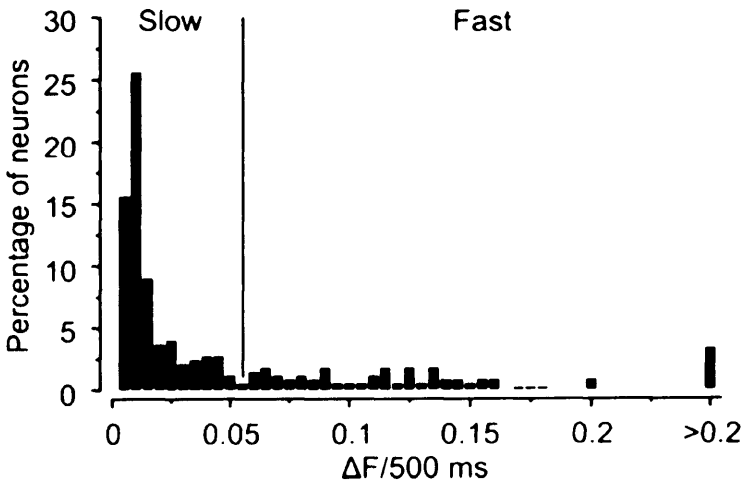

Figure 3.8. Distribution of acutely dissociated cold-sensitive DRG neurons as a function of the rate of onset of the calcium response. The histogram shows a bimodal distribution with a cut-off between fast and slow responders set at 0.055 ΔF/500 ms. n = 319.

Sensory neurons were assessed for functional cold sensitivity with cold ramps starting from 20.3 ± 1.2 °C (STD) or 31.4 ± 1.2 °C (STD). When analysed in terms of activation threshold, increasing the baseline temperature did not alter the distribution of the cold-sensitive population, although responses were shifted to significantly warmer temperatures (Figure 3.10). For the cold-sensitive population as a whole, the mean temperature of activation was 12 ± 0.2 °C when recording from room temperature (n = 319) and 16.9 ± 0.4 °C when recording from warm temperatures (n = 181, $P < 0.001$). Activation thresholds for menthol- and mustard oil-sensitive neurons were likewise altered. For menthol-sensitive cells the threshold was shifted from 14.9 ± 0.4 °C at room temperature (n = 86) to 20.8 ± 0.6 °C at warm temperatures (n = 64, $P < 0.001$), while mustard oil-sensitive neurons responded at 12.5 ± 0.5 °C (n = 68) or 15.5 ± 1 °C (n = 17, $P < 0.001$). Menthol-sensitive cells were activated at significantly warmer temperatures compared to mustard oil-sensitive cells at room temperature ($P < 0.001$) and at 30 °C ($P < 0.001$) (Figure 3.9).

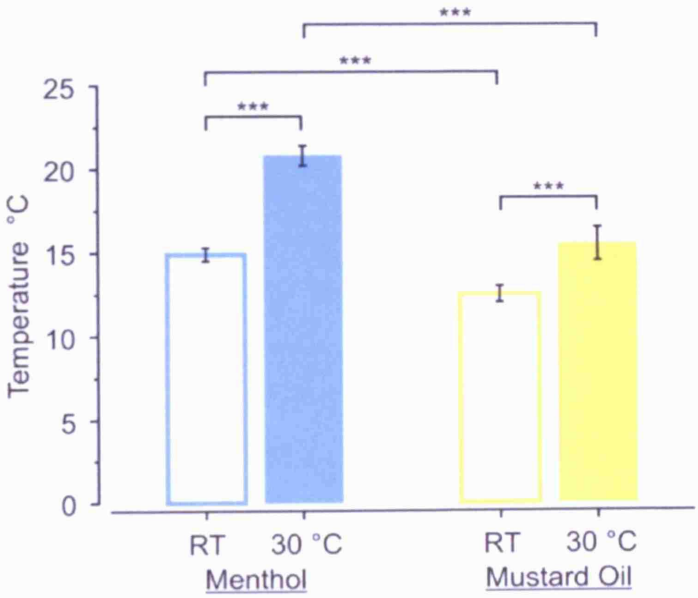

Figure 3.9. Activation thresholds of menthol- and mustard oil-sensitive DRG neurons at room temperature and at 30 °C. Menthol-sensitive neurons had a warmer activation threshold than mustard oil-sensitive neurons. Menthol-sensitive population: n = 86 (room temperature), n = 64 (30 °C); mustard oil-sensitive population: n = 68 (room temperature), n = 17 (30 °C). Data are presented as mean threshold ± SEM. *** $P < 0.001$ (Student's unpaired t-test).

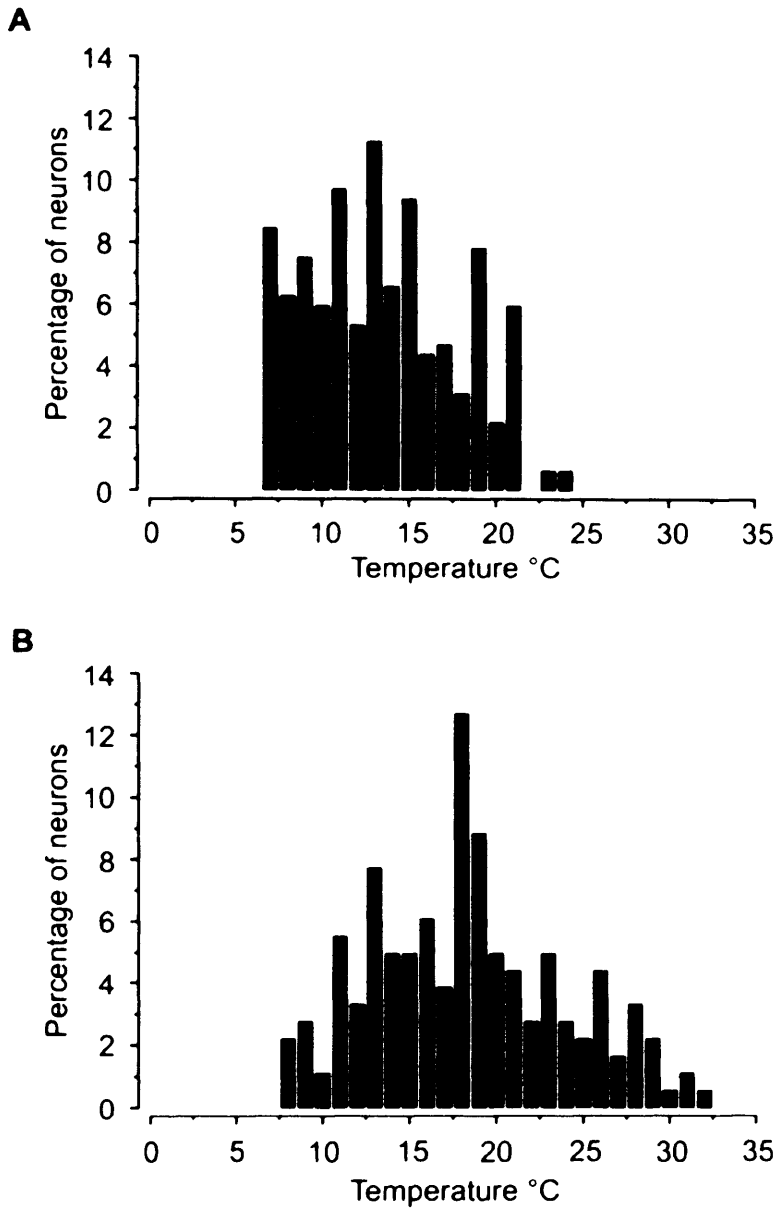

Figure 3.10. Histogram depicting the distribution of cold-sensitive DRG neurons as a function of activation threshold. Recordings were made at room temperature (A) or from a baseline of 30 °C (B). Room temperature: n = 319; 30 °C: n = 181.

3.4.3. TRPM8 mediates innocuous and noxious cold transduction

Within the menthol-sensitive population, 150/172 (94 ± 3 %) neurons responded to cold. In contrast, only 85/444 (22 ± 4 %) mustard oil-sensitive neurons were cold-sensitive. Although mustard oil is a potent agonist of TRPA1, there is some evidence to suggest that it may activate additional receptors and therefore cinnamaldehyde was

also tested, which has been suggested to be a more specific TRPA1 agonist (Bandell et al., 2004). From 86 cold-sensitive neurons 7 (9 ± 3 %) responded to cinnamaldehyde, while 7/37 (21 ± 9 %) cinnamaldehyde-responsive neurons were sensitive to cold. There were no significant differences between the mustard oil-sensitive and cinnamaldehyde-sensitive populations in terms of cold sensitivity. Thus, neither the percentage of cold-sensitive neurons responding to cinnamaldehyde is different from the population at large (9 ± 3 % versus 7 ± 4 %, $P > 0.6$) nor is the cold sensitivity in cinnamaldehyde-responsive neurons higher than the general population (21 ± 9 % versus 17 ± 2 %, $P > 0.5$). These data suggest that TRPA1 is unlikely to be an important cold receptor in sensory neurons.

350/500 (65 ± 3 %) cold-sensitive sensory neurons were menthol-insensitive. Of those neurons, 104 (25 ± 4 %) were IB4-positive and 78 (23 ± 3 %) stained for CTB. While the number of CTB-positive neurons was similar in the menthol-sensitive population (24/150 neurons, 19 ± 4 %, $P > 0.4$), the number of IB4-stained cells was significantly lower (9/150 neurons, 6 ± 2 %, $P < 0.001$).

Cell area was measured in 1036 acutely dissociated DRG neurons. The DRG population as a whole showed a normal distribution, with a mean cell area of 500 ± 7 μm^2, while the cold-sensitive population had a mean cell area of 479 ± 19 μm^2 (n = 191). Cold-sensitive neurons which also responded to menthol had a cell area of 370 ± 26 μm^2 (n = 60), which was significantly smaller than the cold-sensitive, menthol-insensitive population (528 ± 23 μm^2, n = 131, $P < 0.001$) (Figure 3.11).

The cold responses of menthol-sensitive and -insensitive neurons differed. Menthol-sensitive neurons were found to have a significantly faster rate of onset than menthol-insensitive cells (menthol-sensitive rate of onset 0.033 ΔF/500 ms [median; upper and lower quartiles 0.083 and 0.013, respectively, n = 86], versus menthol-insensitive rate of onset 0.01 ΔF/500 ms [upper and lower quartiles 0.062 and 0.006, respectively, n = 233], $P < 0.001$, Mann-Whitney U test) (Figure 3.12). In addition, the activation threshold of menthol-sensitive neurons was significantly warmer than the threshold of menthol-insensitive cells. At room temperature, menthol-sensitive neurons had a threshold of 14.9 ± 0.4 °C (n = 86), while menthol-insensitive cells were activated at 10.9 ± 0.3 °C (n = 233, $P < 0.001$). In recordings made at 30 °C, menthol-sensitive neurons responded at 20.8 ± 0.6 °C (n = 64) and menthol-insensitive neurons responded at 14.7 ± 0.4 °C (n = 117, $P < 0.001$) (Figure 3.13).

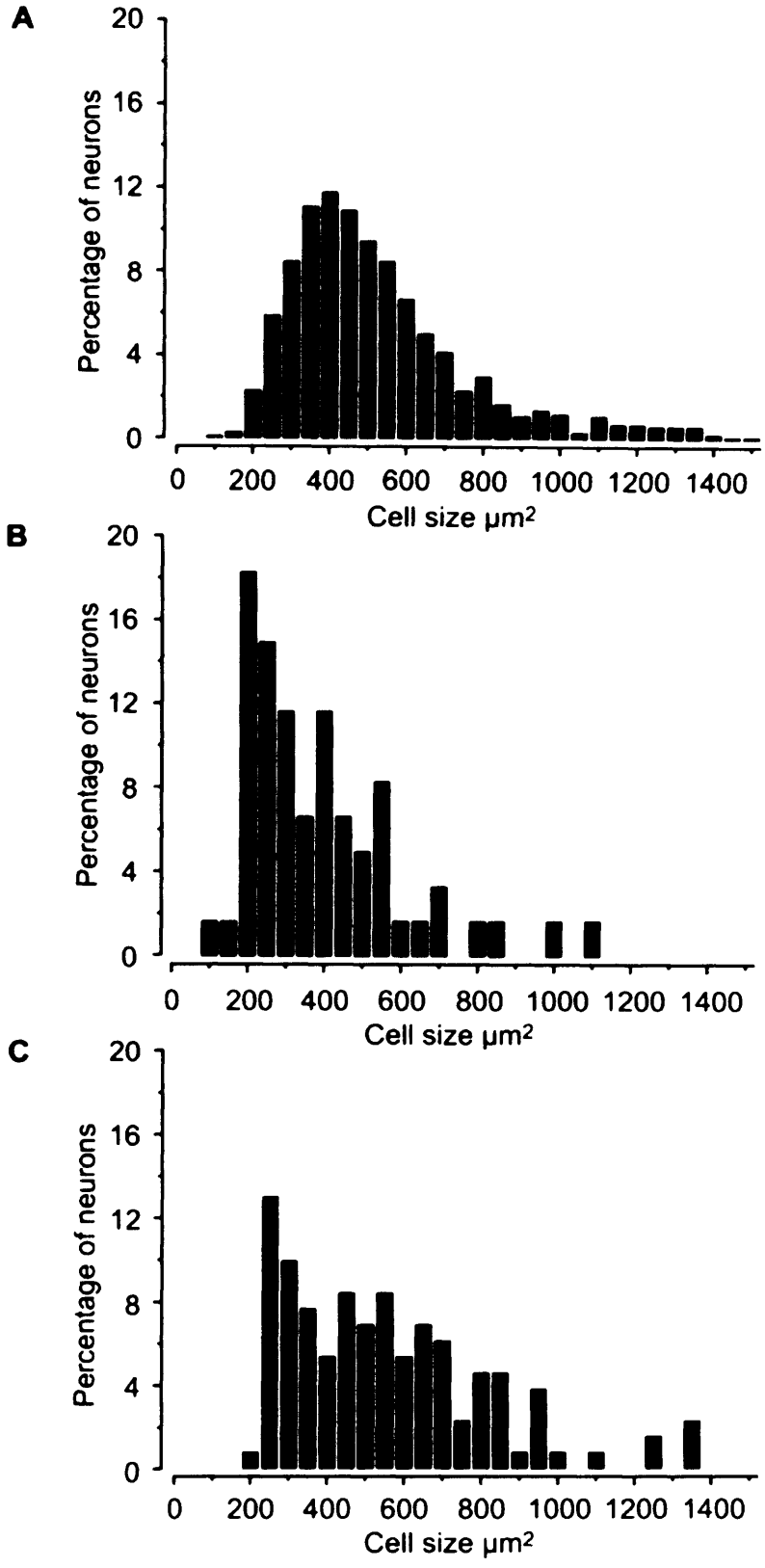

Figure 3.11. (A) Cell size distribution of acutely dissociated DRG neurons. n = 1036. (B) Cell size distribution of cold- and menthol-sensitive DRG neurons. n = 60. (C) Cell size distribution of cold-sensitive, menthol-insensitive DRG neurons. n = 131.

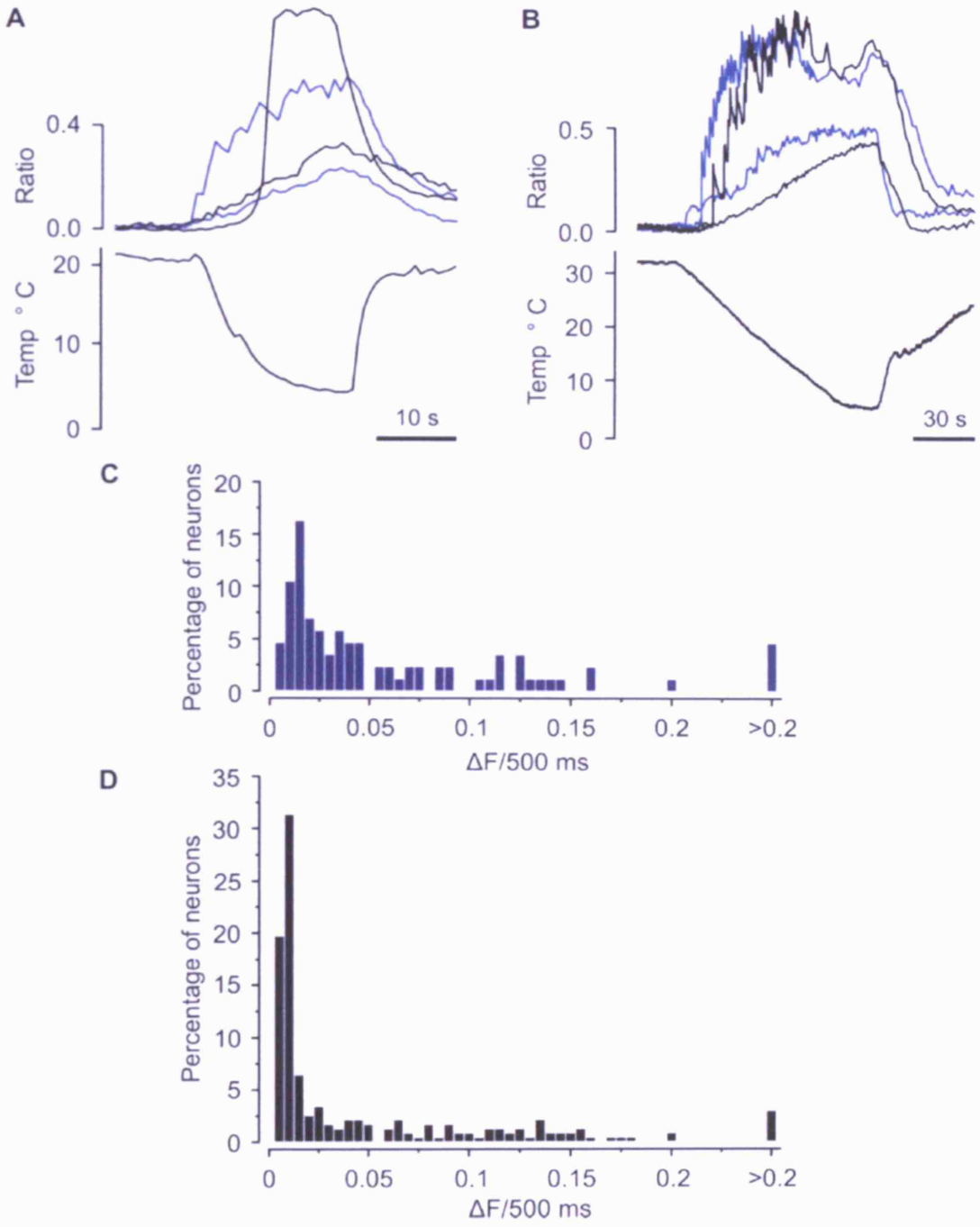

Figure 3.12. (A-B) Representative kinetic profiles of the cold response of two menthol sensitive (blue) and two menthol-insensitive (black) DRG neurons. Two cells have a fast onset and two cells have a slow onset response. Menthol-sensitive and menthol-insensitive neurons showed both fast and slow kinetics. (A) Example of a recording made at room temperature. (B) Example of a recording made at 30 °C. (C-D) Histograms depicting the distribution of menthol sensitive (C) and menthol-insensitive (D) neurons as a function of the rate of onset of the calcium response. Menthol-sensitive neurons: n = 86; menthol insensitive neurons: n = 233.

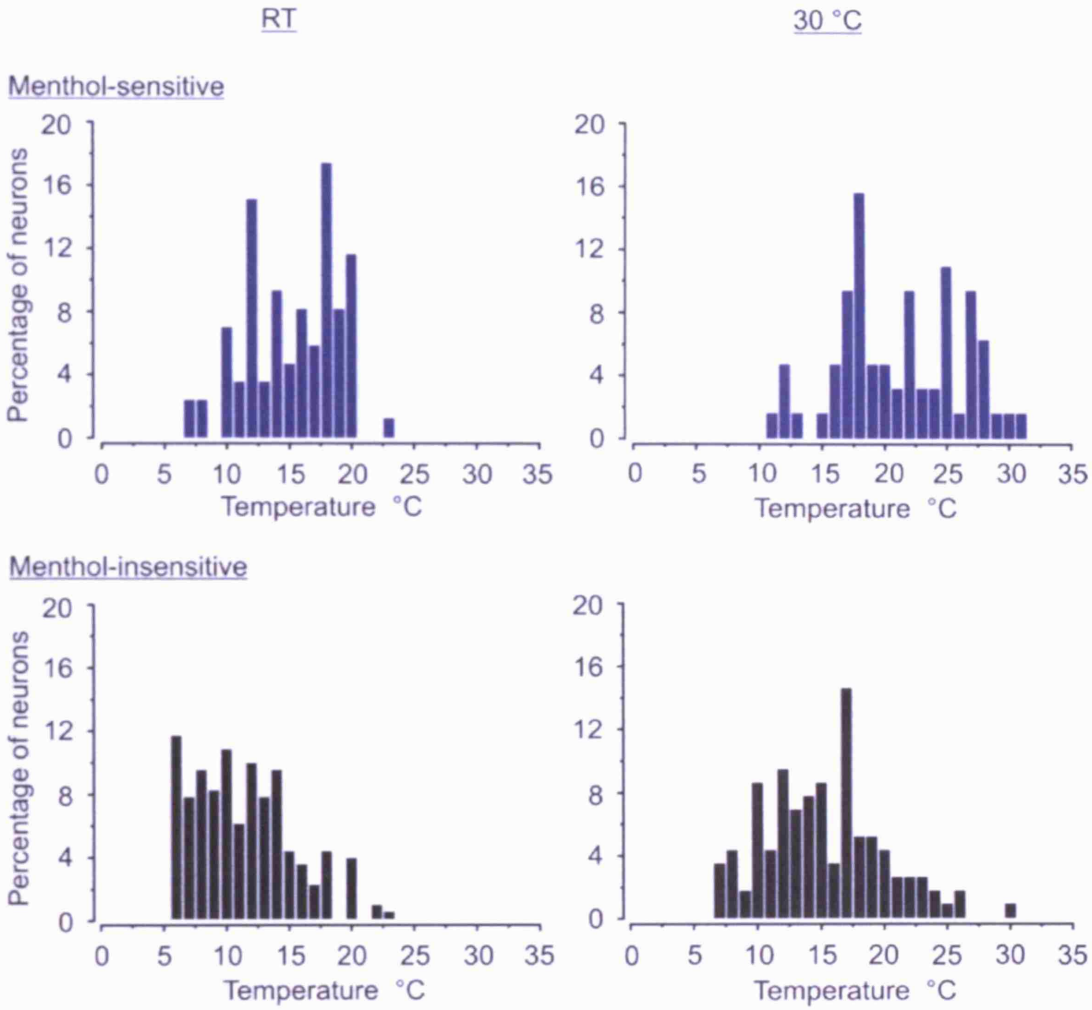

Figure 3.13. Histograms depicting the distribution of menthol-sensitive (blue) and menthol-insensitive (black) DRG neurons as a function of activation threshold. Recordings were made at room temperature (left) or at 30 °C (right). Menthol-sensitive neurons: n = 86 (room temperature), n = 64 (30 °C); menthol-insensitive neurons: n = 233 (room temperature), n = 117 (30 °C).

Psychophysical experiments in humans have shown that topical application of high concentrations of menthol can elicit sensations of pain (Wasner et al., 2004;Namer et al., 2005). From these studies it was unclear whether the pain resulted from a non-specific activation of nociceptors by saturating concentrations of menthol, or whether differential expression of TRPM8 meant that higher concentrations of menthol were required to elicit a response in nociceptive afferents.

In dose response experiments, 89/1101 (8 ± 1 %) neurons were sensitive to 3 mM menthol, of which 85 had already responded at a 10-fold lower concentration (n = 5). This would suggest that high concentrations of menthol do not recruit neurons non-specifically. 46/89 (44 ± 10 %) menthol-sensitive cells responded to 3 μM capsaicin, while within the capsaicin-sensitive population 51/460 (11 ± 4 %) neurons were sensitive to menthol. There was no significant difference in the menthol dose-response curve of capsaicin-sensitive versus capsaicin-insensitive cells, ruling out the possibility that subpopulations of sensory neurons have a differential sensitivity to menthol (Figure 3.14). The results from these experiments suggest that TRPM8 is expressed on nociceptors and may be involved in the transduction of noxious as well as innocuous cold stimuli.

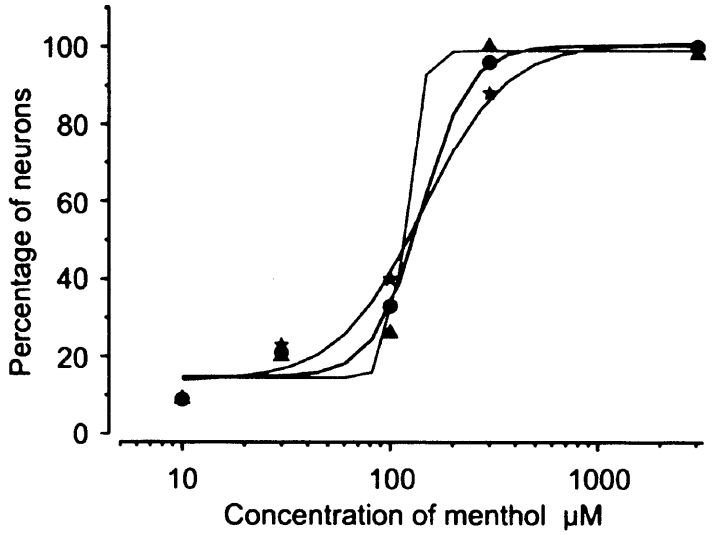

Figure 3.14. Dose-response curve for menthol sensitivity in capsaicin-sensitive (red) and capsaicin-insensitive (green) populations of acutely dissociated DRG neurons. The entire menthol-sensitive population is represented in blue. $n_{animals}$ = 5, n_{cells} = 1101. The total number of responsive neurons is presented as a percentage.

3.4.4. Cold and menthol sensitivity is up-regulated in the IB4-positive population at 24 hours

Sensory neurons cultured for 24 hours in the presence of 50 ng/ml NGF were assessed for sensitivity to cold and TRP channel agonists at room temperature ($n_{animals}$ = 4, n_{cells} = 636) or at 30 °C ($n_{animals}$ = 6, n_{cells} = 1132). From a total of 1768 neurons, 208 were cold-sensitive, 122 responded to menthol, and 755 were sensitive to capsaicin. Of 1132 neurons tested for sensitivity to mustard oil, 215 responded. The percentage of responsive neurons did not differ from acutely cultured cells (cold-sensitive neurons: 17 ± 2 % in acute cultures versus 12 ± 2 % in 24 hour cultures, $P > 0.05$; menthol-sensitive neurons: 6 ± 1 % in acute cultures versus 8 ± 2 % in 24 hour cultures, $P > 0.6$; mustard oil-sensitive neurons: 18 ± 4 % in acute cultures versus 19 ± 5 % in 24 hour cultures, $P > 0.7$; capsaicin-sensitive neurons: 41 ± 4 % in acute cultures versus 43 ± 3 % in 24 hour cultures, $P > 0.7$).

The number of neurons staining for IB4 and CTB was also unaltered in the 24 hour cultures. 729/1768 (41 ± 1 %) neurons labelled with IB4 (versus 39 ± 2 % in acute cultures, $P > 0.2$), and 352 (20 ± 1 %) neurons were CTB-positive (versus 22 ± 2 % in acute cultures, $P > 0.2$).

Within the cold-sensitive population, 67 (30 ± 5 %) neurons responded to menthol, and 112 (54 ± 5 %) were sensitive to capsaicin. 35/100 (32 ± 8 %) neurons were mustard oil-sensitive. The proportion of cold-sensitive neurons responding to TRP channel agonists was unchanged over 24 hours (menthol: $P > 0.3$; mustard oil: $P > 0.08$; capsaicin: $P > 0.6$).

There was however a significant up-regulation in menthol sensitivity within the IB4-positive population. In accordance with previous observations that TRPM8 is not co-expressed with IB4 (Peier et al., 2002a), only 1 ± 0.4 % of IB4-positive cells in acute cultures were menthol-sensitive (Figure 3.16). This number was increased to 10 ± 4 % over 24 hours ($P < 0.05$) (Figure 3.17). The observed up-regulation of menthol sensitivity in IB4-positive neurons was accompanied by a decrease in menthol responsiveness within the IB4-negative population, from 10 ± 1 % in acute cultures to 5 ± 2 % at 24 hours ($P < 0.05$). At the same time, the proportion of menthol-sensitive neurons staining for IB4 also increased. 7 ± 3 % of acutely dissociated neurons were IB4-positive, compared to 41 ± 10 % of neurons at 24 hours ($P < 0.01$).

The up-regulation of menthol sensitivity in IB4-positive neurons was correlated with an increase in cold sensitivity. 8 ± 2 % of IB4-positive neurons in acute cultures were cold-sensitive, compared to 14 ± 2 % in overnight cultures ($P < 0.05$). Similarly, cold sensitivity was decreased in the IB4-negative population, falling from 23 ± 3 % to 11 ± 3 % over 24 hours ($P < 0.01$). As observed in the menthol-sensitive population, the proportion of cold-sensitive cells staining for IB4 was also increased: 18 ± 3 % of acutely dissociated cold-sensitive neurons were IB4-positive, compared to 49 ± 7 % of cells cultured overnight ($P < 0.001$).

The magnitude of the menthol response was measured in IB4-positive and IB4-negative neurons at 24 hours, and was found to be significantly different within the two populations. The magnitude was defined as the change in Fura fluorescence ratio (ΔF) from baseline to the peak of the stimulus-induced calcium response. IB4-positive neurons had a ΔF of 0.278 ± 0.017 ($n = 53$), while IB4-negative neurons had a ΔF of 0.532 ± 0.05 ($n = 33$, $P < 0.001$) (Figure 3.15). Cold responses had a similar magnitude in both the IB4-positive and the IB4-negative populations (0.259 ± 0.02, $n = 53$, versus 0.282 ± 0.022, $n = 47$, $P > 0.4$).

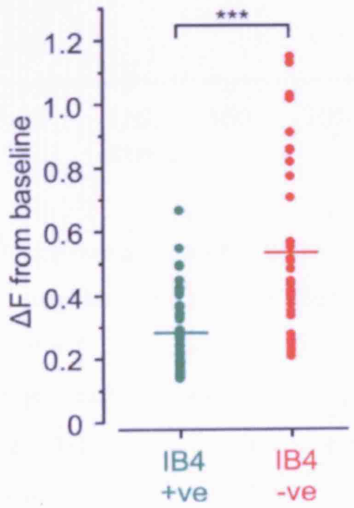

Figure 3.15. Scatter plot showing the magnitude of the menthol response in IB4-positive versus IB4-negative DRG neurons cultured for 24 hours in NGF. Each data point represents one cell, and the mean value is indicated by the horizontal bar. IB4-positive neurons: $n = 53$; IB4-negative neurons: $n = 33$. *** $P < 0.001$ (Student's unpaired *t*-test).

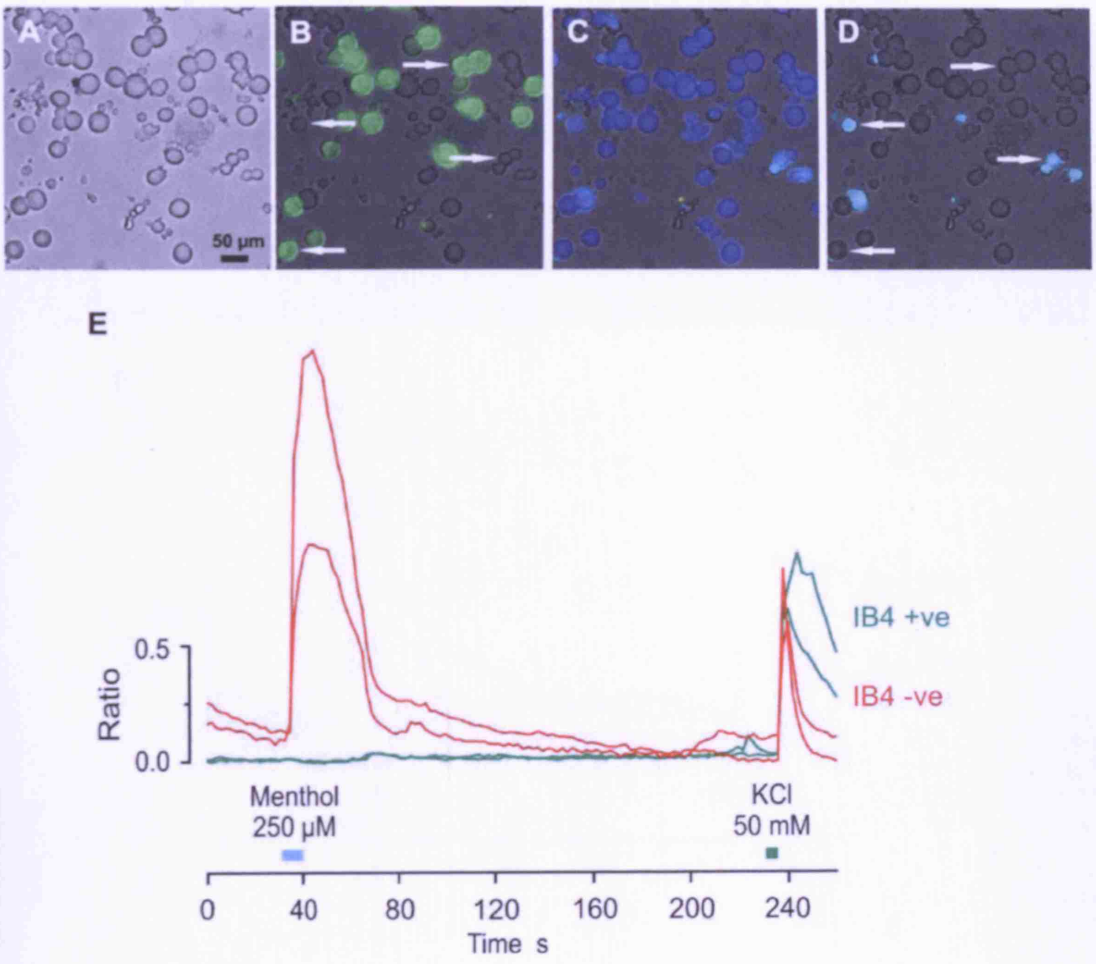

Figure 3.16. Pseudocolour fluorescence images of acutely dissociated DRG neurons responding to menthol. (A) Brightfield image. (B) IB4 staining. (C) Background Fura fluorescence. (D) DRG neurons responding to menthol. (E) Representative kinetic profiles of the responses of two IB4-negative, menthol-sensitive DRG neurons (red) and two IB4-positive, menthol-insensitive neurons (green). The kinetic profiles correspond to the cells marked with an arrow in images (B) and (D).

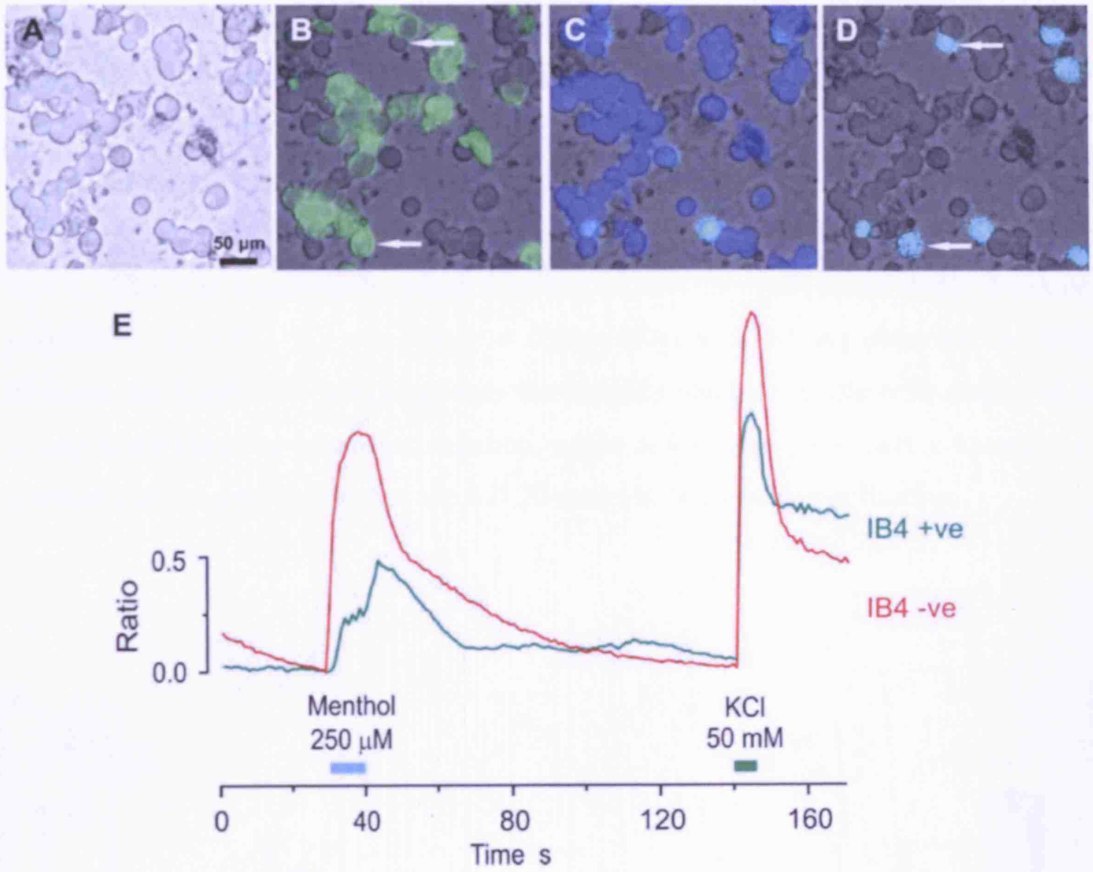

Figure 3.17. Pseudocolour fluorescence images of dissociated DRG neurons cultured for 24 hours responding to menthol. (A) Brightfield image. (B) IB4 staining. (C) Background Fura fluorescence. (D) DRG neurons responding to menthol. (E) Representative kinetic profiles of the responses of two menthol-sensitive neurons, one of which was IB4-negative (red) and one of which was IB4 positive (green). The kinetic profiles correspond to the cells marked with an arrow in images (B) and (D).

3.4.5. Cold-sensitive sympathetic neurons do not respond to TRP channel agonists

Acutely dissociated SCG neurons were analysed for functional sensitivity to cold and TRP channel agonists. From a total of 369 cells, 139 (39 ± 9 %) responded to a cold stimulus (n = 4). In contrast to DRG neurons, very few cells responded to TRP channel agonists. Only 1 cell out of the 369 assayed responded to menthol (0.3 ± 0.3 %), 7 were mustard oil-sensitive (2 ± 1 %), and 8 (2 ± 0.5 %) were sensitive to capsaicin. Within the cold-sensitive population, 1 neuron responded to menthol and 3 were sensitive to mustard oil stimulation (Figure 3.19).

SCG neurons were stimulated with a cold ramp starting from a baseline temperature of 20 ± 1.2 °C (STD). The average threshold for activation of SCG cells was 10.2 ± 0.3 °C. This was significantly colder than that of DRG neurons tested under the same conditions (12 ± 0.2 °C, n = 319, P < 0.001) (Figure 3.18). As observed in DRG neurons, the kinetics of cold responses were highly variable. Some cells displayed a strong sharp response to cold stimulation, while others showed a gradual increase in intracellular calcium levels over the full 20 seconds of stimulus application.

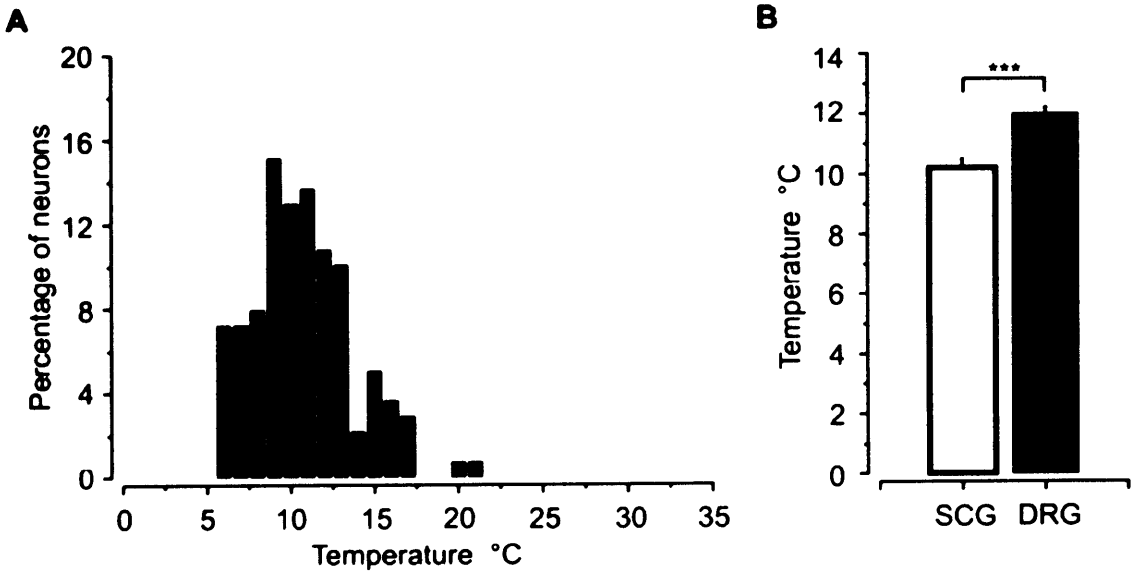

Figure 3.18. (A) Histogram depicting the distribution of cold-sensitive SCG neurons as a function of activation threshold. (B) DRG neurons had a warmer activation threshold than SCG neurons. SCG neurons: $n_{animals}$ = 4, n_{cells} = 139; DRG neurons: $n_{animals}$ = 4, n_{cells} = 319. Data are presented as mean threshold ± SEM. *** P < 0.001 (Student's unpaired t-test).

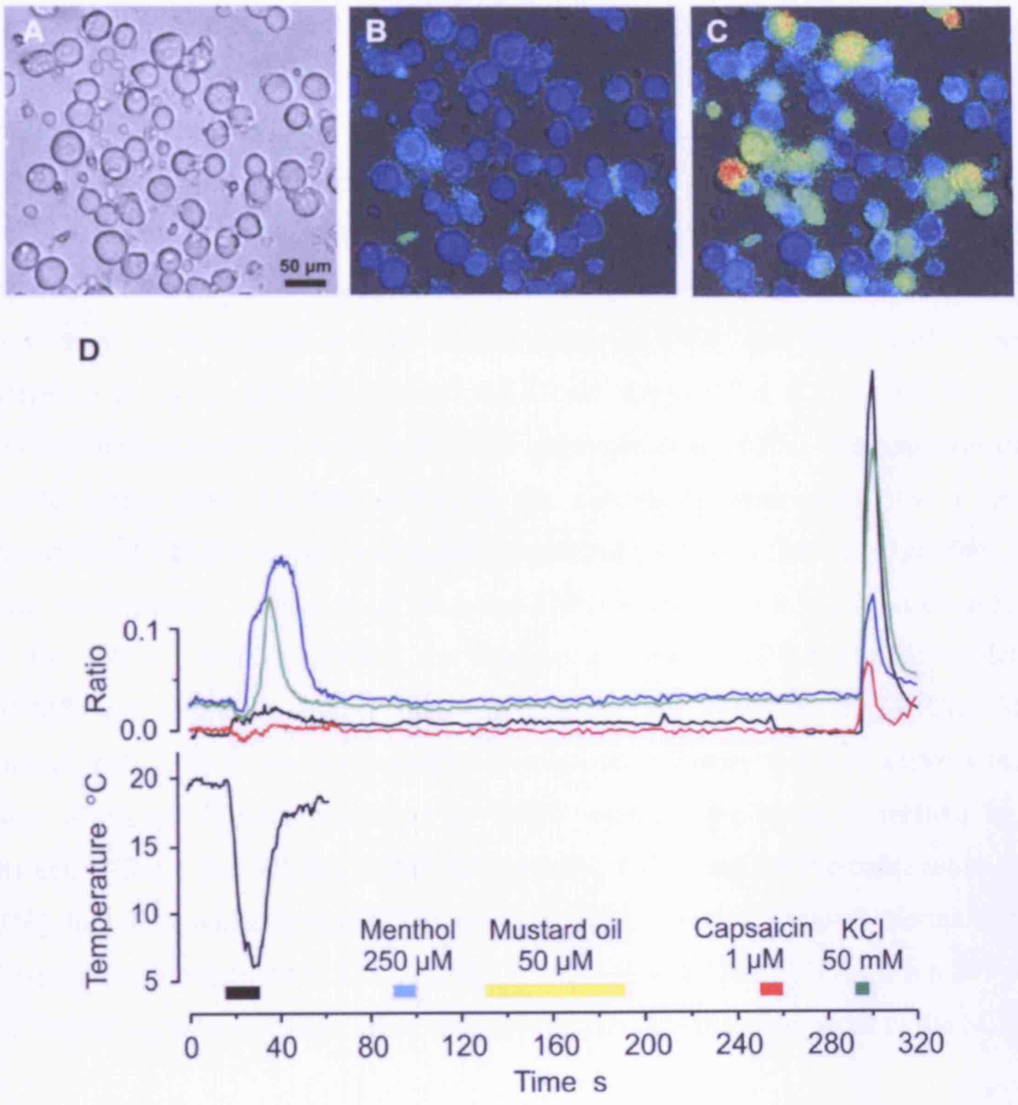

Figure 3.19. Fura fluorescence images of acutely dissociated SCG neurons responding to a brief cold stimulus. (A) Brightfield image. (B) Background Fura fluorescence. (C) Neurons responding to the cold stimulus with an increase in Fura fluorescence levels, indicative of a rise in intracellular calcium concentration. (D) Representative kinetic profiles of the responses of two cold-sensitive (blue and green) and two cold-insensitive (black and red) SCG neurons. All cells respond to KCl, but none to the TRP channel agonists menthol, mustard oil or capsaicin.

3.4.6. Sympathetic neurons do not express TRPM8, and express only low levels of TRPA1

In order to validate the functional data, total RNA from DRG and SCG was probed for the presence of the two cold-sensitive TRP channels TRPM8 and TRPA1 using real-time PCR (n = 4). TRP channel expression was quantified using total RNA or expression levels of UCHL1 or GAPDH as reference.

All four transcripts were expressed in DRG, whereas no TRPM8 was found in SCG (Figure 3.20). With equal amounts of starting RNA, UCHL1 and GAPDH transcripts were found to be present at very similar levels in DRG and SCG, with a mean difference in cycle threshold (Ct) of 0.6 ± 0.1 and 0.55 ± 0.3 for UCHL1 and GAPDH, respectively ($P > 0.5$). In the DRG expression of TRPA1 was approximately 20-fold higher than TRPM8, reflecting the functional observation that a larger proportion of DRG neurons responded to mustard oil than menthol. Therefore, the mean difference in Ct between UCHL1 and TRPM8 was 7.9 ± 0.9, compared to 5.9 ± 0.3 for TRPA1, and in addition the starting amount of cDNA needed to detect TRPM8 was five-times higher than required for the detection of TRPA1. SCG neurons, only 2 % of which responded to mustard oil, were found to express much lower levels of TRPA1 compared to DRG neurons: the mean difference in Ct between UCHL1 and TRPA1 in the SCG was 9.2 ± 3.2, and twelve-times more SCG cDNA had to be added to the PCR reaction in order to detect a signal. Normalisation of expression in relation to UCHL1 or to GAPDH showed that TRPA1 has a 109-fold or 130-fold higher expression level, respectively, in the DRG compared to the SCG.

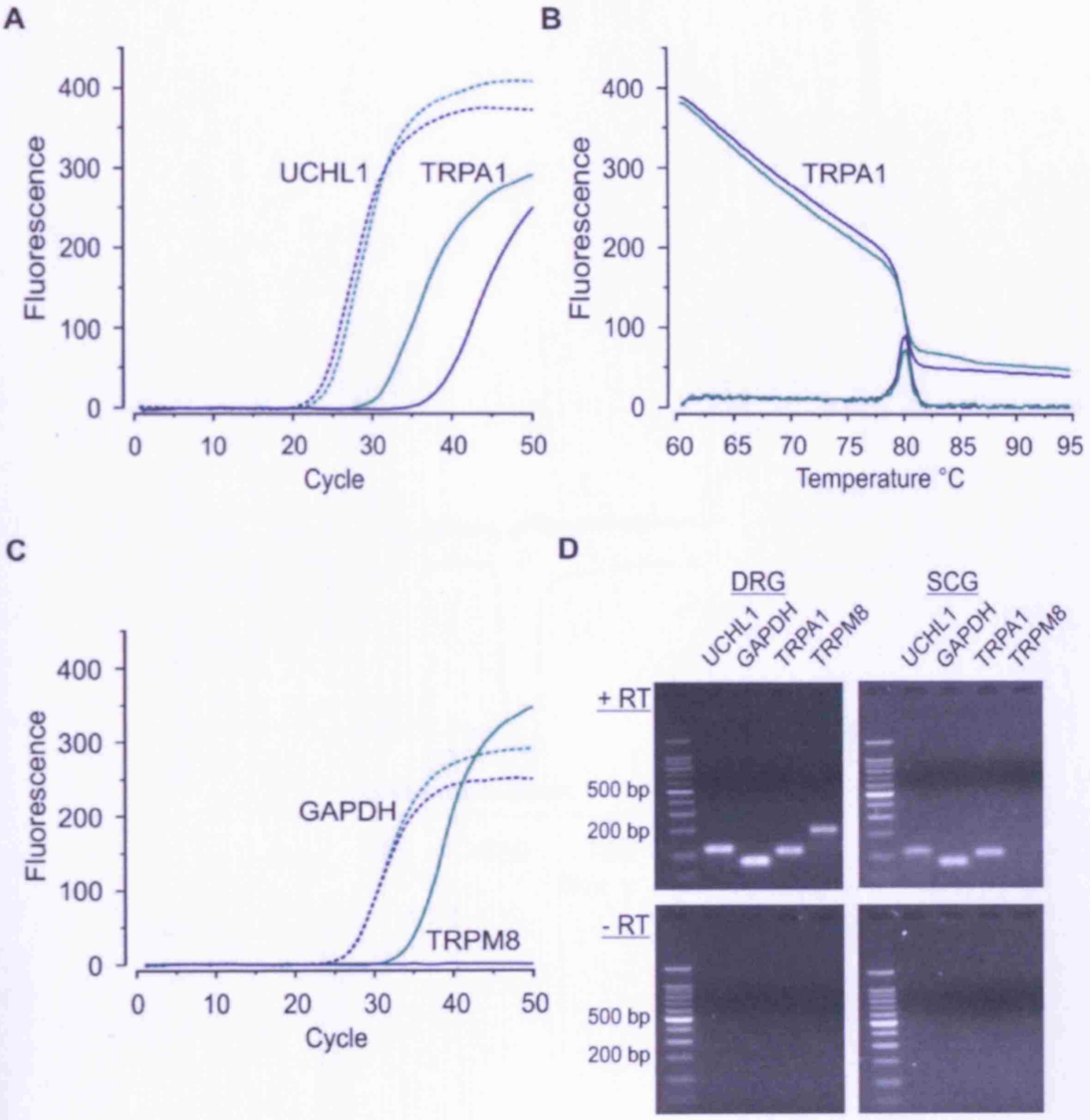

Figure 3.20. Quantitative rt-PCR for TRP channel expression in DRG and SCG. The cDNA of 250 pg (UCHL1, GAPDH), 1.25 ng (TRPM8) or 3 ng (TRPA1) total RNA equivalents were amplified. (A) Illustration of rt-PCR for UCHL1 and TRPA1. Whereas there were similar cycle threshold (Ct) values for UCHL1, there was a much lower Ct value for the TRPA1 transcript in DRG (green) compared to SCG (blue). (B) Melt curve analysis for TRPA1 showed the presence of only one amplification product. (C) Illustration of rt-PCR for GAPDH and TRPM8. DRG and SCG showed similar Ct values for GAPDH, but while DRG expressed the TRPM8 transcript, it was absent in SCG as demonstrated by the lack of a fluorescent product. (D) All PCR products were analysed on a 2 % agarose gel. Estimated product sizes were 117 bp (UCHL1), 81 bp (GAPDH), 107 bp (TRPA1) and 190 bp (TRPM8). –RT, RNA without reverse transcription.

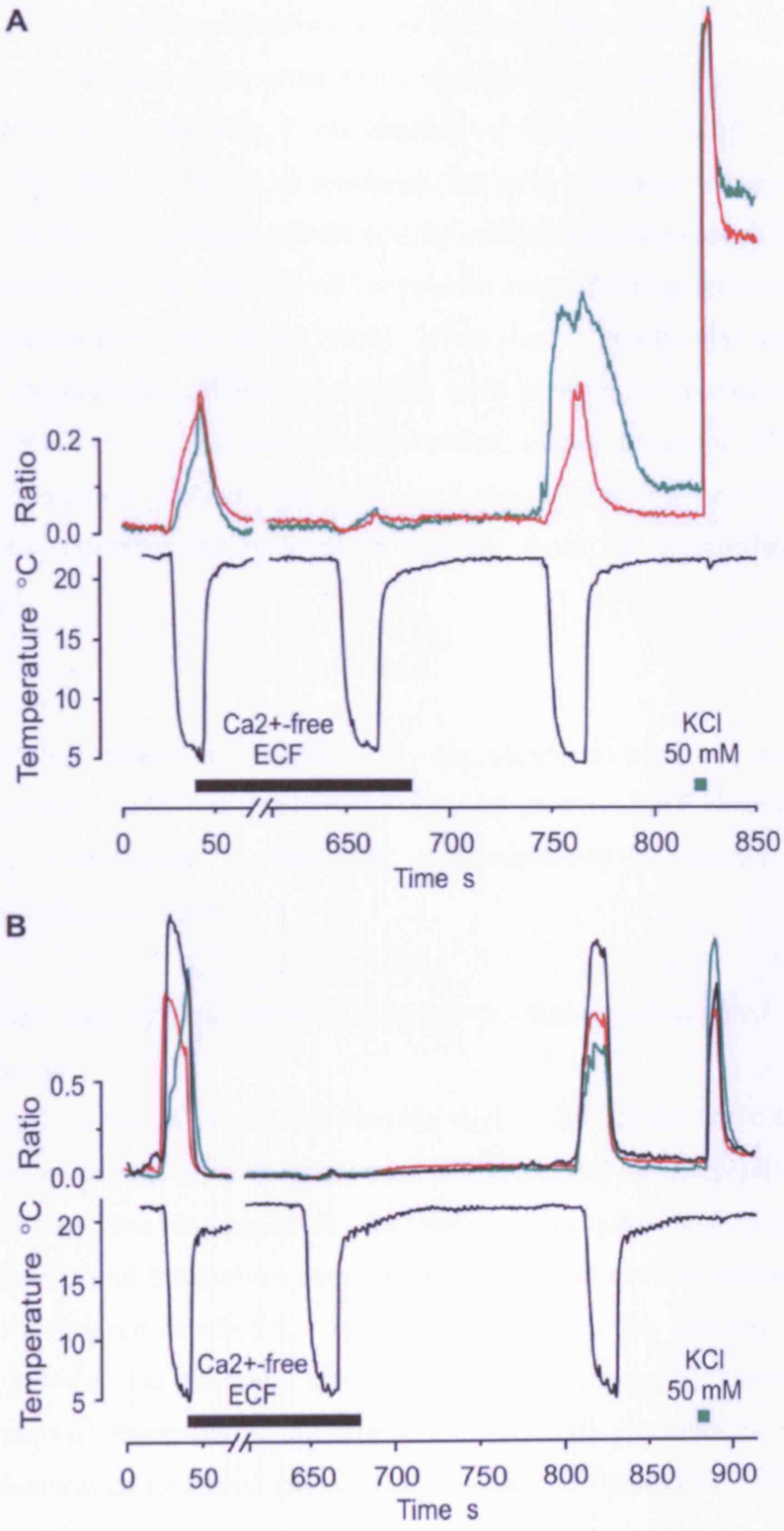

Figure 3.21. Representative kinetic profiles of two cold-sensitive DRG neurons (A) and three cold-sensitive SCG neurons (B) whose responses were abolished following the removal of calcium from the extracellular solution. Cold responses were restored with the addition of calcium.

3.4.7. Cold-induced calcium influx in sensory and sympathetic neurons

The data presented above demonstrate that a significant percentage of DRG and SCG neurons display cold sensitivity in the absence of functional TRPM8 and TRPA1 expression. In order to further characterise the cold response experiments were designed to address the question of whether the cold-induced increase in intracellular calcium concentration was due to the influx of ions across the membrane or due to the release of calcium from intracellular stores. When a cold stimulus was applied in the absence of extracellular calcium, responses were completely abolished in 88 % (29/33) of DRG neurons, and substantially reduced in the remaining 12 % of cells. Likewise, intracellular calcium transients were absent in all (46/46) cold-sensitive SCG neurons following the removal of calcium from the extracellular solution (Figure 3.21).

3.5. Discussion

The main findings from this study are that sympathetic neurons, and many sensory neurons, respond to cold in the absence of the cold-sensitive TRP channels, TRPM8 and TRPA1. Furthermore, menthol and cold sensitivity in sensory neurons is regulated over time in culture.

3.5.1. Identification of cold-sensitive neurons in freshly dissociated cells using calcium imaging

In recent years the use of dissociated neurons as a model for the nerve terminal has become widely adopted, since the discovery that ion channels and peptides found at the terminal are also expressed in the soma (Baccaglini and Hogan, 1983). Dissociated cells lend themselves very well to techniques such as calcium imaging, which is an appropriate method for use in studies such as this one due to the close correlation between the threshold for the generation of action potentials in cold-sensitive neurons determined electrophysiologically and increases in intracellular calcium concentration measured with microfluorometry (Viana et al., 2002;Madrid et al., 2006).

Very few studies of cold sensitivity have been performed on acutely dissociated neurons, despite the fact that cells are known to alter protein expression patterns over time in culture. In the present study 17 % of acutely dissociated DRG neurons were cold-sensitive. This percentage is higher than in studies where neurons were

maintained in cultures for more than a few hours (Reid et al., 2002), but in agreement with work on freshly dissociated cells which reported around 20 % of rat DRG neurons to be cold-sensitive (Babes et al., 2004;Babes et al., 2006). This proportion is also in good agreement with the percentage of cold-sensitive neurons estimated from teased fibre recording of peripheral nerves in rodents (Koltzenburg, 2004). It is therefore possible that acutely dissociated cells reflect the native cold sensitivity of neurons more accurately than cells maintained for longer periods in culture.

This view is also endorsed by findings from this and other studies which have shown that not only is time in culture important, but that the availability of growth factors such as NGF can influence menthol responsiveness (Story et al., 2003;Babes et al., 2004). Previous studies have suggested that the presence of NGF specifically up-regulates menthol sensitivity in sensory neurons, and the findings presented here would seem to agree with this. However, additional experiments have demonstrated that the observed changes in menthol sensitivity are not dependent on the presence of NGF. Furthermore, while other studies describe an effect which can last for several days, data from our laboratory suggest that the up-regulation in responsiveness to menthol in IB4-positive cells is only transient, returning to baseline levels by 48 hours (AlQatari et al., 2007). The reasons behind these discrepancies are unclear, although species-specific differences should be taken into account. Whether there is a physiological relevance to these findings is also currently unknown, but these studies do demonstrate the potential for culture conditions to significantly alter neuronal phenotype and the importance of being aware of such changes when investigating functional sensitivity in vitro. It may be the case that changes in menthol sensitivity, and presumably TRPM8 expression, will contribute to the development of cold hypersensitivity, a common symptom of neuropathic pain conditions (Scadding and Koltzenburg, 2005), and the transient nature of the up-regulation in menthol sensitivity observed in vitro could be due to the absence of additional regulatory factors normally present in vivo.

3.5.2. There is limited overlap of functional responses to cold and TRP channel agonists in sensory neurons

Many cold-responsive sensory neurons were also sensitive to menthol and mustard oil, chemical agonists of TRPM8 and TRPA1, respectively, although a large population of cells did not respond to either stimulus. In the present study 6 % of

DRG cells responded to the TRPM8 agonist menthol, but more than 90 % of the menthol-sensitive cells were cold-responsive. This corresponds well with the finding that TRPM8 is present in 5-10 % of adult mouse DRG neurons (McKemy et al., 2002;Peier et al., 2002a), and that most native DRG cells expressing TRPM8 are cold-sensitive or that cold sensitivity can be induced in cold-insensitive neurons by transfection of TRPM8 (Nealen et al., 2003;de la Pena et al., 2005). Knockout of the TRPM8 gene has been shown to result in a significant, although not total, loss of cold sensitivity, in vitro and in vivo (Dhaka et al., 2007;Colburn et al., 2007;Bautista et al., 2007).

Functional sensitivity to mustard oil was detected in 18 % of the DRG cells, agreeing with recent reports that TRPA1 is expressed in approximately 20 % of sensory neurons (Jordt et al., 2004;Bautista et al., 2005). However, only 5 % of the cold-sensitive population in this study responded to both menthol and mustard oil. This is in agreement with histological studies that TRPM8 and TRPA1 are expressed on distinct subpopulations of cells in the mouse (Story et al., 2003), but is in contrast to the 20-60 % overlap reported for the rat (Bandell et al., 2004;Babes et al., 2004). This discrepancy may simply be due to species-specific differences, however a much larger overlap (> 60 %) was recorded when neurons had been kept in culture over a period of days, in the presence of NGF (Bandell et al., 2004), than in freshly dissociated neurons without NGF (Babes et al., 2004). Indeed in the results of this study there was a trend for an increase in the overlap between menthol and mustard oil sensitivity in cells maintained for 24 hours compared to acute cultures (11 % versus 5 %, $P > 0.2$).

Responses of DRG neurons to cinnamaldehyde were also examined. Previous studies had suggested that cinnamaldehyde activated a smaller population of DRG cells than mustard oil, and that this discrepancy could be due to the activation by mustard oil of other receptors on sensory neurons (Bandell et al., 2004). Recent studies of TRPA1 knockout mice failed to resolve this issue, since one group reported a complete loss of responses to mustard oil (Bautista et al., 2006), while another group still found mustard oil-sensitive neurons in the absence of TRPA1 (Kwan et al., 2006). In fact, the dose response data presented in this study show that saturating concentrations of cinnamaldehyde and mustard oil activate a similar proportion of DRG neurons, but that the EC_{50} value for mustard oil is almost four-times lower than that of cinnamaldehyde. Therefore variability in the number of cinnamaldehyde- or mustard

oil-sensitive neurons can be explained by differences in potency between the two compounds.

The number of cold-sensitive cells that responded to cinnamaldehyde was much lower in this study than has been reported previously in the rat (9 % versus 39 %) (Bandell et al., 2004), but this is probably due to differences between acute and long-term cultures, since additional experiments showed 39 % of cold-sensitive neurons responding to cinnamaldehyde after 24 hours in NGF ($n_{animals} = 2$, $n_{cells} = 362$). There was no difference between the mustard oil-sensitive and cinnamaldehyde-sensitive populations in terms of cold sensitivity, despite the more potent action of mustard oil. This means that the functional association between TRPA1 activation and cold is not systematic, but reflects the distribution in the population at large. More importantly, only a minority of those cells that did respond to mustard oil or to cinnamaldehyde were also cold-sensitive. This means that there are other, TRP-independent mechanisms that control cold sensation in a significant proportion of DRG neurons. This possibility is also endorsed by single unit recordings from sensory neurons innervating rat skin which found a substantial proportion of cold-sensitive units that were not excited by menthol or mustard oil (Vastani et al., 2005).

Based on the activation thresholds of the recombinant channels, TRPA1 was traditionally thought to be involved in the detection of noxious cold, while TRPM8 was implicated in innocuous cool sensing (McKemy et al., 2002;Peier et al., 2002a;Story et al., 2003). However, there is now increasing evidence that TRPM8 may detect noxious, as well as innocuous, cold stimuli. Even at low micromolar concentrations of menthol, there was a significant overlap with functional capsaicin sensitivity in sensory neurons. It had been suggested from previous studies that this was due to an up-regulation of TRPM8 within the TRPV1-expressing population over time in culture, driven by the presence of NGF (Story et al., 2003;Babes et al., 2004). The cells analysed in this study however were acutely dissociated and cultured without NGF, arguing that TRPM8 is expressed in nociceptive neurons in vivo. In support of this hypothesis, behavioural studies in TRPM8 knockout mice indicate there may be some deficit in the detection of noxious cold stimuli (Dhaka et al., 2007;Colburn et al., 2007;Bautista et al., 2007).

In this study cold sensitivity in DRG neurons was assessed using cold ramps applied from room temperature or from 30 °C. Increasing the baseline resulted in a significant shift of activation thresholds to warmer temperatures. Despite this shift the

distribution of the activation thresholds in the population at large, as well as that of menthol-sensitive or menthol-insensitive cells, was not substantially altered. In addition, the kinetics of cold responses were comparable under the two conditions. Temperature has been shown to have an effect on the activation of TRPV1 by capsaicin (Vlachova et al., 2001), and accordingly a higher percentage of capsaicin-sensitive cells was recorded at warmer temperatures. However, there was no significant difference in the proportion of menthol- or mustard oil-sensitive cells at room temperature or at warmer temperatures, either in the population at large or within the cold-sensitive population. This is expected for TRPA1 where mustard oil or cinnamaldehyde responses of the cloned receptor are not temperature-dependent (Bandell et al., 2004), but is unexpected for TRPM8 in which menthol-induced currents of the cloned channel are modulated by temperature (Peier et al., 2002a). This might point to differences in the regulation of TRPM8 sensitivity in native sensory neurons and heterologous expression systems, as already demonstrated for threshold and adaptation properties of the menthol-sensitive cold current (Reid, 2005).

It has been suggested that the activation of specific neurons by cold is dependent on the rate at which the cold stimulus is applied (Reid, 2005). However, both fast (mean rate of temperature change 1.4 °C/s) and slow (mean rate of temperature change 0.3 °C/s) cold ramps were used in this study, and no differences were found in the properties of the cold-sensitive population in terms of distribution, kinetics, or sensitivity to menthol and mustard oil. This is in agreement with findings on the cloned TRPM8 channel whose activation threshold is not influenced by the rate of temperature change (McKemy et al., 2002).

3.5.3. Absence of TRPM8 and TRPA1 responses in cold-responsive sympathetic neurons provides further evidence for TRP-independent mechanisms of cold sensitivity in peripheral neurons

Confirming previous work, a significant proportion of sympathetic neurons were found to respond to cold, and TRPA1 was found to be expressed in the SCG (Smith et al., 2004). However the suggestion that TRPA1 is the channel for cold transduction is not supported by the data of this study. Less than 4 % of cold-sensitive sympathetic neurons were activated by either menthol or mustard oil. Furthermore quantitative rt-PCR showed that sympathetic neurons do not express TRPM8 and express only very

little TRPA1. The higher proportion of cold-sensitive sympathetic neurons recorded in functional studies compared to sensory neurons contrasts with the more than 100-fold smaller amount of TRPA1 transcript in the SCG.

It is clear from this data that while TRP channels appear to play a role in cold transduction in many sensory neurons, the virtual absence of a functional response to menthol or mustard oil in sympathetic neurons suggests the presence of TRP-independent mechanisms of cold detection. The large discrepancy between responsiveness to cold and to TRP channel agonists in DRG, and especially in SCG, neurons means there are mechanisms for cold transduction that cannot be identified on the basis of sensitivity to cooling compounds, such as menthol or icilin. Besides TRPM8 and TRPA1, voltage-gated potassium and sodium channels have also been implicated in the regulation of cold sensation.

Despite obvious differences in transduction mechanisms between sensory and sympathetic neurons, there are similarities in the properties of the cold response itself. In calcium-free extracellular solution the cold-induced calcium transients were abolished in both DRG and SCG neurons. This indicates that the observed responses are mediated by an influx of calcium rather than by release from intracellular stores, which even in the presence of TRP channels is likely to result from the activation of voltage-gated calcium channels.

In conclusion, the principal finding of this study is that cold sensitivity in sympathetic neurons and a large proportion of sensory neurons is not mediated through TRPM8 and TRPA1.

4. The role of potassium channels in cold transduction

4.1. Background

It has been suggested that potassium channels may have an important role to play in the regulation of cold sensitivity in sensory neurons. In 2001, a study by Reid and Flonta showed that when a cold solution was applied to DRG neurons, the input resistance of the cells increased, due to the cold-induced inhibition of a background potassium conductance (Reid and Flonta, 2001). Leak potassium currents are mediated primarily via members of the two-pore domain potassium channel subfamily, some of which have been shown to be temperature-sensitive (Maingret et al., 2000;Kang et al., 2005). One channel in particular, TREK-1, was implicated in the regulation of cold sensitivity following the demonstration that it could be inhibited by cooling (Maingret et al., 2000), however rt-PCR on cold-sensitive sensory neurons failed to show any correlation between functional cold sensitivity and the expression of TREK-1 (Nealen et al., 2003).

In a further study of potassium conductance in sensory neurons, it was found that not only was the cold-sensitive background potassium current greater in cold-sensitive neurons, but conversely that cold-insensitive cells expressed higher levels of a transient potassium current, sensitive to the broad spectrum potassium channel blocker 4-AP (Viana et al., 2002). It was suggested that the transient current was acting as an excitability brake in cold-insensitive neurons, preventing the cells from firing when a cold stimulus was applied.

Blockade of the transient potassium conductance with 4-AP and another broad spectrum antagonist TEA was found to induce novel cold sensitivity in 30-60 % of previously unresponsive sensory neurons, both in dissociated cultures and in the intact trigeminal ganglion (Viana et al., 2002;Cabanes et al., 2003).

4.2. Aims

The aim of this study was to further investigate the role that voltage-gated potassium channels play in constitutive and induced cold sensitivity in sensory and sympathetic neurons.

4.3. Methods

This section provides specific information on the experiments carried out in this study. For detailed protocols, please refer to Chapter 2.

4.3.1. Primary tissue culture

DRG and SCG from adult male C57/B6 mice were digested in papain followed by collagenase and dispase, and dissociated mechanically with fire-polished glass pipettes. Neurons were re-suspended in F-12 medium, which for SCG cultures was supplemented with 10 % foetal bovine serum, 50 ng/ml rhNGF and 30 mM glucose. DRG neurons were not cultured in NGF unless otherwise stated. Neurons were plated onto poly-L-lysine and laminin-coated coverslips and maintained in culture for up to 24 hours. Acutely dissociated neurons were used for imaging experiments within 3-5 hours of plating.

4.3.2. Ratiometric calcium imaging

Neurons were loaded with Fura-2 and stained with IB4-FITC and CTB-Alexa 594. Coverslips were positioned inside a custom-made chamber and solutions were applied to the cells via a gravity-driven application system.

To produce dose-response curves, DRG neurons were stimulated with potassium channel blockers at increasing concentrations. Stock solutions of 4-AP (100 mM, Sigma), TEA (250 mM, Sigma), XE991 (10 mM, Tocris, UK) and apamin (100 μM, Alomone Laboratories, Israel) were made up in distilled water and diluted in ECF to the required working concentration on the day of the experiment. 4-AP and TEA are both broad spectrum inhibitors of voltage-gated potassium channels, while XE991 blocks slow delayed rectifier channels (the KCNQ subfamily) and apamin targets small-conductance calcium-activated potassium channels (SK channels). 4-AP was tested at concentrations of 10 μM, 30 μM, 100 μM, 300 μM, 1 mM, 3 mM and 10 mM. TEA was applied to neurons at concentrations of 1 mM, 3 mM, 10 mM, 30 mM and 100 mM. Activation of cells by XE991 was assessed at concentrations of 1 μM, 3 μM, 10 μM, 30 μM and 100 μM, while apamin was tested at concentrations of 10 nM, 30 nM, 100 nM, 300 nM and 1 μM. All compounds were applied for 30 seconds. Neurons were additionally stimulated with 3 μM capsaicin, in order to functionally identify a subpopulation of nociceptive neurons.

Various stimulation protocols were assessed for their efficiency in determining the effects of potassium channel blockade on cold sensitivity. In the first instance, the potassium channel blocker was applied to the neurons for 30-40 seconds, followed immediately by a cold stimulus. Two issues were raised with this approach: firstly, TEA in particular washed out very rapidly, and therefore any effects the compound was having on the cold response were very small. Secondly, the channel blocker was diluted on application of the cold stimulus, and consequently the exact concentration of blocker surrounding the cells was unknown. The protocol was therefore modified so that the potassium channel blocker was applied to the cells at room temperature for 20-30 seconds, before being cooled down to approximately 5 °C. Since a significant proportion of neurons were activated by the potassium channel blocker itself, it was difficult to distinguish any additional activation when the cold stimulus was applied. Additional experiments showed that the response to the potassium channel blocker was kinetically distinct from the cold response, and it was also very reproducible. Therefore a protocol was adopted whereby neurons were stimulated with the potassium channel blocker for 40 seconds, followed by a 2 minute wash with ECF and a second application of the blocker (for 20 seconds at room temperature and 20 seconds while being cooled to 5 °C). Subsequently neurons were assessed for sensitivity to 250 μM menthol (10 second application) and 3 μM capsaicin (10 second application). All experiments were done at room temperature, and fast non-linear cold ramps were applied over a 20 second period. Temperature was continuously monitored with a thermocouple positioned just outside the field of vision, opposite the stream of the inflow. Experiments assessing the effects of TEA (10 mM), XE991 (10 μM), apamin (100 nM), α-dendrotoxin (DTX) (1 μM) and BDS (250 nM) were performed on acutely dissociated DRG and SCG neurons. 4-AP (300 μM and 3 mM) was also tested on acutely dissociated DRG and SCG neurons, as well as DRG neurons that had been maintained for 24 hours in the presence of 50 ng/ml NGF. DTX and BDS (Alomone Laboratories, Israel) were dissolved directly in ECF to working concentrations on the day of the experiment. In control experiments, the potassium channel blocker was omitted and replaced with ECF.

For calcium-free experiments, calcium was removed from the ECF and replaced with magnesium. In addition, the ECF was supplemented with 1 mM EDTA to ensure complete removal of extracellular calcium ions.

Ratiometric images were recorded at intervals of 0.5 seconds for the duration of the cold stimulus and 1-2 seconds thereafter, using the TillPhotonics system. One field of vision per coverslip was analysed and only vital neurons that responded to a concentrated (50 mM) potassium stimulus were included in the analysis.

4.3.3. Quantitative rt-PCR

Total RNA was extracted from dissociated DRG and SCG neurons, and 10 ng were reverse transcribed into cDNA for use in real-time PCR. cDNA was probed for the expression of Kv1 and Kv3 voltage-gated potassium channels, using SYBR green dye. All Kv1 primers were optimised for annealing temperature and gave a linear correlation between cycle threshold and cDNA concentration in serial dilutions (Figure 4.1). The Kv3 primers were obtained from the Quantitect Primer Assay range, and were manufactured to have the same annealing properties. For quality control purposes, the Kv3.1 and Kv3.4 primers were optimised for annealing temperature in the laboratory and were found to give identical results. For the purposes of this study therefore, all Quantitect Kv3 primers were treated in the same way. Reaction products gave single peaks on melt curve analysis and single bands of expected size on a 2 % agarose gel.

Relative quantification of rt-PCR products was performed, using the expression of housekeeping genes with the $\Delta\Delta$ method as a reference.

4.3.4. Statistics

Calcium imaging experiments were performed on four separate cultures over two experimental days, unless otherwise stated. Each culture usually consisted of several coverslips. The results from the coverslips of one culture were pooled and were used as one data point for subsequent analysis. For rt-PCR experiments, DRG and SCG from 3-4 animals each were processed separately for cDNA and all PCR reactions were run in duplicate. All quantitative comparisons are presented as mean ± SEM. Unless otherwise stated, Student's unpaired *t*-test was used for all statistical analyses.

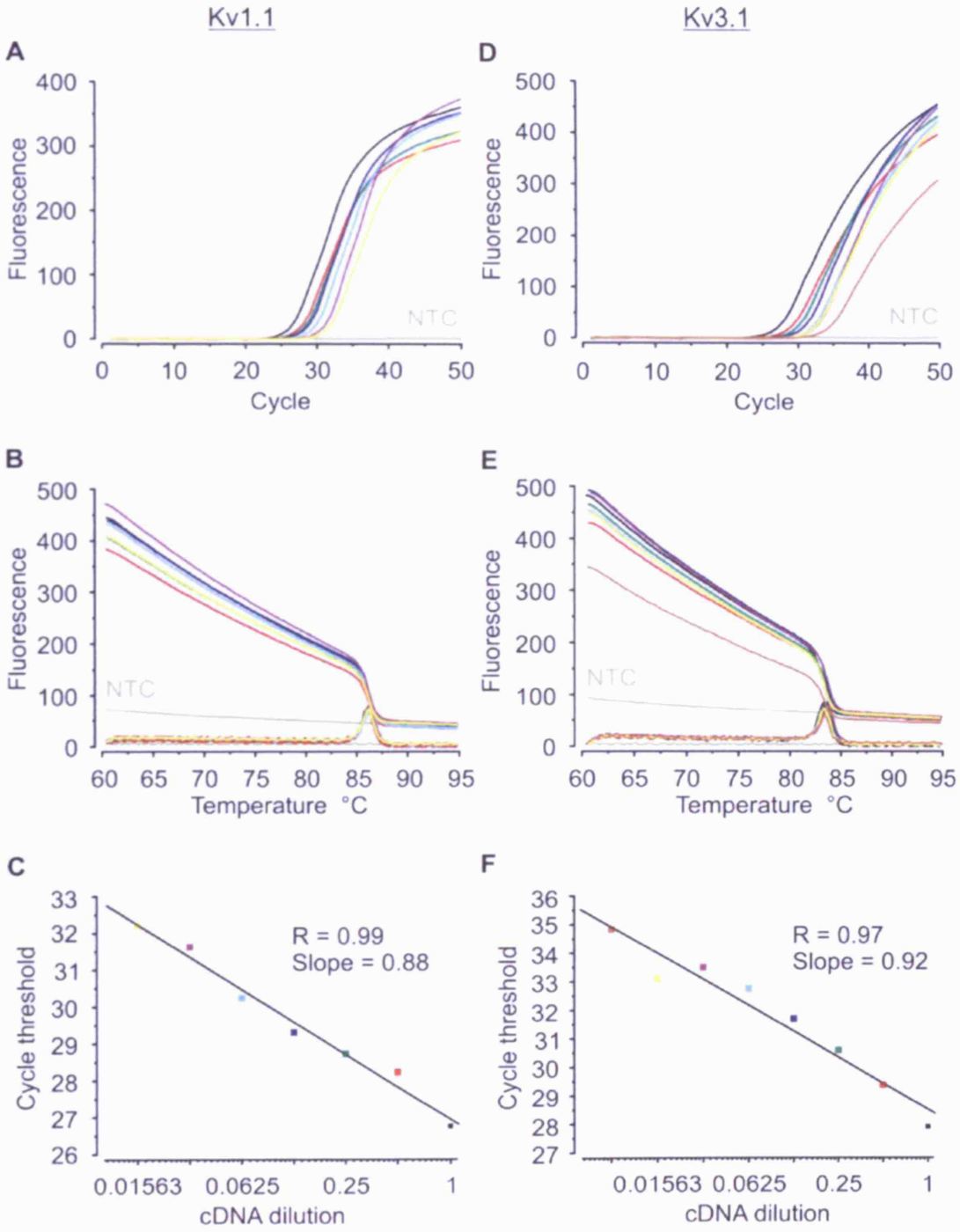

Figure 4.1. Primers used in rt-PCR for the detection of voltage-gated potassium channel transcripts produced a linear reaction in serial dilution experiments. Data from experiments using primers for the Kv1.1 (A-C) and Kv3.1 (D-F) transcripts are shown as representative examples. (A, D) Illustration of rt-PCR for Kv1.1 and Kv3.1 showing an increase in cycle threshold (Ct) with decreasing amounts of starting cDNA. (B, E) Melt curve analysis showed the presence of only one amplification product. (C, F) Ct is plotted as a function of cDNA dilution, demonstrating the linearity of the PCR reaction. NTC, non-template control.

4.4. Results

4.4.1. Dose-dependent activation of sensory neurons by potassium channel blockers

Acutely dissociated DRG neurons were assessed for sensitivity to increasing concentrations of the potassium channel antagonists 4-AP, TEA, XE991 and apamin. 4-AP is a broad spectrum potassium channel blocker, commonly used to inhibit the transient outward current mediated via members of the Kv1, Kv3 and Kv4 subfamilies, while TEA blocks the delayed rectifier current mediated via Kv1, Kv2 and Kv3 channels, as well as the large-conductance calcium-activated current. It should be noted that many voltage-gated potassium channels are sensitive to blockade by both 4-AP and TEA when applied at concentrations in the micromolar to millimolar range, regardless of the type of current they pass. A total of 1494 neurons were tested for sensitivity to concentrations of 4-AP ranging from 10 μM-1 mM (n = 6), and a further 722 cells were stimulated with higher concentrations between 1-10 mM (n = 2). All neurons responded to 10 mM 4-AP, with an EC_{50} of 2 mM (Figure 4.2). 32 ± 1 % of neurons were also capsaicin-sensitive. 1794 neurons were assessed for responsiveness to increasing concentrations of TEA (n = 5). Of those cells, 1357 (72 ± 5 %) responded to 100 mM TEA, with an EC_{50} of 9 mM (Figure 4.3). Within the TEA-sensitive population, 33 ± 3 % responded to capsaicin. It should be noted that capsaicin sensitivity was not restricted to those neurons responding to the highest concentrations of 4-AP or TEA, and when the dose-response curves of capsaicin-sensitive and capsaicin-insensitive neurons were overlayed, there was no difference between them (Figure 4.5).

XE991 is a specific blocker for members of the Kv7 or KCNQ subfamily, which underlie slow delayed rectifier currents (M-currents). 81 neurons were tested for sensitivity to XE991, of which 28 (35 %) responded to 100 μM (Figure 4.4). Of those neurons, 29 % were capsaicin-sensitive. The EC_{50} for XE991 was 10 μM. As observed with 4-AP and TEA, there was no difference between the dose-response curves for capsaicin-sensitive versus capsaicin-insensitive neurons (Figure 4.5).

Apamin specifically blocks the small-conductance calcium-activated potassium current mediated via SK channels. This compound was tested on 178 cells, but was found to activate neurons in a non-dose-dependent manner. 27 cells (15 %) were excited by the lowest concentration of apamin used (10 nM), but only 14 neurons (8 %) responded to the highest concentration (1 μM).

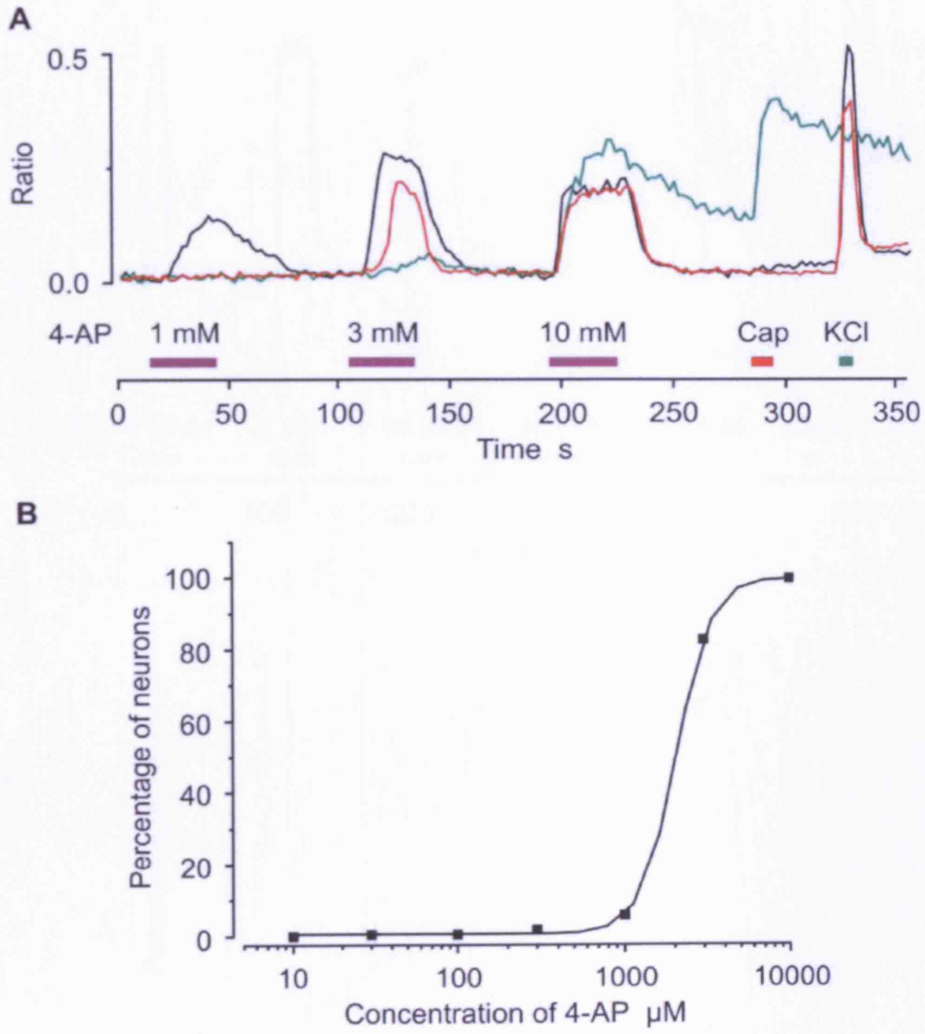

Figure 4.2. (A) Representative kinetic profiles of the responses of three 4-AP-sensitive DRG neurons. The three cells required different concentrations of 4-AP to elicit a response. One cell was also capsaicin-sensitive (green). (B) Dose-response curve for 4-AP in acutely dissociated DRG neurons. $n_{animals}$ = 2-6, n_{cells} = 2216. Data are presented as mean percentage of responding neurons ± SEM.

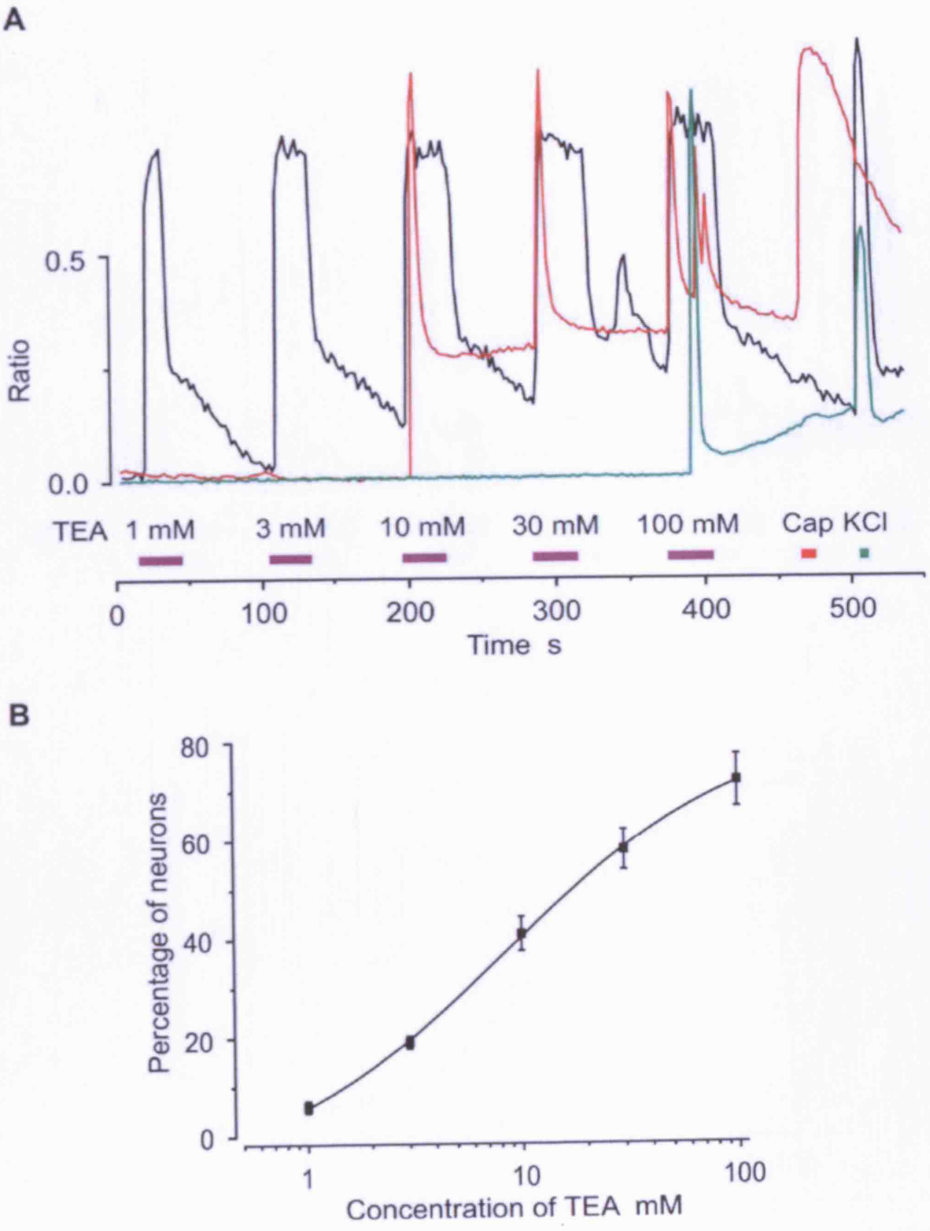

Figure 4.3. (A) Representative kinetic profiles of the responses of three TEA-sensitive DRG neurons. The three cells required different concentrations of TEA to elicit a response. One cell was also capsaicin-sensitive (red). (B) Dose-response curve for TEA in acutely dissociated DRG neurons. $n_{animals} = 5$, $n_{cells} = 1794$. Data are presented as mean percentage of responding neurons ± SEM.

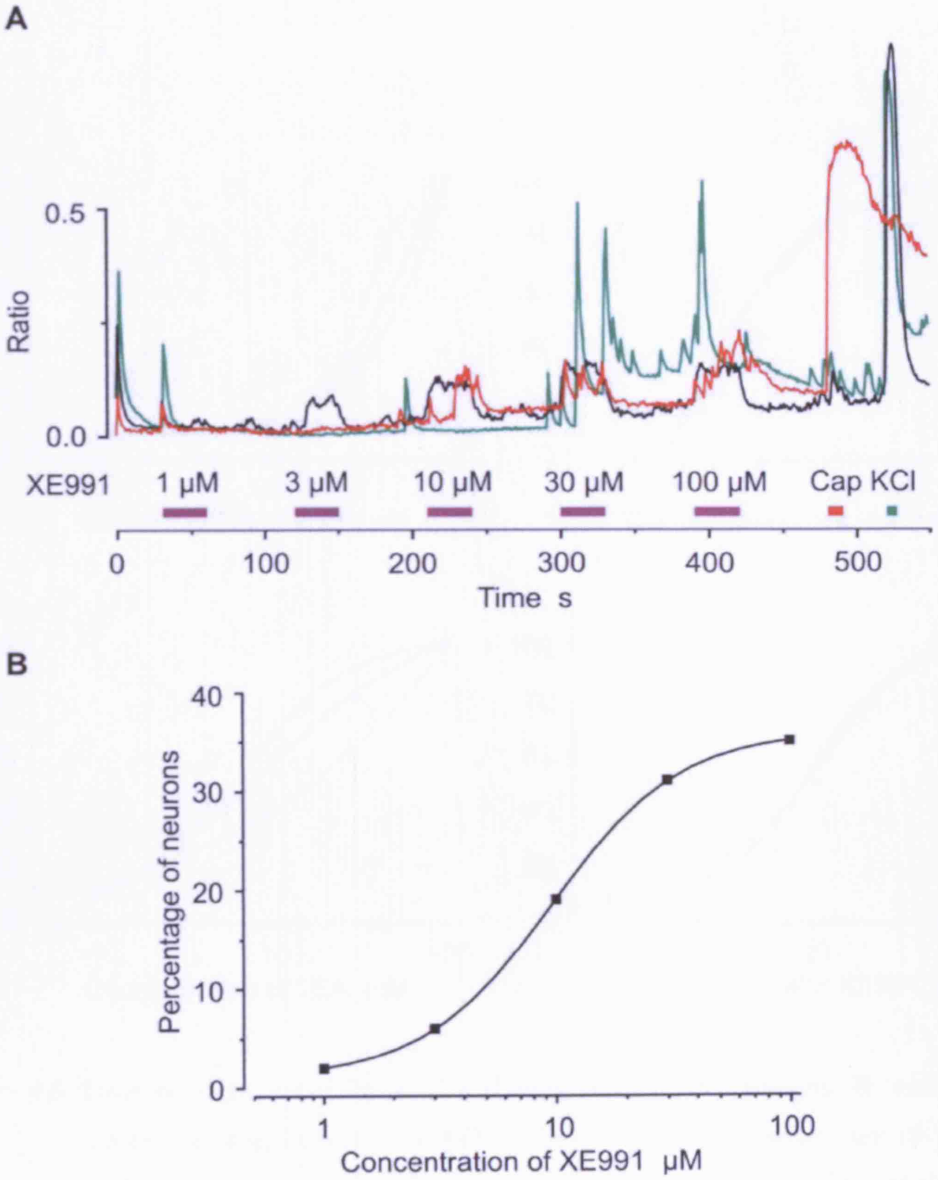

Figure 4.4. (A) Representative kinetic profiles of the responses of three XE991-sensitive DRG neurons. The three cells required different concentrations of XE991 to elicit a response. One cell was also capsaicin-sensitive (red). (B) Dose-response curve for XE991 in acutely dissociated DRG neurons. n_{cells} = 81. Data are presented as percentage of responding neurons.

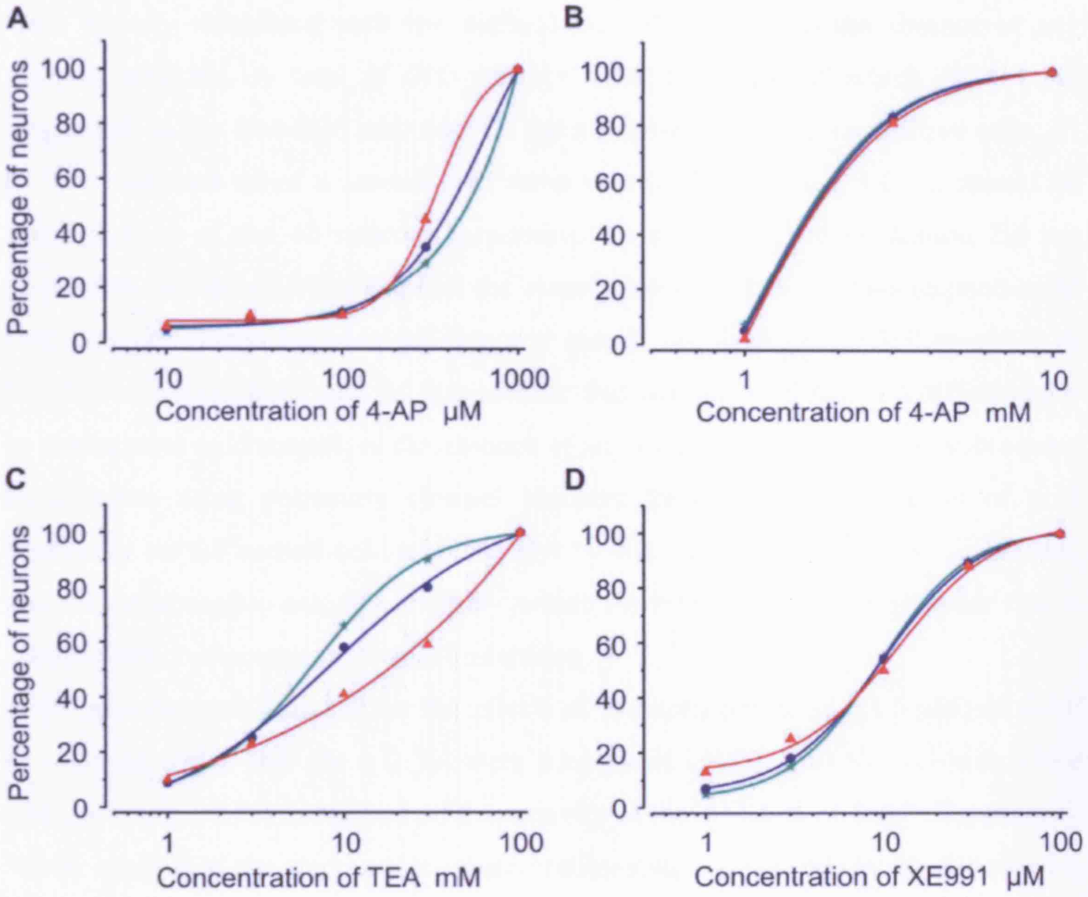

Figure 4.5. Dose response curve for 4-AP (A: micromolar concentrations, B: millimolar concentrations), TEA (C) and XE991 (D) sensitivity in capsaicin-sensitive (red) and capsaicin-insensitive (green) populations of acutely dissociated DRG neurons. The entire population is represented in blue. 4-AP: $n_{animals}$ = 2-6, n_{cells} = 2216; TEA: $n_{animals}$ = 5, n_{cells} = 1794; XE991: n_{cells} = 81. The total number of responsive neurons is presented as a percentage.

4.4.2. Pharmacological blockade of voltage-gated potassium channels induces novel cold sensitivity in sensory neurons

Acutely dissociated DRG neurons were assessed using Fura calcium imaging for constitutive and induced cold responses following the application of various voltage-gated potassium channel blockers. To establish a baseline response, DRG neurons were initially stimulated with two consecutive cold stimuli in the absence of any channel blockers. A total of 310 neurons were analysed, of which 43 (14 %) responded on the first cold stimulus. Of the remaining 267 cold-insensitive cells, 17 (6 %) responded when a second cold ramp was applied (Figure 4.6). It should be noted that 10 of the 43 neurons responding on the first cold application did not respond to the second, meaning that the overall percentage of neurons responding to cold was not altered between the first and second applications (50/310 neurons, 16 %). Nevertheless, these data do demonstrate that neurons will respond differentially to consecutive cold stimuli, in the absence of any external factors. During subsequent experiments using potassium channel blockers therefore, any induction of cold sensitivity on the second cold stimulus $\leq$ 6 % was not considered to be significant, and was attributed to natural variability within the neuronal population, rather than a specific effect of potassium channel inhibition.

1209 neurons were analysed for the effects of low concentrations (300 μM) of 4-AP (n = 6), of which 266 (24 ± 2 %) were cold-sensitive. Of the 943 cold-insensitive cells, 365 (37 ± 5 %) developed cold sensitivity in the presence of 4-AP (Figure 4.7). When applied in the micromolar concentration range 4-AP will block the slowly-inactivating transient current (commonly referred to as I_D), whereas millimolar concentrations will also inhibit the fast-inactivating current (I_A). Neurons were therefore also tested using a higher concentration of 4-AP (3 mM). From a total of 510 cells (n = 3), 71 (13 ± 3 %) were cold-sensitive, and of the 439 remaining cold-insensitive neurons, 87 (20 ± 2 %) responded to cold following the application of 4-AP. Increasing the concentration of 4-AP from 300 μM to 3 mM did not affect the percentage of neurons displaying induced cold responses (37 ± 5 % versus 20 ± 2 %, $P > 0.05$). The following data were taken from experiments using 300 μM 4-AP. Neurons displaying an induced cold response in the presence of the potassium channel blocker will be referred to as the 'induced cold population'.

There was not a direct relation between neuronal activation by the potassium channel blocker and the induction of cold sensitivity. Thus, of the 365 neurons showing an induced cold response, 54 (18 ± 4 %) were sensitive to the application of 4-AP. Conversely, 148 (14 ± 2 %) cells were 4-AP-sensitive, of which 33 ± 6 % showed an induced cold response.

Neurons were also assessed for sensitivity to the TRP channel agonists menthol and capsaicin. Within the induced cold population, 117 (34 ± 7 %) neurons responded to capsaicin, but only 3 (1 ± 1 %) were sensitive to menthol. The lack of overlap between cold induction and menthol sensitivity means that TRPM8 is not involved in the transduction of cold stimuli in these neurons, and that the induced responses are therefore mediated via a TRP-independent mechanism.

Subpopulations of neurons were identified on the basis of staining for IB4 and CTB. Of the cells displaying an induced cold response, 287 (74 ± 4 %) were IB4-positive, while 54 (21 ± 5 %) stained for CTB (Figure 4.8).

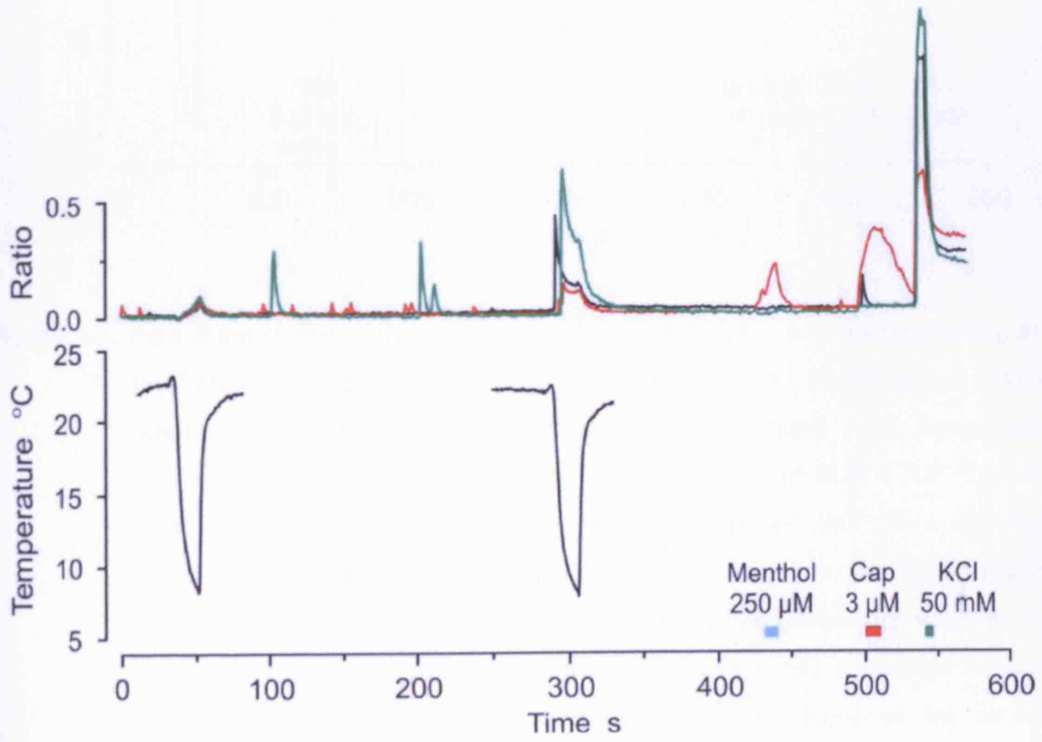

Figure 4.6. Representative kinetic profiles of the responses of three DRG neurons responding to a cold stimulus on the second application only, in the absence of potassium channel blockers. One cell was also weakly menthol- and capsaicin-sensitive (red).

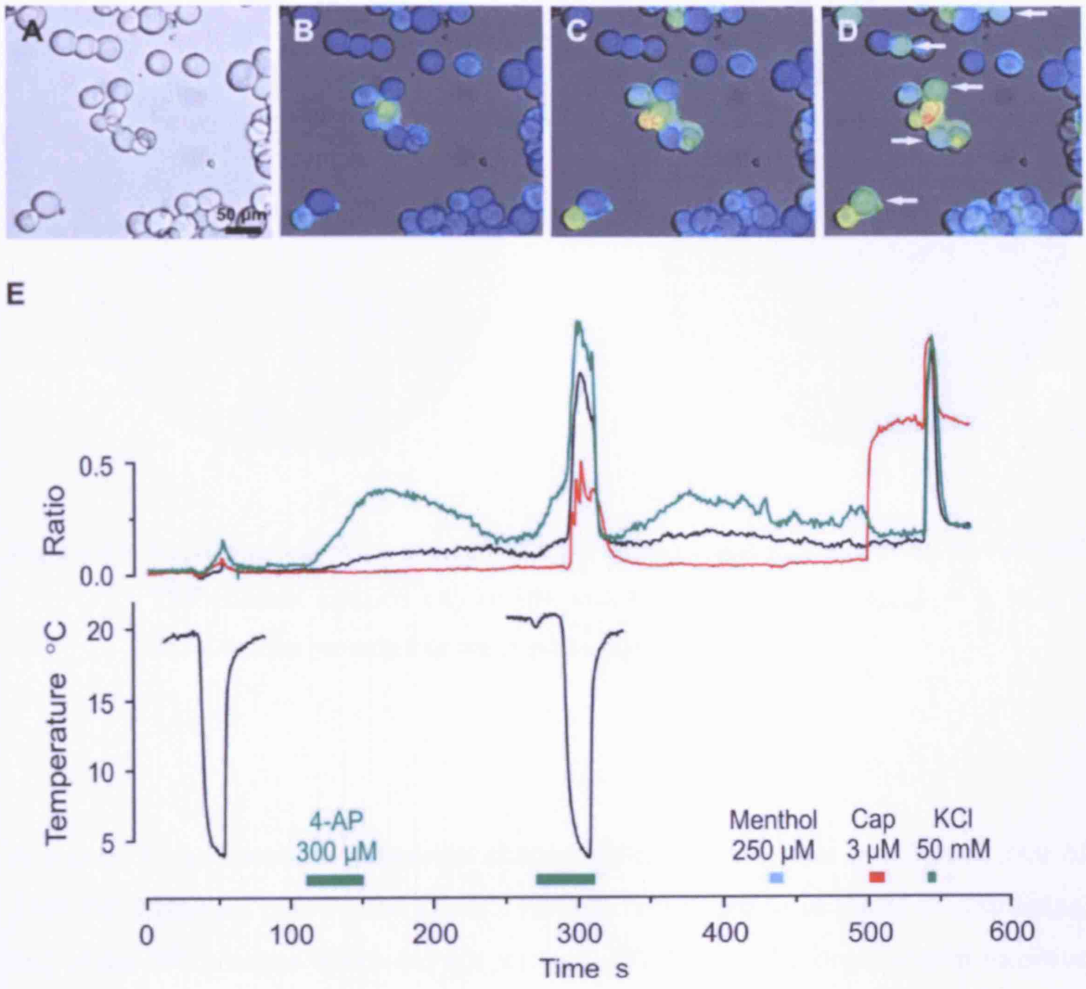

Figure 4.7. Fura fluorescence images of acutely dissociated DRG neurons responding to a brief cold stimulus before and during application of the Kv potassium channel blocker 4-AP. (A) Brightfield image. (B) Background Fura fluorescence. (C) DRG neurons responding to cold before the application of 4-AP. (D) DRG neurons responding to cold during the application of 300 µM 4-AP. Cells displaying induced cold sensitivity are marked with an arrow. (E) Representative kinetic profiles of the responses of three DRG neurons displaying induced cold sensitivity following the application of 4-AP. One cell responded to 4-AP (green), and one cell was capsaicin-sensitive (red). None of the neurons responded to menthol.

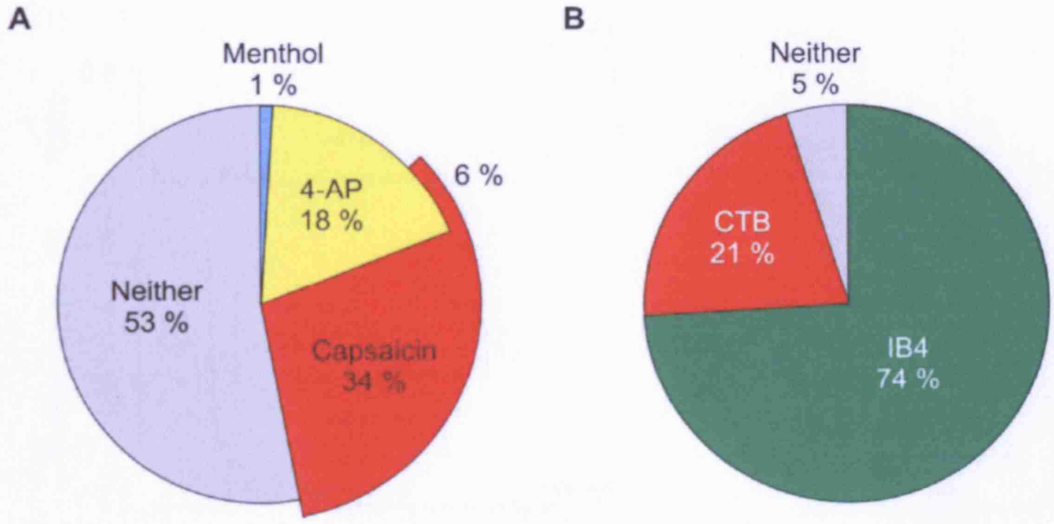

Figure 4.8. Representation of the induced cold population in terms of sensitivity to 4-AP and TRP channel agonists (A) or IB4 and CTB staining (B). $n_{animals}$ = 6, n_{cells} = 365. Data are presented as mean percentage of neurons.

A second broad spectrum potassium channel blocker, TEA, was tested on a total of 1245 DRG neurons (n = 4). 250 (20 ± 2 %) cells responded to an initial cold stimulus, and of the 995 neurons which did not respond, 292 (30 ± 4 %) became cold-sensitive on application of 10 mM TEA (Figure 4.9). Induction of cold sensitivity was not correlated with sensitivity to TEA. 514 (44 ± 5 %) neurons were TEA-responsive, of which 85 (16 ± 3 %) showed an induced cold response. Within the induced cold population, 29 ± 3 % were TEA-sensitive. Neurons were also analysed for sensitivity to TRP channel agonists, and within the induced cold population 1 cell responded to menthol and 102 (32 ± 6 %) to capsaicin.

138 (47 ± 5 %) of the 292 neurons showing an induced cold response following TEA application stained for IB4, while 78 (30 ± 7 %) were CTB-positive (Figure 4.9). Unlike 4-AP therefore, the effects of which were recorded primarily in the IB4-binding non-peptidergic C-fibre population, TEA induced significant levels of cold sensitivity in both IB4- and CTB-positive cells: the ratio of IB4-positive to CTB-positive neurons was 5.3 in the 4-AP-induced population, and just 1.8 in the TEA-induced population.

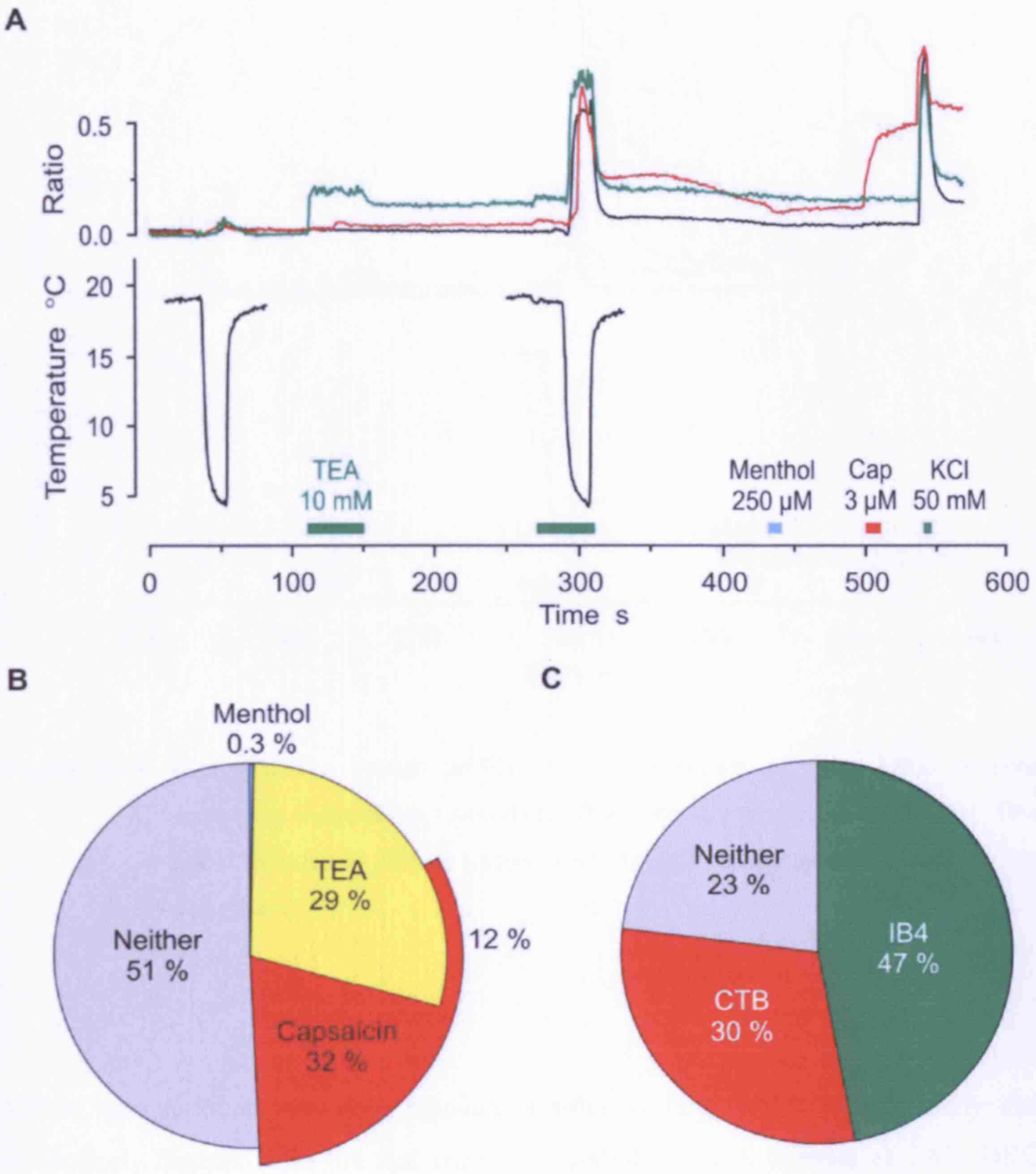

Figure 4.9. (A) Representative kinetic profiles of the responses of three DRG neurons displaying induced cold sensitivity following the application of TEA. One cell responded to TEA (green), and one cell was capsaicin-sensitive (red). None of the cells responded to menthol. (B) Representation of the proportion of neurons displaying induced cold sensitivity that also responded to TEA and TRP channel agonists. (C) Representation of the proportion of neurons displaying induced cold sensitivity that stained for IB4 or CTB. $n_{animals}$ = 4, n_{cells} = 292. Data are presented as mean percentage of neurons.

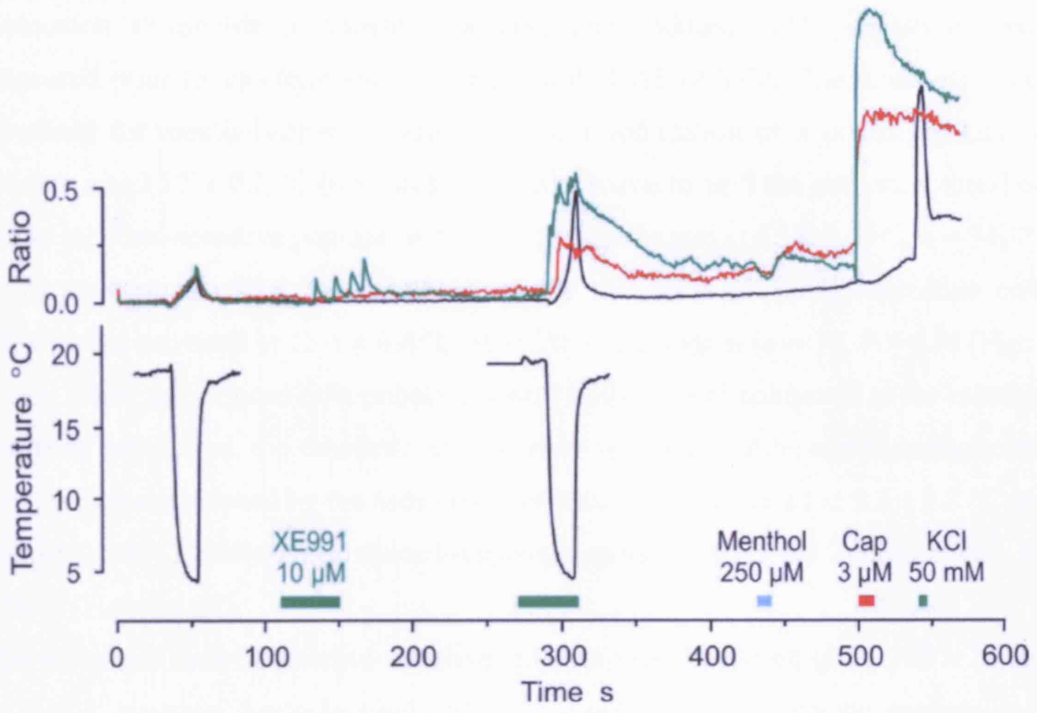

Figure 4.10. Representative kinetic profiles of the responses of three DRG neurons displaying induced cold sensitivity following the application of XE991. One cell responded to XE991 (green) and two cells were capsaicin-sensitive (red and green).

XE991 acts to block the slow delayed rectifier current, which is kinetically and molecularly distinct from the fast current inhibited by TEA. A total of 1246 DRG neurons were tested with XE991 for changes in cold sensitivity ($n = 4$). 281 (23 ± 3 %) neurons showed constitutive cold sensitivity, while 61/965 (6 ± 1 %) cells responded to cold only after the application of 10 µM XE991 (Figure 4.10). However, the same percentage of neurons were found to have an 'induced' cold response in control experiments where the potassium channel blocker was omitted and replaced with ECF. This would suggest that XE991 does not induce a novel cold sensitivity in sensory neurons (see page 106).

Likewise, blockade of the small-conductance calcium-activated potassium channels with 100 nM apamin did not induce cold sensitivity in DRG neurons. 233 cells were analysed and only 4 (2 %) displayed an induced cold response ($n = 2$).

Activation thresholds of menthol-sensitive and induced cold populations were measured prior to and following treatment with 4-AP or TEA. The mean activation threshold for menthol-sensitive neurons before application of a potassium channel blocker was 15.5 ± 0.2 °C (n = 182). 4-AP was found to shift the activation threshold of the menthol-sensitive population to colder temperatures (14.5 ± 0.4 °C, n = 74, $P < 0.05$). In contrast, TEA had no effect on the threshold of menthol-sensitive cells, which were activated at 15.5 ± 0.4 °C after TEA application (n = 75, $P > 0.9$) (Figure 4.11). When the induced cold population was analysed and compared to the menthol-sensitive population, the threshold of activation was found to be significantly colder. Cold responses induced by the application of 4-AP were activated at 9.2 ± 0.2 °C (n = 365, $P < 0.001$), while TEA-induced responses came on at 9.3 ± 0.2 °C (n = 292, $P < 0.001$) (Figure 4.12).

The mean cell area of menthol-sensitive neurons was calculated to be 370 ± 26 μm^2 (n = 60). Neurons displaying induced cold sensitivity following the application of either 4-AP or TEA were significantly larger in size. The 4-AP-induced cold population had a cell area of 479 ± 6 μm^2 (n = 350, $P < 0.001$), while the TEA-induced cold population had a cell size of 484 ± 12 μm^2 (n = 278, $P < 0.001$) (Figure 4.13).

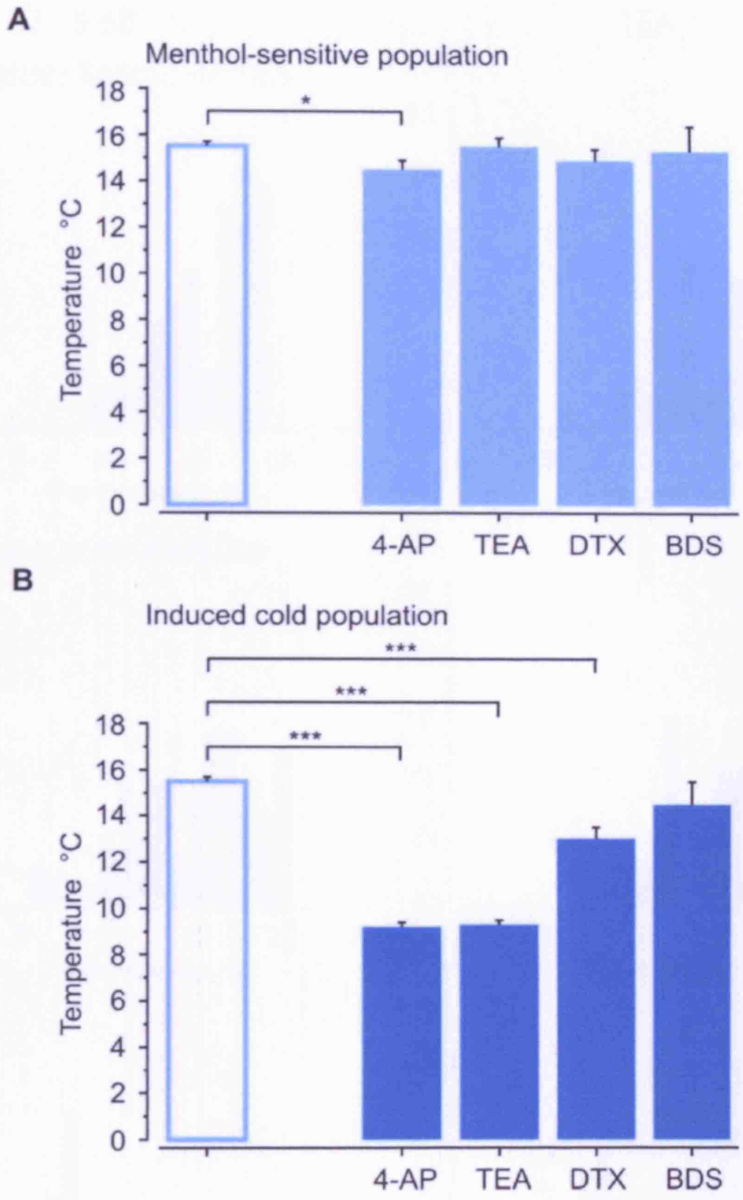

Figure 4.11. (A) Activation thresholds of the menthol-sensitive DRG population before (n = 182) and after application of various potassium channel blockers. 4-AP shifted the threshold to colder temperatures (n = 74), but neither TEA (n = 75), DTX (n = 25) nor BDS (n = 5) affected the activation threshold of menthol-sensitive neurons. (B) Activation thresholds of DRG neurons displaying induced cold sensitivity following the application of various potassium channel blockers. Thresholds of induced cold responses were compared to the threshold of the menthol-sensitive population measured prior to application of the blocker. Cold responses induced by 4-AP (n = 365), TEA (n = 292) and DTX (n = 74) were activated at colder temperatures than menthol-sensitive neurons, while BDS induced cold responses had a similar threshold (n = 33). Data are presented as mean threshold ± SEM. * $P < 0.05$, *** $P < 0.001$ (Student's unpaired t-test).

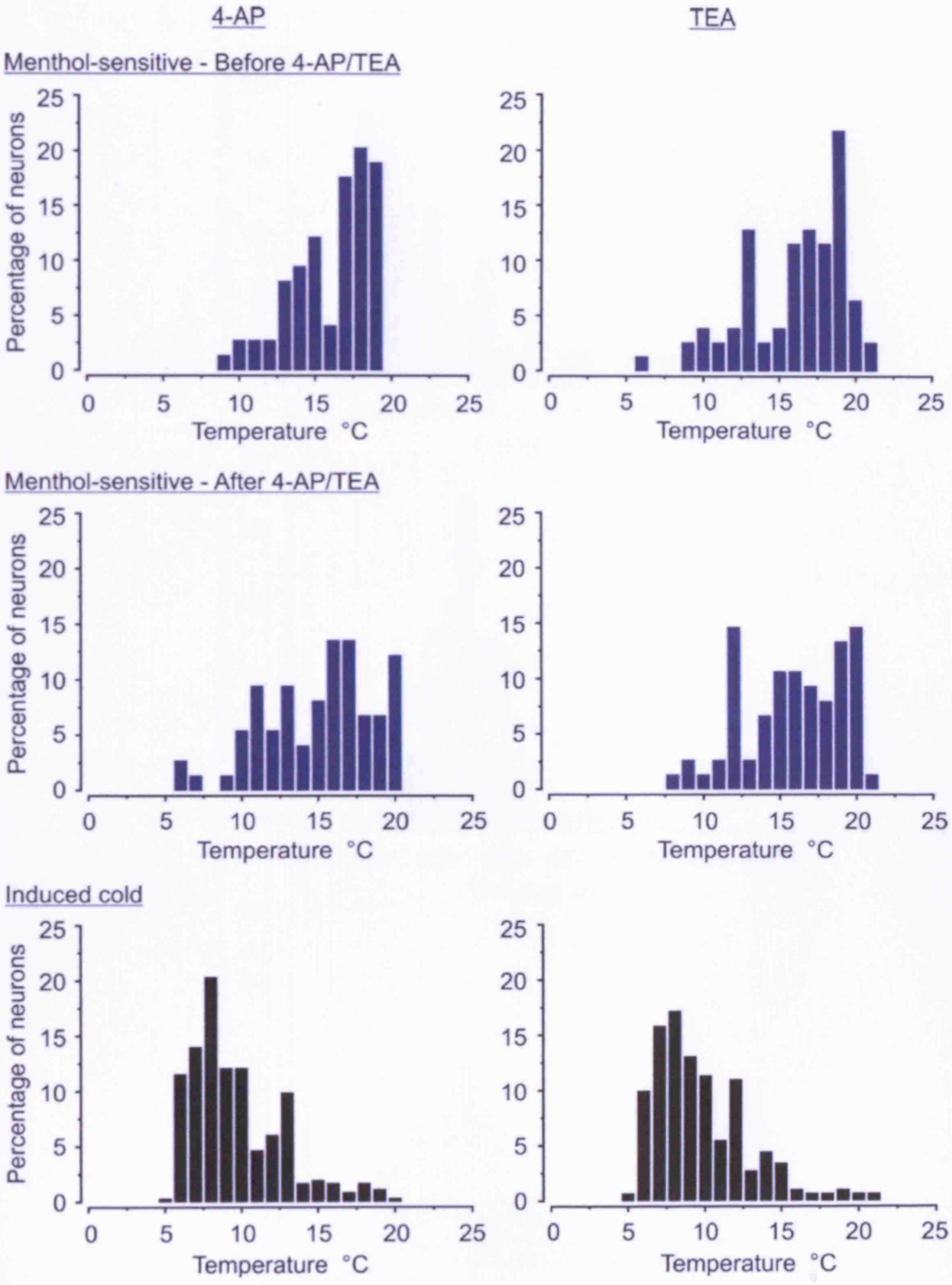

Figure 4.12. Histograms depicting the distribution of menthol-sensitive (blue) and induced cold-sensitive (black) DRG neurons as a function of activation threshold. Thresholds were measured before and after the application of 4-AP (left) or TEA (right). Menthol-sensitive neurons: $n = 74$ (4-AP), $n = 78$ (TEA); induced cold-sensitive neurons: $n = 365$ (4-AP), $n = 292$ (TEA).

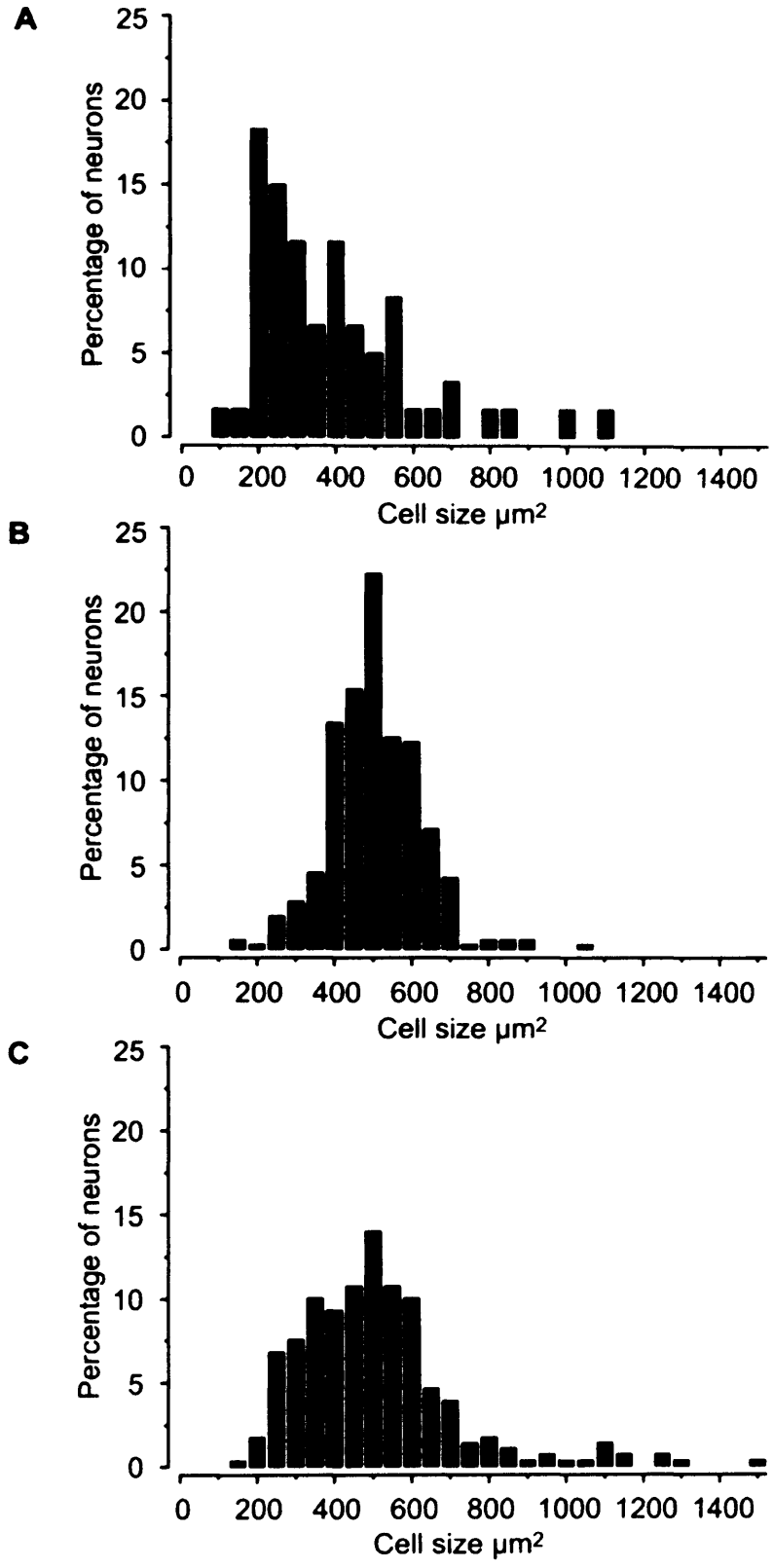

Figure 4.13. (A) Cell size distribution of menthol-sensitive DRG neurons. n = 60. (B) Cell size distribution of 4-AP-induced cold-sensitive DRG neurons. n = 350. (C) Cell size distribution of TEA-induced cold-sensitive DRG neurons. n = 278.

4.4.3. Cold-induced calcium influx in sensory neurons displaying an induced cold response

The 4-AP-induced cold response was studied under calcium-free conditions in order to ascertain whether the observed increase in intracellular calcium was due to an influx of ions from the external milieu (as is the case for constitutive cold responses), or whether it was caused by the release of calcium from intracellular stores. From a total of 208 cells examined, 62 were cold-sensitive in the presence of 4-AP ($n = 2$). In 92 % (57/62) of neurons the cold response was completely abolished following the removal of calcium from the extracellular solution (Figure 4.14).

4.4.4. 4-AP-induced cold sensitivity is not altered at 24 hours

DRG neurons were also assessed for 4-AP-induced cold sensitivity after 24 hours in 50 ng/ml NGF ($n = 4$). 436 neurons were analysed, of which 156 showed constitutive cold sensitivity, and 50 responded to the application of 4-AP. 126/280 previously unresponsive neurons became cold-sensitive in the presence of 4-AP. There was no alteration in the number of neurons either responding to 4-AP or showing an induced cold response at 24 hours compared to acutely dissociated cells (4-AP-sensitive neurons: 14 ± 2 % in acute cultures versus 12 ± 2 % in 24 hour cultures, $P > 0.5$; induced cold sensitivity: 37 ± 5 % in acute cultures versus 46 ± 5 % in 24 hour cultures, $P > 0.2$).

Although the overall percentage of neurons displaying an induced cold response was not altered, there was an increase of induced cold sensitivity within the 4-AP-responsive population. In acute cultures 54/148 (33 ± 6 %) 4-AP-sensitive neurons showed an induced cold response, compared to 26/50 (53 ± 5 %) cells at 24 hours ($P < 0.05$). In contrast there was no change in the number of neurons with induced cold sensitivity that also responded to 4-AP (18 ± 4 % in acute cultures versus 20 ± 3 % in 24 hour cultures, $P > 0.6$).

In line with previous observations that menthol sensitivity is up-regulated in the IB4-positive population at 24 hours, there was a significant increase in the number of cells responding to menthol within the induced cold population. In acutely cultured neurons, only 1 ± 1 % of cells with an induced cold response were menthol-sensitive, but this increased to 15 ± 4 % at 24 hours ($P < 0.01$) (Figure 4.15).

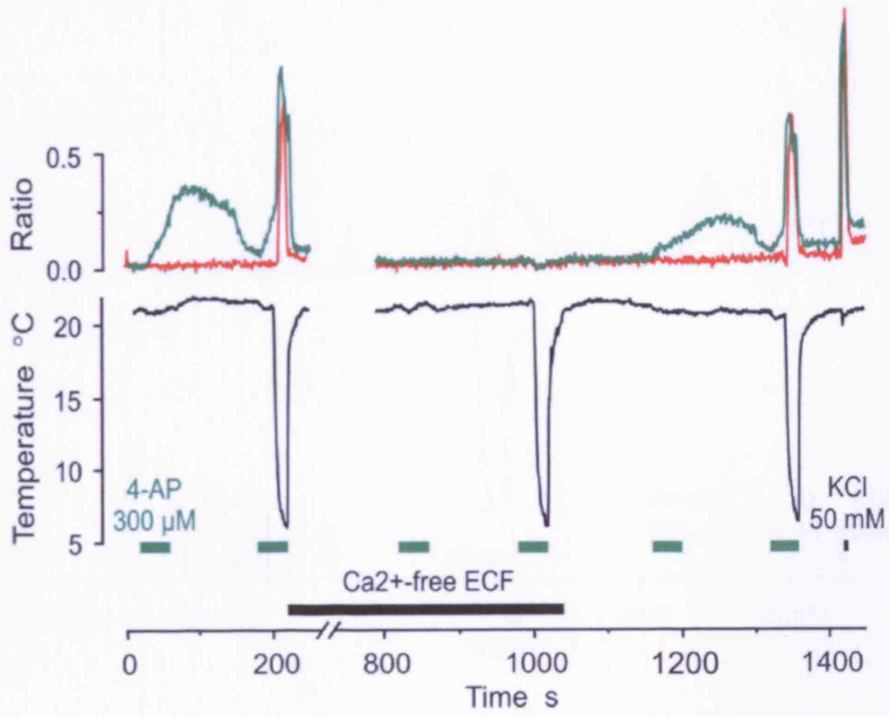

Figure 4.14. Representative kinetic profiles of two cold- and 4-AP-sensitive DRG neurons whose responses were abolished following the removal of calcium from the extracellular solution. Cold and 4-AP responses were restored with the addition of calcium.

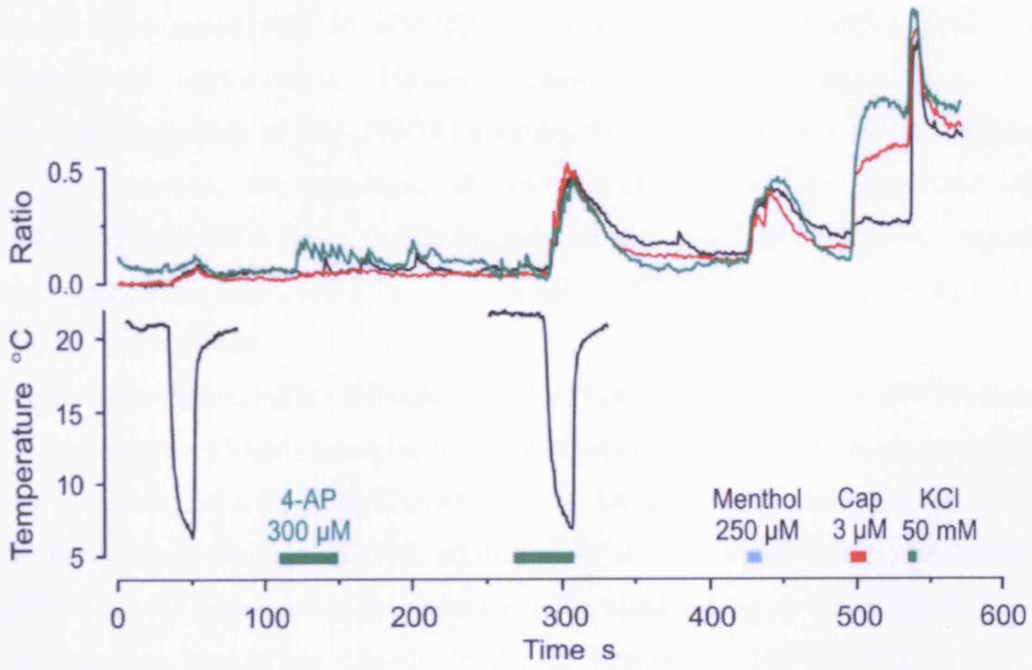

Figure 4.15. Representative kinetic profiles of the responses of three DRG neurons assessed for 4-AP-induced cold sensitivity following 24 hours in culture. One cell was sensitive to 4-AP (green) and two cells responded to capsaicin (green and red). All cells were menthol-sensitive.

4.4.5. Pharmacological blockade of voltage-gated potassium channels induces novel cold sensitivity in sympathetic neurons

Acutely dissociated SCG neurons were similarly tested with a range of potassium channel blockers for alterations to cold sensitivity. A total of 138 neurons were analysed with 300 μM 4-AP (n = 3). 77 (54 ± 6 %) neurons were cold-sensitive, and of the 61 cold-insensitive cells, 21 (35 ± 9 %) showed a novel cold response on the application of 4-AP (Figure 4.16). Only 1 neuron responded to 4-AP itself.

TEA was found to have a much greater effect on SCG neurons than 4-AP. 316 neurons were tested with 10 mM TEA (n = 4), of which 215 (62 ± 8 %) were constitutively cold-sensitive. However, nearly all neurons responded to cold following application of TEA (99/101 neurons, 98 ± 2 %) (Figure 4.16). As observed in DRG neurons, the induction of cold sensitivity was not correlated with responsiveness to TEA. Thus, within the induced cold population, 17 (16 ± 6 %) cells also responded to TEA, while 18 ± 7 % of the 86 TEA-sensitive neurons showed an induced cold response.

In contrast to the negligible influence of XE991 on cold sensitivity in DRG neurons, SCG neurons were highly sensitive to the blockade of KCNQ channels. A total of 597 cells were assessed with 10 μM XE991 (n = 5). 349 (61 ± 8 %) neurons responded to cold before application of XE991, while 162 of the remaining 248 cold-insensitive cells (74 ± 5 %) responded in the presence of the blocker (Figure 4.17). Of the 82 (7 ± 3 %) neurons responding directly to the application of XE991, 31 (14 ± 9 %) belonged to the induced cold population, while just 7 ± 5 % of cells with a novel cold response were XE991-sensitive.

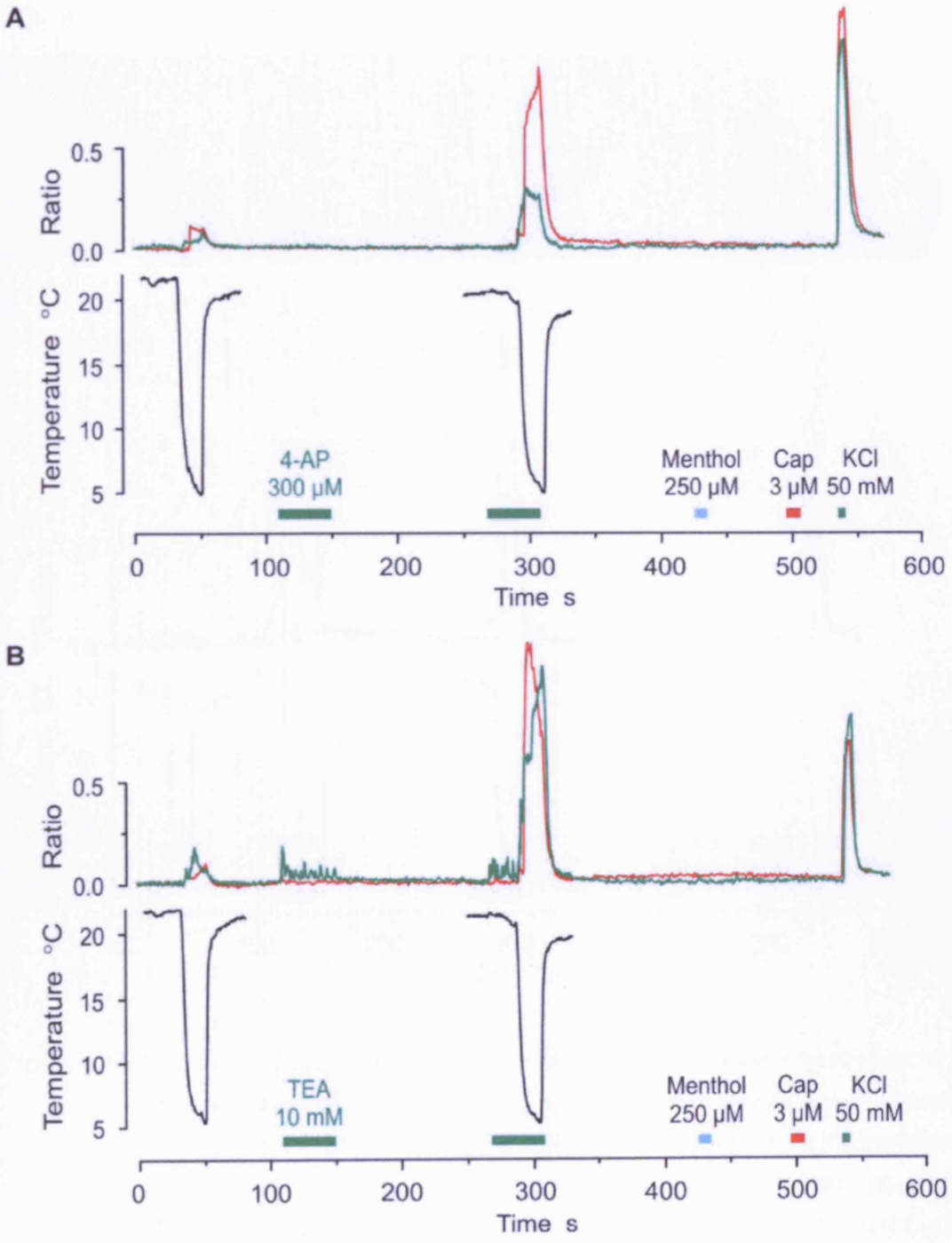

Figure 4.16. (A) Representative kinetic profiles of the responses of two SCG neurons displaying induced cold sensitivity following the application of 4-AP. (B) Representative kinetic profiles of the responses of two SCG neurons displaying induced cold sensitivity following the application of TEA. One cell was TEA-sensitive (green).

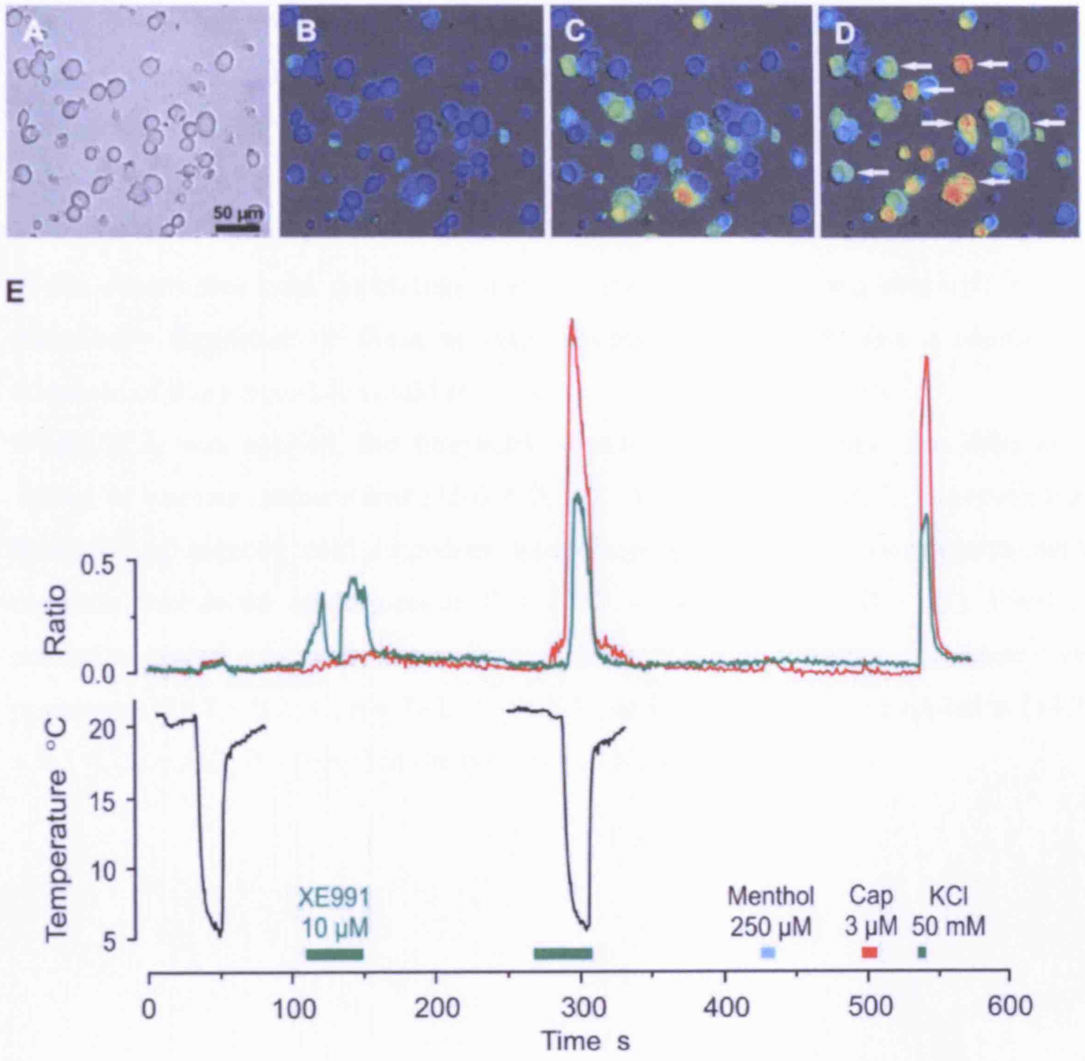

Figure 4.17. Fura fluorescence images of acutely dissociated SCG neurons responding to a brief cold stimulus before and during application of the Kv potassium channel blocker XE991. (A) Brightfield image. (B) Background Fura fluorescence. (C) SCG neurons responding to cold before the application of XE991. (D) SCG neurons responding to cold during the application of 10 µM XE991. Cells displaying induced cold sensitivity are marked with an arrow. (E) Representative kinetic profiles of the responses of two SCG neurons displaying induced cold sensitivity following the application of XE991. One cell was XE991-sensitive (green).

The different potassium channel blockers had varied effects on the activation threshold of constitutive and induced cold responses. Constitutively cold-sensitive SCG neurons had an activation threshold of 12.9 ± 0.1 °C before application of a potassium channel blocker (n = 640). In the presence of 4-AP both the constitutive and induced cold populations were activated at colder temperatures (constitutive cold population: 12.1 ± 0.3 °C, n = 73, $P < 0.05$; induced cold population: 9.9 ± 0.5 °C, n = 21, $P < 0.001$) (Figure 4.18). It should be noted that the shift in activation threshold in the constitutive cold population was however very small, and although it was statistically significant in these in vitro studies, it is unlikely that a change in threshold of this magnitude would prove to be physiologically relevant.

When TEA was applied, the threshold of constitutively cold-sensitive cells was shifted to warmer temperatures (16.6 ± 0.2 °C, n = 215, $P < 0.001$). However, the threshold of induced cold responses was closer to that of the constitutive cold response prior to the application of TEA (13.5 ± 0.4 °C, n = 99, $P > 0.1$). Warmer activation thresholds were recorded in both the constitutively cold-sensitive population (14.8 ± 0.2 °C, n = 347, $P < 0.001$), and the induced cold population (14.7 ± 0.3 °C, n = 162, $P < 0.001$) in the presence of XE991 (Figure 4.19).

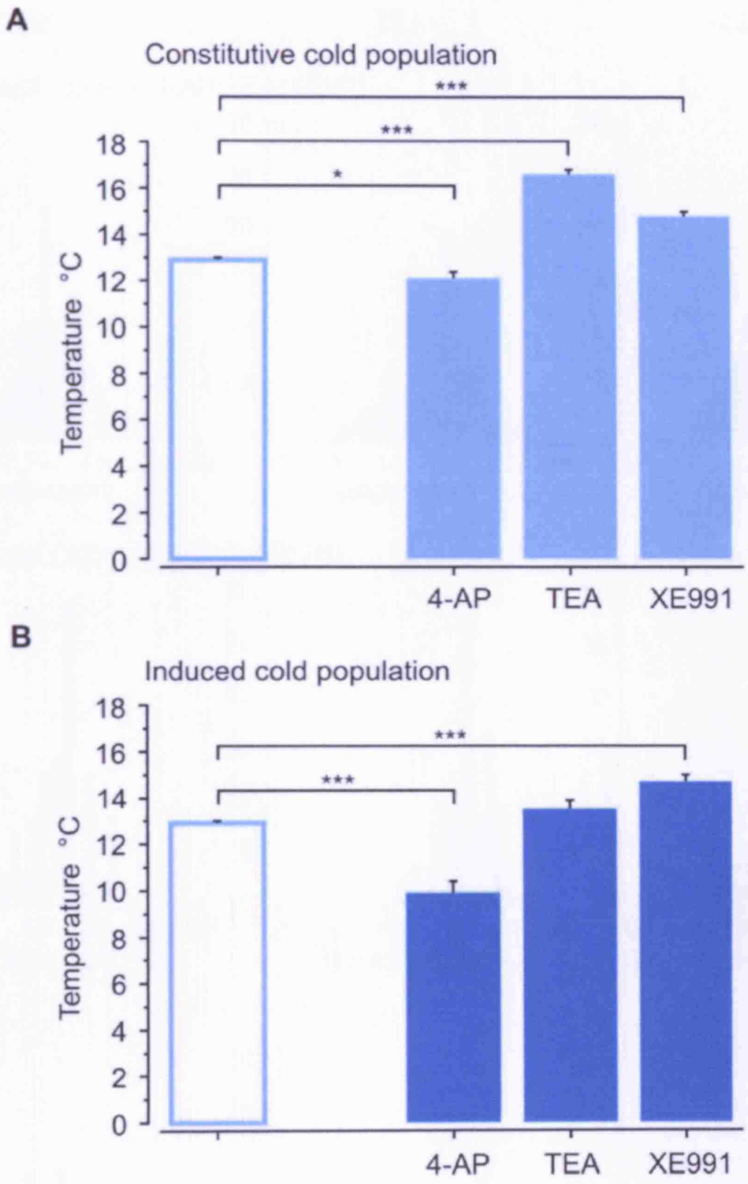

Figure 4.18. (A) Activation thresholds of constitutively cold-sensitive SCG neurons before (n = 640) and after application of various potassium channel blockers. 4-AP shifted the threshold to colder temperatures (n = 73), while TEA (n = 215) and XE991 (n = 347) shifted the threshold to warmer temperatures. (B) Activation thresholds of SCG neurons displaying induced cold sensitivity following the application of various potassium channel blockers. Thresholds of induced cold responses were compared to the threshold of constitutive cold responses measured prior to application of the blocker. Cold responses induced by 4-AP were activated at colder temperatures than constitutive cold responses (n = 21), while XE991-induced cold responses had a warmer activation threshold (n = 162). The threshold of cold responses induced by TEA did not differ from the constitutive cold response (n = 99). Data are presented as mean threshold ± SEM. * $P < 0.05$, *** $P < 0.001$ (Student's unpaired t-test).

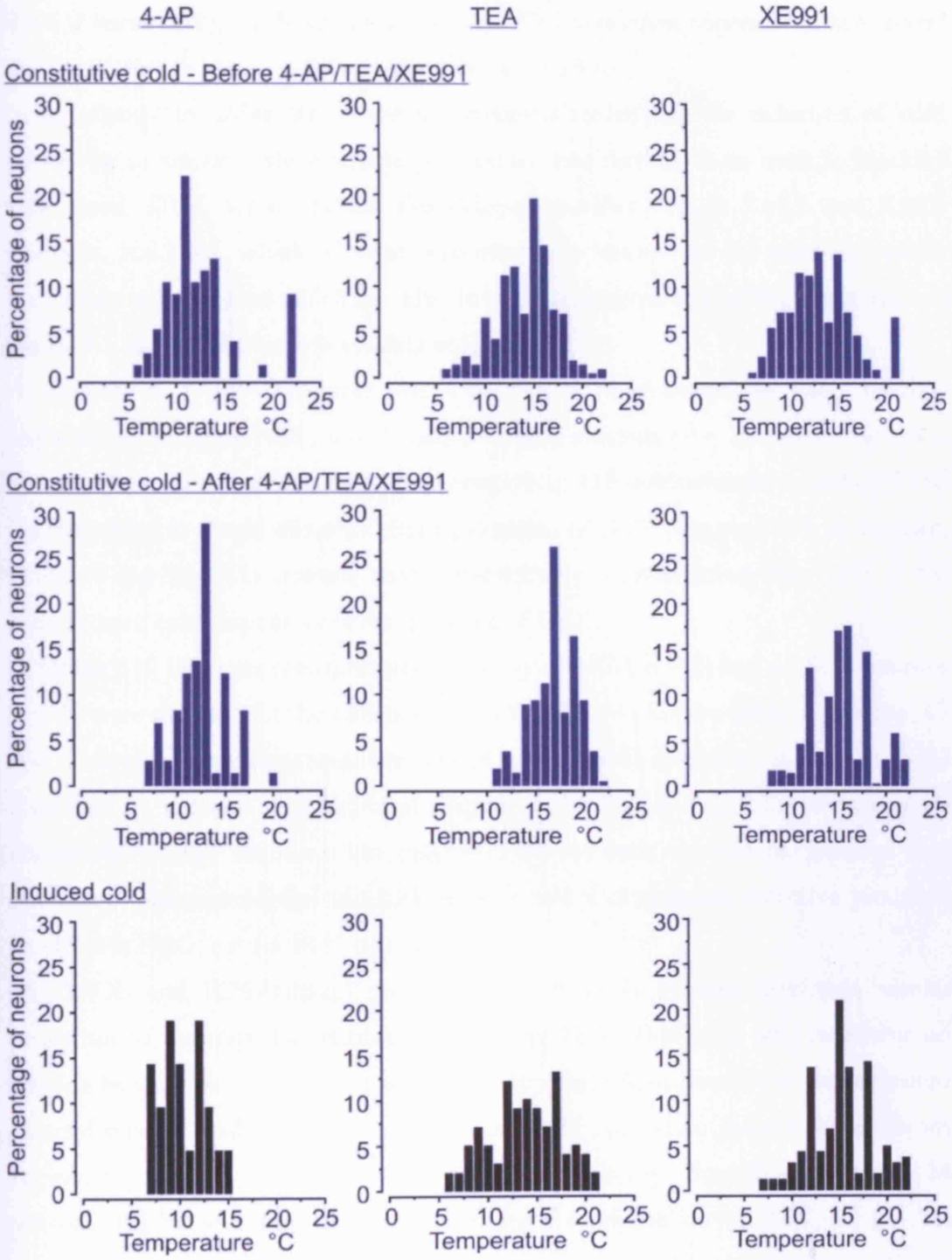

Figure 4.19. Histograms depicting the distribution of constitutively cold-sensitive (blue) and induced cold-sensitive (black) SCG neurons as a function of activation threshold. Thresholds were measured before and after the application of 4-AP (left), TEA (middle) or XE991 (right). Constitutively cold-sensitive neurons: n = 77 (4-AP), n = 215 (TEA), n = 348 (XE991); induced cold-sensitive neurons: n = 21 (4-AP), n = 99 (TEA), n = 162 (XE991).

4.4.6. Pharmacological blockade of Kv1 and Kv3 potassium channels induces novel cold sensitivity in sensory, but not sympathetic, neurons

In an attempt to define the potassium channels underlying the induction of cold sensitivity in sensory and sympathetic neurons, two further, more specific blockers were used: DTX, which blocks the delayed rectifier Kv1.1, Kv1.2 and Kv1.6 channels, and BDS, which is commonly used as a blocker for the transient current mediated via Kv3.4, but which has also been demonstrated to inhibit current through the Kv3.1 and Kv3.2 channels (Yeung et al., 2005).

A solution of 1 μM DTX was tested on 504 acutely dissociated DRG neurons (cultured in 50 ng/ml NGF, n = 2) and 170 SCG neurons (n = 2). 94 (19 %) DRG neurons were cold-sensitive and of the remaining 410 cold-insensitive cells, 74 (18 %) responded to a cold stimulus after application of DTX (Figure 4.20). In contrast, while 79 (44 %) SCG neurons were constitutively cold-sensitive, only 2/91 (3 %) cells became cold-responsive in the presence of DTX.

A further 319 DRG neurons (cultured in 50 ng/ml NGF, n = 2) and 41 SCG neurons (n = 2) were assessed for the effects of 250 nM BDS. Within the DRG population, 43 (14 %) neurons were cold-sensitive, and of the 276 cold-insensitive cells, 33 (13 %) displayed an induced cold response (Figure 4.21). 20 (50 %) SCG neurons were constitutively cold sensitive, but only 1/21 (4 %) cells showed an induced cold sensitivity. Pharmacological blockade of Kv1 and Kv3 channels therefore produced an effect in DRG, but not SCG neurons.

The DTX- and BDS-induced cold response in DRG neurons displayed similar properties to the response induced by 4-AP or TEA. That is to say, there was no relation between the induction of cold sensitivity and responsiveness to the potassium channel blocker, and that within the induced cold population there was significant capsaicin sensitivity, but very little menthol sensitivity. Specifically, of the 74 neurons that became cold-sensitive following the application of DTX, 32 (44 %) responded to DTX itself, 41 (56 %) were sensitive to capsaicin, and only 1 cell was menthol-sensitive. 85 (17 %) neurons were DTX-sensitive, of which 39 % showed an induced cold response. Neurons were additionally analysed for binding of the cell-specific markers IB4 and CTB. Within the induced cold population, 40 (54 %) were IB4-positive and 15 (20 %) stained for CTB (Figure 4.20).

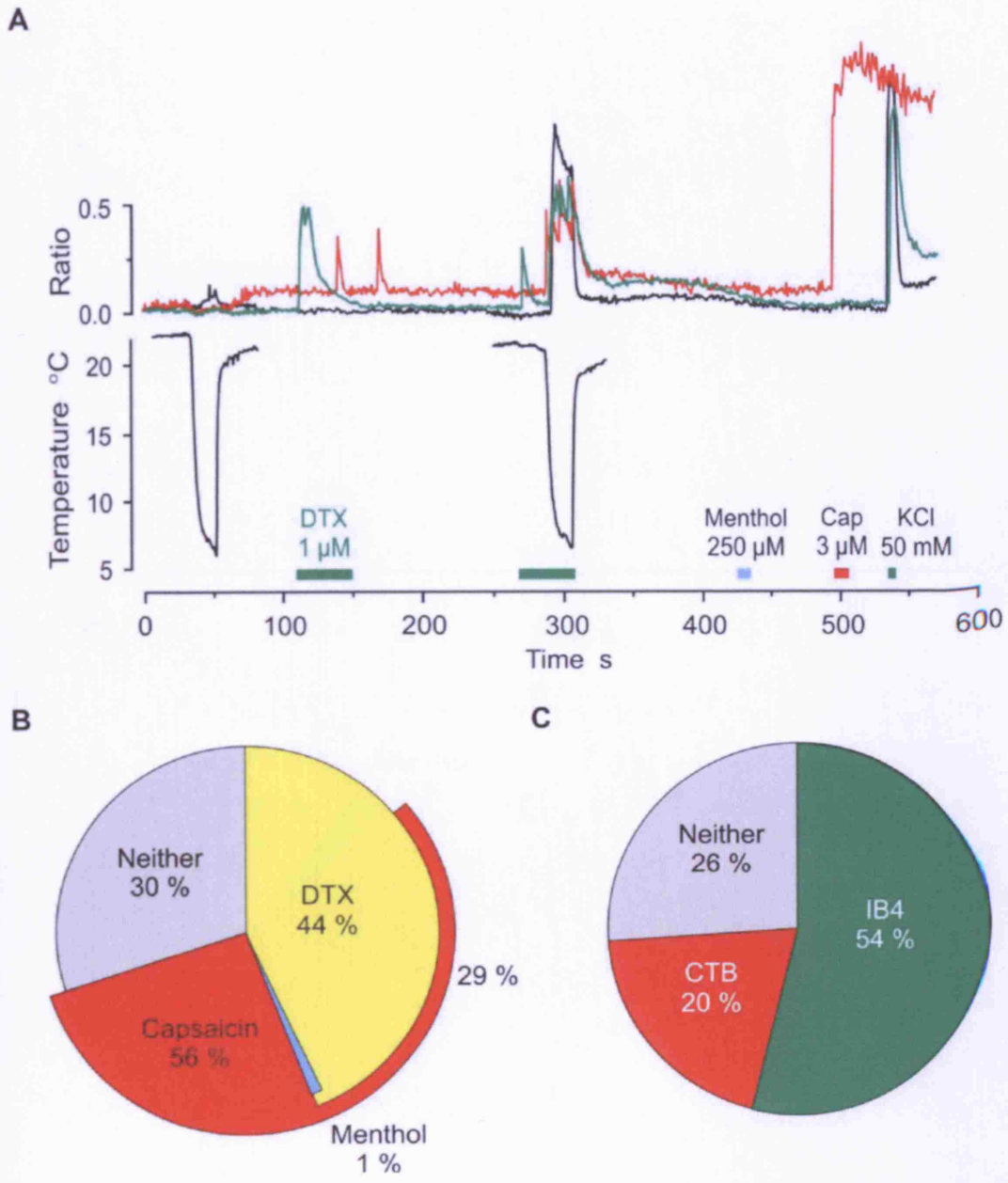

Figure 4.20. (A) Representative kinetic profiles of the responses of three DRG neurons displaying induced cold sensitivity following the application of DTX. One cell responded to DTX (green), and one cell was capsaicin-sensitive (red). None of the cells responded to menthol. (B) Representation of the proportion of neurons displaying induced cold sensitivity that also responded to DTX and TRP channel agonists. (C) Representation of the proportion of neurons displaying induced cold sensitivity that stained for IB4 or CTB. $n_{animals} = 2$, $n_{cells} = 74$. Data are presented as mean percentage of neurons.

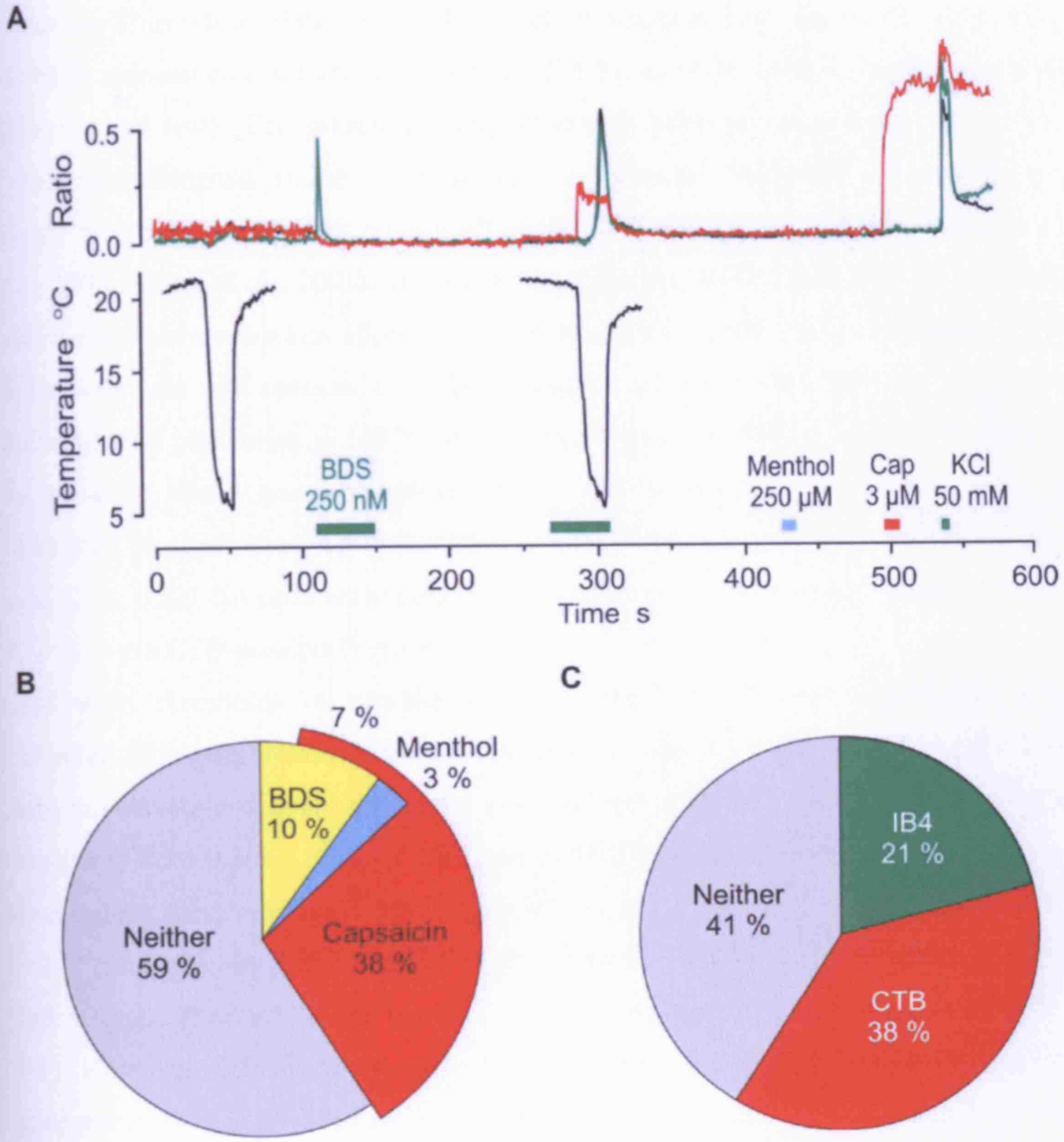

Figure 4.21. (A) Representative kinetic profiles of the responses of three DRG neurons displaying induced cold sensitivity following the application of BDS. One cell responded to BDS (green), and one cell was capsaicin-sensitive (red). None of the cells responded to menthol. (B) Representation of the proportion of neurons displaying induced cold sensitivity that also responded to BDS and TRP channel agonists. (C) Representation of the proportion of neurons displaying induced cold sensitivity that stained for IB4 or CTB. $n_{animals} = 1$, $n_{cells} = 29$. Data are presented as percentage of neurons.

Two variants of BDS were tested, both of which are described as blockers of Kv3.4, but which were found to have very different effects on cold sensitivity in DRG neurons. Thus while BDS I induced a novel cold response in only 4/149 (3 %) cells, BDS II induced cold sensitivity in 29/127 (23 %) cells ($P < 0.001$, Yates' corrected Chi-squared test). The reason for the observed difference in potency is unclear. Electrophysiological studies monitoring Kv3 channel inhibition in heterologous expression systems reported similar efficacies between the two isoforms (Diochot et al., 1998;Yeung et al., 2005). It may be the case that BDS I and BDS II will react differently however when administered to primary cultures. As a consequence, the following data will concern only those neurons assessed with BDS II. Within the induced cold population, 3 (10 %) cells were sensitive to BDS, 11 (38 %) responded to capsaicin, and 1 was menthol-sensitive. 13 (9 %) neurons responded to BDS, of which 23 % showed an induced cold response. When neurons were stained for IB4 and CTB, 6 (21 %) cells with induced cold sensitivity were also IB4-positive and 11 (38 %) were CTB-positive (Figure 4.21).

Activation thresholds of menthol-sensitive and induced cold populations were recorded following treatment with DTX or BDS, and compared to the thresholds of menthol-sensitive neurons measured prior to application of the potassium channel blocker (15.5 ± 0.2 °C). Neither DTX nor BDS affected the threshold for activation of menthol-sensitive neurons (DTX: 14.9 ± 0.5 °C, $n = 25$, $P > 0.3$; BDS: 15.3 ± 1 °C, $n = 5$, $P > 0.8$) (Figure 4.11). In addition cold responses induced in the presence of BDS had a similar threshold to the menthol-sensitive population (14.5 ± 1 °C, $n = 33$, $P > 0.1$). However, DTX-induced cold responses were activated at significantly colder temperatures (13 ± 0.5 °C, $n = 74$, $P < 0.001$) (Figure 4.22).

The cell area of neurons showing an induced cold response was measured, and, as reported for the 4-AP- and TEA-induced cold-sensitive neurons, was found to be significantly larger than the menthol-sensitive population. DTX-induced cold-sensitive cells had an area of 464 ± 20 μm^2 ($n = 72$, $P < 0.01$), and the BDS-induced cold population had a cell area of 535 ± 59 μm^2 ($n = 28$, $P < 0.001$) (Figure 4.23).

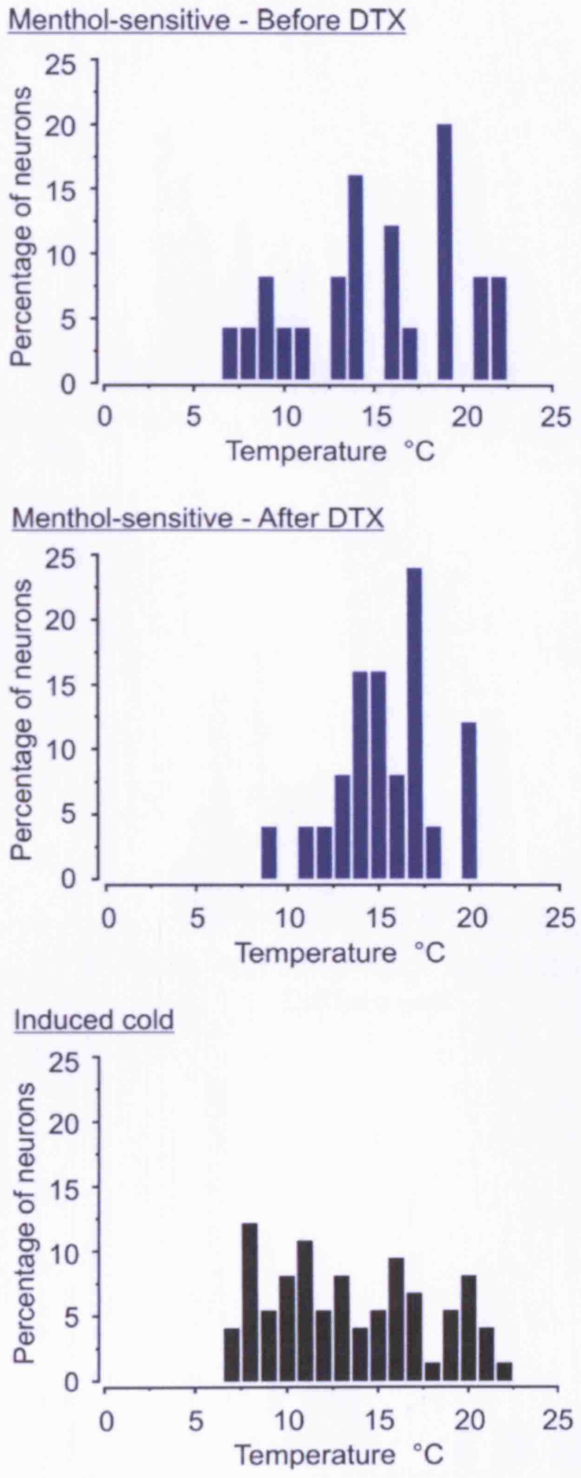

Figure 4.22. Histograms depicting the distribution of menthol-sensitive (blue) and induced cold-sensitive (black) DRG neurons as a function of activation threshold. Thresholds were measured before and after the application of DTX. Menthol-sensitive neurons: $n = 25$; induced cold-sensitive neurons: $n = 74$.

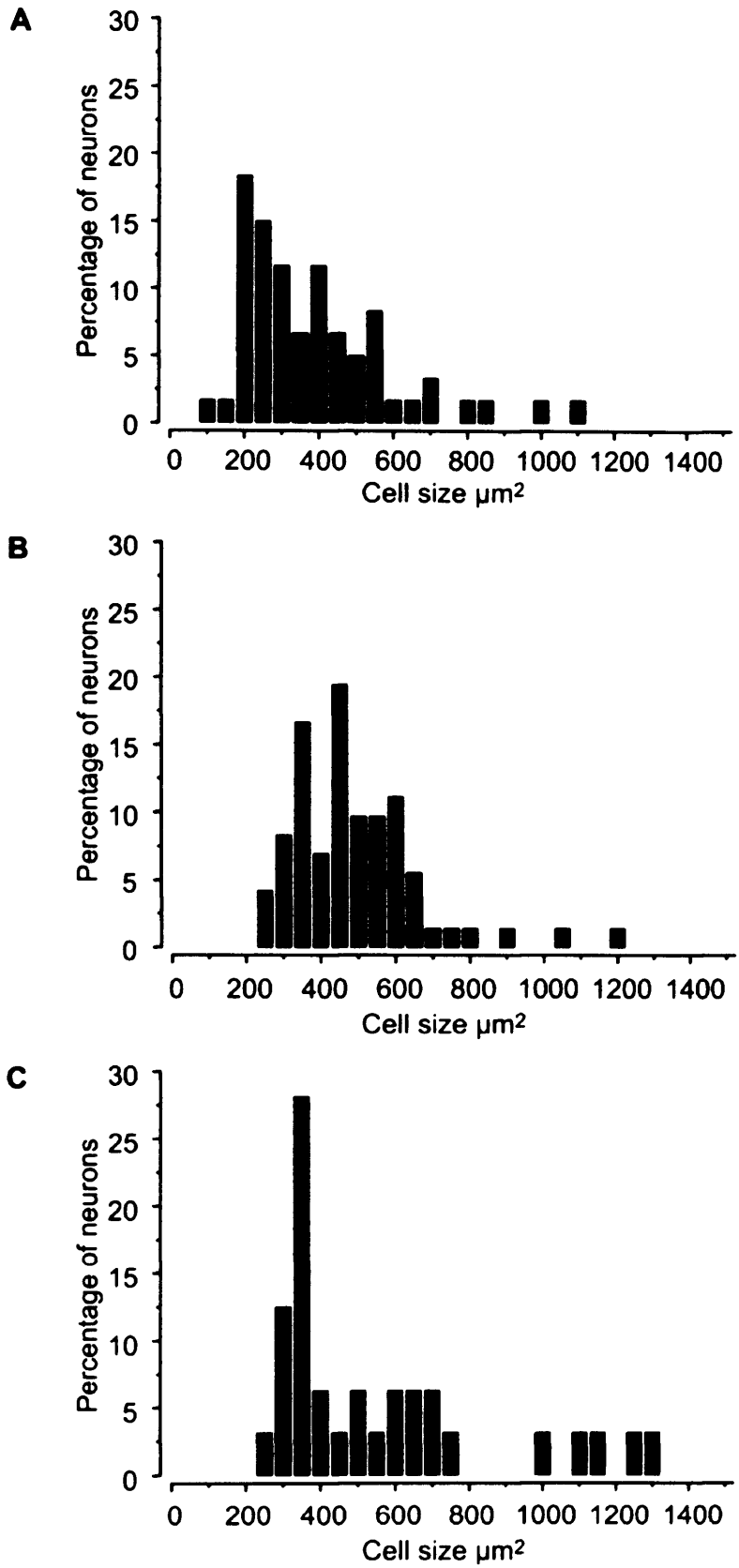

Figure 4.23. (A) Cell size distribution of menthol-sensitive DRG neurons. n = 60. (B) Cell size distribution of DTX-induced cold-sensitive DRG neurons. n = 72. (C) Cell size distribution of BDS-induced cold-sensitive DRG neurons. n = 28.

4.4.7. Sympathetic neurons express Kv1 and Kv3 potassium channels

It has been previously reported that the SCG expresses both Kv1 and Kv3 potassium channels (Dixon and McKinnon, 1996). This being the case, the observed differences in the induction of cold sensitivity in functional studies may be due to variation in expression between the DRG and SCG. To assess this possibility, quantitative rt-PCR was used to investigate Kv1 and Kv3 channel expression in sensory and sympathetic neurons ($n = 3$).

As observed in previous experiments the two housekeeping genes UCHL1 and GAPDH were expressed at similar levels in DRG and SCG, with mean cycle threshold (Ct) values of 27.9 ± 1 and 29.1 ± 0.4 for UCHL1 in DRG and SCG, respectively ($P > 0.3$), and 28.5 ± 0.3 and 29.2 ± 0.7 for GAPDH ($P > 0.3$). DTX specifically targets three members of the Kv1 subfamily, Kv1.1, Kv1.2 and Kv1.6, and all three transcripts were expressed in both DRG and SCG (Figure 4.24). In the DRG Kv1.1 and Kv1.2 were expressed at similar levels, but there was lower expression of Kv1.6. The mean difference in Ct between UCHL1 and the potassium channels was 3.5 ± 0.3 for Kv1.1, 3.6 ± 0.3 for Kv1.2, and 5.3 ± 0.7 for Kv1.6.

In the SCG, expression of Kv1.6 was similar to that observed in the DRG (mean difference in Ct between UCHL1 and Kv1.6 was 5 ± 1), but Kv1.1 and Kv1.2 were both expressed at lower levels. The mean difference in Ct between UCHL1 and the potassium channels was 4.7 ± 0.6 for Kv1.1 and 6.5 ± 1.4 for Kv1.2. Normalisation of expression relative to UCHL1 or GAPDH showed that Kv1.1 had a 2-fold or 3-fold higher expression level, respectively, in the DRG compared to SCG, while Kv1.2 was expressed 8-fold or 13-fold more, respectively. There was no difference in expression levels of Kv1.6 (Figures 4.24 and 4.25).

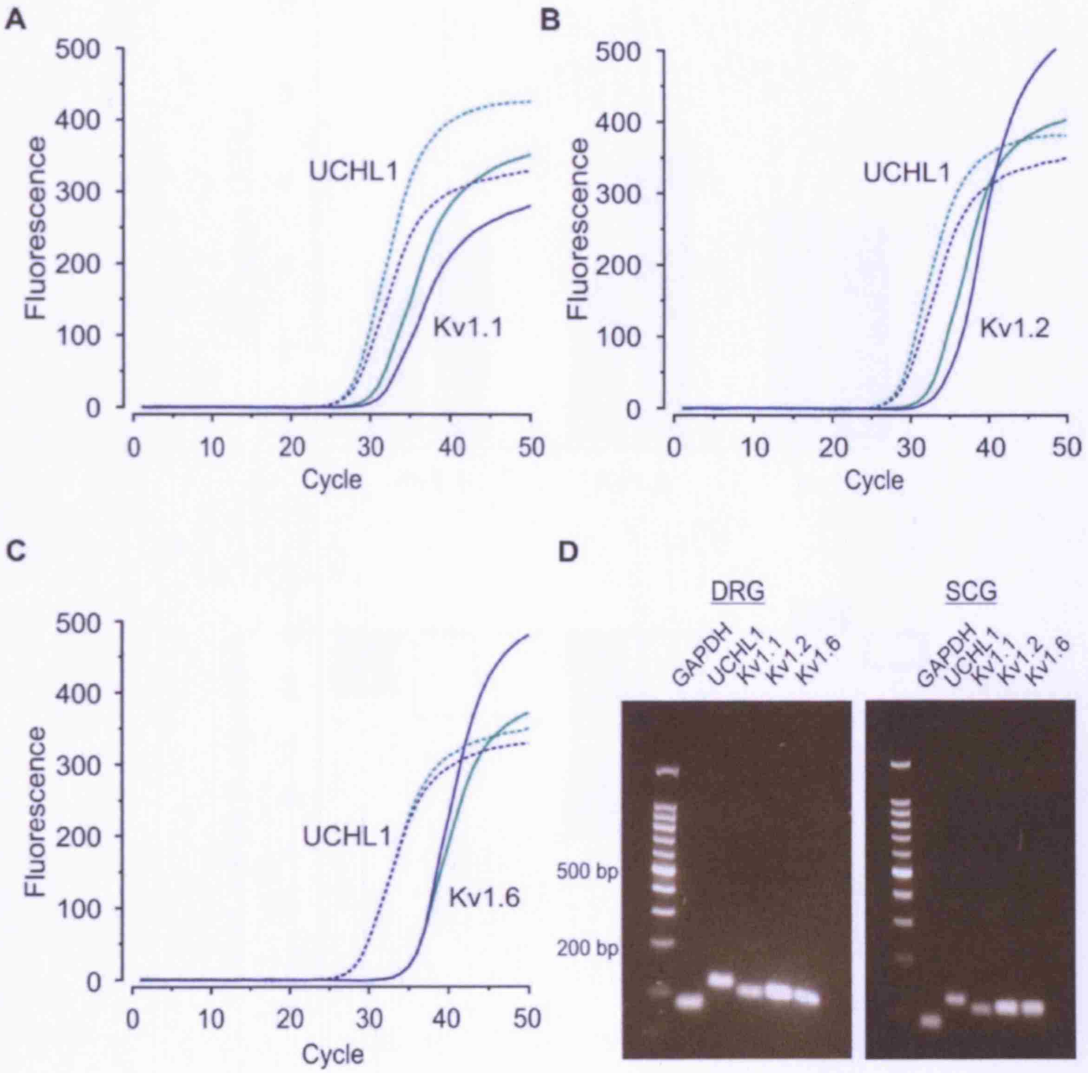

Figure 4.24. Quantitative rt-PCR for Kv1 channel expression in DRG and SCG. The cDNA of 250pg total RNA equivalents were amplified. (A-C) Illustration of rt-PCR for UCHL1 and Kv1.1 (A), Kv1.2 (B), or Kv1.6 (C). The cycle threshold (Ct) values for UCHL1 were similar in DRG (green) and SCG (blue). There was a lower Ct value for both Kv1.1 and Kv1.2 in DRG compared to SCG, but Kv1.6 was expressed at similar levels. (D) All PCR products were analysed on a 2 % agarose gel. Estimated product sizes were 81 bp (GAPDH), 117 bp (UCHL1) and 100 bp (Kv1.1, Kv1.2, Kv1.3).

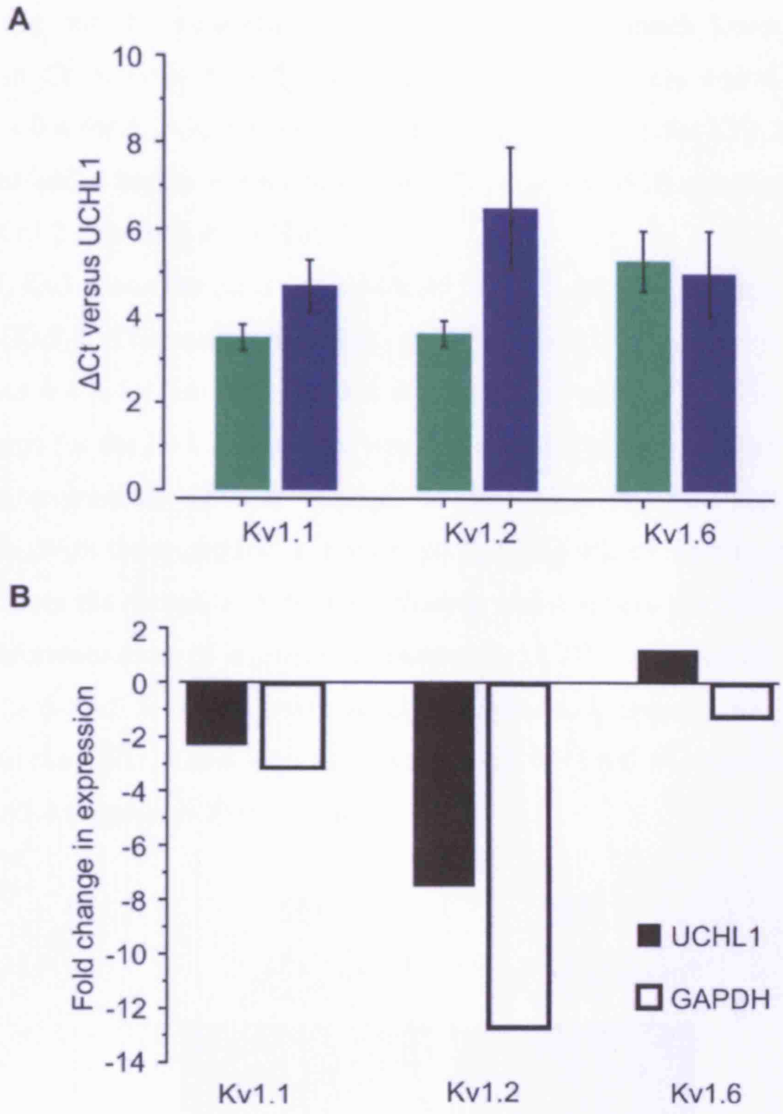

Figure 4.25. (A) Difference in cycle threshold (Ct) values between UCHL1 and the Kv1 potassium channels in DRG (green) and SCG (blue). The cDNA of 250 pg total RNA equivalents were added to all PCR reactions. Data are presented as mean difference in Ct ± SEM. (B) Quantification of the difference in Kv1 channel expression in the SCG compared to the DRG, relative to the expression of UCHL1 or GAPDH. Kv1.1 and Kv1.2 are expressed at lower levels in the SCG, but there is no difference in the expression of Kv1.6 between the two ganglia.

The DRG was also found to express all four members of the Kv3 subfamily of potassium channels (Figure 4.26). Kv3.1, Kv3.3 and Kv3.4 were all expressed at similar levels, but the expression levels of Kv3.2 were much lower. The mean difference in Ct between UCHL1 and the potassium channels was 6.1 ± 1.3 for Kv3.1, 5.6 ± 0.4 for Kv3.3, 5.3 ± 0.4 for Kv3.4, and 8.8 ± 1.5 for Kv3.2. It was also necessary to add a higher concentration of cDNA to the PCR reaction in order to detect the Kv3.2 transcript in the DRG.

In the SCG, Kv3.4 was the most prominent of the Kv3 channels present, followed by Kv3.1 and Kv3.3. The mean difference in Ct between UCHL1 and the potassium channels was 6.4 ± 1.1 for Kv3.1, 3.3 ± 0.6 for Kv3.3 and 5.3 ± 0.03 for Kv3.4. A positive signal for the Kv3.2 transcript was detected in only one of the three samples tested, and expression of this channel in the SCG therefore appears to be insignificant. With the exception of Kv3.4, greater amounts of starting material were needed to detect the presence of the Kv3 channel transcripts in the SCG compared to the DRG. Normalisation of expression relative to UCHL1 or GAPDH showed that Kv3.1 had a 6-fold or 8-fold lower level of expression, respectively, in the SCG compared to the DRG. There was no difference in the level of expression of either Kv3.3 or Kv3.4 (Figures 4.27 and 4.28).

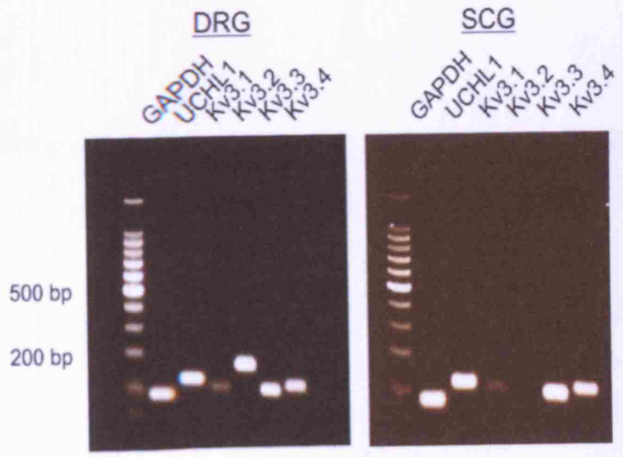

Figure 4.26. Kv3 potassium channel expression in DRG and SCG. All PCR products were analysed on a 2 % agarose gel. All four Kv3 transcripts were expressed in the DRG, but only three channels, Kv3.1, Kv3.3 and Kv3.4, were expressed at significant levels in the SCG. Estimated product sizes were 81 bp (GAPDH), 117 bp (UCHL1), 101 bp (Kv3.1), 150 bp (Kv3.2), 93 bp (Kv3.3) and 109 bp (Kv3.4).

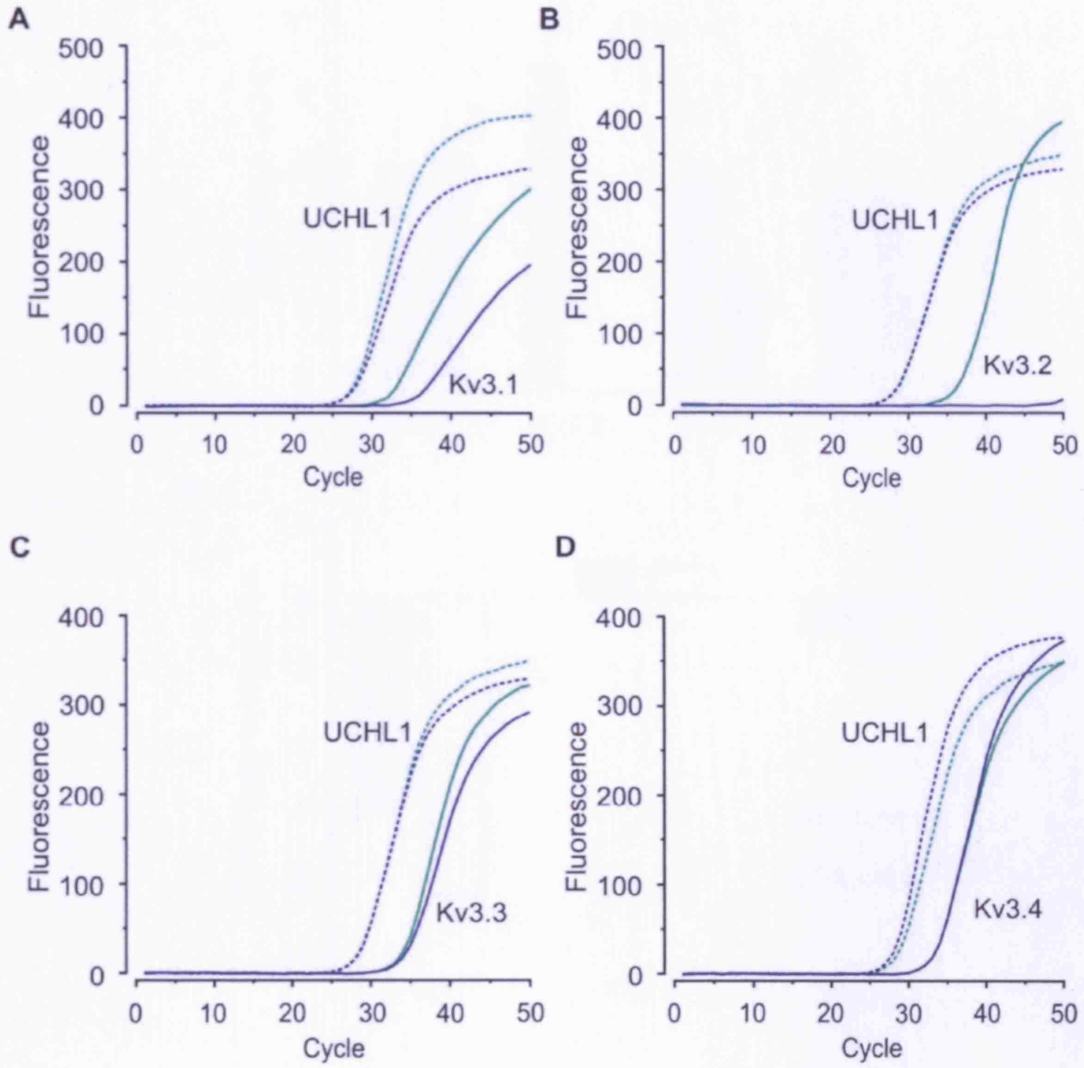

Figure 4.27. Quantitative rt-PCR for Kv3 channel expression in DRG and SCG. The cDNA of 250 pg (UCHL1, GAPDH, Kv3.4), 1.25 ng (Kv3.1, Kv3.3) or 3 ng (Kv3.2) total RNA equivalents were amplified. (A-D) Illustration of rt-PCR for UCHL1 and Kv3.1 (A), Kv3.2 (B), Kv3.3 (C), or Kv3.4 (D). The cycle threshold (Ct) values for UCHL1 were similar in DRG (green) and SCG (blue). There was a lower Ct value for Kv3.1 in DRG compared to SCG, but Kv3.3 and Kv3.4 were expressed at similar levels. Kv3.2 was not expressed in the SCG.

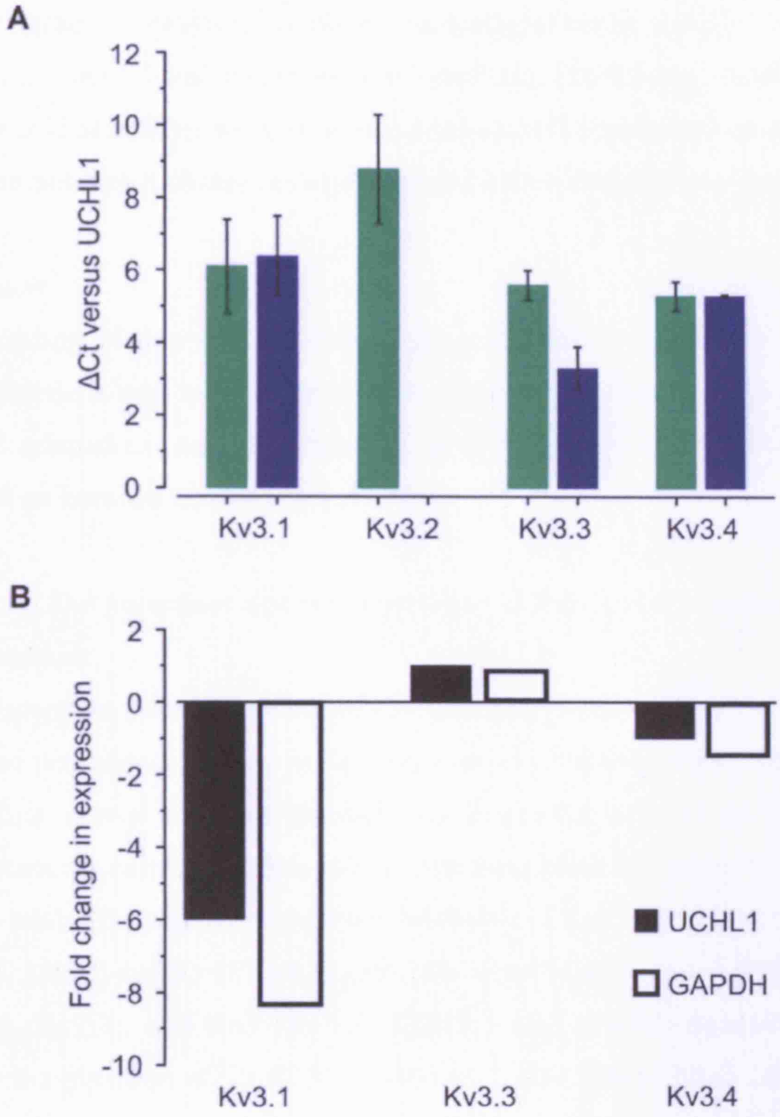

Figure 4.28. (A) Difference in cycle threshold (Ct) values between UCHL1 and the Kv3 potassium channels in DRG (green) and SCG (blue). For the DRG, cDNA of 250 pg (Kv3.1, Kv3.3 and Kv3.4) or 1.25 ng (Kv3.2) total RNA equivalents were amplified. For the SCG, cDNA of 250 pg (Kv3.4), 1.25 ng (Kv3.1 and Kv3.3) or 3 ng (Kv3.2) total RNA equivalents were amplified. Data are presented as mean difference in Ct ± SEM. (B) Quantification of the difference in Kv3 channel expression in the SCG compared to the DRG, relative to the expression of UCHL1 or GAPDH. Kv3.1 is expressed at lower levels in the SCG, but there is no difference in the expression of Kv3.3 or Kv3.4 between the two ganglia. Kv3.2 is not expressed in the SCG.

The rt-PCR data confirm that while both the DRG and the SCG express Kv1 and Kv3 potassium channels, expression levels are generally lower in the SCG compared to the DRG. This would therefore support the hypothesis that the lack of effect of DTX and BDS on cold sensitivity in sympathetic neurons in the functional studies is due to differences in potassium channel expression between the two neuronal populations.

4.5. Discussion

The main finding of this study is that pharmacological blockade of voltage-gated potassium channels can induce novel cold sensitivity in previously unresponsive sensory and sympathetic neurons, although the specific complement of ion channels involved differs between neuronal populations.

4.5.1. Kv1 and Kv3 potassium channels contribute to the regulation of cold sensitivity in sensory neurons

Two broad spectrum potassium channel blockers were used to investigate the role of voltage-gated potassium channels in the regulation of cold sensitivity. Both 4-AP and TEA can block several different channels, encompassing both delayed rectifier and transient potassium currents. At the concentrations used in this study 4-AP would be expected to inhibit the activity of members of the Kv1 (Kv1.1, Kv1.3, Kv1.4, Kv1.5), Kv3 (Kv3.1, Kv3.2) and Kv4 (Kv4.3) subfamilies, while Kv1 (Kv1.1, Kv1.3, Kv1.6), Kv2 (Kv2.1, Kv2.2), and Kv3 (Kv3.1, Kv3.2, Kv3.3, Kv3.4) channels would be affected by the presence of TEA (see Table 1.2). The two blockers were found to induce a novel response to cold in 30-40 % of previously insensitive DRG neurons. These figures are in good agreement with previous work carried out in dissociated neurons and in intact trigeminal ganglia (Viana et al., 2002;Cabanes et al., 2003).

Specific blockade of Kv1 and Kv3 potassium channels by DTX and BDS, respectively, was found to induce a novel cold sensitivity in around 20 % of sensory neurons. Expression data from rt-PCR suggests that Kv1.1 and Kv1.2, as the channels with the higher levels of expression, are important in mediating the DTX-induced effects on cold sensitivity, while by the same reasoning BDS is likely to be exerting its effects through the inhibition of Kv3.1 and Kv3.4. The induction of cold responsiveness in sensory neurons by DTX or BDS alone was lower than recorded with either 4-AP or TEA. There are two possible explanations for this: either 4-AP and TEA are acting on both Kv1 and Kv3 channels in different populations of

neurons, resulting in a greater induction of cold sensitivity; or there are further, as yet unidentified, channels involved in this regulation. Possible candidates would include Kv1.4 and Kv4.3, both of which have been shown to be highly expressed in IB4-positive non-peptidergic DRG neurons, the subpopulation affected primarily by 4-AP (Vydyanathan et al., 2005;Chien et al., 2007).

The complexity of potassium ion channel expression in sensory neurons and its importance in regulating cold sensitivity is highlighted by the fact that each chemical blocker was found to influence different subpopulations of neurons. This is particularly evident when considering the effects of 4-AP and TEA: while over 70 % of neurons displaying an induced cold response following treatment with 4-AP belonged to the non-peptidergic, IB4-binding C-fibre population, TEA-induced cold responsiveness was prevalent in both myelinated and unmyelinated neurons. No two blockers were applied in combination in this study, but previous work in TG neurons demonstrated that the application of TEA alongside 4-AP produced a cumulative effect on the induction of cold sensitivity (Viana et al., 2002), suggesting that the potential for sensory neurons to develop responsiveness to cold could be much greater than demonstrated here.

Despite the fact that the different channel blockers were targeting distinct neuronal subpopulations, the properties of the induced cold response were very consistent. There was no overlap between induced cold sensitivity and menthol responsiveness, and on the basis of cell size measurements, the induced cold population could be clearly distinguished from the menthol-sensitive population. This finding demonstrates that TRPM8 is not involved in the transduction of the induced cold response, and lends further support to the argument that TRP-independent mechanisms are important in mediating cold sensitivity in peripheral neurons. Many of the cells showing a novel cold response were capsaicin-sensitive however, which would imply that a significant proportion of nociceptive neurons were being recruited to the cold-sensitive population. In addition, it was found that cells displaying an induced cold response had a significantly colder threshold for activation than menthol-sensitive neurons, demonstrating a requirement for a noxious stimulus to elicit activation. It was suggested previously that the 4-AP-sensitive potassium current could influence the temperature threshold of constitutively cold-sensitive neurons, following the discovery that the current was present in these cells also, albeit at much lower levels than recorded in the cold-insensitive population (Viana et al.,

2002). Data from this study supports this claim to some extent, as the application of 4-AP resulted in a small but significant shift of threshold in menthol-sensitive neurons to colder temperatures. The remaining three potassium channel blockers however had no effect on the activation threshold of the menthol-sensitive population, indicating that the involvement of potassium channels in setting the activation threshold of constitutively cold-sensitive neurons is limited.

4.5.2. KCNQ potassium channels regulate cold sensitivity in sympathetic neurons

Cold sensitivity in sympathetic neurons is also susceptible to modulation through the blockade of voltage-gated potassium channels, and like DRG neurons both 4-AP and TEA induced novel cold responses in a significant proportion of previously insensitive cells. Unlike DRG neurons however, the effects cannot be attributed to members of the Kv1 or Kv3 channel subfamilies, as neither DTX nor BDS were able to induce cold sensitivity in SCG neurons. This is in spite of the fact that the SCG was found to express Kv1.1, Kv1.2 and Kv1.6, as well as Kv3.1, Kv3.3 and Kv3.4. The two principal Kv1 channels expressed in the DRG, Kv1.1 and Kv1.2, were expressed approximately 3-fold and 8-fold lower, respectively, in the SCG, which may offer some explanation for the lack of effect of DTX. However, the channel targeted primarily by BDS, Kv3.4, was expressed at comparable levels in both sensory and sympathetic ganglia, suggesting that differences in channel expression between DRG and SCG cannot entirely account for the results of the calcium imaging experiments. These data would strongly indicate that while cold sensitivity in both sensory and sympathetic neurons can be regulated by the inhibition of voltage-gated potassium current, the specific complement of ion channels involved in this process differs significantly between the two neuronal types. Earlier studies characterising the transient and delayed rectifier currents in SCG neurons concluded that the Kv1.4, Kv4.2 and Kv4.3 channels underlie the transient potassium current, while members of the Kv2 subfamily mediate the delayed rectifier current (Malin and Nerbonne, 2000;Malin and Nerbonne, 2001;Malin and Nerbonne, 2002), which would explain the reason an effect was seen with 4-AP and TEA, but not with DTX or BDS.

In DRG neurons, both transient and delayed rectifier-type currents contributed to the induction of cold sensitivity, whereas in SCG neurons the delayed rectifier current was dominant. This was demonstrated by the fact that TEA and XE991, blockers of fast and slow delayed rectifier currents, respectively, were capable of inducing a

novel cold response in over 70 % of previously insensitive sympathetic neurons. In particular, there was an obvious difference in the effect produced by XE991, which was large in SCG neurons, most of which express the KCNQ-mediated M-current (Hadley et al., 2003), but negligible in sensory neurons. This is in spite of the fact that DRG neurons have been shown to express KCNQ channels, and that their excitability can be modulated with KCNQ agonists or antagonists (Passmore et al., 2003). Interestingly the M-current was found to be the dominant subthreshold current in small DRG neurons, in contrast to large cells where it made little contribution, and in this study those neurons that did show a change in cold sensitivity following the application of XE991 were small in size (average cell size 387 ± 32 μm^2, n = 58). This finding adds further support to the theory that different ion channels are critical in the regulation of cold transduction in sensory and sympathetic neurons.

4.5.3. The down-regulation of voltage-gated potassium channels following nerve injury may contribute to the development of cold hypersensitivity

Several studies have shown that potassium channel expression is modulated following nerve injury. Transient and delayed rectifier currents are reduced in DRG neurons following axotomy of the sciatic nerve or chronic compression of the DRG (Everill and Kocsis, 1999;Tan et al., 2006;Yang et al., 2004), and this is reflected by a down-regulation of potassium channel expression (Rasband et al., 2001;Ishikawa et al., 1999;Yang et al., 2004). It is therefore reasonable to conclude from the data presented here that the down-regulation of voltage-gated potassium channels following nerve injury will lead to an increase in responsiveness to cold stimuli, and may contribute to the development of cold hypersensitivity. Interestingly, expression of Kv1.1 and Kv1.2 is significantly reduced by nerve injury, while expression of Kv1.6 is relatively unaltered (Ishikawa et al., 1999;Yang et al., 2004), lending support to the proposed hypothesis that the observed effects of DTX are mediated primarily via the two former channels. Although there is currently no evidence linking potassium channels to the development of cold sensitivity in vivo, a recent study has demonstrated that selective knockdown of Kv3.4 or Kv4.3 is sufficient to induce mechanical hypersensitivity in rats (Chien et al., 2007). Thermal responses were not affected, although as this study has demonstrated, the pattern of ion channel expression appears to be an important factor. Chien et al. also reported a significant overlap in expression of potassium channels in nociceptive C-fibres, and surmised that this co-expression

may enable a neuron to reflect different intensities of incoming stimuli. Subsequently, reduced expression of potassium channels would result in an inability to accurately reflect stimulus intensity, leading to a state of allodynia, where normally innocuous stimuli are felt as painful.

Throughout this chapter, the effect produced by the blockade of potassium channels has been referred to as an induction of cold sensitivity. However, rather than cells acquiring a novel responsiveness to cold as this term would suggest, it is more likely that the neurons constitutively express the ability to respond to a cold stimulus, but that under normal conditions the response is dampened by the expression of voltage-gated potassium channels (Viana et al., 2002). Inhibition of these channels would therefore unmask, rather than induce, the cold response and allow the neuron to reach firing threshold. As already mentioned, TRPM8 does not mediate the cold response in these cells, and as a consequence the ion channels underlying transduction of this cold stimulus remain unidentified.

Inhibition of voltage-gated potassium channels would be expected to increase the input resistance of the neuronal membrane, and it could be suggested that this alone is sufficient to induce firing in cells displaying a novel response. There are several lines of evidence to suggest that this is not the case. Firstly, there was no correlation between the direct activation of neurons by the potassium channel blocker and the induction of cold sensitivity, indicating that neurons open to potassium channel blockade did not necessarily possess the capacity to respond to cold. Secondly, low concentrations of 4-AP (100 μM) were not found to alter the input resistance of TG neurons (Cabanes et al., 2003). Thirdly, in single unit recordings from sensory neurons, 4-AP and TEA were found to induce cold sensitivity, but have little effect on heat or mechanical sensitivity (Vastani and Koltzenburg, 2007).

In conclusion, the principal finding of this study is that inhibition of voltage-gated potassium channels can induce novel cold sensitivity in sensory and sympathetic neurons. This is likely to be relevant to the development of cold hypersensitivity following nerve injury.

5. The role of sodium channels in cold transduction

5.1. Background

Oxaliplatin is a platinum-based chemotherapeutic drug used in the treatment of colorectal, ovarian, breast and lung cancers. The platinum compounds present in the drug form adducts with DNA, blocking replication and transcription, and leading to apoptosis of actively dividing cells. Many of the platinum-based drugs currently used in the treatment of cancer have severe dose-limiting side effects, such as nephrotoxicity, myelotoxocity and hematologic toxicity, symptoms that are not induced by oxaliplatin (Desoize and Madoulet, 2002).

Like all platinum derivatives, however, cumulative doses of oxaliplatin do induce a peripheral sensory neurotoxicity, characterised by paraesthesias, numbness, a loss of vibratory sensation, and a loss of deep tendon reflexes. This form of chronic neuropathy is thought to be caused by the accumulation of platinum-based biotransformation products in the DRG and peripheral nerves (Luo et al., 1999;Cavaletti et al., 2001). Human patients show decreased sensory nerve action potential amplitude and a loss of sensory fibres (Lehky et al., 2004), while studies in rodents have demonstrated that the neuropathy is associated with a reduced sensory nerve conduction velocity, a loss of large myelinated fibres, and axonal degeneration (Cavaletti et al., 2001;Jamieson et al., 2005).

Unlike other platinum-based drugs, oxaliplatin can also induce an acute sensory neuropathy, which has a very rapid onset (in some cases the symptoms can develop during the infusion of the oxaliplatin itself), is reversible within days, and which can increase in duration and severity with repeated drug administration. Symptoms include paraesthesias and dysaesthesias, often affecting the perioral and laryngo-pharyngeal areas as well as the limbs, muscle spasms and cramps in the limbs, muscle tightness in the throat and jaw, and eye pain (Cersosimo, 2005;Pasetto et al., 2006). This neuropathy is induced or exacerbated by exposure to cold, and affects over 80 % of patients. Behavioural studies in rats show an acute oxaliplatin-induced mechanical allodynia and cold hyperalgesia (Ling et al., 2007). Interestingly, in human patients, no abnormalities in sensory nerve fibres could be detected, but there was a marked hyperexcitability of motor nerves, associated with repeated neuromyotonic discharge (Wilson et al., 2002;Lehky et al., 2004).

Recent *in vitro* studies have implicated sodium channels in the development of the acute oxaliplatin-induced neuropathy. The application of oxaliplatin to nerve fibres or dissociated sensory neurons has been shown to result in an increased refractory period, a reduction in sodium conductance, a shift in peak activation and inactivation to hyperpolarised potentials, and a slowing of the inactivation kinetics of sodium channels (Adelsberger et al., 2000;Grolleau et al., 2001;Webster et al., 2005;Benoit et al., 2006).

5.2. Aims

The aims of this study were to investigate the effects of oxaliplatin and sodium channel activation on constitutive and induced cold sensitivity in dissociated sensory neurons.

5.3. Methods

This section provides specific information on the experiments carried out in this study. For detailed protocols, please refer to Chapter 2.

5.3.1. Primary tissue culture

DRG from adult C57/B6 mice were digested in papain followed by collagenase and dispase, and dissociated mechanically with fire-polished glass pipettes. Neurons were re-suspended in F-12 medium and plated on poly-L-lysine and laminin-coated coverslips. In the first instance, cells were treated with an acute dose of the drug, whereby the oxaliplatin was perfused directly onto the neurons during calcium imaging. Later experiments were designed to investigate the effects of chronic oxaliplatin exposure. The drug was diluted to 600 μM in F-12 medium, and the freshly plated neurons were incubated in the oxaliplatin for 4-6 hours prior to the start of the imaging experiment. All cultures were used for calcium imaging experiments within a few hours of plating.

5.3.2. Ratiometric calcium imaging

Neurons were loaded with Fura-2 and stained with IB4-FITC and CTB-Alexa 594. Coverslips were positioned inside a custom-made chamber and solutions were applied to the cells via a gravity-driven application system.

To assess whether sodium channel activation is sufficient to influence cold transduction, the sodium channel agonist veratridine was analysed for its ability to induce a novel cold sensitivity in acutely dissociated sensory neurons. Stock solutions of veratridine (75 mM, Sigma), menthol (2 M) and capsaicin (20 mM) were made up in ethanol, and diluted to the required working concentration on the day of the experiment. The imaging protocol was adapted from previous experiments looking at the role of potassium channel blockade on cold sensitivity (see Chapter 4). Neurons were stimulated with an initial application of cold ECF (5 °C), followed by 25 μM veratridine (40 second application). The drug was then washed out of the chamber before being reapplied in the presence of a second cold stimulus. Cells were subsequently assessed for sensitivity to 250 μM menthol (10 second application) and 1 μM capsaicin (10 second application). All experiments were done at room temperature, and fast non-linear cold ramps were applied over a 20 second period. Temperature was continuously monitored with a thermocouple positioned just outside the field of vision, opposite the stream of the inflow.

To assess the effects of oxaliplatin on cold sensitivity in sensory neurons, a number of different imaging protocols and drug concentrations were tried. A stock solution of oxaliplatin (10 mM, Sanofi Aventis, France) was made up in distilled water, divided into aliquots and stored at -80 °C. Once diluted to working concentration, the efficacy of oxaliplatin is reduced by 10 % every 30 minutes. A fresh working solution was therefore prepared at the start of each imaging experiment. A solution of 400 μM oxaliplatin was used initially, but the concentration was increased to 600 μM for later experiments.

In the first instance, experiments were designed to investigate whether an acute application of oxaliplatin would alter functional cold sensitivity in dissociated sensory neurons. Previous studies have reported effects on sodium currents within minutes of applying oxaliplatin to cells (Adelsberger et al., 2000). Neurons were exposed to cold ECF prior to and following a 30 minute incubation in 400 μM oxaliplatin (Figure 5.1, Experiment 1). This approach however produced little change in the responsiveness of sensory neurons to the cold stimulus. Several modifications were therefore introduced to the protocol. Firstly, studies carried out in the laboratory using oxaliplatin on the skin-nerve preparation had shown that fibres induced to become cold-sensitive by the presence of the drug only responded when a second cold ramp was applied following the incubation in oxaliplatin. Consequently all subsequent

experiments included two consecutive cold stimuli before and after the oxaliplatin treatment (Figure 5.1, Experiment 2). Secondly, an *in vitro* study of the effects of oxaliplatin at the neuromuscular junction found that stimulation of the nerve was required to unmask the changes in nerve function induced by the drug (Webster et al., 2005). In some experiments therefore an additional 50 mM potassium chloride stimulus (6 second application) was placed between the two cold ramps following drug application (Figure 5.1, Experiment 3). Thirdly, in the initial experiments, the oxaliplatin was washed out immediately after the 30 minute incubation period. In dissociated cell preparations, the effects of oxaliplatin are reported to be completely reversible within minutes of drug washout (Adelsberger et al., 2000) and therefore, in order to ensure any effect the oxaliplatin was having on cold sensitivity would be recorded, the drug was applied continuously throughout the cold stimulation.

In all of the experimental protocols outlined above, the oxaliplatin was washed into the recording chamber, the flow was stopped, and the cells were left to incubate for 30 minutes. A significant proportion of cells were found to respond during the incubation period, even in the presence of ECF (control experiments were carried out, using the identical imaging protocols but replacing the oxaliplatin with ECF). The responses were not due to a drop in temperature, which was monitored throughout the experiment, but may have been due to changes in the pH of the solution as the cells were left to incubate. In any case, it was not possible to accurately assess the proportion of neurons responding directly to the oxaliplatin. To overcome this problem, further experiments were carried out in which the flow of oxaliplatin into the chamber was maintained throughout the incubation period. The 30 minute incubation time had been chosen because a previous study using a phrenic nerve preparation had shown that a longer incubation time was needed to see oxaliplatin-induced changes in function (Webster et al., 2005), a finding supported by experiments on the skin-nerve preparation in the laboratory. For dissociated neurons however, it may not be necessary to apply oxaliplatin for such long periods in order to induce an effect (Adelsberger et al., 2000). Consequently, the incubation time was shortened to 15 minutes, but the concentration of oxaliplatin increased to 600 μM to invoke the maximal effect (Figure 5.1, Experiment 4).

Oxaliplatin is believed to exert its effects via the modulation of sodium channel function, and as mentioned earlier may require an additional stimulation for the effects to become apparent. In some experiments therefore, cells were incubated in

oxaliplatin alone for 15 minutes, and then in a solution of 600 μM oxaliplatin mixed with 25 μM veratridine (the sodium channel agonist) during two consecutive cold ramps (Figure 5.1, Experiment 5).

To assess whether chronic exposure to oxaliplatin would influence cold sensitivity in sensory neurons, cells were plated in F-12 medium containing 600 μM oxaliplatin, and left to incubate for up to 6 hours before imaging. Oxaliplatin was added to the Fura-2 and IB4-CTB solutions, and the coverslips were placed directly into oxaliplatin in the recording chamber. Neurons were stimulated with two consecutive cold stimuli, but without the additional potassium chloride stimulus (Figure 5.1, Experiment 6).

In all experiments looking at the effects of oxaliplatin on cold sensitivity, neurons were additionally analysed for responsiveness to 250 μM menthol (10 second application) and 1 μM capsaicin (10 second application). For control experiments, the oxaliplatin and/or veratridine were replaced with ECF. All experiments were carried out at room temperature. Cold ECF and oxaliplatin solutions were warmed to approximately 23 °C and slow linear cold ramps were applied over a 100 second period. Temperature was continuously monitored with a thermocouple positioned just outside the field of vision, opposite the stream of the inflow.

Ratiometric images were recorded at intervals of 0.5 seconds for the duration of the cold stimulus and 1 second thereafter, using the TillPhotonics system. Only vital neurons that responded to a concentrated (50 mM) potassium stimulus were included in the analysis.

5.3.3. Statistics

Calcium imaging experiments were performed on at least two separate cultures. Each culture usually consisted of several coverslips. The results from the coverslips of one culture were pooled and were used as one data point for subsequent analysis. All quantitative comparisons are presented as mean ± SEM where appropriate. Student's unpaired *t*-test was used for all statistical analyses.

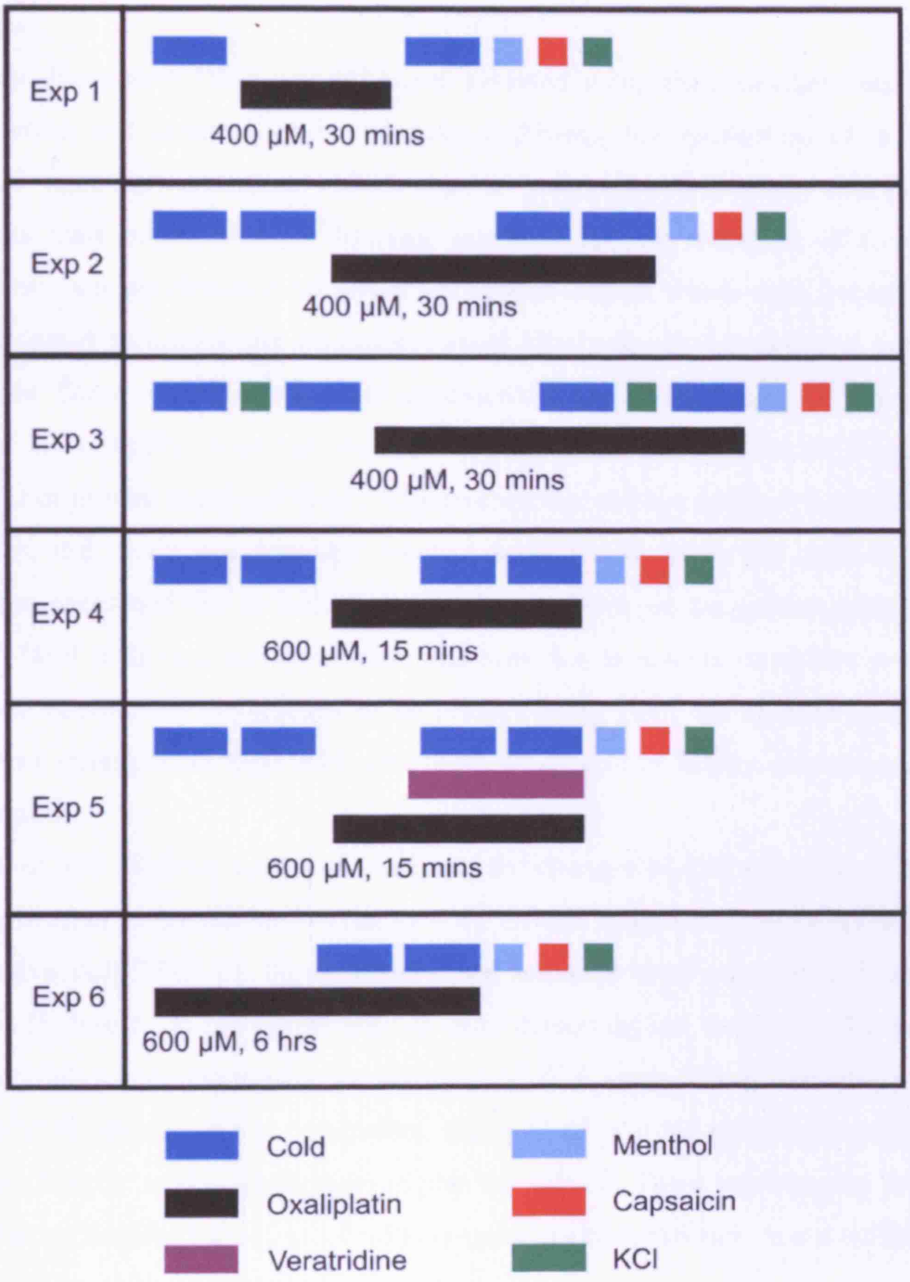

Figure 5.1. Schematic representation of the different experimental protocols employed in the investigation of the effects of oxaliplatin on cold sensitivity in dissociated DRG neurons. The concentration of oxaliplatin used and the incubation time are noted for each experiment.

5.4. Results

5.4.1. Activation of sodium channels does not induce novel cold sensitivity in sensory neurons

Acutely dissociated DRG neurons were assessed using Fura calcium imaging for constitutive and induced cold responses following the application of a sodium channel agonist, veratridine, which opens voltage-gated sodium channels and prevents their inactivation. A baseline response for the induction of novel cold sensitivity was previously established for experiments in which cold responsiveness was assessed following the pharmacological blockade of voltage-gated potassium channels. These control experiments are described in detail in Chapter 4 (please refer to page 106). Briefly, it was shown that in the absence of any additional factors such as drugs or growth factors, 6 % of DRG neurons that did not respond to an initial cold stimulus, did produce a response when a second cold ramp was applied. It was therefore concluded that an induction of cold sensitivity on the second cold stimulus of $\leq$ 6 % of cells was not significant, and was due to natural variability within the neuronal population, as opposed to an effect arising from ion channel modulation. The same criteria were used when assessing the effects of sodium channel activation in this study.

A total of 950 DRG neurons were analysed for changes in cold sensitivity following the application of 25 μM veratridine (n = 4). Of 894 neurons that were initially cold-insensitive, only 37 (4 ± 1 %) showed a novel response when a second cold ramp was applied (Figure 5.2). The percentage of cells displaying an 'induced' cold response was not higher than observed in the presence of ECF alone. This is unlikely to be due to a lack of potency of the veratridine, since 42 (5 ± 1 %) neurons were found to respond directly to the application of the compound. These experiments therefore demonstrate that the activation of voltage-gated sodium channels is not sufficient to induce cold sensitivity in sensory neurons.

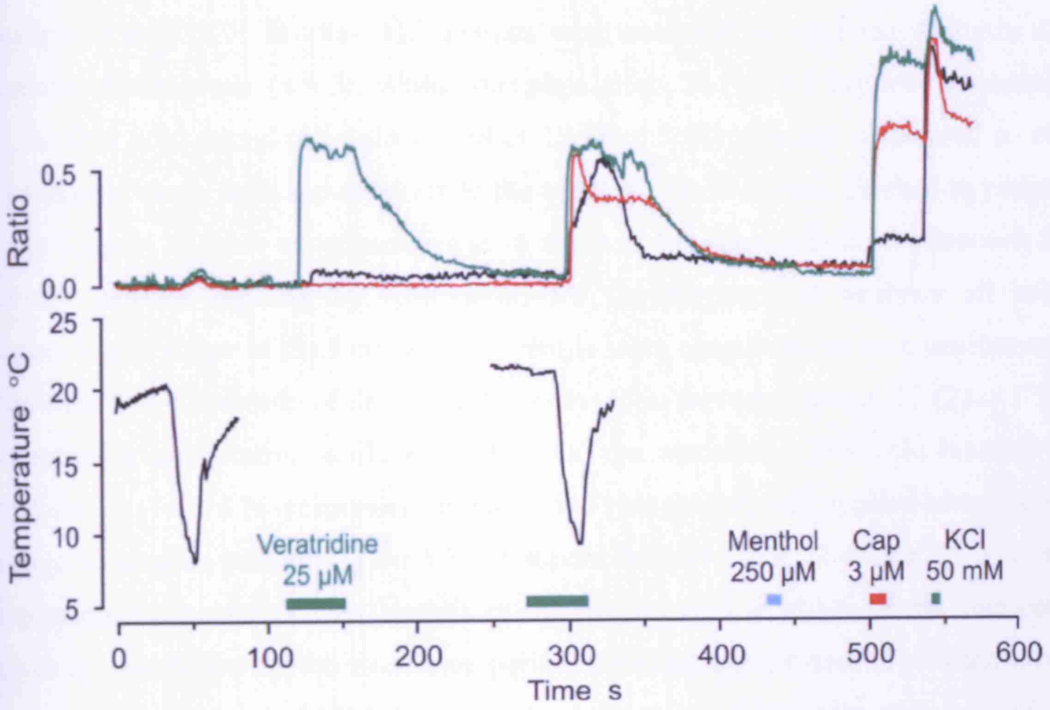

Figure 5.2. Representative kinetic profiles of the responses of three DRG neurons displaying induced cold sensitivity following the application of veratridine. One cell responded to veratridine (green) and two cells were capsaicin-sensitive (green and red). None of the neurons responded to menthol.

5.4.2. Acute exposure to oxaliplatin does not induce novel cold sensitivity in sensory neurons

Acutely dissociated DRG neurons were assessed for changes to functional cold sensitivity following acute treatment with the chemotherapeutic drug oxaliplatin. In the first set of experiments, neurons were stimulated with two pairs of consecutive cold stimuli either side of a 30 minute incubation in 400 μM oxaliplatin (Figure 5.1, Experiment 2). To establish a baseline for the induction of cold sensitivity by the drug, experiments were carried out using the same protocol, but replacing the oxaliplatin with ECF. In total, 313 neurons were analysed for cold sensitivity in the absence of oxaliplatin (n = 3). Within this population, 56 (18 ± 3 %) cells responded to the first cold stimulus, while a further 19 (8 ± 3 %) neurons responded to the second cold ramp, both applied prior to the onset of the 30 minute incubation period. Since the aim of these experiments was to measure the change in cold sensitivity in sensory neurons induced by oxaliplatin, for the purposes of analysis all cells responding to either of the first two cold ramps were considered to be constitutively cold-sensitive. Therefore, of the 313 cells analysed in this experiment, 75 (25 ± 5 %) expressed a constitutive cold sensitivity. Of the remaining 238 cold-insensitive neurons, 26 (14 ± 4 %) responded to one of the two cold stimuli applied after the 30 minute incubation period (Figure 5.3). It should be noted that 22 of the 75 neurons displaying a constitutive cold sensitivity did not respond to either of the two cold ramps applied following the incubation period, meaning that the overall percentage of neurons responding to cold before or after the incubation was not altered (a total of 75 neurons responded before the incubation period, 25 ± 5 %, and 79 cells responded after the incubation period, 28 ± 4 %, $P > 0.6$).

The experiment was subsequently repeated with the addition of oxaliplatin, and out of a total of 394 cells that were analysed, 68 (17 %) responded to either of the initial two cold stimuli, and were therefore classed as constitutively cold-sensitive (n = 2). In the presence of oxaliplatin, of the remaining 326 cold-insensitive neurons, only 26 (9 %) displayed a novel cold response (Figure 5.4).

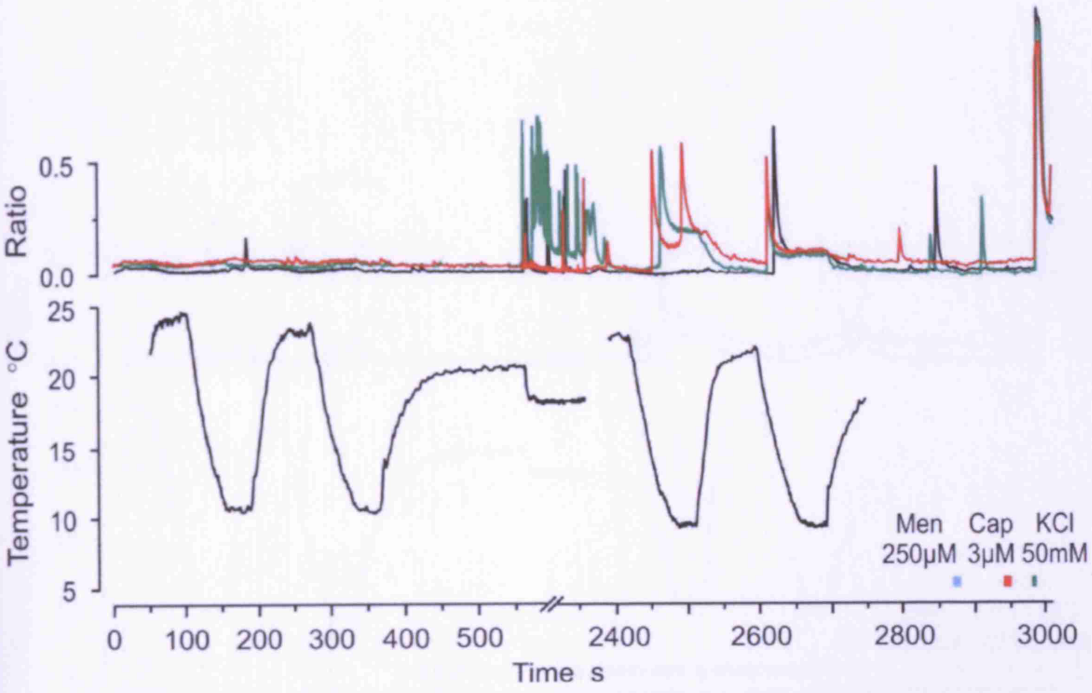

Figure 5.3. Representative kinetic profiles of the responses of three DRG neurons responding to a cold stimulus only after the 30 minute incubation period, in the absence of oxaliplatin. Two cells responded on the first cold ramp (green and red), and one cell responded to the second cold stimulus only (black). Note the continued firing of one cell throughout the incubation period even once the temperature was stable (green).

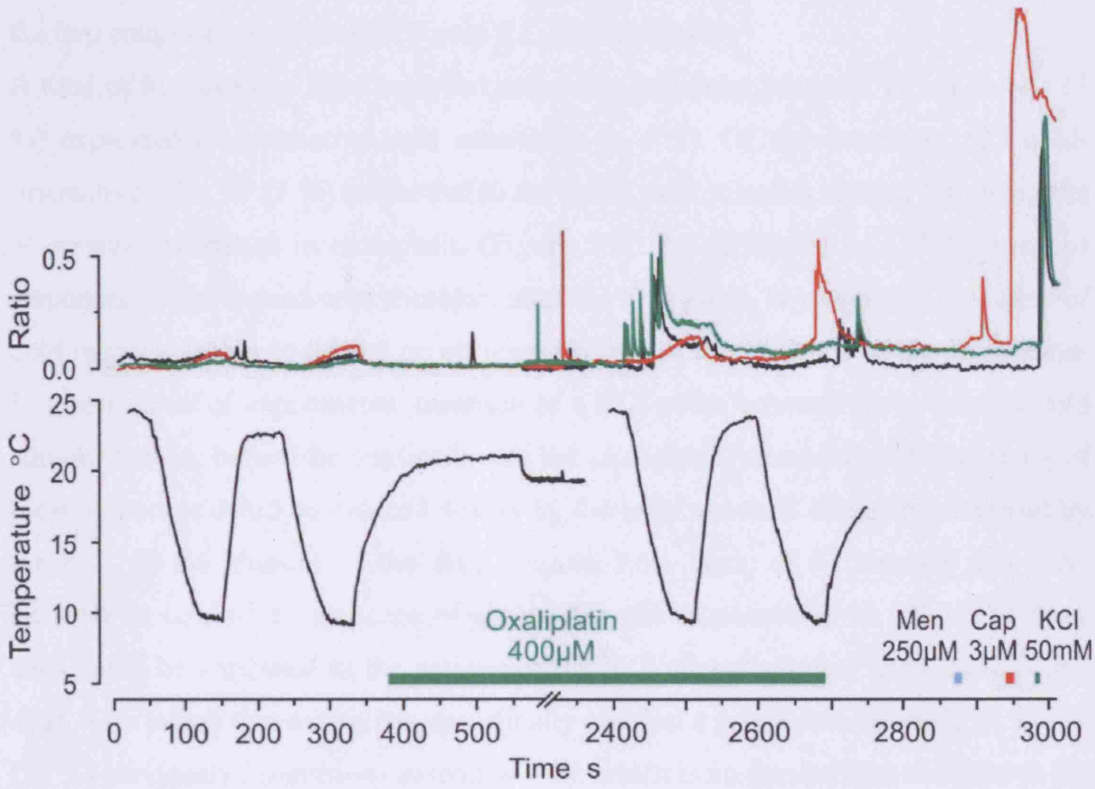

Figure 5.4. Representative kinetic profiles of the responses of three DRG neurons displaying induced cold sensitivity following a 30 minute incubation in 400 µM oxaliplatin. Two cells responded on the first cold oxaliplatin ramp (green and black), while one cell responded to the second cold oxaliplatin stimulus only (red). One neuron also responded to capsaicin (red), but none were menthol-sensitive.

Using this first experimental protocol, the extent of the induction of cold sensitivity by the addition of oxaliplatin was no greater than observed in the ECF control experiments (14 % in ECF versus 9 % in oxaliplatin). Previous studies using oxaliplatin on a phrenic nerve preparation had found that stimulation of the nerve was required to unmask changes in nerve function induced by the presence of the drug (Webster et al., 2005). Therefore, in order to see whether this could also be the case for dissociated neuronal preparations, a 50 mM KCl stimulus was introduced between the two cold oxaliplatin ramps (Figure 5.1, Experiment 3).

A total of 611 neurons were analysed using this particular protocol, of which 86 (13 %) expressed a constitutive cold sensitivity (n = 2). Of the remaining 525 cold-insensitive cells, 37 (9 %) responded to the initial cold stimulus applied following the 30 minute incubation in oxaliplatin (Figure 5.5). An additional 64 (12 %) neurons responded to the second cold stimulus, after the KCl pulse, however this induction of cold responsiveness could not be attributed solely to the presence of the oxaliplatin. In a second set of experiments, insertion of a KCl pulse between the initial two cold stimuli (that is, before the application of the oxaliplatin) demonstrated that many of these responses could be induced simply by the brief neuronal stimulation evoked by the KCl, in the absence of the drug (Figure 5.6). Thus, of 52 neurons that were sensitive to cold in the presence of oxaliplatin, the responses of 16 (31 %) of these cells could be attributed to the actions of the KCl stimulus rather than those of the drug. This means that oxaliplatin specifically induced a novel cold response in 36/279 (13 %) previously insensitive neurons (n = 2), which is no greater than recorded in the presence of ECF alone. Therefore, neuronal stimulation was not sufficient to unmask a novel induction of cold sensitivity by oxaliplatin in dissociated sensory neurons.

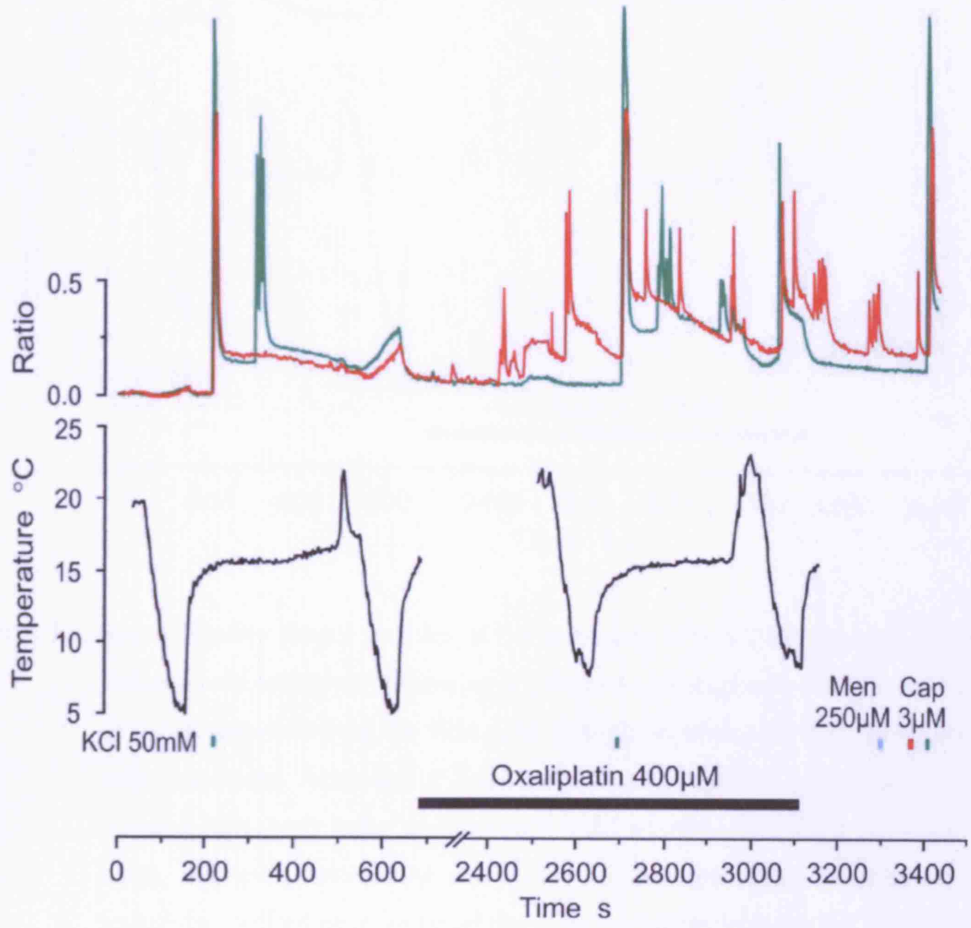

Figure 5.5. Representative kinetic profiles of the responses of two DRG neurons displaying induced cold sensitivity following a 30 minute incubation in 400 μM oxaliplatin, and a brief KCl stimulus. One cell responded on the first cold oxaliplatin stimulus (red), while one cell only responded following the KCl pulse (green).

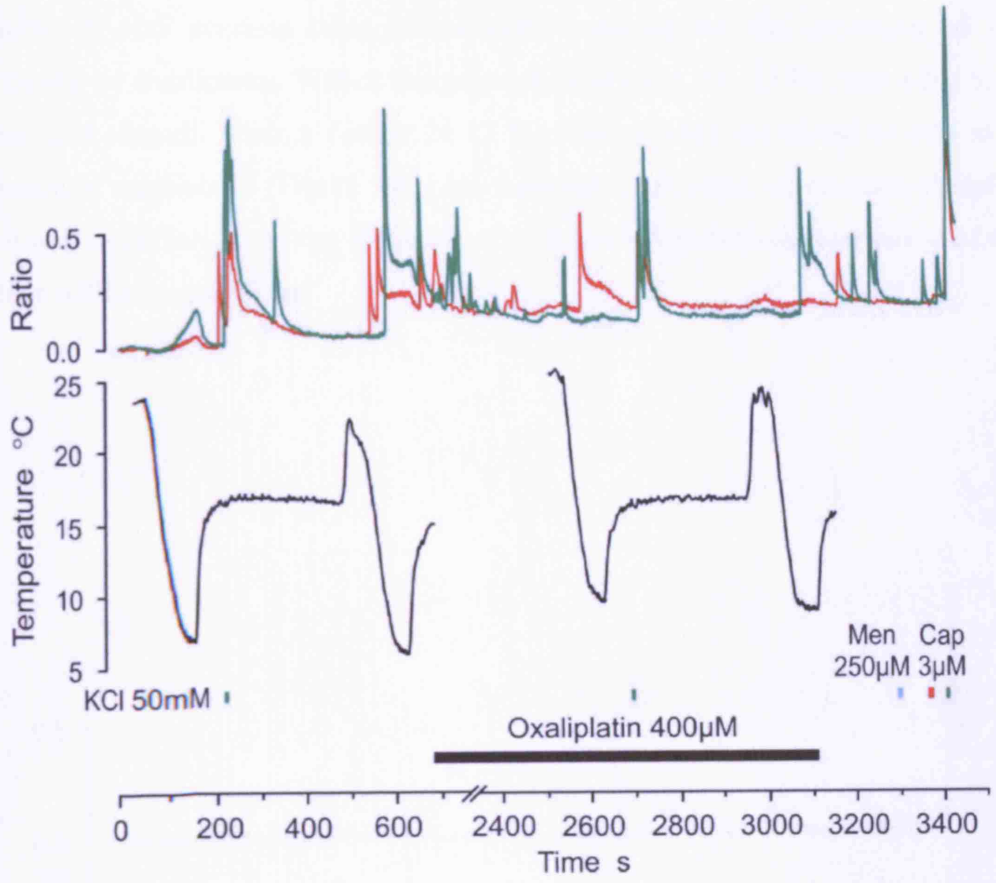

Figure 5.6. Representative kinetic profiles of the responses of two DRG neurons displaying induced cold sensitivity following a 30 minute incubation in 400 μM oxaliplatin. One cell responded on the first cold oxaliplatin stimulus (red), while one cell only responded following a brief KCl stimulus (green). It should be noted however that both cells were already cold-sensitive following an initial KCl pulse, applied prior to the incubation in the drug. The induction of cold sensitivity in these neurons could therefore not be attributed to the oxaliplatin.

The experimental protocol was further modified so that neurons were stimulated with a higher concentration of oxaliplatin (600 μM), but for a shorter period of time (15 minutes) (Figure 5.1, Experiment 4). In addition, the flow of oxaliplatin was maintained throughout the incubation period. In initial control experiments, where the oxaliplatin was replaced with ECF, 60/420 (15 %) DRG neurons were constitutively cold-sensitive ($n = 2$). Of the 360 cold-insensitive neurons, 25 (7 %) responded to one of the two cold ramps applied following the 15 minute incubation period (Figure 5.7).

A total of 406 neurons were subsequently assessed for the induction of cold sensitivity by oxaliplatin. Within this population of cells, 53 (13 %) responded to the initial cold stimuli, while a further 24 (7 %) neurons only responded to cold in the presence of oxaliplatin (Figure 5.8). As observed in previous experiments therefore, there was no difference in the induction of cold sensitivity between neurons incubated with or without oxaliplatin.

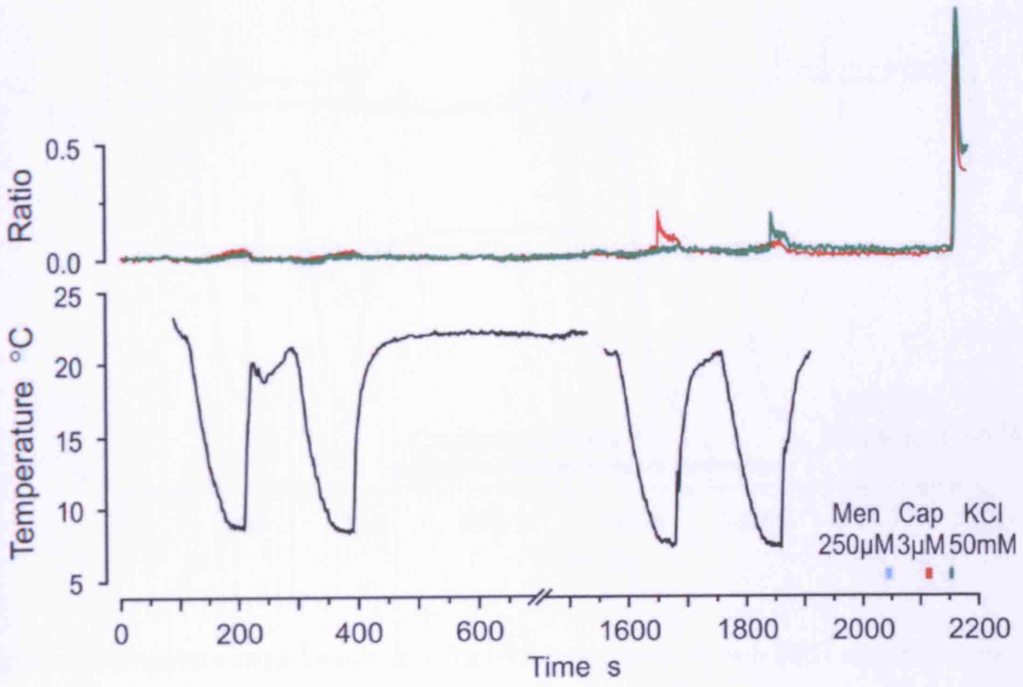

Figure 5.7. Representative kinetic profiles of the responses of two DRG neurons responding to a cold stimulus only after the 15 minute incubation period, in the absence of oxaliplatin. One cell responded on the first cold stimulus (red), while one cell only responded to the second cold ramp (green).

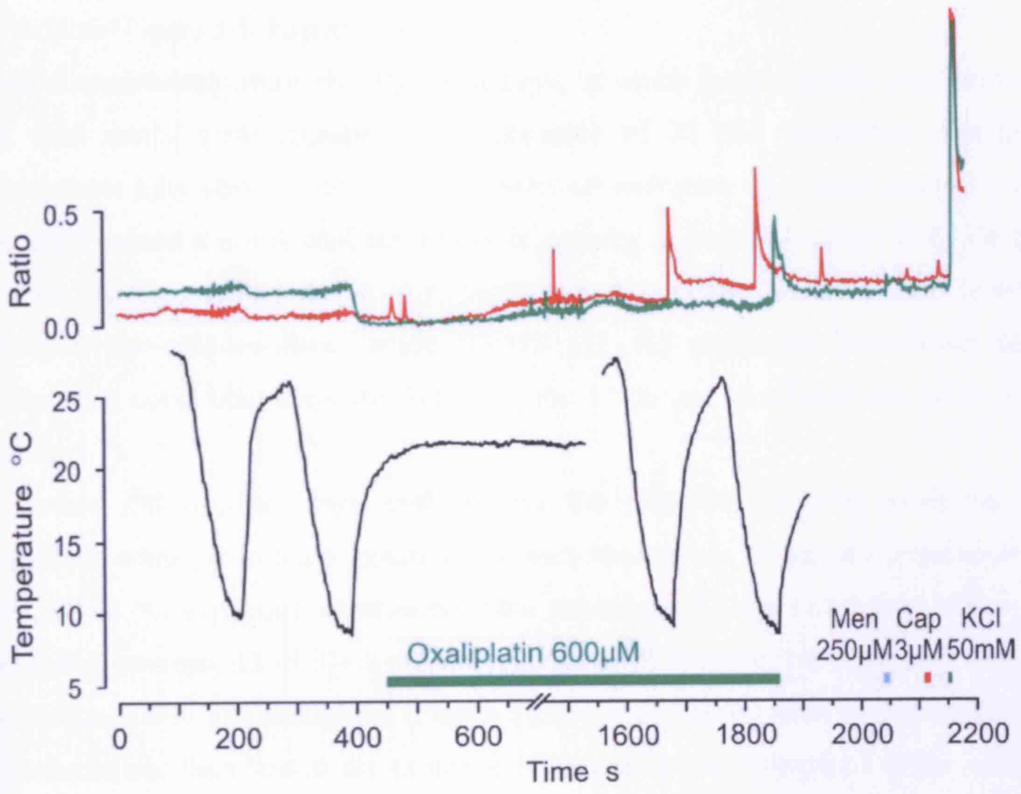

Figure 5.8. Representative kinetic profiles of the responses of two DRG neurons displaying induced cold sensitivity following a 15 minute incubation in 600 µM oxaliplatin. One cell responded on the first cold oxaliplatin stimulus (red), while one cell only responded to the second application of cold oxaliplatin (green).

5.4.3. Activation of sodium channels does not promote the induction of novel cold sensitivity by oxaliplatin in sensory neurons

Oxaliplatin is believed to exert its effects through an action on voltage-gated sodium channels. Given that application of oxaliplatin alone was insufficient to modify cold sensitivity in sensory neurons, it was hypothesised that the drug would be more effective if exposed to pre-activated sodium channels. In order to test this theory therefore, cold oxaliplatin was applied in the presence of the sodium channel agonist veratridine (Figure 5.1, Experiment 5).

Control experiments were initially carried out, in which the oxaliplatin was omitted, but cold ramps were applied in the presence of 25 μM veratridine. Previous experiments have shown that veratridine-evoked activation of sodium channels will not itself induce a novel cold sensitivity in sensory neurons (see page 148). Of the 358 acutely dissociated DRG neurons analysed in these experiments, 40 (10 %) were constitutively cold-sensitive, while 30/318 (11 %) previously insensitive cells displayed a novel cold response following the 15 minute incubation period (n = 2) (Figure 5.9).

A further 290 neurons were analysed for the induction of cold sensitivity by oxaliplatin when presented in combination with veratridine. Within this population of cells, 27 (9 %) expressed constitutive cold sensitivity. Of the remaining 263 cold-insensitive neurons, 22 (8 %) displayed a novel cold response following a 15 minute incubation in 600 μM oxaliplatin (Figure 5.10). There was no additional induction of cold sensitivity therefore in the presence of the oxaliplatin compared to the control experiments.

During the 15 minute incubation, oxaliplatin was flowed continuously onto the cells, preventing any alterations in temperature or pH that could elicit cellular activity, and allowing for an accurate measure of the amount of activation evoked by the application of the drug. In the presence of ECF, 21/358 (5 %) neurons showed some response during the incubation period, while in the presence of oxaliplatin, 8/290 (3 %) cells were activated. These data demonstrate that oxaliplatin itself does not induce activity in dissociated sensory neurons.

In conclusion, a number of experimental protocols and drug concentrations were tried in an attempt to elicit changes in cold transduction in sensory neurons by oxaliplatin. However, all of the data presented here show that the acute application of oxaliplatin to dissociated neurons does not induce novel cold sensitivity.

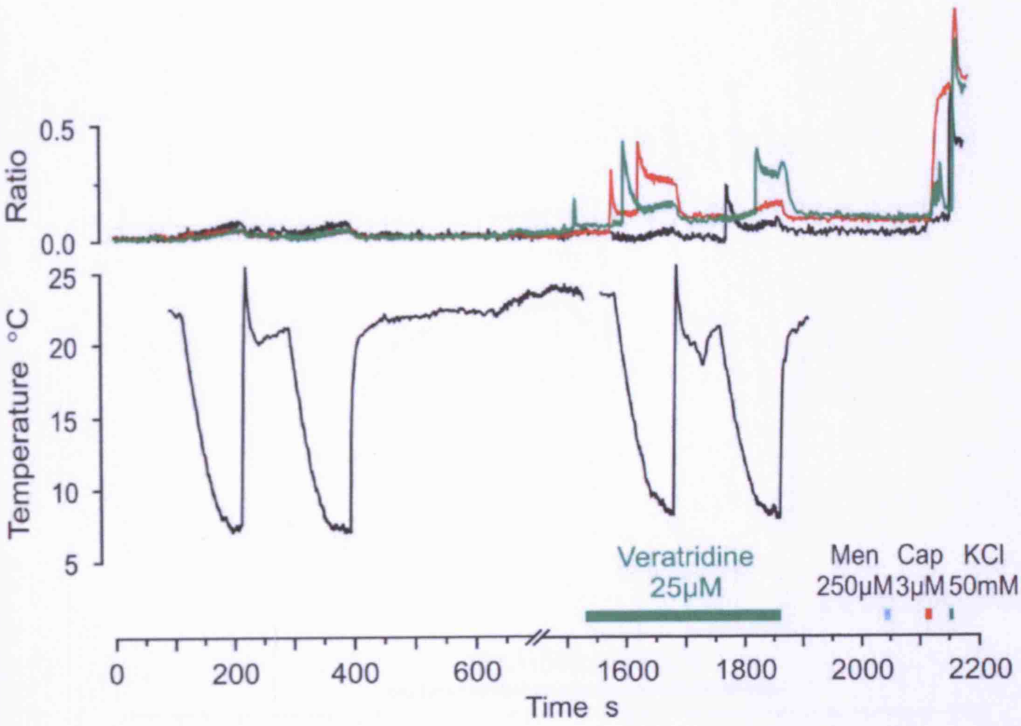

Figure 5.9. Representative kinetic profiles of the responses of three DRG neurons responding to a cold stimulus only after the 15 minute incubation period, in the presence of 25 μM veratridine, but the absence of oxaliplatin. Two cells responded on the first cold veratridine stimulus (red and green), while one cell only responded to the second cold ramp (black). One neuron was also capsaicin-sensitive (red).

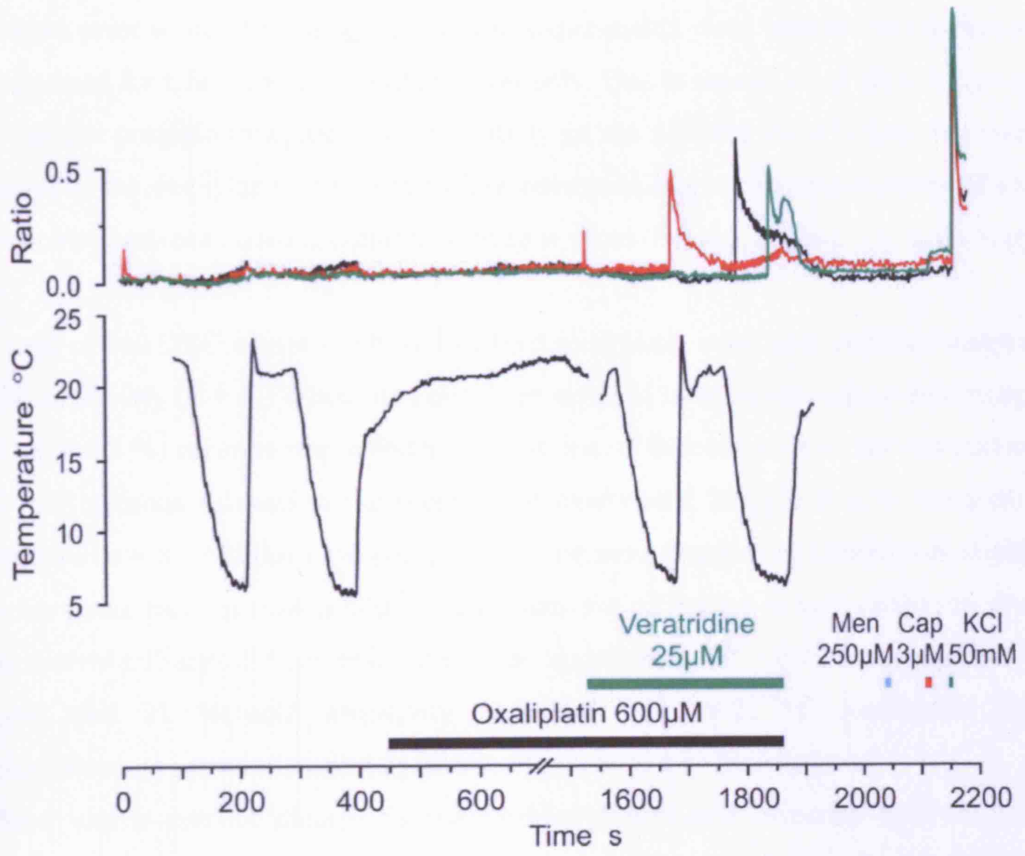

Figure 5.10. Representative kinetic profiles of the responses of three DRG neurons displaying induced cold sensitivity following a 15 minute incubation in 600 μM oxaliplatin, and in the presence of veratridine. One cell responded to the first cold oxaliplatin stimulus (red), while two cells only responded on the second application of cold oxaliplatin (green and black).

5.4.4. Chronic exposure to oxaliplatin induces a qualitative change in sensory neuron cold responses

Following the discovery that acute exposure to oxaliplatin does not alter cold sensitivity in sensory neurons, experiments were designed to investigate whether chronic exposure to the drug would have any effect. Following dissociation, DRG neurons were plated in F-12 medium containing 600 μM oxaliplatin and left for up to 6 hours prior to calcium imaging. Control experiments were carried out on neurons maintained for a few hours in F-12 medium only. Due to the nature of the experiment, it was not possible to assess cold sensitivity in the cultured cells before they were placed in the oxaliplatin. It was therefore only possible to compare the overall cold sensitivity between neurons cultured with or without the drug (Figure 5.1, Experiment 6).

A total of 910 DRG neurons cultured without oxaliplatin were analysed for functional cold sensitivity (n = 4). When the cells were exposed to two consecutive cold ramps, 103 (12 ± 3 %) neurons responded to at least one of the cold stimuli. By comparison, of 1518 neurons cultured in the presence of oxaliplatin, 298 (21 ± 4 %) were cold-sensitive (n = 5). Although the percentage of neurons responding to cold was slightly higher in the cultures maintained in oxaliplatin, the difference in cold sensitivity from the control cultures did not reach statistical significance ($P > 0.1$). It should also be noted that 21 % cold sensitivity is within the range of constitutive cold responsiveness recorded in acutely dissociated, untreated DRG neurons.

There was a marked change in the profile of the cold response following the incubation in oxaliplatin. Cold responses are heterogeneous, but can be classed into three broadly defined groups according to their different profiles. The first group of neurons respond with a gradual increase in calcium levels over the period of cold application, often reaching a plateau before calcium levels drop as the solution is rewarmed. The second group of cells respond rapidly, displaying a sharp peak in calcium concentration before it falls back to baseline. The calcium response is usually over before the cold stimulus has been fully applied. The final group of neurons also respond sharply to the drop in temperature, but rather than a single peak in the calcium curve, there are often several, with the calcium concentration increasing with each step (Figure 5.11).

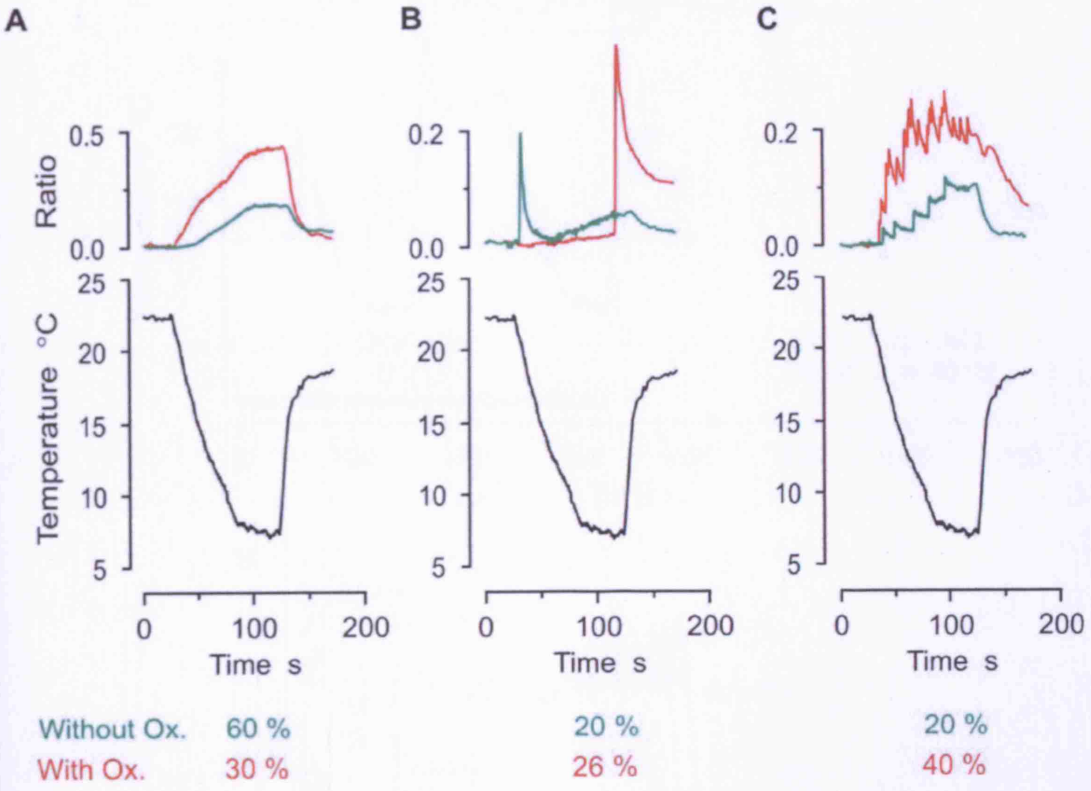

Figure 5.11. (A-C) Representative kinetic profiles of cold responses showing the characteristic features of each type of response. See text for details. The application of oxaliplatin induced a change in the cold response profile, so that a higher percentage of cells displayed sharp stepping responses (C) as opposed to gradual increases in calcium levels (A). The approximate percentage of neurons displaying each type of response in the absence (without ox.) or presence (with ox.) of oxaliplatin is shown below each figure. Note that a small percentage (4 %) of neurons developed a novel bursting response following the incubation in oxaliplatin (see Figure 5.12).

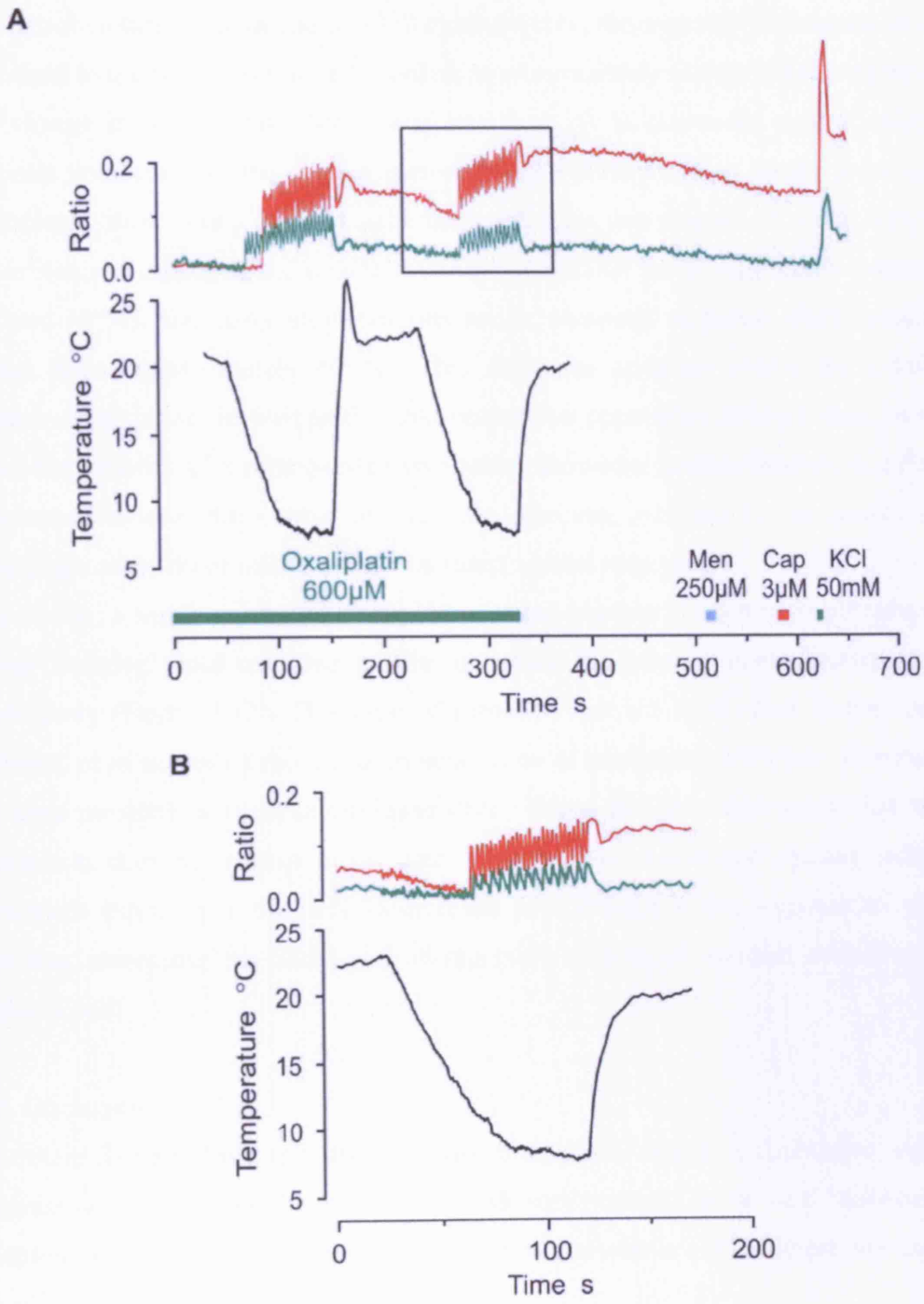

Figure 5.12. (A) Representative kinetic profiles of two DRG neurons responding to cold following a 6 hour incubation in 600 µM oxaliplatin. Note the 'bursting' profile of the cold response, which was only observed in neurons treated with a chronic dose of oxaliplatin. Note also the slow decline of calcium levels back to baseline following the cold stimuli (red). The boxed area in (A) is enlarged in (B).

In control cultures maintained in F-12 medium only, the majority of neurons (60 %) belonged to the first group of cells, and showed a relatively slow, gradual response to the change in temperature. Moreover, less than 20 % responded with a stepping increase in calcium levels, as demonstrated by the third grouping. In the presence of oxaliplatin, there was a marked shift between these two classes of cells, such that fewer neurons displayed the gradual increase in calcium levels typified by group one (around 30 %), and many more neurons had a 'stepping' response characteristic of group three (approximately 40 %). This shift was apparent within the menthol-sensitive population, as well as the cold-responsive population at large: thus, in ECF alone the majority of menthol-sensitive neurons showed a gradual increase in calcium concentration over the course of the cold stimulus, whereas in the presence of oxaliplatin many more cells displayed a sharp, spiked response.

In addition, a small number of oxaliplatin-treated neurons (11/298, 4 %) displayed a novel 'bursting' cold response profile, in which the calcium concentration spiked repetitively (Figure 5.12). This type of response was not seen either in the control cultures, or in neurons exposed to an acute dose of oxaliplatin. Of those 11 neurons, all were menthol- and capsaicin-insensitive. These data therefore show that while oxaliplatin does not induce novel cold sensitivity in dissociated sensory neurons, prolonged exposure to the drug does result in a change in the response to a cold stimulus, increasing the likelihood of repetitive spiking of calcium concentrations within a cell.

5.5. Discussion

The main findings from this study are that oxaliplatin induces a qualitative, but not quantitative, change in the response of sensory neurons to a cold stimulus. In addition, the activation of voltage-gated sodium channels is not sufficient to induce a novel cold sensitivity in DRG neurons.

5.5.1. The effects of oxaliplatin on cold sensitivity are not visible at the cell soma

The chemotherapeutic drug oxaliplatin is closely associated with the development of two types of peripheral sensory neuropathy. As with all platinum-based compounds, repetitive doses result in the accumulation of platinum derivatives in the DRG and peripheral sensory nerves, leading to a chronic neurotoxicity characterised by abnormal mechanical sensation and a loss of myelinated afferents (Luo et al.,

1999;Cavaletti et al., 2001;Lehky et al., 2004;Jamieson et al., 2005). Oxaliplatin also gives rise to a cold-induced acute sensory neuropathy, affecting over 80 % of patients, the symptoms of which have been well-characterised, and include paraesthesias, muscle spasms and muscle tightness (Wilson et al., 2002;Lehky et al., 2004;Cersosimo, 2005;Pasetto et al., 2006). Rats administered with a single injection of oxaliplatin display mechanical allodynia and cold hyperalgesia that can last up to a week after the injection (Ling et al., 2007), mirroring symptoms seen in patients (Binder et al., 2007).

This study was designed to investigate whether some of the acute neuropathic symptoms experienced by patients undergoing oxaliplatin treatment could be caused by a change in cold sensitivity within peripheral sensory neurons. In spite of trying a number of different experimental protocols, drug concentrations and incubation times however, oxaliplatin did not alter functional sensitivity to a cold stimulus in dissociated DRG neurons. The concentration of oxaliplatin used in this study is slightly higher than used in previous studies on dissociated neurons (100-500 μM) (Adelsberger et al., 2000;Grolleau et al., 2001), but is in line with concentrations applied to *in vitro* nerve preparations (400-500 μM) (Webster et al., 2005;Vastani and Koltzenburg, 2007). Similarly, whereas the effects of oxaliplatin on sodium currents in dissociated DRG neurons were apparent within a minute of applying the drug (Adelsberger et al., 2000), other studies, both on dissociated neurons and on nerve preparations, required a much longer incubation period before the drug was seen to produce any effect (15-40 minutes) (Grolleau et al., 2001;Webster et al., 2005;Vastani and Koltzenburg, 2007). One study reported greater effects of oxaliplatin on sodium channel function if the drug was applied intracellularly (Grolleau et al., 2001), but other groups have reported similar findings with extracellular application (Adelsberger et al., 2000). It is therefore unlikely that the parameters chosen for this study (drug concentration, incubation time, method of drug application) had an inverse effect on the results.

The inability of oxaliplatin to induce a novel cold sensitivity in dissociated sensory neurons is very surprising given that single unit studies on the saphenous nerve preparation demonstrated a significant induction of cold sensitivity in previously insensitive nerve fibres following incubation in the drug (Vastani and Koltzenburg, 2007). In these experiments, cold sensitivity was induced preferentially in A-fibres, which corresponds well to previous reports that oxaliplatin evokes its effects

primarily on A-fibres, increasing the size and duration of action potentials, with little effect on C-fibres (Adelsberger et al., 2000).

There are several possible explanations for this discrepancy between the dissociated neuron and *in vitro* nerve preparations. Firstly, species-specific differences between mouse (used in the dissociated neuron preparation) and rat (used in the skin-nerve preparation) should be taken into consideration, however preliminary experiments carried out during the course of this study would argue against this possibility. In an acute rat DRG culture, incubated for 30 minutes in 400 μM oxaliplatin, only 12/200 (6 %) cold-insensitive neurons responded to a cold ramp presented after the drug. The extent of induction of cold sensitivity was therefore no different to that recorded in mouse DRG neurons. Furthermore, in the skin-nerve preparation, oxaliplatin was equally capable of inducing a novel cold sensitivity in fibres isolated from mouse as well as rat. Secondly, oxaliplatin is believed to act on sodium channels, and it is highly possible that the specific isoforms susceptible to modulation by oxaliplatin are expressed differentially on the soma and at the nerve terminal. It should be noted that there is currently no direct evidence linking sodium channels with the induction of cold sensitivity, and indeed the findings from this study would argue strongly against this being the case. Alternatively, oxaliplatin may require the presence of additional factors to regulate cold transduction, which again may be expressed differentially at the nerve terminal. Rat DRG neurons that had been cultured for 48 hours and had started to put out processes were assessed for cold sensitivity following a 30 minute incubation in 400 μM oxaliplatin. In this experiment, just 4/82 (5 %) previously insensitive cells responded to a cold stimulus applied after the oxaliplatin, indicating again the lack of a novel cold induction. This was only a preliminary experiment, and further investigation into the possibility of differences in ion channel expression and oxaliplatin modulation between the soma and nerve terminal is warranted. Ideally, the effects of oxaliplatin would be assessed in an *in vitro* model such as a DRG-Schwann cell co-culture, comprising neurons with well-established nerve terminals and associated cells that may also influence how oxaliplatin exerts its effects.

5.5.2. Cold enhances oxaliplatin-induced neuronal hyperexcitability

Chronic exposure of DRG neurons to oxaliplatin resulted in a marked alteration in the profile of the calcium response to a cold stimulus. The responses were more often 'spiky' in nature, reflecting repeated increases in intracellular calcium concentration.

Responses of this type have been described previously, in an *in vitro* model of autonomic transmission, where oxaliplatin-induced bursts of rapid calcium transients were observed at the nerve terminal (Webster et al., 2005). The transients were consistent with spontaneous action potential generation, and were associated with neurotransmitter release. The spontaneous activity could be blocked by application of the sodium channel antagonist tetrodotoxin, suggesting it was caused by alterations to voltage-gated sodium channels induced by the presence of oxaliplatin. In this study, the cells that displayed a bursting response to a cold stimulus were insensitive to both menthol and capsaicin, and therefore are likely to constitute a subpopulation of A-fibre neurons. Interestingly, in single unit recordings, mechanically-sensitive A-fibres that developed an abnormal sensitivity to cold in the presence of oxaliplatin also demonstrated a typically bursting pattern of firing, and these two recordings may demonstrate distinct functional changes, induced by the drug, within the same population of cells.

A number of recent studies have reported that oxaliplatin affects various aspects of sodium channel function. In dissociated rat DRG neurons, application of the drug resulted in a shift in peak channel activation towards more negative potentials, a reduction in current amplitude, and a slowing of the inactivation kinetics (Adelsberger et al., 2000), findings supported by other studies in dissociated cockroach dorsal unpaired median neurons (Grolleau et al., 2001) and myelinated axons isolated from the frog sciatic nerve (Benoit et al., 2006). In addition, the inactivation-voltage curve of the peak sodium current was shifted to hyperpolarised potentials (Benoit et al., 2006). Each of these modifications to sodium channel function would contribute to increased neuronal excitability as observed in motor and sympathetic nerve fibres (Webster et al., 2005): slowed channel inactivation would allow more sodium current to pass and promote repetitive firing, the shift in channel activation means sodium channels would require a smaller depolarising stimulus to reach maximal conductance, and the shift in channel inactivation would result in a decrease in the duration of action potentials.

It is currently unclear which sodium channels are modulated by oxaliplatin, but there is evidence to suggest that specific isoforms are affected. Alterations in sodium channel function could be observed in peripheral sensory neurons but not in hippocampal neurons, and A-fibres are targeted preferentially over C-fibres (Adelsberger et al., 2000). The affected channel underlies transient sodium current, as

demonstrated by an increase in refractoriness in motor nerves following single or multiple infusions of the drug (Kiernan and Krishnan, 2006), and is expressed in sensory, motor and sympathetic fibres (Webster et al., 2005;Benoit et al., 2006). The most likely candidate is Nav1.6, which is expressed primarily at the Nodes of Ranvier of myelinated axons, although further investigation is required to confirm this hypothesis.

Mutations of the muscle-specific sodium channel isoform Nav1.4 give rise to the condition paramyotonia congenita, which manifests as muscle stiffness triggered by exposure to cold and aggravated by exercise. Several of the mutations underlying this disorder have been characterised, and have been found to impact primarily on channel fast inactivation, causing slowed inactivation kinetics, shifts in the voltage-dependence of inactivation, and increased rate of recovery from inactivation (Fleischhauer et al., 1998;Wu et al., 2001;Bouhours et al., 2003;Mohammadi et al., 2003;Bouhours et al., 2005;Wu et al., 2005). Cooling has been shown to aggravate the defects caused by these mutations, resulting in enhanced slowing of channel kinetics and the development of a persistent sodium current, which in turn further increase neuronal excitability and are believed to lead to the development of myotonia (Fleischhauer et al., 1998;Bouhours et al., 2003;Mohammadi et al., 2003;Bouhours et al., 2005).

The described action of cooling on the paramyotonia congenita mutations could provide an explanation for the actions of oxaliplatin on sensory nerves. The modulation of sodium channel kinetics by oxaliplatin promotes neuronal excitability. In the presence of a cold stimulus, the oxaliplatin-induced defects on sodium channel function would be enhanced, leading to the development of a hyperexcitable state in which responses to cold and mechanical stimuli are exaggerated, as observed in patients and rodent models (Binder et al., 2007;Ling et al., 2007). It is probable that the spiking calcium transients observed in neurons treated with chronic doses of oxaliplatin in this study represent cells in a hyperexcitable state. This theory would also explain how A-fibre mechanoreceptors, which are normally cold-insensitive, can develop a cold-induced hypersensitivity, provided they express the appropriate sodium channel isoforms.

5.5.3. Sodium channels are not involved in the regulation of cold sensitivity

In single unit recordings from the saphenous nerve preparation, a significant induction of cold sensitivity was observed in previously insensitive A-fibres following the application of oxaliplatin (Vastani and Koltzenburg, 2007). Since the primary targets of oxaliplatin are reported to be sodium channels, it could be expected that this induction of responsiveness to cold would arise from the modulation of sodium currents. Indeed there have been previous suggestions that cooling can activate sodium channels and thereby regulate cold transduction (Askwith et al., 2001). The findings from this study however demonstrate that the activation of voltage-gated sodium channels is not sufficient to induce cold sensitivity in sensory neurons.

This then leads to the question as to how oxaliplatin could be mediating its effects on cold transduction. Aside from sodium channels, a recent paper has shown that oxaliplatin also has the capacity to alter potassium conductance in myelinated axons (Benoit et al., 2006). At concentrations of 100 μM, current was reduced by up to 35 %. Drug concentrations used on the skin-nerve preparation were much higher, and may therefore have induced a much stronger block on potassium conductance. Earlier work has shown that pharmacological blockade of voltage-gated potassium channels can lead to a significant induction of cold sensitivity in both sensory and sympathetic neurons (see Chapter 4). From these studies it can be concluded that transient potassium currents, which are normally inhibited by 4-aminopyridine, would not be involved, as the effects of this blocker are observed primarily in the IB4-binding population of non-peptidergic C-fibres. The blocker of delayed rectifier-type channels, however, tetraethylammonium chloride, did induce cold sensitivity in a large proportion of CTB-binding, presumptive myelinated neurons, and this particular subfamily of potassium channels may therefore provide the link between oxaliplatin and cold transduction. Indeed as oxaliplatin is thought to influence the function of certain sodium channel isoforms, the same has been suggested for potassium channels, and the fact that an effect could be recorded in the skin-nerve preparation and not in dissociated neurons may be due to differential ion channel expression between the soma and the nerve terminal. It should be noted that a previous study in dissociated DRG neurons also failed to demonstrate an effect of oxaliplatin on the activity of potassium channels (Adelsberger et al., 2000).

Finally, a recent study in human subjects noted a similarity in the somatosensory profile of cold hyperalgesia between oxaliplatin-induced neuropathy and the hypersensitivity elicited with topical application of menthol (Wasner et al., 2004;Binder et al., 2007). It was suggested that oxaliplatin could be influencing TRP channel activation to induce thermal sensitisation. There have been no studies on the effect of oxaliplatin on TRP channels to date, but given that TRP channel expression is restricted to small-diameter sensory neurons, this hypothesis does not fit with the observations that oxaliplatin alters activity in large-diameter myelinated A-fibres, as well as motor and sympathetic neurons.

In conclusion, the principal finding of this study is that oxaliplatin does not induce novel cold sensitivity in sensory neurons. The drug may however alter the function of voltage-gated sodium channels, which can be further modulated by cold to invoke a hyperexcitable state.

6. The regulation of cold sensitivity and TRP channel expression by NGF

6.1. Background

A recent study of TRP channel expression in embryonic and neonatal sensory neurons demonstrated that the thermosensitive TRP channels, TRPV1, TRPM8 and TRPA1, are all expressed at different stages during development (Hjerling-Leffler et al., 2007). While TRPV1 and TRPM8 are both present embryonically, emerging at E11.5 and E16.5, respectively, TRPA1 is only expressed postnatally, with very low levels of transcript first detectable at P0. Furthermore, the emergence of TRPA1 expression can be defined by two separate waves, with IB4-negative neurons starting to express TRPA1 between P0-P7 and IB4-positive cells expressing TRPA1 from P14 onwards. The mechanisms by which TRP channel expression is regulated are currently unknown, however growth factors have been shown to be important in various aspects of sensory neuron development. At around E10.5 small-diameter sensory neurons start to express the TrkA receptor and subsequently become dependent on NGF. Studies have shown that during embryonic development this growth factor promotes survival of nociceptive DRG neurons (Johnson, Jr. et al., 1980), while postnatally it can influence the sensory phenotype of neurons (Ritter et al., 1991). In adults, the activation of NGF-mediated signalling pathways can alter ion channel expression and function, and much work has focussed on its ability to sensitise and up-regulate TRPV1 (Petruska and Mendell, 2004).

Studies looking at TRPA1 in neonatal sensory neurons have reported high functional expression in cells isolated at P0 and cultured for 2-3 days (Jordt et al., 2004;Bautista et al., 2006), which appears to contradict the finding that the TRPA1 transcript is only expressed postnatally (Hjerling-Leffler et al., 2007). Since neonatal neurons cannot survive in culture without NGF, it is possible that the presence of the growth factor is influencing TRP channel expression in these cells.

6.2. Aims

The aim of this study was to investigate whether NGF could influence cold sensitivity and TRP channel expression in sensory neurons during early postnatal development.

6.3. Methods

This section provides specific information on the experiments carried out in this study. For detailed protocols, please refer to Chapter 2.

6.3.1. Primary tissue culture

Newborn (P0, P2 or P5) C57/B6 mice were killed by decapitation. The skull was opened up and the brain removed to expose the trigeminal ganglia (TG). The spinal column was opened from the dorsal side in situ, following removal of the overlying skin and muscle, and the spinal cord was carefully removed to expose the underlying ganglia. DRG and TG were quickly removed in HBSS and incubated in papain followed by collagenase and dispase. The ganglia were spun down at 2400 rpm (1120 x *g*) for 2 minutes and triturated in 1 ml HBSS. Dissociated neurons were spun down at 2400 rpm for 2 minutes and re-suspended in F-12 medium containing 10 % horse serum, 100 U/ml penicillin and 0.1 mg/ml streptomycin, and supplemented with either 100 ng/ml rhNGF or 75 μM Caspase Inhibitor 1 (Z-Val-Ala-Asp(OMe)-CH_2F, also called Z-VAD-(OMe)-FMK), a pan-caspase inhibitor (Calbiochem, UK). Neurons were plated onto poly-L-lysine and laminin-coated coverslips placed in 12-well plates, and were maintained at 37 °C under 5 % CO_2. Acutely dissociated P2 and P5 neurons were used for imaging experiments within 3-5 hours of plating, while neurons dissociated at P0 were maintained in culture for 2 (P0+2) or 5 days (P0+5) before use. In long-term cultures, 500 μl of culture medium were carefully removed and replaced with fresh F-12 every 2-3 days.

6.3.2. Ratiometric calcium imaging

Neurons were loaded with Fura-2 and stained with IB4-FITC and CTB-Alexa 594. Coverslips were positioned inside a custom-made chamber and solutions were applied to the cells via a gravity-driven application system.

Stock solutions of menthol (2 M), cinnamaldehyde (2 M), mustard oil (1 M) and capsaicin (20 mM) were made up in ethanol and diluted in ECF to the required working concentration on the day of the experiment. Neurons were stimulated with cold ECF (5 °C), 250 μM menthol (10 second application), 100 μM cinnamaldehyde (60 second application), 100 μM mustard oil (60 second application), and 1 μM capsaicin (10 second application). Temperature was continuously monitored with a thermocouple positioned just outside the field of vision, opposite the stream of the

inflow. In all experiments fast non-linear cold ramps were applied from room temperature. Responses of sensory neurons that had been maintained for 2 or 5 days in 100 ng/ml NGF were compared to acutely dissociated age-matched controls.
Ratiometric images were recorded at intervals of 0.5 seconds for the duration of the cold stimulus and 1 second thereafter, using the TillPhotonics system. One field of vision per coverslip was analysed and only vital neurons that responded to a concentrated (50 mM) potassium stimulus were included in the analysis.

6.3.3. Quantitative rt-PCR

Total RNA was extracted from cultured DRG and TG neurons (after calcium imaging) and 10 ng were reverse transcribed into cDNA for use in real-time PCR. cDNA was probed for expression of the housekeeping genes UCHL1 and GAPDH, along with TRPM8, TRPA1 and TRPV1, using SYBR green dye. All primers had been previously optimised and shown to give a linear correlation between cycle threshold and cDNA concentration in serial dilution experiments. Reaction products gave single peaks on melt curve analysis and single bands of expected size on a 2 % agarose gel.
Relative quantification of rt-PCR products was performed, using either the amount of total starting RNA or the expression of housekeeping genes with the $\Delta\Delta$ method as a reference.

6.3.4. Statistics

Calcium imaging experiments were performed on at least three separate cultures over two experimental days, unless otherwise stated. Each culture usually consisted of several coverslips. The results from the coverslips of one culture were pooled and were used as one data point for subsequent analysis. For rt-PCR experiments, DRG and TG from 3-4 cultures each were processed separately for cDNA, and each PCR reaction was run in duplicate. All quantitative comparisons are presented as mean ± SEM. For all statistical analyses, Student's unpaired *t*-test was used.

6.4. Results

6.4.1. Neonatal sensory neurons respond to cold and TRP channel agonists

Acutely dissociated DRG neurons from P2 or P5 animals were assessed using Fura calcium imaging for functional sensitivity to cold and TRP channel agonists. A total of 962 P2 DRG neurons were analysed ($n = 5$), of which 146 (14 ± 3 %) responded to a brief cold stimulus and 345 (34 ± 5 %) were capsaicin-sensitive. In contrast, very few neurons responded to either menthol, cinnamaldehyde or mustard oil: just 36 (4 ± 0.4 %) cells were menthol-sensitive, 8 (1 ± 1 %) responded to cinnamaldehyde, and 24 (2 ± 1 %) were sensitive to mustard oil.

At P5, 125/705 (19 ± 3 %) DRG neurons were cold-sensitive, 37 (6 ± 1 %) responded to menthol, 5 (1 ± 0.2 %) were sensitive to cinnamaldehyde, 22 (3 ± 0.4 %) were mustard oil-sensitive, and 209 (31 ± 3 %) responded to capsaicin ($n = 4$) (Figure 6.1). There was no significant change in the sensitivity of DRG neurons to cold or TRP channel agonists between the ages of P2 and P5 (cold: $P > 0.2$; menthol: $P > 0.09$; cinnamaldehyde: $P > 0.6$; mustard oil: $P > 0.3$; capsaicin: $P > 0.6$).

TG neurons from P2 and P5 animals were similarly assessed for responsiveness to cold and TRP channel agonists. Of 644 P2 neurons, 237 (33 ± 5 %) responded to a cold stimulus, 83 (14 ± 1 %) were menthol-sensitive, 10 (1 ± 0.5 %) were sensitive to cinnamaldehyde, 38 (6 ± 1 %) responded to mustard oil, and 213 (34 ± 2 %) were capsaicin-sensitive ($n = 4$).

As in DRG neurons, there was no change in the sensitivity of TG neurons to the different stimuli between P2 and P5. Thus, within a population of 366 P5 neurons ($n = 4$), 88 (25 ± 3 %) were cold-sensitive ($P > 0.2$), 39 (11 ± 2 %) were sensitive to menthol ($P > 0.3$), 14 (4 ± 1 %) responded to cinnamaldehyde ($P > 0.05$), 33 (9 ± 1 %) were sensitive to mustard oil ($P > 0.1$), and 126 (35 ± 2 %) responded to capsaicin ($P > 0.6$) (Figure 6.2).

There were however significant differences between the DRG and TG populations in terms of functional sensitivity to cold and TRP channel agonists. At P2, a greater number of TG neurons were responsive to cold ($P < 0.05$), menthol ($P < 0.001$) and mustard oil ($P < 0.05$) compared to DRG neurons, while at P5 a larger proportion of TG cells were sensitive to menthol ($P < 0.05$), cinnamaldehyde ($P < 0.05$) and mustard oil ($P < 0.01$). There was no difference in capsaicin sensitivity at either time point (P2: $P > 0.9$; P5: $P > 0.2$) (Figure 6.3).

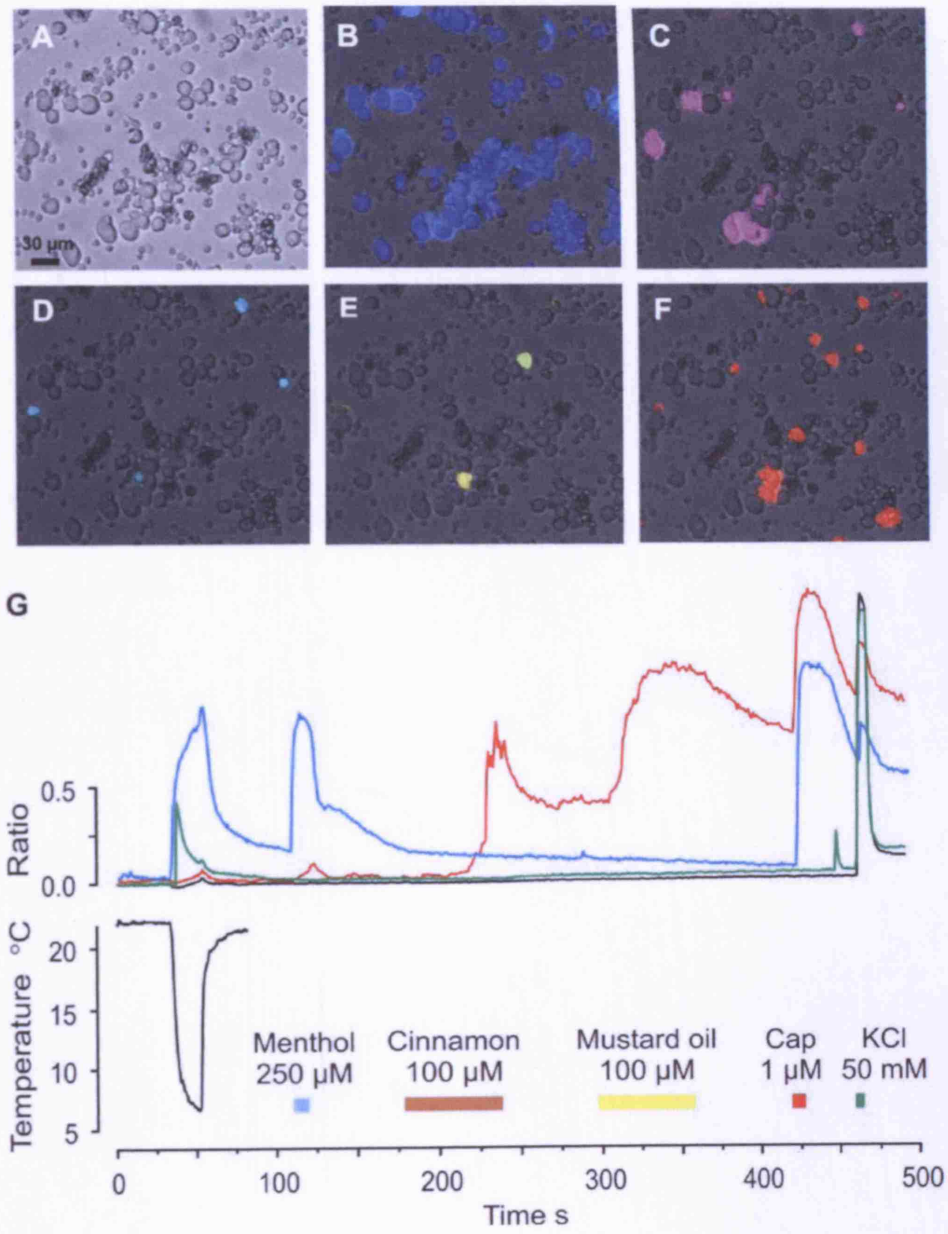

Figure 6.1. Pseudocolour fluorescence images of acutely dissociated P5 DRG neurons. (A) Brightfield image. (B) Background Fura fluorescence. (C-F) DRG neurons responding to cold and TRP channel agonists are colour-coded. (C) Cold-sensitive neurons. (D) Menthol-sensitive neurons. (E) Cinnamaldehyde-sensitive neurons are shown in green, and mustard oil-sensitive neurons are shown in yellow. (F) Capsaicin-sensitive neurons. (G) Representative kinetic profiles of the responses of four P5 DRG neurons. Two cells are cold-sensitive (blue and green), one of which also responds to menthol and capsaicin (blue). One cell is sensitive to cinnamaldehyde, mustard oil and capsaicin (red), and one cell does not respond to any of the applied stimuli (black). All cells respond to the non-specific depolarising stimulus KCl.

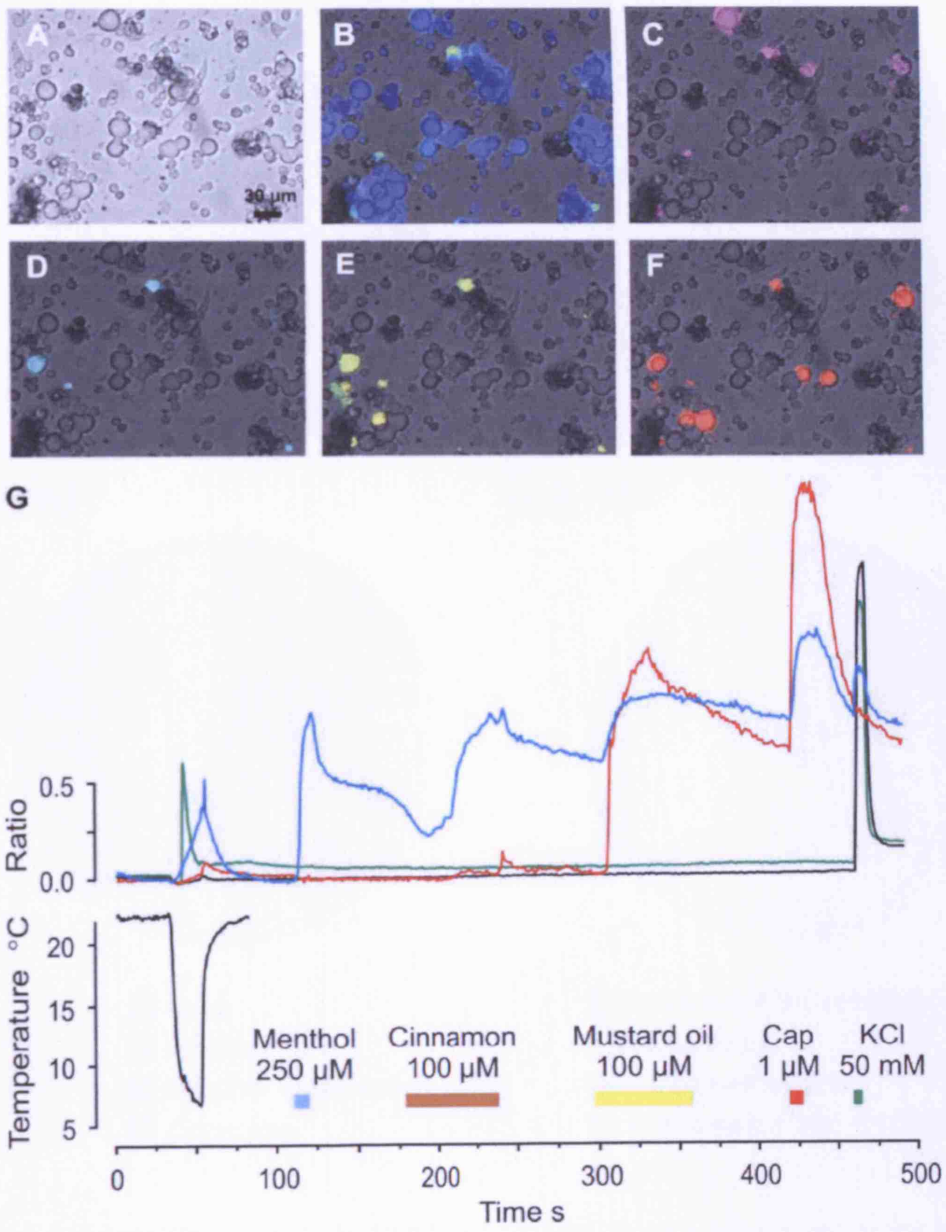

Figure 6.2. Pseudocolour fluorescence images of acutely dissociated P5 TG neurons. (A) Brightfield image. (B) Background Fura fluorescence. (C-F) TG neurons responding to cold and TRP channel agonists are colour-coded. (C) Cold-sensitive neurons. (D) Menthol-sensitive neurons. (E) Cinnamaldehyde-sensitive neurons are shown in green, and mustard oil-sensitive neurons are shown in yellow. (F) Capsaicin-sensitive neurons. (G) Representative kinetic profiles of the responses of four P5 TG neurons. Two cells are cold-sensitive (blue and green), one of which also responds to menthol, cinnamaldehyde, mustard oil and capsaicin (blue). One cell is sensitive to mustard oil and capsaicin (red), and one cell does not respond to any of the applied stimuli (black). All cells respond to the non-specific depolarising stimulus KCl.

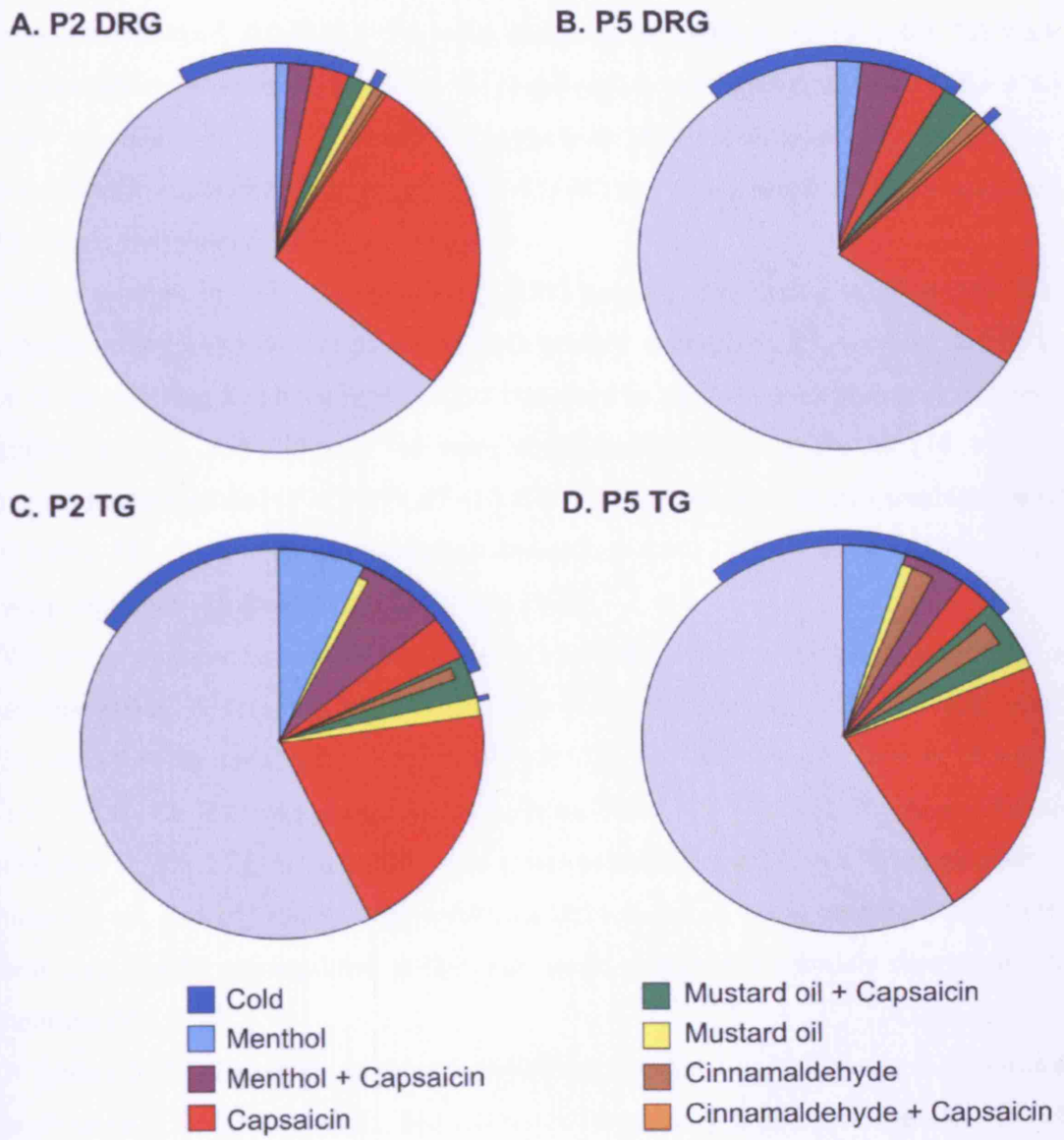

Figure 6.3. Representation of the proportion of neonatal sensory neurons responding to cold and TRP channel agonists. (A) P2 DRG neurons. $n_{animals} = 5$, $n_{cells} = 962$. (B) P5 DRG neurons. $n_{animals} = 4$, $n_{cells} = 705$. (C) P2 TG neurons. $n_{animals} = 4$, $n_{cells} = 644$. (D) P5 TG neurons. $n_{aniamls} = 4$, $n_{cells} = 366$. Data are presented as mean percentage of responding neurons.

6.4.2. NGF up-regulates functional sensitivity to cold and TRP channel agonists

In order to ascertain whether NGF could influence cold sensitivity and TRP channel expression in neonatal sensory neurons, DRG and TG neurons from P0 mice were maintained in 100 ng/ml NGF for 2 or 5 days, and their responses were compared to acutely dissociated age-matched controls. A total of 953 DRG neurons were analysed following two days treatment with NGF ($n = 5$). Of those cells, 247 (24 ± 8 %)

responded to cold, 42 (4 ± 1 %) were sensitive to menthol, 20 (2 ± 0.4 %) were cinnamaldehyde-sensitive, 57 (6 ± 1 %) responded to mustard oil, and 666 (72 ± 4 %) were capsaicin-sensitive. Two days exposure to NGF resulted in a significant up-regulation in sensitivity to mustard oil ($P < 0.01$) and capsaicin ($P < 0.001$) compared to acutely dissociated P2 DRG neurons.

After five days in NGF the number of DRG neurons responding to all stimuli was significantly greater than recorded in both acutely dissociated P5 neurons as well as in those cells that had been kept for just two days in NGF. Therefore, out of 693 cells tested ($n = 5$), 365 (50 ± 5 %) were cold-sensitive ($P < 0.05$), 86 (14 ± 2 %) responded to menthol ($P < 0.05$), 83 (10 ± 3 %) were sensitive to cinnamaldehyde ($P < 0.05$), 172 (24 ± 3 %) responded to mustard oil ($P < 0.001$), and 647 (93 ± 1 %) were capsaicin-sensitive ($P < 0.01$) (Figure 6.4).

When the experiment was repeated in TG neurons, NGF was found to produce a similar effect. A total of 264 TG neurons maintained for two days in NGF were assessed for functional sensitivity to cold and TRP channel agonists ($n = 3$), of which 132 (53 ± 12 %) were found to be cold-sensitive, 30 (11 ± 1 %) responded to menthol, 9 (3 ± 2 %) were sensitive to cinnamaldehyde, 28 (10 ± 1 %) responded to mustard oil, and 143 (56 ± 7 %) were capsaicin-sensitive. Only capsaicin sensitivity was significantly up-regulated at this time point compared to acutely dissociated P2 neurons ($P < 0.05$).

A further 513 TG neurons were maintained for five days in NGF prior to functional analysis ($n = 5$). Of those cells, 244 (49 ± 4 %) responded to the cold stimulus, 75 (14 ± 2 %) were menthol-sensitive, 34 (6 ± 1 %) were sensitive to cinnamaldehyde, 93 (17 ± 2 %) responded to mustard oil, and 323 (60 ± 7 %) were sensitive to capsaicin. Unlike DRG neurons, there was no difference in sensitivity to any of the applied stimuli between those neurons kept for two days or those maintained for five days in NGF. There was however a significant increase in responsiveness to cold ($P < 0.01$), mustard oil ($P < 0.05$) and capsaicin ($P < 0.05$) after five days in NGF compared to acutely dissociated age-matched controls (Figure 6.5).

In contrast to acutely dissociated P5 cultures where TG neurons displayed greater sensitivity to menthol, cinnamaldehyde and mustard oil compared to DRG neurons, there was no difference in responsiveness to any of these chemical stimuli following five days treatment with NGF. However, a larger proportion of DRG neurons responded to capsaicin after NGF compared to TG neurons ($P < 0.01$).

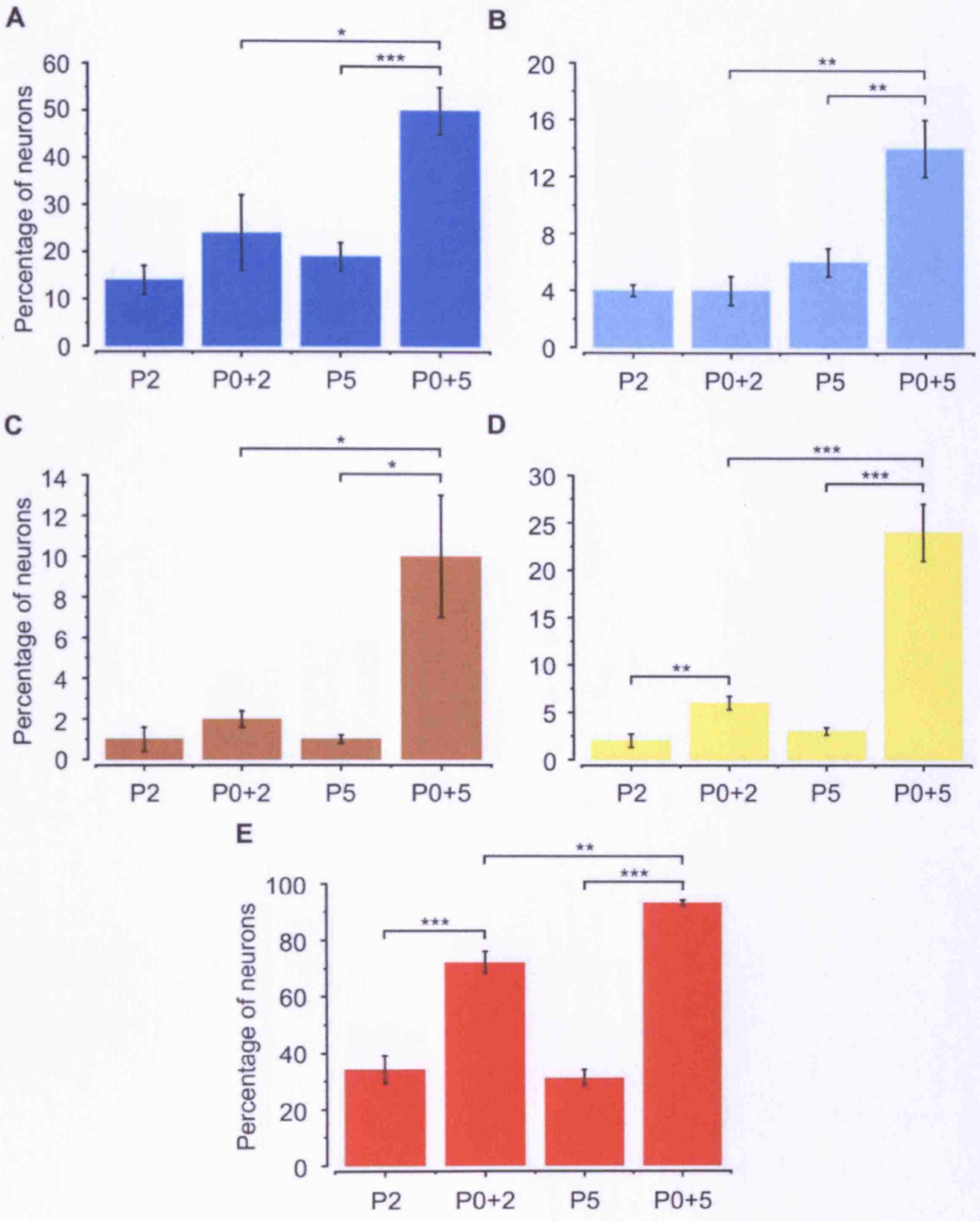

Figure 6.4. NGF induced a significant up-regulation in functional sensitivity to cold (A), menthol (B), cinnamaldehyde (C), mustard oil (D) and capsaicin (E) in neonatal DRG neurons. Neurons were cultured for two (P0+2) or five (P0+5) days in NGF, and compared to acutely dissociated neurons from P2 or P5 mice. P2: $n_{animals} = 5$, $n_{cells} = 962$; P0+2: $n_{animals} = 5$, $n_{cells} = 953$; P5: $n_{animals} = 4$, $n_{cells} = 705$; P0+5: $n_{animals} = 5$, $n_{cells} = 693$. Data are presented as mean percentage of responding neurons ± SEM. * $P < 0.05$, ** $P < 0.01$, *** $P < 0.001$ (Student's unpaired *t*-test).

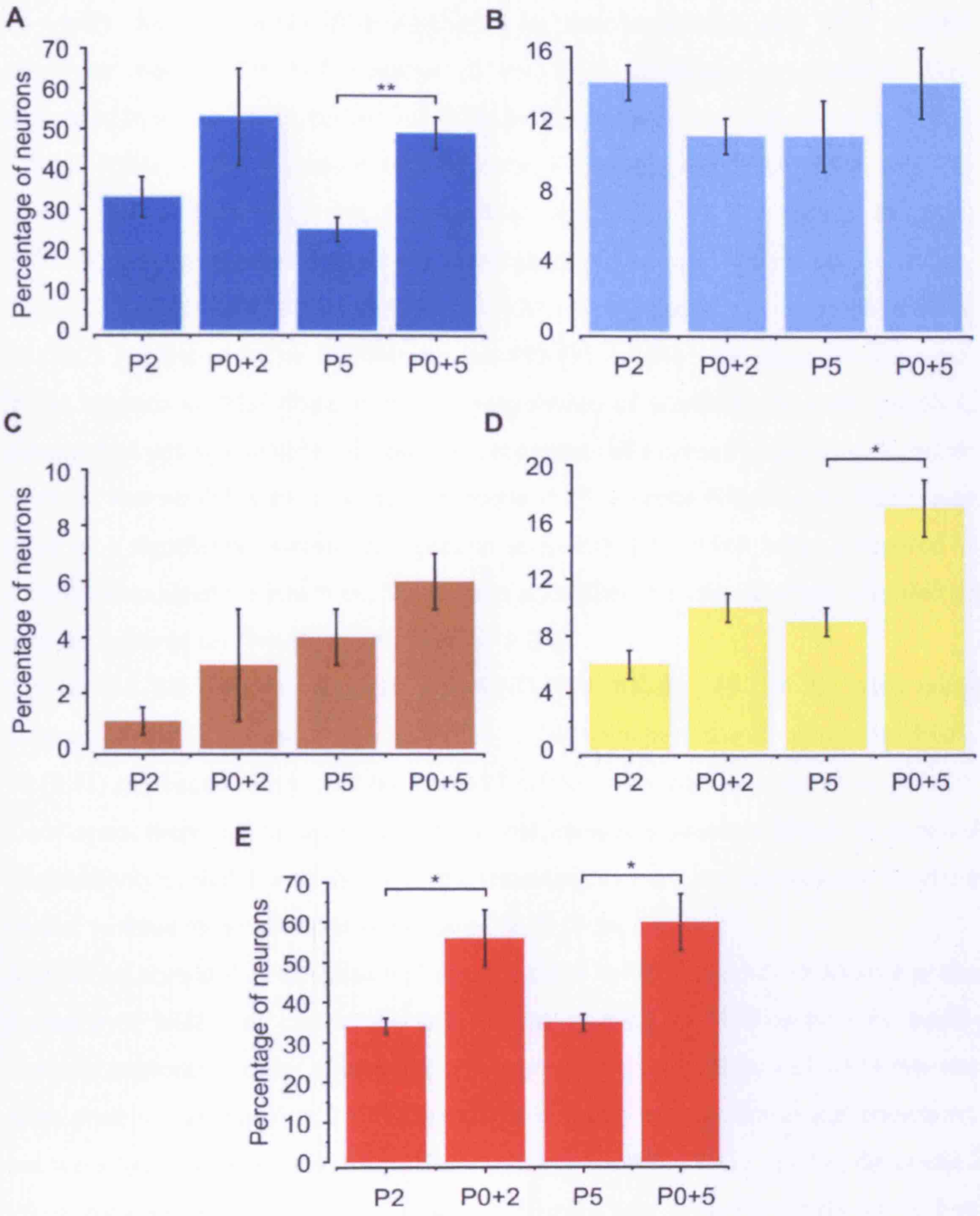

Figure 6.5. NGF induced a significant up-regulation in functional sensitivity to cold (A), menthol (B), cinnamaldehyde (C), mustard oil (D) and capsaicin (E) in neonatal TG neurons. Neurons were cultured for two (P0+2) or five (P0+5) days in NGF, and compared to acutely dissociated neurons from P2 or P5 mice. P2: $n_{animals} = 4$, $n_{cells} = 644$; P0+2: $n_{animals} = 3$, $n_{cells} = 264$; P5: $n_{animals} = 4$, $n_{cells} = 366$; P0+5: $n_{animals} = 5$, $n_{cells} = 513$. Data are presented as mean percentage of responding neurons ± SEM. * $P < 0.05$, ** $P < 0.01$ (Student's unpaired *t*-test).

To verify that the observed up-regulation in functional cold and TRP channel sensitivity was due to the presence of the NGF, additional experiments were performed in which NGF was left out of the culture medium and replaced with 75 μM Z-VAD-(OMe)-FMK, a pan-caspase inhibitor, to prevent cell death. DRG and TG neurons were cultured at P0 and left in culture for five days prior to calcium imaging. 486 DRG neurons were analysed (n = 3), of which 63 (14 ± 5 %) were cold-sensitive, 17 (4 ± 2 %) responded to menthol, 4 (1 ± 0.3 %) were sensitive to cinnamaldehyde, 11 (3 ± 1 %) responded to mustard oil, and 453 (93 ± 1 %) were capsaicin-sensitive. In the absence of NGF there was no up-regulation of sensitivity to cold, menthol, cinnamaldehyde or mustard oil, and the proportion of neurons responding to either stimulus was no different to acutely dissociated P5 neurons (Figure 6.6). There was however a significant increase in capsaicin sensitivity ($P < 0.001$ when compared to acutely dissociated P5 neurons), which was no different to the increase recorded in neurons cultured for five days with NGF ($P > 0.9$).

Out of 251 TG neurons cultured in Z-VAD-(OMe)-FMK, 46 (18 %) were cold-sensitive, 7 (3 %) responded to menthol, 4 (2 %) were sensitive to cinnamaldehyde, 19 (8 %) responded to mustard oil, and 197 (79 %) were capsaicin-sensitive (n = 2). Once again, there was no up-regulation in cold, menthol, cinnamaldehyde or mustard oil sensitivity in the absence of NGF, but responses to capsaicin did increase to levels similar to those recorded in the presence of NGF (Figure 6.7).

It could be argued that the observed up-regulation in TRP channel sensitivity in the presence of NGF was due to the preferential survival of NGF-responsive small-diameter neurons. In order to investigate this possibility, the cell size of DRG neurons from acutely dissociated or NGF-maintained cultures was measured and compared, but were found to be very similar. Thus, the average cell area of acutely dissociated P5 neurons was 319 ± 4 μm^2 (n = 688), whereas the size of neurons cultured for five days in NGF was 324 ± 4 μm^2 (n = 673, $P > 0.3$) (Figure 6.8). Even though the cell size distribution in the population at large was unaltered, there was a significant increase in cell area within the cold-sensitive (302 ± 11 μm^2, n = 123, versus 323 ± 5 μm^2, n = 358, $P < 0.05$), menthol-sensitive (223 ± 15 μm^2, n = 37, versus 266 ± 11 μm^2, n = 84, $P < 0.05$), and capsaicin-sensitive populations (278 ± 6 μm^2, n = 208, versus 319 ± 4 μm^2, n = 627, $P < 0.001$) in the presence of NGF.

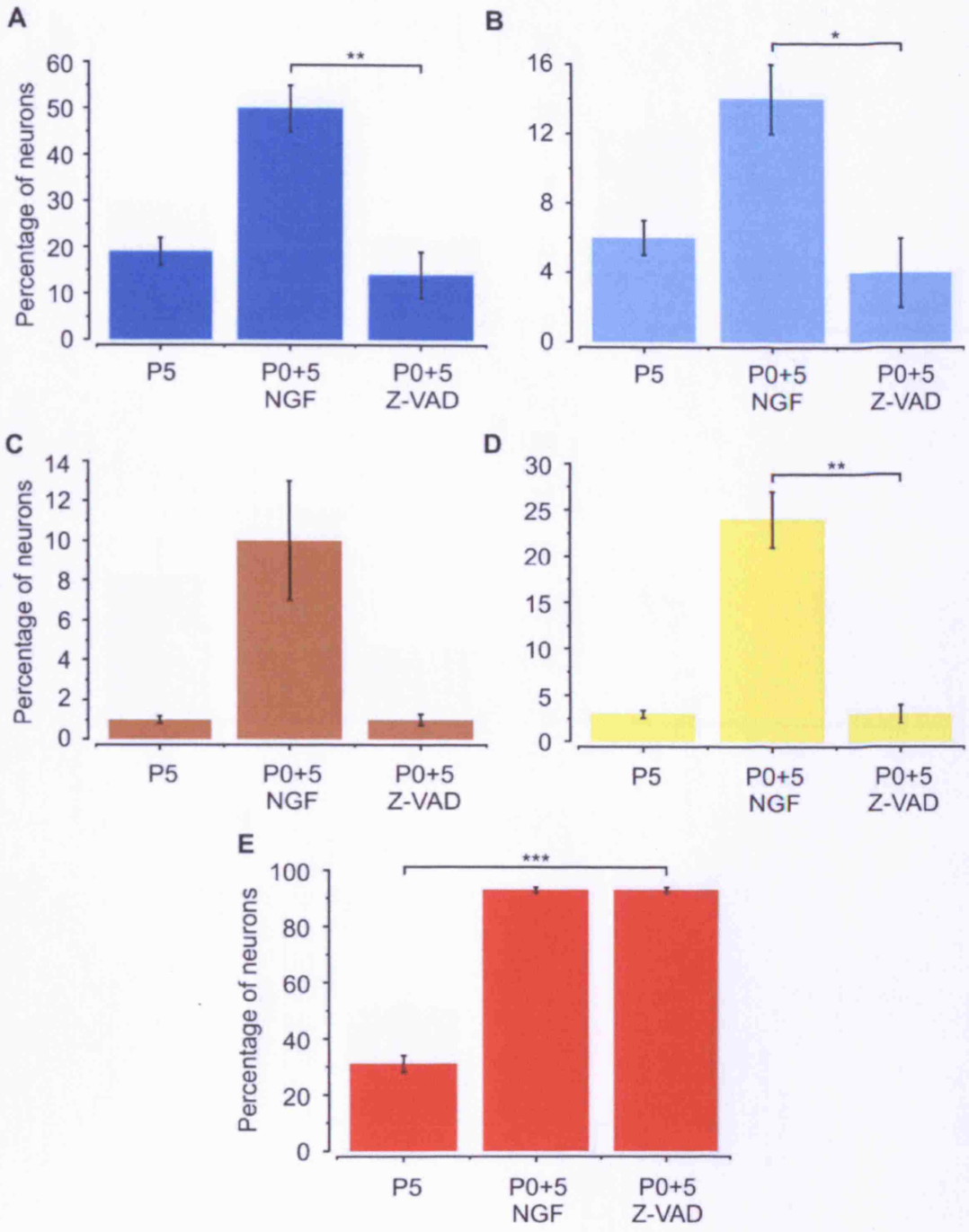

Figure 6.6. Up-regulation in functional sensitivity to cold (A), menthol (B), cinnamaldehyde (C) and mustard oil (D) in neonatal DRG neurons was NGF-dependent, whereas capsaicin sensitivity increased even in the absence of NGF (E). Neurons were cultured for five days in 100 ng/ml NGF (P0+5 NGF) or 75 μM Z-VAD-(OMe)-FMK (P0+5 Z-VAD), and compared to acutely dissociated neurons from P5 mice. P5: $n_{animals}$ = 4, n_{cells} = 705; P0+5 NGF: $n_{animals}$ = 5, n_{cells} = 693; P0+5 Z-VAD: $n_{animals}$ = 3, n_{cells} = 486. Data are presented as mean percentage of responding neurons ± SEM. * $P < 0.05$, ** $P < 0.01$, *** $P < 0.001$ (Student's unpaired *t*-test).

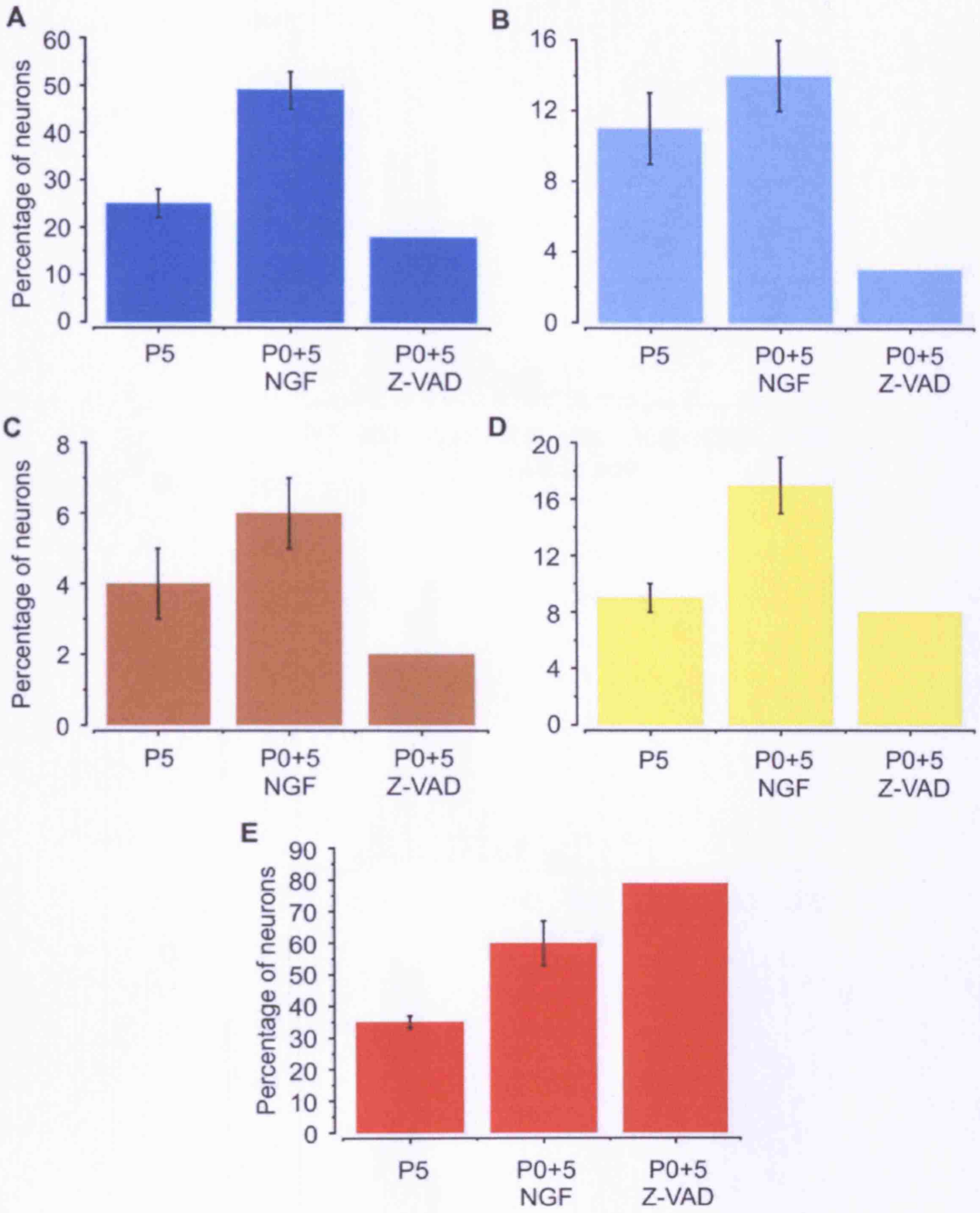

Figure 6.7. Up-regulation in functional sensitivity to cold (A), menthol (B), cinnamaldehyde (C) and mustard oil (D) in neonatal TG neurons was NGF-dependent, whereas capsaicin sensitivity increased even in the absence of NGF (E). Neurons were cultured for five days in 100 ng/ml NGF (P0+5 NGF) or 75 µM Z-VAD-(OMe)-FMK (P0+5 Z-VAD), and compared to acutely dissociated neurons from P5 mice. P5: $n_{animals} = 4$, $n_{cells} = 366$; P0+5 NGF: $n_{animals} = 5$, $n_{cells} = 513$; P0+5 Z-VAD: $n_{animals} = 2$, $n_{cells} = 251$. Data are presented as mean percentage of responding neurons ± SEM.

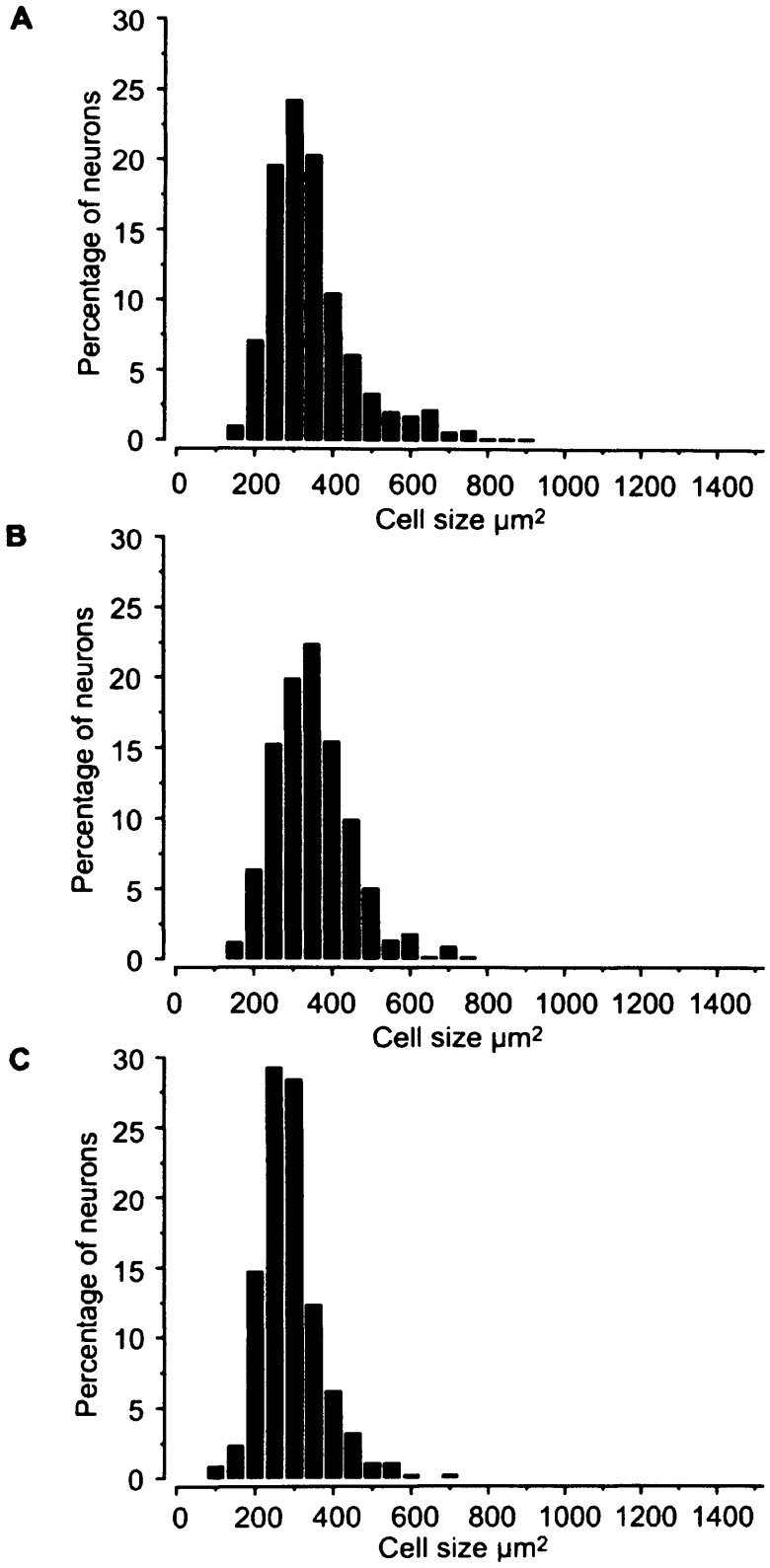

Figure 6.8. (A) Cell size distribution of acutely dissociated P5 DRG neurons. n = 688. (B) Cell size distribution of DRG neurons cultured for five days in NGF. n = 673. (C) Cell size distribution of DRG neurons maintained for five days in Z-VAD-(OMe)-FMK. n = 468.

Interestingly, the average cell area of neurons maintained for five days in Z-VAD-(OMe)-FMK was significantly smaller than either the acutely dissociated or the NGF-treated neurons (266 ± 4 μm^2, n = 468, $P < 0.001$) (Figure 6.8). While the enrichment of small-diameter neurons in these cultures could explain the recorded up-regulation in capsaicin sensitivity, the lack of increased responsiveness to other TRP channel agonists would argue against this possibility.

All DRG and TG cultures were stained for IB4 and CTB prior to calcium imaging with the aim of detecting whether the NGF-mediated up-regulation in cold and TRP channel sensitivity was restricted to a particular neuronal subpopulation. Over time in culture, however, there was a dramatic down-regulation in the number of cells labelling with IB4 (Figure 6.9). In acutely dissociated P2 and P5 DRG neurons, IB4 labelled 264/962 (31 ± 5 %) and 195/705 (29 ± 3 %) cells, respectively, while 87 (12 ± 5 %) and 169 (26 ± 4 %) neurons stained for CTB. After two days in culture, there was already a marked decrease in IB4 staining, with only 95/953 (11 ± 2 %) neurons displaying a fluorescent signal ($P < 0.01$ when compared to acutely dissociated P2 neurons), and after five days in culture, just 24/867 (2 ± 1 %) cells were labelled ($P < 0.001$ when compared to acutely dissociated P5 neurons). This effect was observed both in the presence and absence of NGF. CTB staining did not undergo such a dramatic reduction, although significantly fewer cells were labelled with CTB also on the fifth day in culture (46/486 neurons, 10 ± 3 %, $P < 0.05$).

In acutely dissociated TG cultures, IB4 labelled 106/644 (18 ± 2 %) P2 neurons and 79/366 (22 ± 3 %) P5 cells, while 94 (21 ± 8 %) and 67 (16 ± 8 %) cells stained for CTB, respectively. As observed in DRG neurons, IB4 labelling was down-regulated between 2-5 days in culture, independently of NGF. Of the 264 TG neurons analysed after two days in culture, 24 (8 ± 3 %) were stained for IB4 ($P < 0.05$), whereas just 8/764 (1 ± 0.4 %) cells were IB4-positive following five days of culture ($P < 0.001$). In contrast to DRG, the number of TG neurons staining for CTB remained constant over time in culture (99/764 cells were labelled after five days in culture, 14 ± 3 %, $P > 0.8$) (Figure 6.10).

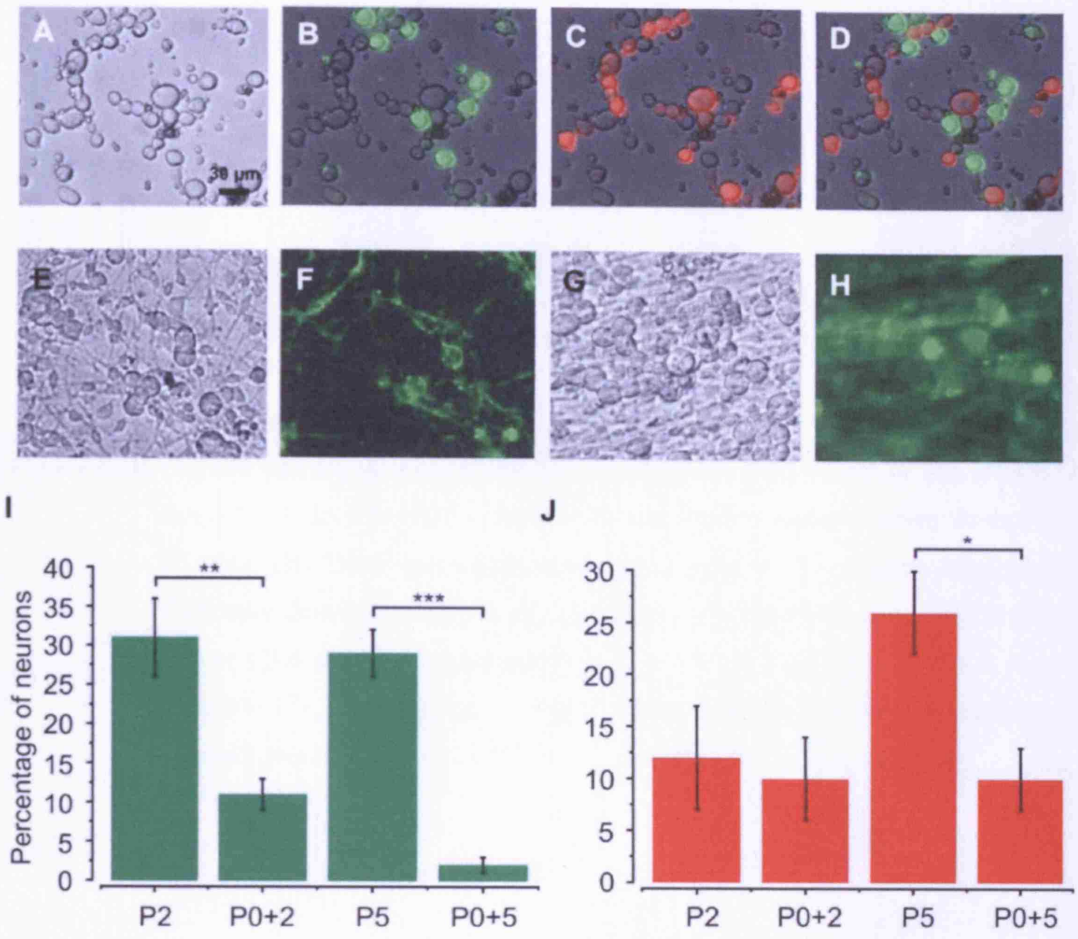

Figure 6.9. (A-D) Representative example of IB4 (green) and CTB (red) staining in acutely dissociated P5 DRG neurons. (A) Brightfield image. (B) IB4 staining. (C) CTB staining. (D) Overlay of IB4 and CTB staining. (E-F) Representative example of IB4 staining in DRG neurons cultured for two days in NGF. (E) Brightfield image. (F) IB4 staining. (G-H) Representative example of IB4 staining in DRG neurons cultured for five days in NGF. (G) Brightfield image. (H) IB4 staining. (I) IB4 staining was down-regulated in DRG neurons cultured for two (P0+2) or five (P0+5) days in NGF compared to acutely dissociated neurons from P2 or P5 mice. (J) CTB staining was down-regulated in DRG neurons cultured for five days in NGF compared to acutely dissociated age-matched controls. P2: $n_{animals}$ = 5, n_{cells} = 962; P0+2: $n_{animals}$ = 5, n_{cells} = 953; P5: $n_{animals}$ = 4, n_{cells} = 705; P0+5: $n_{animals}$ = 6 or 3 (for IB4 or CTB staining, respectively), n_{cells} = 867 or 486. Data are presented as mean percentage of labelled neurons ± SEM. * $P < 0.05$, ** $P < 0.01$, *** $P < 0.001$ (Student's unpaired *t*-test).

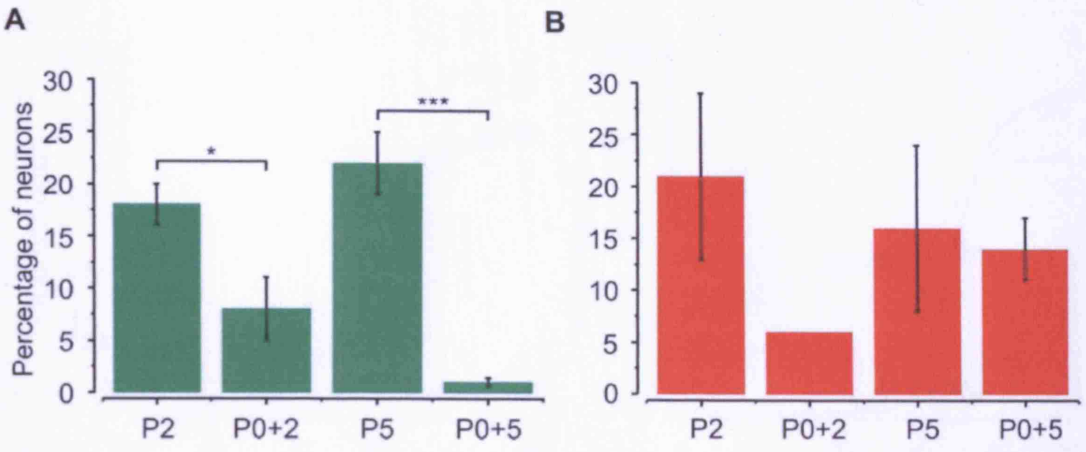

Figure 6.10. (A) IB4 staining was down-regulated in TG neurons cultured for two (P0+2) or five (P0+5) days in NGF compared to acutely dissociated neurons from P2 or P5 mice. (B) There was no change in the number of TG neurons labelling for CTB over time in culture. P2: $n_{animals} = 4$, $n_{cells} = 644$; P0+2: $n_{animals} = 3$ or 2 (for IB4 or CTB staining, respectively), $n_{cells} = 143$ or 264; P5: $n_{animals} = 4$, $n_{cells} = 366$; P0+5: $n_{animals} = 7$, $n_{cells} = 764$. Data are presented as mean percentage of labelled neurons. * $P < 0.05$, *** $P < 0.001$ (Student's unpaired *t*-test).

6.4.3. NGF up-regulates expression of TRP channel mRNA

Following the calcium imaging experiments, DRG and TG neurons were analysed for the expression of TRP channels in order to see whether the observed functional up-regulation in menthol, cinnamaldehyde, mustard oil and capsaicin sensitivity was matched by an increase in TRPM8, TRPA1 and TRPV1 transcript levels (DRG: $n = 4$; TG: $n = 3$-4). The two housekeeping genes UCHL1 and GAPDH were chosen as genes of reference for quantification purposes. However, whereas the expression of UCHL1 remained stable, the amount of GAPDH present increased significantly over time in culture. Thus, while there was no difference in GAPDH expression between acutely dissociated P2 and P5 neurons, after two days in NGF (P0+2 cultures) the transcript was up-regulated 6-fold or 7-fold in DRG and TG neurons, respectively, relative to UCHL1 (Figure 6.11). The reason for this observed increase in GAPDH expression is likely to be the high rate of proliferation of non-neuronal cells present in the culture. As a result all quantification of TRP channel expression was performed relative to the expression of the neuron-specific marker UCHL1 only.

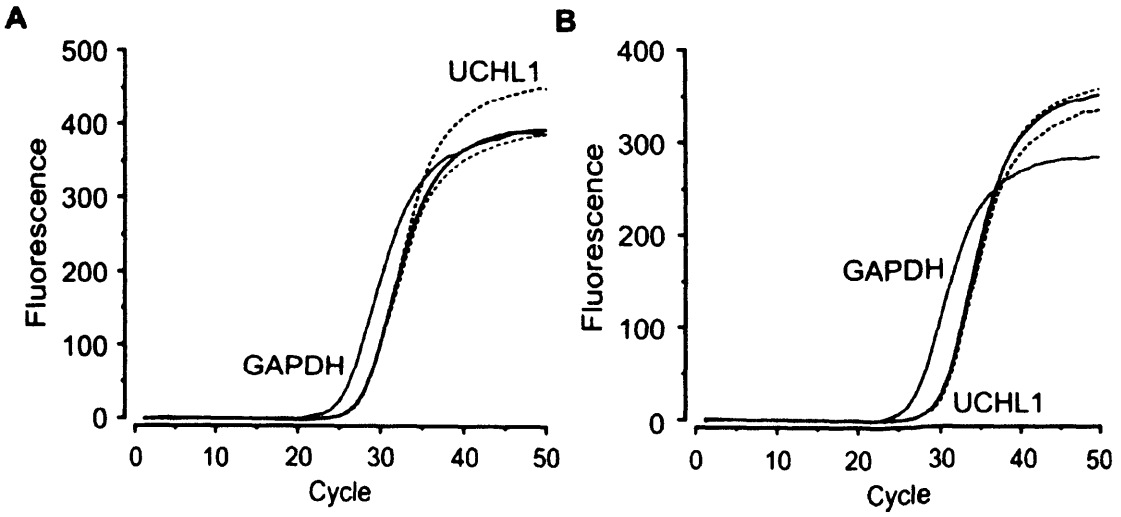

Figure 6.11. Illustration of rt-PCR for UCHL1 and GAPDH in neonatal DRG (A) and TG (B) neurons. The cDNA of 250 pg total RNA equivalents were amplified. The cycle threshold (Ct) values for UCHL1 (dashed lines) were similar in acutely dissociated P2 neurons (blue) and cells that had been cultured for two days in NGF (P0+2, green). However, there was a lower Ct value for GAPDH (solid lines) in neurons maintained in culture for two days compared to acutely dissociated age-matched controls.

The increase in non-neuronal mRNA in cultures maintained for a period of days resulted in a dilution of neuron-specific transcripts. Thus, with equal amounts of starting RNA, 2-5 day-old DRG cultures had up to 3-fold less UCHL1 compared to acutely dissociated age-matched controls, as assessed by the cycle threshold (Ct) value. The difference in mean Ct value between acutely dissociated and long-term cultures was not significant, however. In acutely dissociated P2 DRG neurons, the Ct value for UCHL1 was 28.5 ± 1.1, compared to 29.6 ± 1.1 in neurons cultured for two days in NGF ($P > 0.4$), while in acutely dissociated P5 neurons the Ct value was 27.5 ± 0.7 versus 28.9 ± 1.1 in five day-old cultures ($P > 0.3$). The same was true for TG neurons: acutely dissociated P2 cells had a Ct value of 30.5 ± 0.9 for UCHL1, compared to 30.3 ± 1.2 in neurons maintained for two days in NGF ($P > 0.8$), whereas the Ct values were recorded as 31.4 ± 0.9 and 30.2 ± 1.2 in acutely dissociated P5 neurons and cells kept for five days in culture, respectively ($P > 0.4$).

TRP channel expression was examined in neurons maintained for two (P0+2) or five (P0+5) days in NGF, and compared to that of acutely dissociated age-matched controls (at P2 or P5, respectively). In addition, data from acutely dissociated neurons were used to monitor the evolution of TRP channel expression during the early postnatal stages of development.

Reflecting the observation that functional responses to cinnamaldehyde and mustard oil were up-regulated in DRG and TG neurons cultured in NGF, expression of the TRPA1 channel was elevated compared to the age-matched control cultures. In acutely dissociated DRG neurons, between the ages of P2 and P5, there was no change in the amount of TRPA1 transcript present. However in P0+2 cultures, the presence of NGF was sufficient to induce a significant 2.5-fold increase in expression of the ion channel, relative to neurons isolated at P2. There was no further up-regulation of TRPA1 in neurons maintained for up to five days in NGF, where the amount of transcript present was 2-fold higher than in acutely dissociated P5 neurons (Figure 6.12).

In TG neurons, there was a 1.6-fold increase in TRPA1 expression between days P2 and P5, which was exacerbated by the presence of NGF. Whereas there was no difference in expression between acutely dissociated P2 neurons and cells kept for two days in NGF, matching the absence of a functional change in responsiveness to cinnamaldehyde or mustard oil, after five days in NGF there was a 1.4-fold up-regulation in TRPA1 expression compared to acutely dissociated P5 neurons (Figure 6.12).

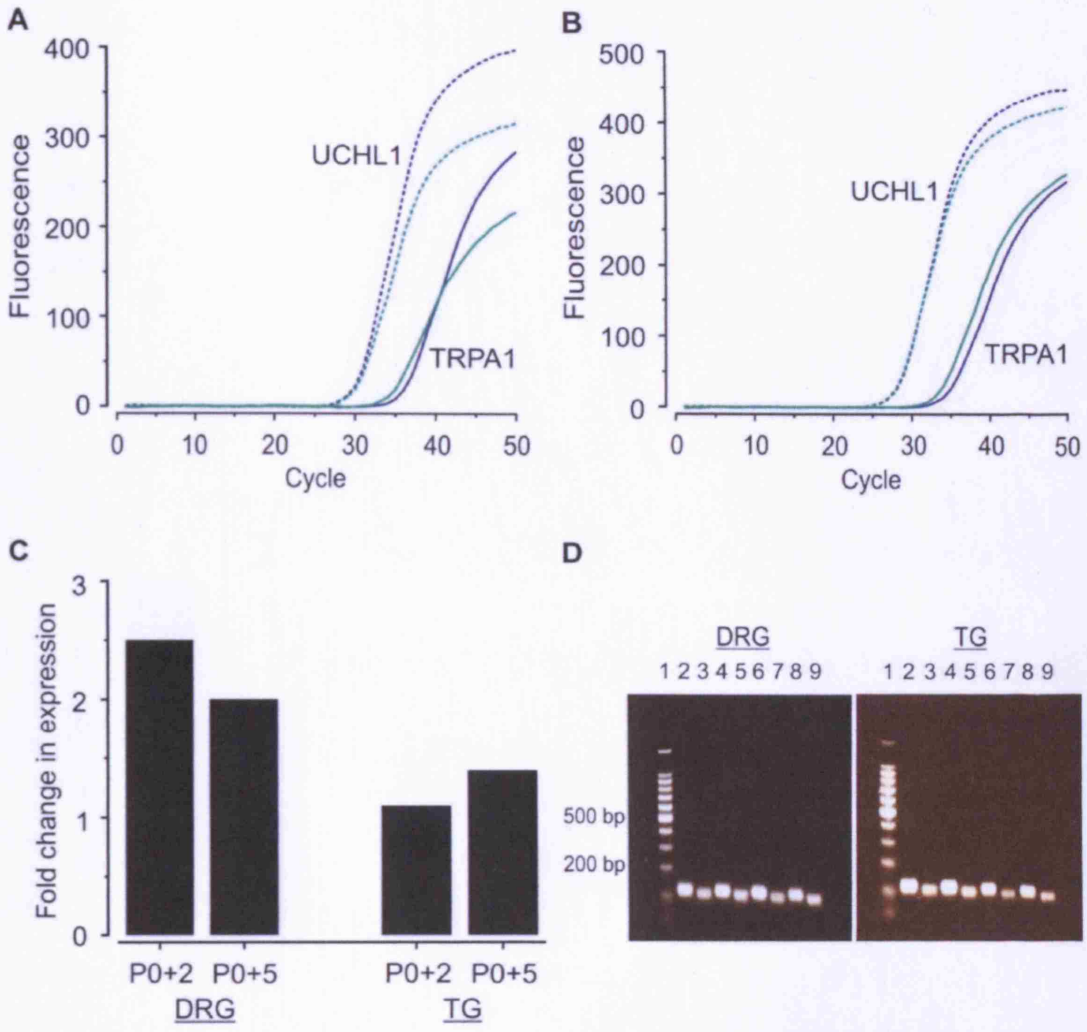

Figure 6.12. Quantitative rt-PCR for TRPA1 expression in neonatal DRG and TG neurons. The cDNA of 250 pg (UCHL1) or 1.25 ng (TRPA1) total RNA equivalents were amplified. (A) Illustration of rt-PCR for UCHL1 and TRPA1 in DRG neurons. Whereas there were similar cycle threshold (Ct) values for UCHL1, there was a lower Ct value for the TRPA1 transcript in cells maintained for 2-5 days in NGF (green) compared to acutely dissociated neurons (blue). (B) Illustration of rt-PCR for UCHL1 and TRPA1 in TG neurons. (C) Quantification of the up-regulation in TRPA1 expression in DRG and TG neurons following two (P0+2) or five days (P0+5) culture in NGF relative to acutely dissociated cells at P2 and P5, respectively. (D) All PCR products were analysed on a 2 % agarose gel. Estimated product sizes were 117 bp (UCHL1, Lanes 2, 4, 6, 8) and 107 bp (TRPA1, Lanes 3, 5, 7, 9). Lane 1: marker. Lanes 2, 3: acutely dissociated P2 neurons. Lanes 4, 5: neurons cultured for two days in NGF. Lanes 6, 7: acutely dissociated P5 neurons. Lanes 8, 9: neurons cultured for five days in NGF.

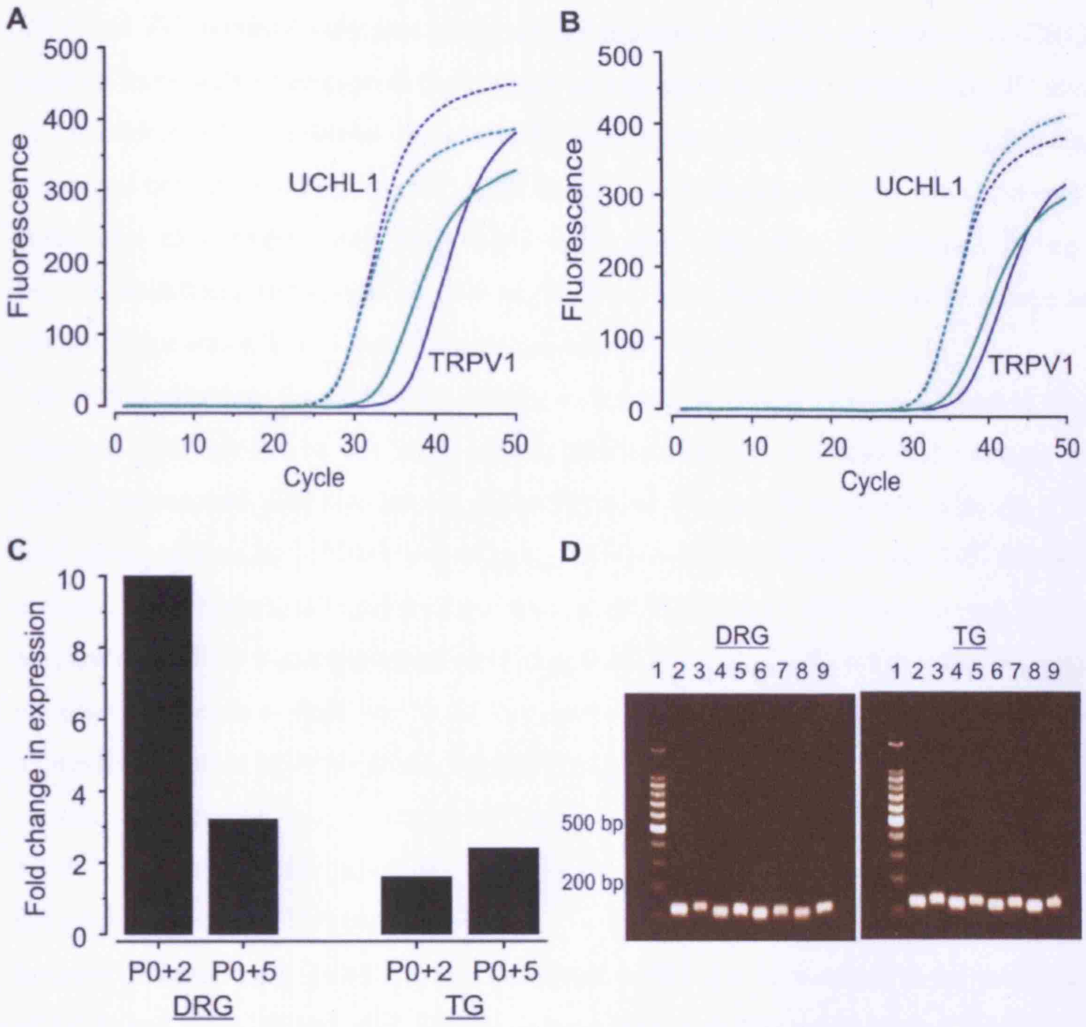

Figure 6.13. Quantitative rt-PCR for TRPV1 expression in neonatal DRG and TG neurons. The cDNA of 250 pg (UCHL1) or 1.25 ng (TRPV1) total RNA equivalents were amplified. (A) Illustration of rt-PCR for UCHL1 and TRPV1 in DRG neurons. Whereas there were similar cycle threshold (Ct) values for UCHL1, there was a lower Ct value for the TRPV1 transcript in cells maintained for 2-5 days in NGF (green) compared to acutely dissociated neurons (blue). (B) Illustration of rt-PCR for UCHL1 and TRPV1 in TG neurons. (C) Quantification of the up-regulation in TRPV1 expression in DRG and TG neurons following two (P0+2) or five days (P0+5) culture in NGF relative to acutely dissociated cells at P2 and P5, respectively. (D) All PCR products were analysed on a 2 % agarose gel. Estimated product sizes were 117 bp (UCHL1, Lanes 2, 4, 6, 8) and 120 bp (TRPV1, Lanes 3, 5, 7, 9). Lane 1: marker. Lanes 2, 3: acutely dissociated P2 neurons. Lanes 4, 5: neurons cultured for two days in NGF. Lanes 6, 7: acutely dissociated P5 neurons. Lanes 8, 9: neurons cultured for five days in NGF.

DRG and TG neurons were also analysed for changes in TRPV1 expression. In DRG neurons there was no change in the amount of transcript present between days P2 and P5. However, P0+2 cultures showed a 10-fold up-regulation in TRPV1 expression compared to acutely dissociated P2 cells. In contrast to the observation that functional sensitivity to capsaicin remained high even after five days in culture, the up-regulation in transcript levels was not maintained. Thus between two and five days in culture, there was a 3-fold down-regulation in TRPV1 mRNA (Figure 6.13).

Like DRG neurons, functional sensitivity to capsaicin was also up-regulated in TG neurons, although not to the same extent, and accordingly the recorded increase in TRPV1 expression was also not as great. Between P2 and P5 there was already a 2-fold up-regulation in TRPV1 expression, which was amplified in the 2-5 day-old cultures. TG neurons cultured for two days in NGF showed a 1.6-fold increase in the amount of TRPV1 transcript compared to acutely dissociated P2 cells, while neurons maintained for five days in NGF demonstrated a 2.4-fold increase in channel expression relative to P5 neurons (Figure 6.13). Functional studies demonstrated that capsaicin sensitivity was up-regulated in sensory neurons even in the absence of NGF. It is probable that transcript expression is also regulated independently of NGF, although this was not investigated here.

Sensory neurons were found to have increased sensitivity to menthol in the presence of NGF, and, like TRPA1 and TRPV1, it was surmised that the increased functional sensitivity would be matched by an up-regulation in TRPM8 expression. Accordingly, an attempt was made to quantify the amount of TRPM8 transcript present in different neuronal samples, however instead of the expected up-regulation in channel expression, a 4-fold down-regulation was recorded in DRG neurons cultured for five days in NGF compared to acutely dissociated P5 neurons (Figure 6.14). As changes in the expression of GAPDH demonstrated, there was a significant increase in the amount of non-neuronal transcripts present in long-term cultures. It is possible that, like UCHL1, the increased expression of these genes resulted in a dilution of the TRPM8 transcript, so that a greater amount of starting material was required to detect its presence. Since NGF does not up-regulate TRPM8 mRNA, it is likely that the increased sensitivity to menthol reflects an NGF-directed modulation of channel function as opposed to expression.

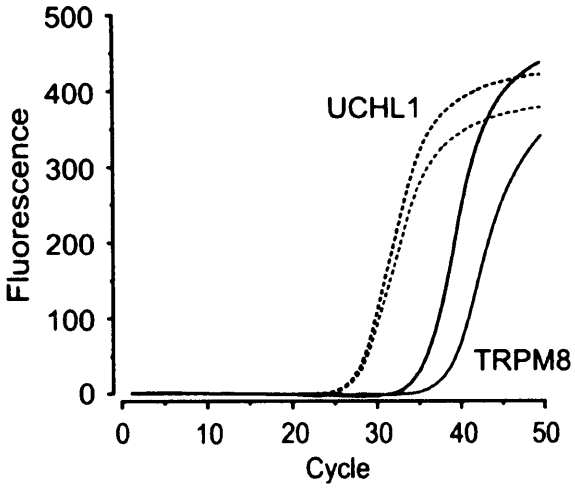

Figure 6.14. Illustration of rt-PCR for UCHL1 and TRPM8 in neonatal DRG neurons. The cDNA of 250 pg (UCHL1), 1.25 ng (TRPM8, acutely dissociated P5 neurons), or 2.5 ng (TRPM8, P0+5 neurons) total RNA equivalents were amplified. The cycle threshold (Ct) values for UCHL1 (dashed lines) were similar in acutely dissociated P5 neurons (blue) and cells that had been cultured for five days in NGF (P0+5, green). However, there was a higher Ct value for TRPM8 (solid lines) in neurons maintained in culture for five days compared to acutely dissociated age-matched controls.

6.5. Discussion

The main finding of this study is that NGF up-regulates functional sensitivity to cold and TRP channel agonists in neonatal sensory neurons, and achieves this by increasing expression of TRP ion channels. The expression and function of TRPV1 are also regulated over time in culture, but independently of the presence of NGF.

6.5.1. The first two postnatal weeks represent a period of ongoing sensory neuronal development

The proportion of acutely dissociated sensory neurons found to respond to cold and TRP channel agonists corresponds very well with the findings from a previous study, in which approximately 30 % of DRG cells were cold-sensitive between the ages of P0-P7, 6 % responded to menthol, up to 5 % were responsive to cinnamaldehyde, and 40 % were capsaicin-sensitive (Hjerling-Leffler et al., 2007). Sensitivity to cold, menthol, cinnamaldehyde and mustard oil was higher in the neuronal population

isolated from the TG compared to that of the DRG. This observation is not without precedence however, as other groups have noted that the TG harbours a larger population of TRPM8- and TRPA1-positive neurons than the DRG (McKemy et al., 2002;Jordt et al., 2004;Kobayashi et al., 2005).

When studying the properties of neonatal sensory neurons, acutely dissociated cells appear to provide a more accurate representation of the *in vivo* phenotype than neurons maintained in culture for longer than a few hours. When grown *in vitro* neonatal neurons are dependent on growth factors in the culture medium for survival, and as the results from this study demonstrate, the presence of NGF induces a marked alteration in the sensory phenotype, that is, a significantly larger proportion of cells displayed functional sensitivity to cold and TRP channel agonists after treatment with NGF compared to age-matched controls. With regards to TRPA1 in particular, the onset of channel expression is postnatal, with the first functional responses observed in less than 1 % of cells at P0, and even by P7 only 5 % of DRG neurons will respond to a cinnamaldehyde stimulus (Hjerling-Leffler et al., 2007). Data from this study are in accordance with these previous observations, and in addition show that at P5 sensitivity to another TRPA1 agonist, mustard oil, is present in just 3 % and 9 % of DRG and TG neurons, respectively. In contrast other groups have reported a significantly greater sensitivity to mustard oil in early postnatal sensory neurons (Jordt et al., 2004;Bautista et al., 2006). This apparent discrepancy can be explained by the fact that in the latter studies, the neurons were cultured in NGF for up to two days before examination, and were therefore induced to express a higher sensitivity to the TRPA1 agonist by the presence of the growth factor. The reported percentage of cells responding to mustard oil was 25-35 %, which is much higher than recorded in this study and with lower concentrations of agonist used (20-50 μM). The only obvious difference between the investigations that could explain this discrepancy was the use of neurons from mouse (this study) versus rat (Jordt et al., 2004;Bautista et al., 2006). In support of this reasoning, preliminary experiments in the laboratory showed that a much higher percentage of neonatal rat DRG neurons (around 25 %) displayed mustard oil sensitivity following two days exposure to NGF compared to mouse (J. Hjerling-Leffler, unpublished observations).

It is recognised that during the first two postnatal weeks, sensory neurons continue to undergo significant developmental changes that will determine the adult phenotype. Included in those changes are cold sensitivity and TRP channel expression, which are

regulated throughout embryonic development and into the postnatal period (Hjerling-Leffler et al., 2007). Functional sensitivity to cold and capsaicin first appears at E11.5. Between the ages of E12.5 and E18.5, there is a substantial increase in the percentage of responsive neurons, so that the number of cells responding to either stimulus greatly exceeds that seen in the adult. The subsequent decrease in sensitivity, which continues postnatally, was attributed to a down-regulation in receptor expression, rather than cell death. This suggests that a large proportion of neurons may retain the capacity to respond to cold or capsaicin, even if they do not normally express it. Sensitivity to menthol and cinnamaldehyde is not detected until E16.5 and P0, respectively, from which time there is a gradual increase in the numbers of responsive neurons up to and beyond P14. The continued development of TRP channel expression in postnatal neurons could explain the up-regulation in TRPV1 and TRPA1 transcript expression recorded in P5 TG neurons compared to cells isolated at P2, although it should be noted that there was no corresponding functional change in responsiveness to either capsaicin, mustard oil or cinnamaldehyde.

Given that the first two postnatal weeks do represent a period of ongoing change and development, it is perhaps not surprising that changes in the concentration of available growth factors could have such marked effects on the properties of neonatal neurons. Indeed, evidence from previous studies demonstrates that NGF can have a significant influence on phenotype during these early stages. On the one hand, anti-NGF treatment between P4-P11 results in a phenotypic switch in a subpopulation of Aδ-fibres, whose properties change from high-threshold mechanoreceptors to low-threshold D-hair afferents, while the same treatment between P2-P14 causes a population of mechanoheat-sensitive C-fibres to be replaced by afferents sensitive to mechanical stimuli only. On the other hand, the administration of excess NGF in the first two postnatal weeks leads to increased sensitivity to mechanical stimuli in Aδ-fibres (Lewin and Mendell, 1993).

6.5.2. NGF regulates TRP channel expression in sensory neurons

The increased sensitivity to cinnamaldehyde and mustard oil in neonatal sensory neurons was reflected in an NGF-mediated up-regulation in the expression of TRPA1. On the other hand, increased responsiveness to menthol was not matched by an up-regulation in TRPM8 mRNA, suggesting an NGF-directed modulation of channel function rather than expression. The fact that the majority of the functional changes

were observed only after the neurons had been cultured in NGF for five days as opposed to two suggests that sustained exposure to the growth factor is required and supports a situation in which transcriptional or post-translational alterations precede the functional up-regulation.

NGF-mediated regulation of TRPA1 expression has been described previously in adult sensory neurons. One study in TG neurons demonstrated a dose-dependent up-regulation in TRPA1 mRNA expression *in vitro* and *in vivo* that was correlated with an increase in mustard oil-evoked currents from neurons recorded in the whole-cell configuration (Diogenes et al., 2007). Furthermore *in vivo* experiments have shown that NGF achieves its effect via activation of the p38 mitogen-activated protein kinase (MAPK) signalling pathway (Obata et al., 2005). Concurrent up-regulation of the p75 neurotrophin receptor in small-diameter neurons facilitates the binding of NGF to TrkA and maintains the receptor in a phosphorylated state, resulting in enhanced TrkA signalling and gene transcription (Obata et al., 2006). The up-regulation in TRPA1 recorded in these latter studies was not matched by an increase in TRPM8 expression, although data from this and other studies suggests that NGF can up-regulate functional sensitivity to menthol in dissociated neonatal and adult DRG neurons *in vitro* (Story et al., 2003;Babes et al., 2004). This apparent discrepancy could be due to the presence of additional regulating factors *in vivo*, and it should be mentioned that the *in vivo* data was obtained from animals in a state of inflammatory or neuropathic pain. In this regard the release of inflammatory mediators *in vivo* could be especially important, as a recent report showed that bradykinin and prostaglandin E_2 can desensitise the response to a cooling stimulus in cold- and menthol-sensitive DRG neurons (Linte et al., 2007). The presence of NGF certainly does appear to be very important for the expression of TRPM8 in developing cells, however: TRPM8 expression in the DRG was greatly reduced at P0 in NGF knockout mice (Luo et al., 2007).

There are three main intracellular signalling pathways through which NGF mediates its various effects on cell survival, cell growth and ion channel expression (Huang and Reichardt, 2003) (Figure 6.15). The first involves the activation of phospholipase C-gamma (PLCγ), which catalyses the hydrolysis of phosphatidylinositol 4,5-bisphosphate (PIP_2) to inositol tris-phosphate (IP3) and diacylglycerol (DAG). IP3 catalyses the release of calcium from intracellular stores, while DAG stimulates the activation of protein kinase C (PKC), which in turn can phosphorylate MAPK and ion

channels to regulate gene transcription or channel function, respectively. Secondly, the generation of P3-phosphorylated phosphoinositides by the phosphatidylinositide 3-kinase (PI3-K) allows subsequent activation of the phosphatidylinositide-dependent protein kinase (PDK-1). PDK-1 then activates PKC and protein kinase B (PKB), the latter promoting cell survival. Finally, activation of the Ras GTPase initiates the MAPK phosphorylation cascade, resulting eventually in gene transcription or post-translational modification of proteins. It is highly unlikely that NGF would have acted via either the PLCγ or the PI3-K pathways to alter menthol sensitivity, since the hydrolysis of PIP_2 and the activation of PKC have both been shown to result in desensitisation of the TRPM8 channel, the latter via dephosphorylation of the receptor (Rohacs et al., 2005;Liu and Qin, 2005;Premkumar et al., 2005;Abe et al., 2006). It is therefore probable that the increase in TRPM8 function, as indicated by the up-regulated sensitivity to menthol, was effected through the activation of the MAPK signalling pathway, as previously described for TRPA1 (Obata et al., 2005).

Unlike TRPM8 and TRPA1, the influence of NGF on the expression and function of TRPV1 has been the subject of much investigation. Acute application of NGF to dissociated sensory neurons potentiates the response to heat and capsaicin, whereas the release of NGF following nerve injury or inflammation *in vivo* has been shown to up-regulate expression of the TRPV1 channel, which underlies the development of thermal hyperalgesia (Petruska and Mendell, 2004). With regards to the mechanisms controlling these effects, all three NGF-mediated signalling pathways have been implicated in the acute regulation of TRPV1 (Chuang et al., 2001;Bonnington and McNaughton, 2003;Zhang et al., 2005;Zhu and Oxford, 2007), while the up-regulation in channel expression following nerve injury or inflammation is effected via Ras and MAPK signalling (Ji et al., 2002;Bron et al., 2003).

The finding that capsaicin sensitivity was up-regulated independently of NGF in neonatal sensory neurons was therefore unexpected, although it is not the first time this phenomenon has been reported: a study of TRPV1 expression in mouse TG neurons isolated at P10-P14 demonstrated an elevation in TRPV1 mRNA and protein in neurons cultured for up to four days without NGF, compared to the intact ganglion (Simonetti et al., 2006). Furthermore, the addition of NGF did not increase the number of capsaicin-sensitive neurons. The authors concluded that the changes in protein expression reflected the plasticity of neurons maintained in culture, although gave no explanation for the mechanisms underlying the observed up-regulation. They

did however measure the amount of endogenous NGF released into the culture medium by the neurons, which was found to be in the low picogram range. While this was almost double the amount of NGF recovered from intact ganglia, concentrations of NGF of this magnitude are not sufficient to promote survival of late embryonic (E19) TG neurons *in vitro* (Davies et al., 1993), and would be unlikely to induce a functional up-regulation in TRPV1 expression of the extent recorded in this study.

It was observed that the average cell size of neurons cultured in the presence of the caspase inhibitor Z-VAD-(OMe)-FMK was significantly smaller than either acutely dissociated neurons or cells maintained in NGF. This raises the possibility that the preferential survival of small-diameter cells resulted in an enrichment, and apparent up-regulation, in TRPV1-positive neurons. However, the fact that neither menthol, cinnamaldehyde nor mustard oil sensitivity were altered in these cultures argues against this possibility. At P7, approximately 60 % of menthol-responsive and the majority of cinnamaldehyde-sensitive neurons are also capsaicin-sensitive, meaning that an enrichment of the TRPV1-positive population would incur an increase in the TRPM8- and TRPA1-positive populations also (Hjerling-Leffler et al., 2007). The observed decrease in cell size is most likely due to neuronal hypotrophy, induced by an absence of growth factors. By the same reasoning, the recorded increase in cell size of cold-, menthol- and capsaicin-sensitive neurons in the presence of NGF would be explained by neuronal hypertrophy evoked by the addition of excess neurotrophic factor to the culture medium. Both phenomena have been noted in previous studies (Luo et al., 2007;Anand et al., 2006).

The NGF-independent up-regulation in TRPV1 expression could be explained by the following scenario. As previously mentioned, between E14.5 and P7 TRPV1 expression is down-regulated in a subset of sensory neurons (Hjerling-Leffler et al., 2007), which implies that a mechanism of transcriptional repression is switched on during this period in order to attain adult levels of receptor expression. When neonatal neurons are placed into culture, this repression mechanism may become disrupted or inhibited, leading to an uncontrolled up-regulation in TRPV1 expression, which cannot be further influenced by growth factors. Incidentally, the capsaicin response in neonatal neurons can be potentiated by the acute application of NGF, demonstrating that channel activity is still modulated by growth factors to some extent (Bonnington and McNaughton, 2003;Simonetti et al., 2006).

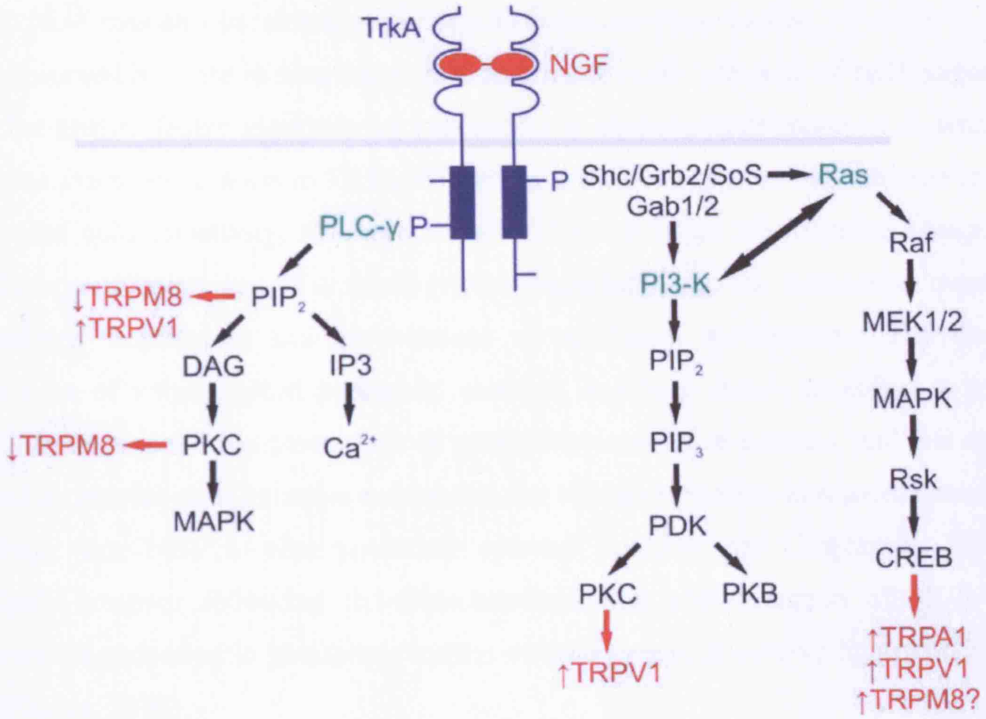

Figure 6.15. Schematic of the intracellular signalling pathways initiated by the binding of NGF to its receptor, TrkA. Binding of ligand induces autophosphorylation of the receptor and allows the recruitment of proteins that have the ability to interact with phosphotyrosine residues. These interactions subsequently trigger the activation of the phospholipase C (PLCγ), phosphatidylinositide 3-kinase (PI3-K) and Ras signalling pathways, which result in a number of outcomes, including gene transcription, cell survival, proliferation, and post-translational modification of proteins. Activation of the signalling pathways has various effects on TRP channel function and expression. The hydrolysis of phosphatidylinositol 4,5-bisphosphate (PIP_2) and the activation of protein kinase C (PKC) have opposing effects on TRPV1 and TRPM8, activating the former and causing desensitisation of the latter. Activation of the Ras GTPase and mitogen-activated protein kinase (MAPK) signalling cascades results in phosphorylation of the cyclic AMP response element binding (CREB) transcription factor and the up-regulation of TRPV1 and TRPA1. TRPM8 may also be regulated via this pathway. DAG, diacylglycerol; IP3, inositol tris-phosphate; Shc, SH2-containing collagen-related protein; Grb2, growth factor receptor-bound protein; SoS, son of sevenless guanine nucleotide exchange factor; Gab1/2, Grb2-associated binder-1/2; PIP_3, phosphatidylinositol 3,4,5-trisphosphate; PDK, phosphatidylinositide-dependent protein kinase; PKB, protein kinase B; MEK1/2, MAPK/ERK (extracellular signal-regulated) kinase 1/2; Rsk, ribosomal protein S6 kinase.

6.5.3. NGF mediates the development of cold hypersensitivity in vivo

The observed increase in functional cold sensitivity in the presence of NGF suggests that the growth factor regulates the expression of cold-sensitive receptors in sensory neurons. An up-regulation in TRPM8 function would be expected to contribute to the increased cold sensitivity, although it should be noted that the recorded change in cold responsiveness was of a much greater magnitude than the increase in menthol sensitivity, implicating the involvement of additional mechanisms. The down-regulation of voltage-gated potassium channels has been shown to induce a novel cold response in a large percentage of previously insensitive neurons, and this could therefore provide an alternative mechanism for the augmentation in responsiveness to cooling, were NGF to alter potassium channel function (see Chapter 4). This is unlikely however following the demonstration that administration of NGF can prevent the reduction in potassium current evoked by a sciatic nerve ligation (Everill and Kocsis, 2000).

Studies presented here and elsewhere have determined that TRPA1 does not play a significant role in the transduction of cold stimuli in healthy sensory neurons (see Chapter 3). A series of reports from one group however have suggested a role for TRPA1 in the development of NGF-induced cold hypersensitivity following inflammation and nerve injury (Obata et al., 2005;Katsura et al., 2006;Obata et al., 2006). Administration of TRPA1 antisense oligodeoxynucleotide was found to reduce behavioural cold hyperalgesia induced by injection of complete Freund's adjuvant or a spinal nerve ligation. Cold sensitivity of sensory neurons was not monitored in these studies, however other groups have reported an increase in the number of cold-sensitive cells in the L5 spinal nerve ligation model of neuropathic pain (Djouhri et al., 2004;Ji et al., 2007). Furthermore, single unit recordings provided evidence for a phenotypic switch in Aδ- and C-fibres, possibly corresponding to a de novo expression of cold-sensitive receptors in previously insensitive neurons. The data from these studies would imply that up-regulated TRPA1 expression could underlie the increased cold sensitivity recorded in neonatal sensory neurons following NGF treatment.

Taking these previous findings into account, the NGF-mediated increase in cold sensitivity and TRP channel expression in sensory neurons is likely to contribute to the development of cold hypersensitivity *in vivo*. Injury of neonatal neurons can produce long-lasting effects and have a significant impact on sensory processing in

the adult. Administration of NGF to neonatal rats resulted in the development of a profound mechanical hyperalgesia which was still present weeks later in the mature animal (Lewin et al., 1993). It was proposed that the hypersensitivity was caused by peripheral sensitisation of Aδ-nociceptors, resulting in a reduction in the mechanical threshold for activation. Inflammation and nerve injury in a neonatal animal can alter the central connectivity of the nociceptive circuitry, and lead to a state of enhanced signalling in the adult (Lidow, 2002). Indeed, studies in adult animals that had suffered an inflammatory insult during the early postnatal period demonstrated an exaggerated hypersensitivity to mechanical and thermal stimuli during a subsequent inflammation. Moreover, neuronal insults can result in long-term changes in gene expression and second messenger pathways which will enhance the response to subsequent sensory challenges (Gold and Flake, 2005). Evidence from this and other studies suggests that cold hyperalgesia is mediated primarily via the up-regulation of cold-sensitive receptors in sensory neurons (Obata et al., 2005;Katsura et al., 2006;Obata et al., 2006;Ji et al., 2007). The NGF-mediated increase in cold sensitivity and TRP channel expression in neonatal neurons may therefore represent the development of a sensitisation to cold temperatures that will result in an enhanced responsiveness to cooling following inflammation or nerve injury in the adult.

In conclusion, the principal finding of this study is that the exposure of neonatal sensory neurons to NGF induces an up-regulation in cold sensitivity and TRP channel expression. This could result in a permanent alteration of sensory phenotype, such that adult neurons will display enhanced hypersensitivity to cold following nerve injury or inflammation.

7. The regulation of cold sensitivity and TRP channel expression by Runx1

7.1. Background

During the first two postnatal weeks, sensory neurons continue to develop and adopt traits characteristic of adult cells, and it is during this period that two subpopulations of C-fibre neurons emerge. During embryonic development, small-diameter neurons express the NGF-specific receptor TrkA. Postnatally, however, the majority of cells down-regulate TrkA and switch dependency to another set of growth factors, the GDNF family (Molliver et al., 1997;Molliver and Snider, 1997). The GDNF receptor is composed of the tyrosine kinase Ret (the signal transducing domain) with one of four alpha subunits (GDNFα1-4, the ligand binding domain). A recent study demonstrated that the onset of Ret expression in DRG neurons was determined by the presence of NGF (Luo et al., 2007) (Figure 7.1).

During embryonic stages of development, the majority of TrkA-positive sensory neurons express the Runx1 transcription factor (Chen et al., 2006b). While the initiation of Runx1 expression is NGF-independent (Kramer et al., 2006) (in fact, in the chick Runx1 was shown to be sufficient to induce TrkA expression (Marmigere et al., 2006)), NGF is required to maintain high levels of Runx1 expression until the early postnatal stages (Luo et al., 2007). After birth, Runx1 is down-regulated in the TrkA-positive population, and its expression in the adult is restricted to Ret-positive neurons (Chen et al., 2006b).

Ret and Runx1 have been implicated in the developmental regulation of TRP channel expression. Conditional knockout of the Runx1 gene was found to abolish expression of both TRPM8 and TRPA1, and lead to reduced expression of TRPV1 (Chen et al., 2006b), whereas the absence of Ret, while not altering expression of either TRPM8 or TRPV1, did eliminate expression of TRPA1 (Luo et al., 2007) (Figure 7.1).

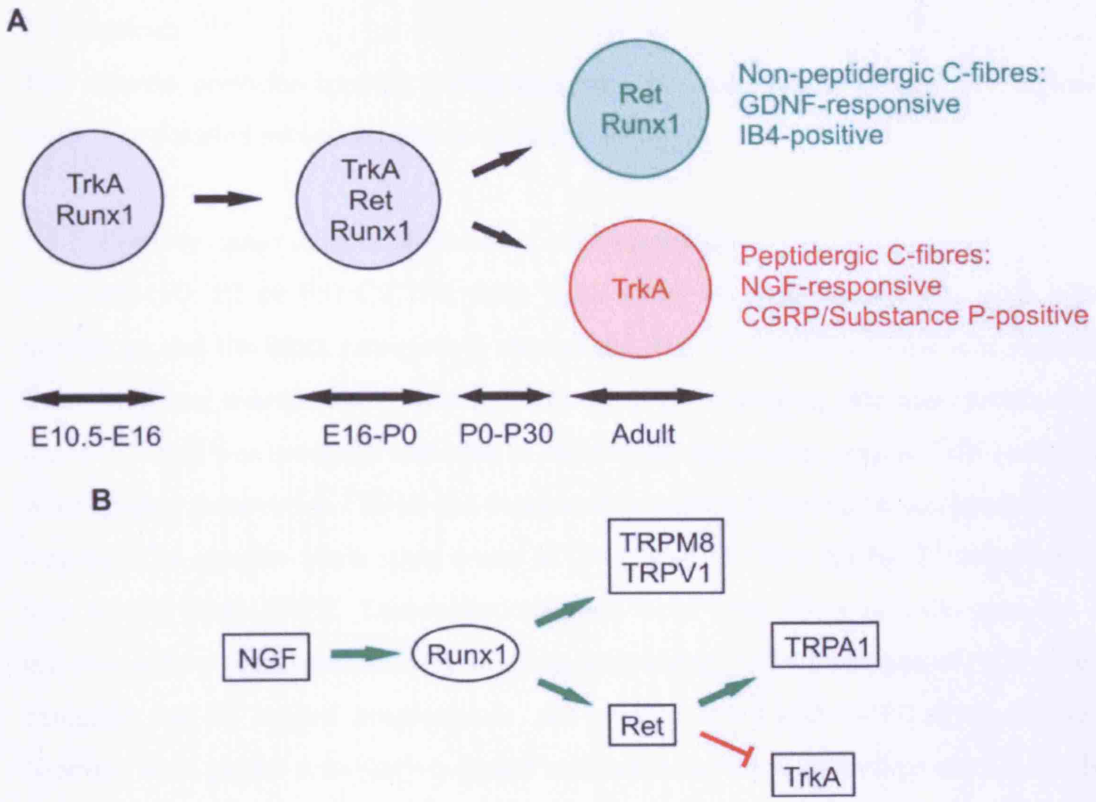

Figure 7.1. (A) Schematic of the development of small-diameter sensory neurons. During the first two postnatal weeks, two populations of C-fibre neurons emerge, expressing either the GDNF receptor Ret (non-peptidergic C fibres) or the NGF receptor TrkA (peptidergic C fibres). The Runx1 transcription factor is down-regulated in the TrkA-positive population, and becomes restricted to Ret-expressing neurons. (B) Schematic of the relationship between NGF, Runx1, Ret and the thermosensitive TRP channels. The expression of TRPM8, TRPV1 and Ret is dependent on Runx1, while TRPA1 expression in non-peptidergic neurons is determined by the presence of the Ret receptor.

7.2. Aims

The previous chapter demonstrated that NGF could up-regulate cold sensitivity and TRP channel expression in neonatal sensory neurons, and the aims of this study were two-fold. The first part of the project was designed to examine whether the presence of NGF would also alter the expression of TrkA, Ret or Runx1 in early postnatal neurons. In the second part, experiments were carried out to investigate whether Runx1 signalling was involved in the NGF-mediated up-regulation of cold sensitivity and TRP channel expression.

7.3. Methods

This section provides specific information on the experiments carried out in this study. For detailed protocols, please refer to Chapter 2.

7.3.1. Primary tissue culture and in vitro electroporation

Newborn (P0, P2 or P5) C57/B6 mice were killed by decapitation. The skull was opened up and the brain removed to expose the TG. The spinal column was opened from the dorsal side in situ, following removal of the overlying skin and muscle, and the spinal cord was carefully removed to expose the underlying ganglia. DRG and TG were quickly removed in HBSS and incubated in papain followed by collagenase and dispase. The ganglia were spun down at 2400 rpm (1120 x *g*) for 2 minutes and triturated in 1 ml HBSS. Dissociated neurons were spun down at 2400 rpm for 2 minutes and re-suspended in F-12 medium containing 10 % horse serum, 100 U/ml penicillin and 0.1 mg/ml streptomycin, and supplemented with 1-100 ng/ml rhNGF. Neurons were plated onto poly-L-lysine and laminin-coated coverslips placed in 12-well plates, and were maintained at 37 °C under 5 % CO_2. RNA was harvested from acutely dissociated P2 and P5 neurons within 3-5 hours of plating. Neurons dissociated at P0 were maintained in culture for 2 (P0+2) or 5 days (P0+5) before being processed for RNA. In long-term cultures, 500 µl of culture medium were carefully removed and replaced with fresh F-12 every 2-3 days.

In a separate set of experiments, DRG from P0 mice were dissociated as described above. Following tritration, neurons were electroporated with 5 µg pCA-Runx1d plus 5 µg pCA-eGFP, or with 5 µg pCA-eGFP alone. Neurons were re-suspended in F-12 medium supplemented with 100 ng/ml rhNGF and plated on poly-L-lysine and laminin-coated coverslips. Neurons were maintained in culture for 5 days prior to calcium imaging.

7.3.2. Ratiometric calcium imaging

Transfected DRG neurons were loaded with Fura-2 and stained with IB4-TRITC. Coverslips were positioned inside a custom-made chamber and solutions were applied to the cells via a gravity-driven application system.

Stock solutions of menthol (2 M), cinnamaldehyde (2 M), mustard oil (1 M) and capsaicin (20 mM) were made up in ethanol and diluted in ECF to the required working concentration on the day of the experiment. Neurons were stimulated with

cold ECF (5 °C), 250 μM menthol (10 second application), 100 μM cinnamaldehyde (60 second application), 100 μM mustard oil (60 second application), and 1 μM capsaicin (10 second application). Temperature was continuously monitored with a thermocouple positioned just outside the field of vision, opposite the stream of the inflow. In all experiments fast non-linear cold ramps were applied from room temperature. Responses of transfected sensory neurons were compared to non-transfected cells, either acutely dissociated at P5 or isolated at P0 and maintained for 5 days in 100 ng/ml NGF.

Due to high cell loss and low transfection efficiency (it was estimated that approximately 5 % of neurons on a coverslip were GFP-positive), it became necessary to image each coverslip twice. To test the viability of this approach, acutely dissociated adult DRG neurons were assessed for the extent of tachyphylaxis induced by repeated application of mustard oil. Neurons were stimulated with five consecutive 60 second applications of 100 μM mustard oil, with intervals of 5-10 minutes between each application. It was found that repeated stimulation with mustard oil induced a significant tachyphylaxis, however this effect was reduced when the interval between consecutive applications was increased (Figure 7.2). Therefore, out of 214 neurons tested with a 5 minute interval between mustard oil applications, 24 responded on the first stimulus, and of those cells 19 (79 %) responded to the second application. Conversely, 36/182 neurons assessed with a 10 minute interval between stimuli responded to the first application of mustard oil, and 35/36 (97 %) cells responded to the second stimulation. In both experiments, approximately 7 % of cells that did not respond to the initial mustard oil stimulus did respond to one or more of the subsequent applications. On the basis of these experiments, each coverslip of transfected cells was analysed twice, with a 15 minute wash in ECF between recordings.

Ratiometric images were recorded at intervals of 0.5 seconds for the duration of the cold stimulus and 1 second thereafter, using the TillPhotonics system. Only vital neurons that responded to a concentrated (50 mM) potassium stimulus were included in the analysis.

7.3.3. Quantitative rt-PCR

Total RNA was extracted from cultured DRG and TG neurons and 10 ng were reverse transcribed into cDNA for use in real-time PCR. cDNA was probed for expression of the housekeeping gene UCHL1, along with TrkA, Ret and Runx1, using SYBR green dye. Primers targeted against TrkA, Ret and Runx1 were obtained from the Quantitect Primer Assay range, similar to the Kv3 primers used in a previous study (see Chapter 4). Since all primers are optimised during manufacture to have the same annealing properties, PCR conditions used for the detection of Kv3 channels were adopted for use with these primers also. Reaction products gave single peaks on melt curve analysis and single bands of expected size on a 2 % agarose gel.

Relative quantification of rt-PCR products was performed, using either the amount of total starting RNA or the expression of housekeeping genes with the $\Delta\Delta$ method as a reference.

7.3.4. Statistics

Calcium imaging experiments were performed on at least four separate cultures over two experimental days. Each culture consisted of several coverslips. Each culture contained few transfected neurons, and therefore results from all coverslips were pooled and data was analysed in terms of the number of transfected cells. For rt-PCR experiments, DRG and TG from 2-4 cultures each were processed separately for cDNA, and each PCR reaction was run in duplicate. All quantitative comparisons are presented as mean ± SEM. For statistical analysis of quantitative rt-PCR data and calcium response magnitude, Student's unpaired *t*-test was used. For statistical analysis of the functional responses of transfected neurons to cold and TRP channel agonists, the raw data were collated in the form of 2 x 2 frequency tables and expected frequencies were calculated for each cell. If three or more of the expected frequency values were over 5, statistical analysis was performed using the Chi-squared test, with Yates' continuity correction. If at least two of the expected frequency values were below 5, Fisher's exact test was used.

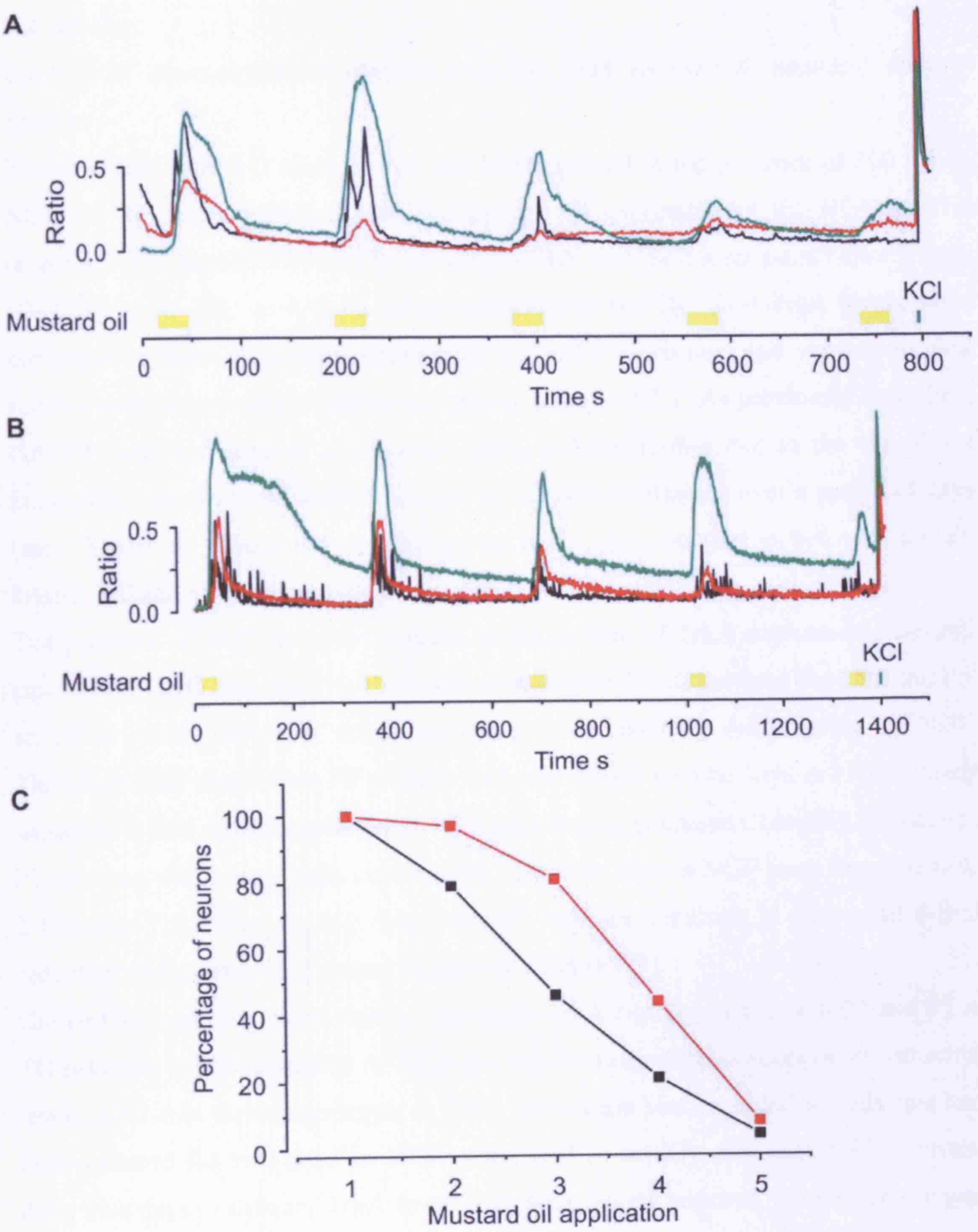

Figure 7.2. Representative kinetic profiles of the responses of three DRG neurons stimulated with 100 μM mustard oil at 5 (A) or 10 (B) minute intervals. Note that the degree of tachyphylaxis was reduced with longer interstimulus intervals. (C) The percentage of neurons responding to mustard oil was reduced with each consecutive stimulus, however this decrease was less in cultures stimulated every 10 minutes (red, n_{cells} = 182, of which 36 were mustard oil-sensitive) compared to those stimulated every 5 minutes (black, n_{cells} = 214, of which 24 were mustard oil-sensitive). Data are presented as percentage of responding neurons, relative to the number of cells responding to the first application of mustard oil.

7.4. Results

7.4.1. NGF down-regulates expression of the TrkA receptor in neonatal sensory neurons

Neonatal DRG and TG neurons that had been cultured in the presence of 100 ng/ml NGF for 2-5 days were analysed for changes in expression of the NGF-specific receptor TrkA, the GDNF-specific co-receptor Ret, and the transcription factor Runx1 (DRG: n = 4; TG: n = 3-4), using quantitative rt-PCR. Transcript levels were compared to those of acutely dissociated P2 and P5 neurons, and were quantified relative to the expression of the housekeeping gene UCHL1. As previously described, GAPDH was not used as a reference gene in these studies due to the significant increase in non-neuronal mRNA species in cultures maintained over a period of days (see Chapter 6). There was no difference in UCHL1 expression between acutely dissociated and long-term cultures.

The presence of NGF led to a decrease in the amount of TrkA expressed in sensory neurons. In DRG neurons TrkA was down-regulated 2-fold between days P2 and P5, an effect which was both accelerated and exacerbated by the presence of NGF. Therefore cells taken from P0 animals and maintained for two days in NGF already showed a 2-fold down-regulation in TrkA expression compared to acutely dissociated P2 neurons, while those cells cultured for up to five days in NGF were found to have 2-fold less TrkA than acutely dissociated P5 neurons, resulting in an overall 4-fold reduction in the amount of transcript present (Figure 7.3).

Unlike DRG neurons, there was no change in TrkA expression between P2 and P5 in TG neurons, but the presence of NGF did induce a significant reduction in transcript levels: a 27-fold down-regulation in TrkA expression was recorded in cells that had been cultured for two days in NGF, compared to acutely dissociated P2 neurons. After five days in culture, TrkA levels had been largely restored, although there was still a 2-fold reduction in the amount of transcript present compared to acutely dissociated P5 neurons (Figure 7.3).

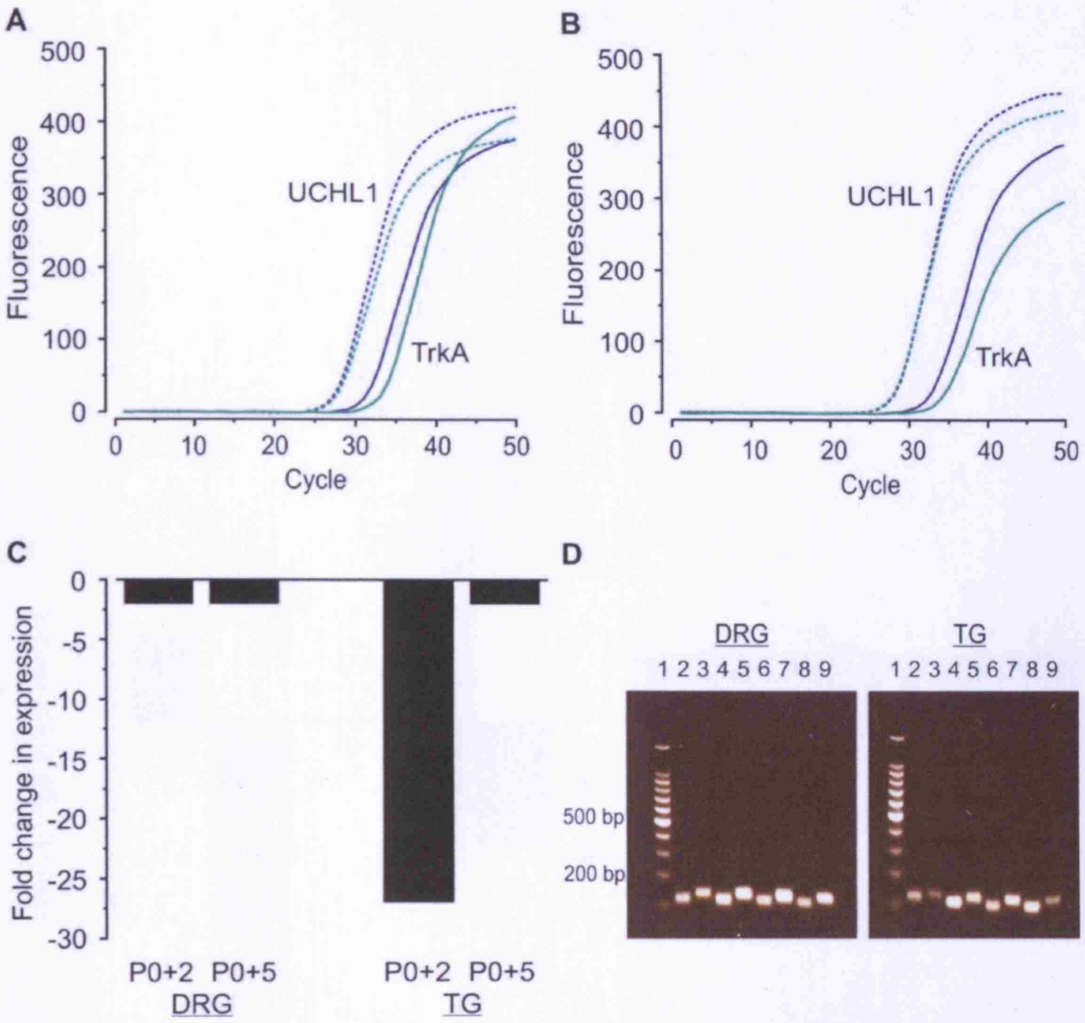

Figure 7.3. Quantitative rt-PCR for TrkA expression in neonatal DRG and TG neurons. The cDNA of 250 pg (UCHL1) or 1.25 ng (TrkA) total RNA equivalents were amplified. (A) Illustration of rt-PCR for UCHL1 and TrkA in DRG neurons. Whereas there were similar cycle threshold (Ct) values for UCHL1, there was a higher Ct value for the TrkA transcript in cells maintained for 2-5 days in NGF (green) compared to acutely dissociated neurons (blue). (B) Illustration of rt-PCR for UCHL1 and TrkA in TG neurons. (C) Quantification of the down-regulation in TrkA expression in DRG and TG neurons following two (P0+2) or five days (P0+5) culture in NGF relative to acutely dissociated cells at P2 and P5, respectively. (D) All PCR products were analysed on a 2 % agarose gel. Estimated product sizes were 117 bp (UCHL1, Lanes 2, 4, 6, 8) and 137 bp (TrkA, Lanes 3. 5. 7. 9). Lane 1: marker. Lanes 2, 3: acutely dissociated P2 neurons. Lanes 4, 5: neurons cultured for two days in NGF. Lanes 6, 7: acutely dissociated P5 neurons. Lanes 8, 9: neurons cultured for five days in NGF.

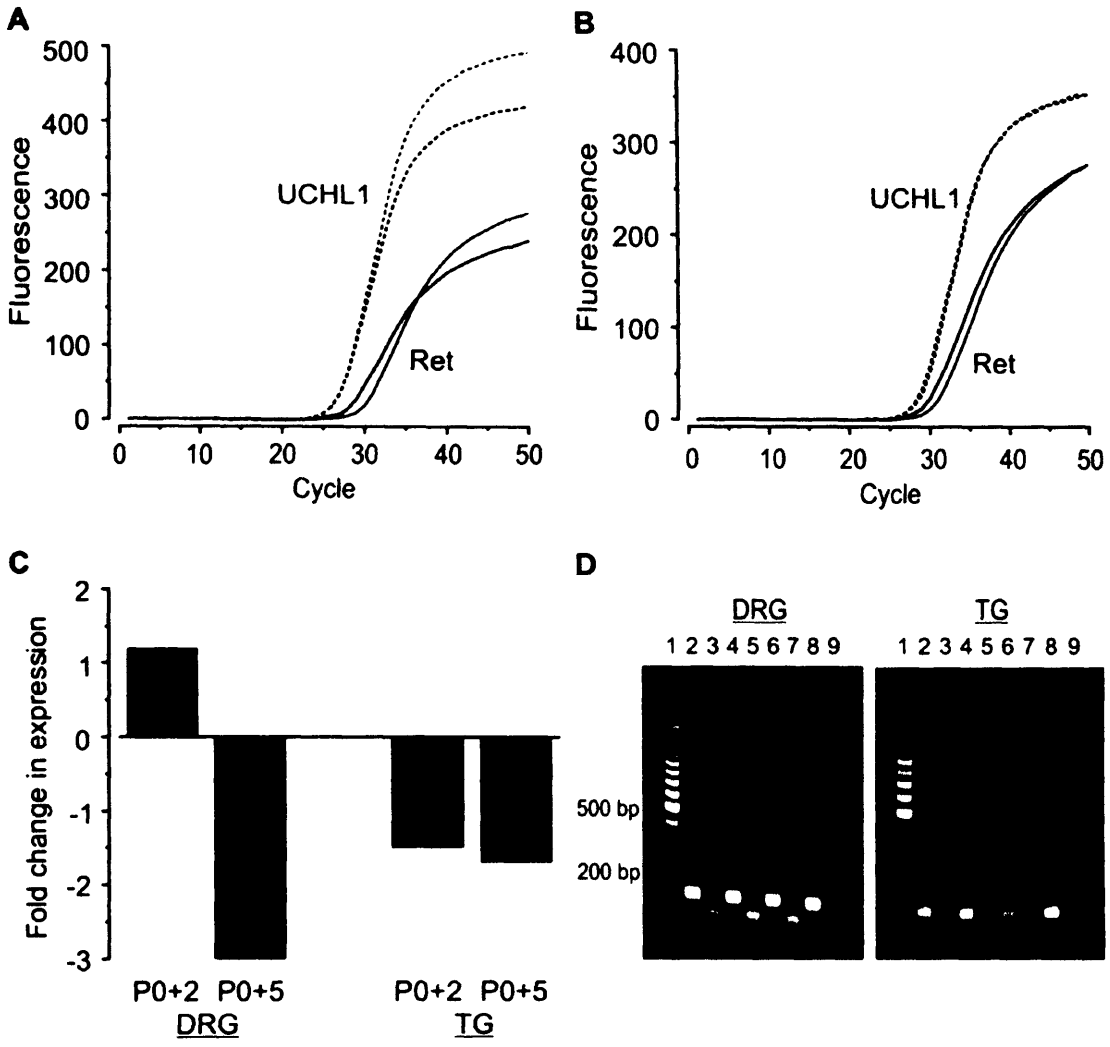

Figure 7.4. Quantitative rt-PCR for Ret expression in neonatal DRG and TG neurons. The cDNA of 250 pg (UCHL1, Ret) total RNA equivalents were amplified. (A) Illustration of rt-PCR for UCHL1 and Ret in DRG neurons. Whereas there were similar cycle threshold (Ct) values for UCHL1, there was a higher Ct value for the Ret transcript in cells maintained for 2-5 days in NGF (green) compared to acutely dissociated neurons (blue). (B) Illustration of rt-PCR for UCHL1 and Ret in TG neurons. (C) Quantification of the down-regulation in Ret expression in DRG and TG neurons following two (P0+2) or five days (P0+5) culture in NGF relative to acutely dissociated cells at P2 and P5, respectively. (D) All PCR products were analysed on a 2 % agarose gel. Estimated product sizes were 117 bp (UCHL1, Lanes 2, 4, 6, 8) and 78 bp (Ret, Lanes 3, 5, 7, 9). Lane 1: marker. Lanes 2, 3: acutely dissociated P2 neurons. Lanes 4, 5: neurons cultured for two days in NGF. Lanes 6, 7: acutely dissociated P5 neurons. Lanes 8, 9: neurons cultured for five days in NGF.

7.4.2. NGF down-regulates expression of the Ret receptor in neonatal sensory neurons

The same DRG and TG neuronal samples were probed for expression of the GDNF co-receptor Ret, which is normally up-regulated postnatally in non-peptidergic nociceptive sensory neurons. In DRG neurons, there was no change in Ret expression between days P2 and P5, and two days culture in NGF were not sufficient to alter transcript levels either. However, neurons that had been maintained for up to five days in 100 ng/ml NGF expressed 3-fold less Ret transcript than acutely dissociated P5 neurons (Figure 7.4).

In TG neurons, a 2-fold up-regulation in Ret expression was observed in acutely dissociated P5 neurons when compared to neurons dissociated at P2. As in DRG neurons, NGF led to a reduction in transcript levels, effectively preventing the postnatal up-regulation of Ret expression. Thus, after two days in NGF, transcript levels were down 1.5-fold compared to acutely dissociated P2 neurons, while on the fifth day in NGF, a 1.7-fold decrease relative to cells dissociated at P5 was recorded (Figure 7.4).

7.4.3. NGF up-regulates expression of the Runx1 transcription factor in neonatal sensory neurons

In contrast to the observed down-regulation in both TrkA and Ret expression in sensory neurons, the presence of NGF was found to induce a significant up-regulation of the Runx1 transcription factor. In DRG neurons there was no change in the expression of Runx1 between days P2 and P5, but after only two days in 100 ng/ml NGF, transcript levels were already 4-fold higher than in acutely dissociated P2 neurons, and by the fifth day of culture, there was a 26-fold difference in expression between acutely dissociated and NGF-cultured cells (Figure 7.5).

The effects of NGF were very similar in TG neurons. Therefore, while there was very little change in Runx1 expression between neurons dissociated at P2 and P5 (there was a 1.8-fold increase in the amount of transcript at P5), two or five days culture in NGF induced an 11-fold or 22-fold up-regulation in the expression of Runx1, respectively, compared to acutely dissociated cells (Figure 7.5).

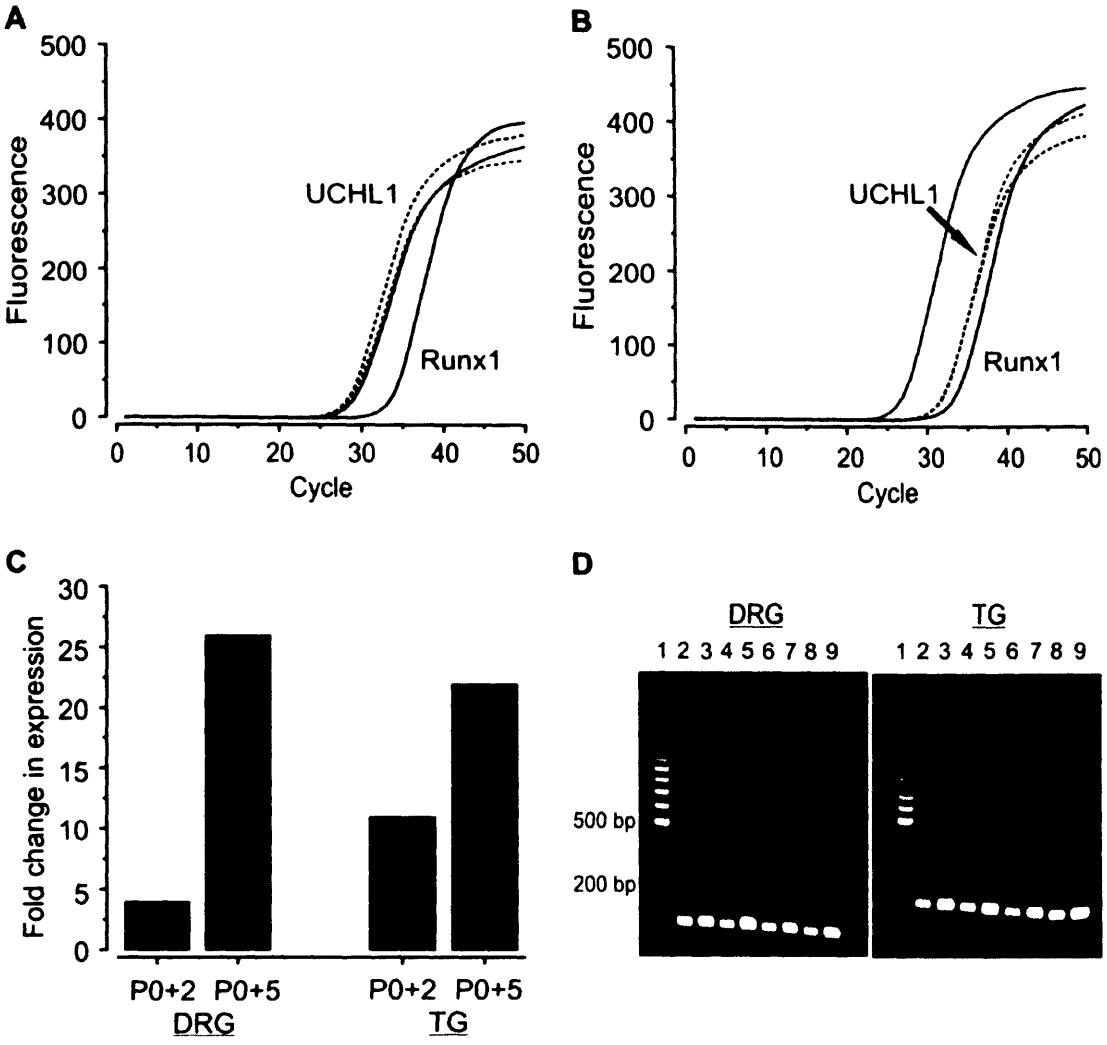

Figure 7.5. Quantitative rt-PCR for Runx1 expression in neonatal DRG and TG neurons. The cDNA of 250 pg (UCHL1) or 1.25 ng (Runx1) total RNA equivalents were amplified. (A) Illustration of rt-PCR for UCHL1 and Runx1 in DRG neurons. Whereas there were similar cycle threshold (Ct) values for UCHL1, there was a lower Ct value for the Runx1 transcript in cells maintained for 2-5 days in NGF (green) compared to acutely dissociated neurons (blue). (B) Illustration of rt PCR for UCHL1 and Runx1 in TG neurons. (C) Quantification of the up-regulation in Runx1 expression in DRG and TG neurons following two (P0+2) or five days (P0+5) culture in NGF relative to acutely dissociated cells at P2 and P5, respectively. (D) All PCR products were analysed on a 2 % agarose gel. Estimated product sizes were 117 bp (UCHL1, Lanes 2, 4, 6, 8) and 120 bp (Runx1, Lanes 3, 5, 7, 9). Lane 1: marker. Lanes 2, 3: acutely dissociated P2 neurons. Lanes 4, 5: neurons cultured for two days in NGF. Lanes 6, 7: acutely dissociated P5 neurons. Lanes 8, 9: neurons cultured for five days in NGF.

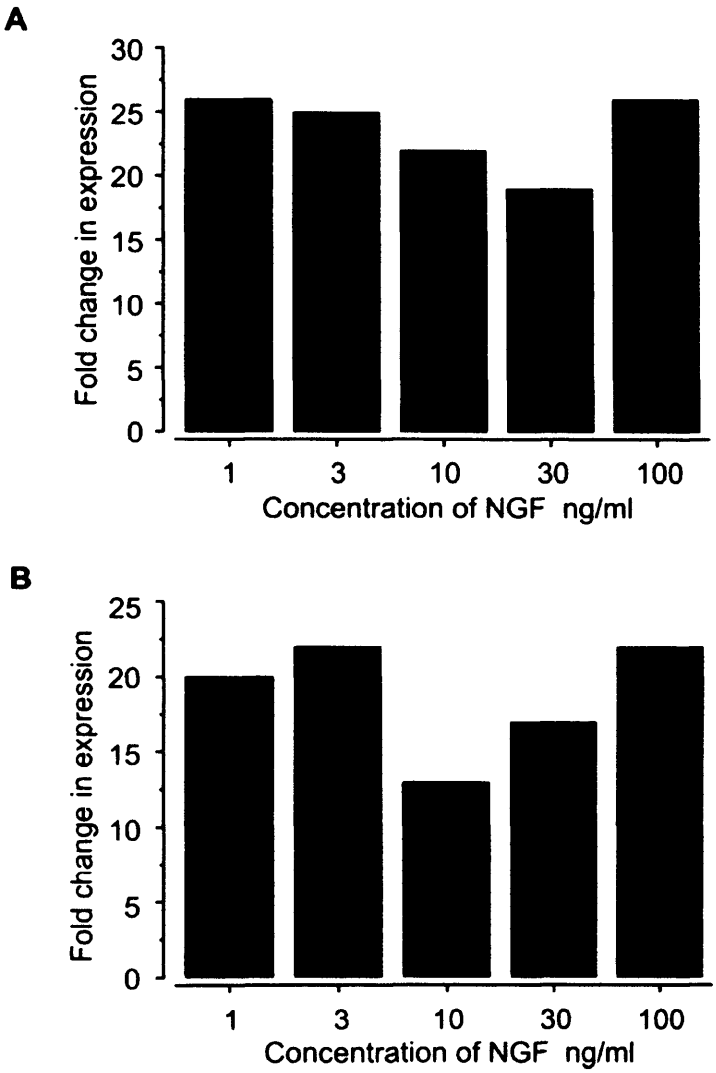

Figure 7.6. The up-regulation in Runx1 expression in neonatal DRG (A) and TG (B) neurons cultured for five days was not dependent on the concentration of NGF included in the culture medium.

Further experiments were performed to determine whether the NGF-mediated up-regulation in Runx1 expression was dose-dependent. DRG (n = 4) or TG (n = 2) neurons dissociated at P0 and cultured for five days in increasing concentrations of NGF (1-100 ng/ml) were analysed for Runx1 expression and compared to acutely dissociated P5 neurons. All quantification was performed relative to the expression of the housekeeping gene UCHL1, which was not affected by varying the concentration of NGF. Thus, DRG neurons cultured in 1 ng/ml NGF had a cycle threshold (Ct) value for UCHL1 of 29.3 ± 0.3, while cells maintained in a 100-fold higher concentration of NGF had a Ct value of 29.5 ± 0.2 ($P > 0.6$, Student's unpaired t-test). In both DRG and TG neurons, the up-regulation in Runx1 expression was not dependent on the concentration of NGF present (Figure 7.6), so that neurons cultured in 1 ng/ml or 100 ng/ml NGF showed comparable increases in the amount of Runx1 transcript present. It should be noted that 1 ng/ml NGF is sufficient to promote maximal survival of late embryonic (E19) TG neurons in culture (Davies et al., 1993). The experiment would therefore need to be repeated using lower concentrations of NGF (within the picogram range) in order to draw any firm conclusions on whether the NGF-mediated up-regulation in Runx1 expression is dose-dependent.

7.4.4. Knockdown of Runx1 prevents the NGF-mediated up-regulation of cold and menthol sensitivity in sensory neurons

Given the significant up-regulation in Runx1 expression induced by NGF, along with its specific presence in small-diameter sensory neurons, it was hypothesised that Runx1 could form part of the signalling pathway underlying the NGF-mediated up-regulation in functional cold and TRP channel sensitivity observed in neonatal sensory neurons (see Chapter 6). In order to test this theory, P0 DRG neurons were transfected with a dominant-negative isoform of Runx1, known as Runx1d (Marmigere et al., 2006). This protein, which is lacking the transactivation domain, blocks Runx activity by binding preferentially to the consensus DNA-binding site. The transfected cells were cultured for five days in 100 ng/ml NGF, and then assessed using Fura calcium imaging for functional sensitivity to cold, menthol, cinnamaldehyde, mustard oil and capsaicin. Control cultures were transfected with GFP only. Data were compared to non-transfected cultures, comprising either acutely dissociated P5 neurons or P0 cells that had been maintained in NGF for five days prior to imaging.

A total of 468 neurons from the control GFP-transfected coverslips were analysed, of which 70 were GFP-positive. Within the GFP-positive population, 46 neurons (66 %) responded to a brief cold stimulus, 4 (6 %) were menthol-sensitive, 4 (6 %) were sensitive to cinnamaldehyde, 7 (10 %) responded to mustard oil, and 57 (81 %) were capsaicin-sensitive. Similarly, within the GFP-negative population taken from the same coverslips, 237/398 (60 %) cells responded to cold, 42 (11 %) were sensitive to menthol, 8 (2 %) were responsive to cinnamaldehyde, 50 (13 %) responded to mustard oil, and 349 (88 %) were capsaicin-sensitive. The proportion of cells responding to each stimulus did not differ between the GFP-positive and GFP-negative populations (cold: $P > 0.4$; menthol: $P > 0.3$; cinnamaldehyde: $P > 0.1$; mustard oil: $P > 0.6$; capsaicin: $P > 0.2$, Yates' corrected Chi-squared test) (Figure 7.7).

As previously described, DRG neurons cultured for five days in NGF show a significant increase in functional cold and TRP channel sensitivity compared to acutely dissociated P5 neurons. In the GFP-transfected population, the observed up-regulation in sensitivity to cold and capsaicin was largely unaltered by the presence of the GFP (Figure 7.7). There was a noticeable down-regulation in responsiveness to cinnamaldehyde and mustard oil in the GFP-transfected cultures compared to the non-transfected five day-old cultures, although the number of responding neurons was still significantly higher than in acutely dissociated cells. Menthol sensitivity was elevated in the GFP-negative population, but it was reduced in GFP-positive cells, to the extent that the percentage of responding neurons was comparable to that recorded in acutely dissociated neurons.

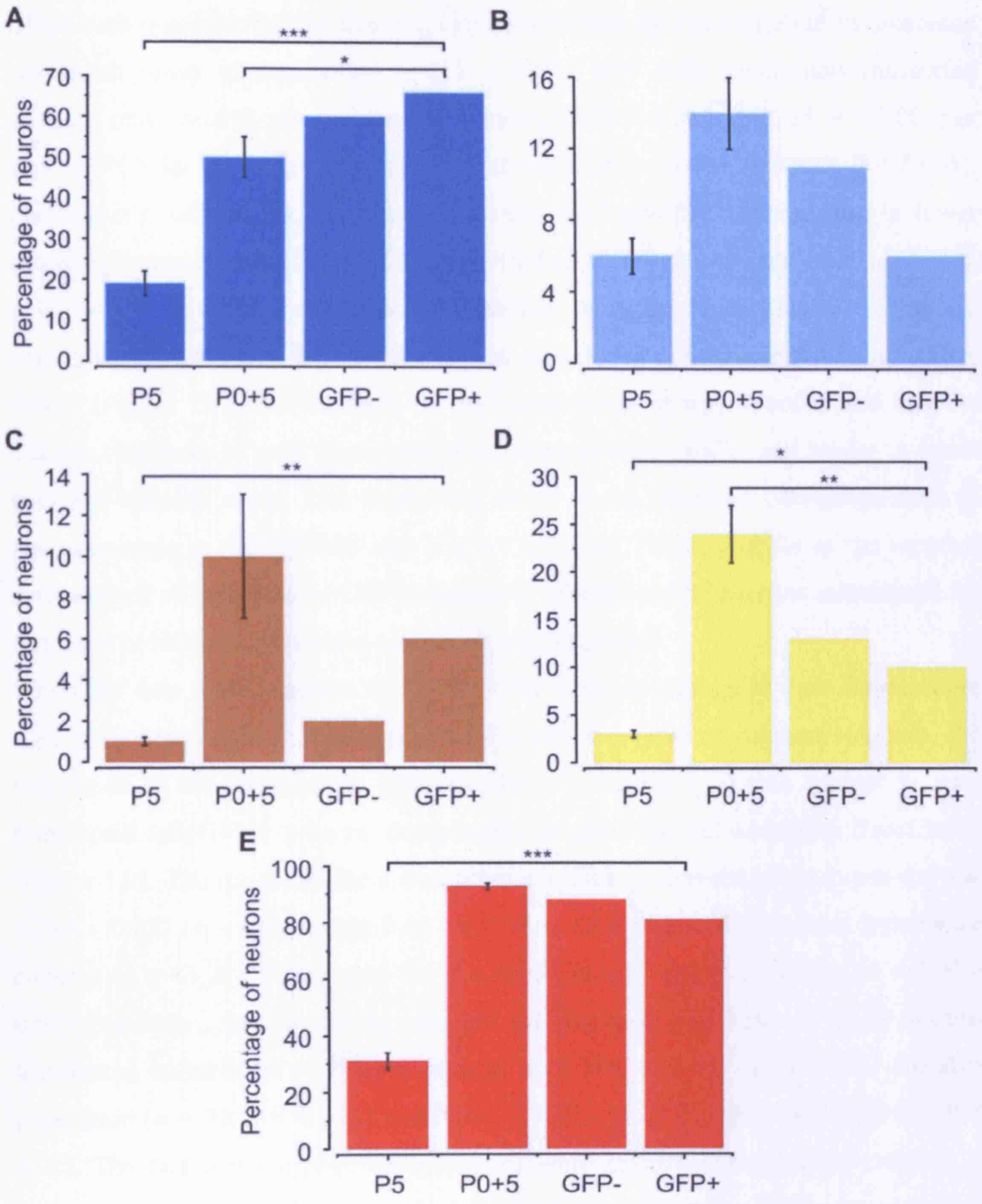

Figure 7.7. Neonatal DRG neurons transfected with GFP (GFP+) were assessed for functional sensitivity to cold (A), menthol (B), cinnamaldehyde (C), mustard oil (D) and capsaicin (E), and compared to GFP-negative neurons from the same coverslips (GFP-), acutely dissociated P5 DRG neurons, and non-transfected DRG neurons maintained for five days in NGF (P0+5). P5: $n_{animals}$ = 4, n_{cells} = 705; P0+5: $n_{animals}$ = 5, n_{cells} = 693; GFP-: n_{cells} = 398; GFP+: n_{cells} = 70. Data are presented as mean percentage of responding neurons ± SEM (P5, P0+5), or as total percentage of responding neurons (GFP-, GFP+). * $P < 0.05$, ** $P < 0.01$, *** $P < 0.001$ (Yates' corrected Chi-squared test).

It had been noted during the imaging experiments that the Fura baseline fluorescence was much lower in transfected (0.225 ± 0.004, n = 468) versus non-transfected cultures, either acutely dissociated (P5 cultures, 0.479 ± 0.003, n = 705, $P < 0.001$) or kept in NGF for up to five days (P0+5 cultures, 0.468 ± 0.003, n = 693, $P < 0.001$). Furthermore, within the transfected cultures, GFP-positive neurons had a lower baseline fluorescence (0.188 ± 0.008, n = 70) than GFP-negative cells (0.231 ± 0.005, n = 398, $P < 0.001$), although the baseline fluorescence for the GFP-negative population was still significantly lower than recorded in non-transfected cultures ($P < 0.001$) (Figure 7.8). On the basis of this observation, it was hypothesised that the calcium responses of cells from transfected cultures were smaller and harder to detect over the baseline noise, thus explaining some of the observed down-regulation in responsiveness to the TRPM8 and TRPA1 agonists. The magnitude of the menthol and mustard oil response of GFP-transfected cultures and of neurons maintained for five days in NGF was therefore measured and compared.

When the data were analysed in terms of the absolute change in Fura fluorescence ratio (ΔF) from baseline to the peak of the stimulus-induced calcium response, the magnitude of the response to both menthol and mustard oil was greater in non-transfected cells (P0+5 cultures) compared to neurons that had undergone transfection (Figure 7.9). The mean ΔF for the menthol response in non-transfected neurons was 0.385 ± 0.027 (n = 86), versus 0.187 ± 0.02 in GFP-negative cells from transfected cultures (n = 42, $P < 0.001$) and 0.145 ± 0.031 in GFP-positive neurons (n = 4, $P > 0.05$). Similarly, the ΔF for the mustard oil response was 0.308 ± 0.014 in non-transfected cultures (n = 172) compared to 0.198 ± 0.031 in the GFP-negative population (n = 50, $P < 0.001$) and 0.084 ± 0.012 in GFP-positive cells (n = 7, $P < 0.01$). The fact that the absolute responses were smaller in transfected cultures is perhaps not surprising given the initial difference in the baseline fluorescence values. However, when the data were expressed as percentage change in fluorescence from baseline, there was no difference in the size of the response between transfected and non-transfected neurons (Figure 7.9). Thus, the mean percentage change in fluorescence from baseline to peak was 70 ± 5 % for the menthol response in non-transfected cells (n = 86) versus 73 ± 6 % in GFP-negative neurons (n = 42, $P > 0.7$) and 74 ± 19 % in GFP-positive cells (n = 4, $P > 0.8$), while the values for the mustard oil responses were 57 ± 3 % in non-transfected neurons (n = 172), 62 ± 7 % in GFP-

negative cells (n = 50, P > 0.4) and 43 ± 8 % in the GFP-positive population (n = 7, P > 0.3).

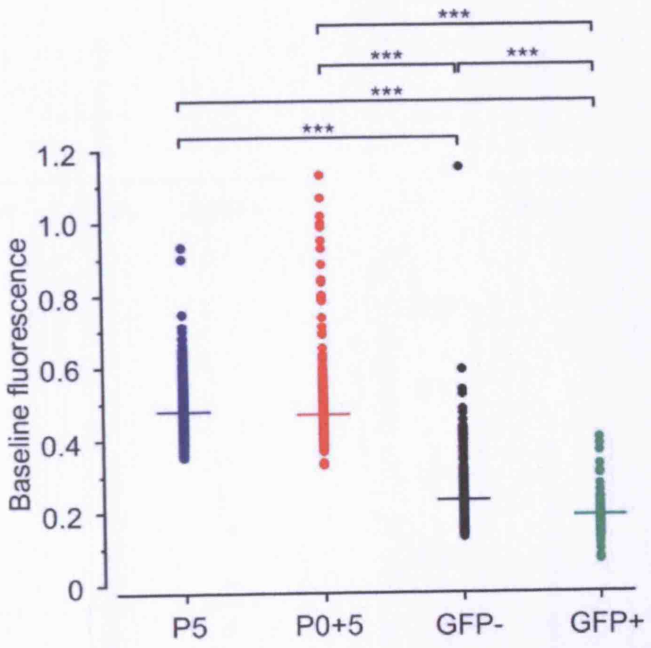

Figure 7.8. Scatter plot showing the Fura baseline fluorescence for non-transfected versus GFP-transfected DRG cultures. Data were taken from acutely dissociated P5 neurons and neurons that had been maintained for five days in NGF (P0+5) (non-transfected cultures), or from GFP-negative (GFP-) and GFP-positive (GFP+) neurons from transfected cultures. Each data point represents one cell, and the mean value is indicated by the horizontal bar. P5 cultures: n = 705; P0+5 cultures: n = 693; GFP-negative neurons: n = 398; GFP-positive neurons: n = 70. *** P < 0.001 (Student's unpaired t-test).

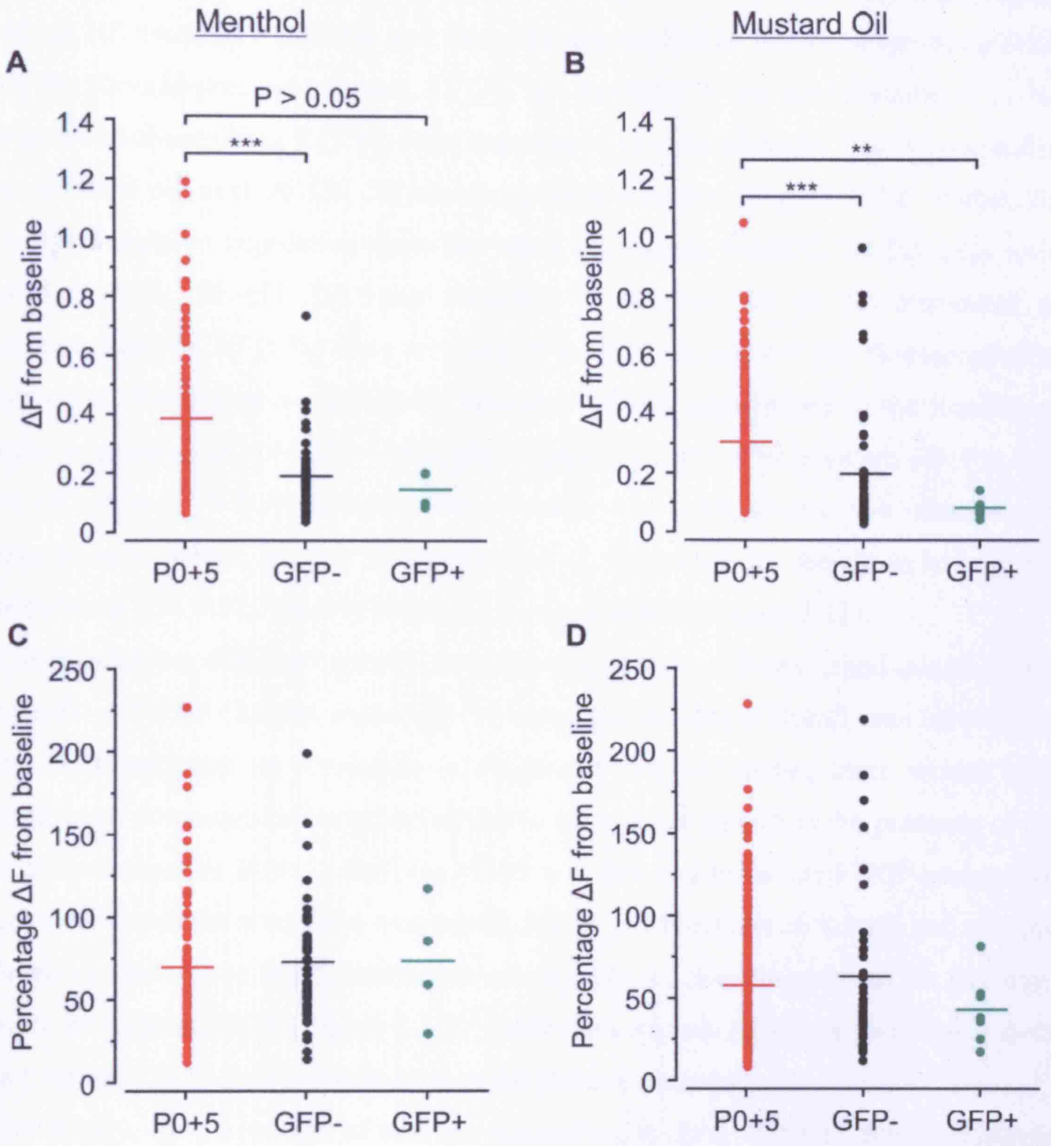

Figure 7.9. Scatter plots comparing the magnitude of the menthol (left-hand column) and mustard oil (right-hand column) responses in non-transfected (P0+5) versus GFP-transfected DRG cultures. Data are presented as absolute change in Fura fluorescence (ΔF) from baseline to the peak of the response (A,B), or as percentage change in fluorescence from baseline to the peak of the response (C,D). Each data point represents one cell, and the mean value is indicated by the horizontal bar. Menthol-sensitive neurons: n = 86 (P0+5 cultures), n = 42 (GFP-negative cells), n = 4 (GFP-positive cells); Mustard oil-sensitive neurons: n = 172 (P0+5 cultures), n = 50 (GFP-negative cells), n = 7 (GFP-positive cells). ** $P < 0.01$, *** $P < 0.001$ (Student's unpaired t-test).

A total of 599 DRG neurons from Runx1d-transfected coverslips were analysed, of which 107 were GFP-positive and therefore assumed to be Runx1d-expressing cells. Of the Runx1d-positive neurons, 23 (21 %) responded to the cold stimulus, 1 (1 %) was menthol-sensitive, 3 (3 %) were sensitive to cinnamaldehyde, 9 (8 %) responded to mustard oil, and 94 (88 %) were capsaicin-sensitive (Figure 7.10). Within the Runx1d-negative population from the same coverslips, 149/492 (30 %) cells were cold-sensitive, 53 (11 %) were sensitive to menthol, 16 (3 %) responded to cinnamaldehyde, 43 (9 %) were sensitive to mustard oil, and 441 (90 %) responded to capsaicin. There was no difference between the two populations in the number of cells responding to cold ($P > 0.08$), cinnamaldehyde ($P > 0.9$), mustard oil ($P > 0.9$) or capsaicin ($P > 0.7$), however the percentage of menthol-sensitive neurons was significantly lower in the Runx1d-positive, compared to the Runx1d-negative population ($P < 0.01$, Yates' corrected Chi-squared test) (Figure 7.11).

The knockdown of Runx1 activity with the introduction of Runx1d had mixed effects on cold and TRP channel sensitivity. It was expected that if Runx1 was involved in the NGF-mediated up-regulation in functional responsiveness, there would be a significant down-regulation in sensitivity to the various stimuli in the presence of the dominant-negative Runx1d isoform, relative to the non-transfected NGF-maintained cultures. Capsaicin sensitivity was unaffected by the blockade of Runx1, and reached levels comparable to those recorded in non-transfected neurons cultured for five days with, or without, NGF (Figure 7.11). These data suggest therefore that Runx1 does not regulate TRPV1 expression in neonatal sensory neurons.

Conversely, the percentage of neurons responding to cold, menthol, cinnamaldehyde and mustard oil was significantly reduced in the Runx1d-transfected population, compared to non-transfected cells. However, while the number of responses to cinnamaldehyde and mustard oil were reduced in Runx1d-positive neurons, there was a similar down-regulation in the Runx1d-negative population. Furthermore, the observed decrease in cinnamaldehyde and mustard oil sensitivity was comparable to that recorded in the GFP-transfected control cultures (Figure 7.12). Thus, 6 % of GFP-transfected neurons responded to cinnamaldehyde, compared to 3 % of Runx1d-transfected cells ($P > 0.2$, Fisher's exact test), while 10 % and 8 % of the GFP- and Runx1d-transfected populations, respectively, were sensitive to mustard oil ($P > 0.9$, Yates' corrected Chi-squared test). This down-regulation in channel function would therefore appear to be a non-specific effect associated with the transfection procedure,

and on the basis of these data, there is no evidence to suggest that Runx1 is involved in the NGF-mediated up-regulation of TRPA1 activity.

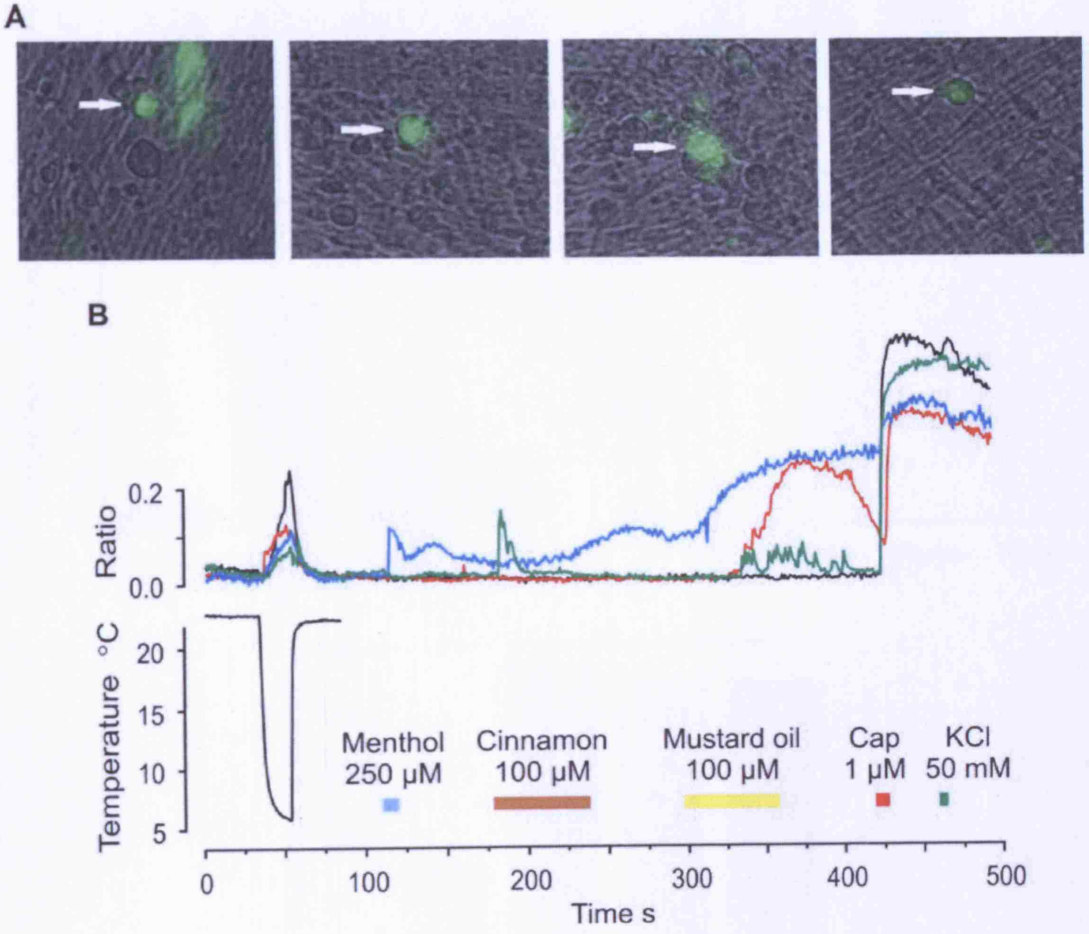

Figure 7.10. (A) Examples of Runx1d-transfected DRG neurons, stained green with GFP. The neurons had been transfected at P0 and cultured for five days in 100 ng/ml NGF. (B) Kinetic profiles of the responses of the four Runx1d-transfected DRG neurons shown in (A). The ability of cells to respond to cold and TRP channel agonists was not affected by the presence of Runx1d.

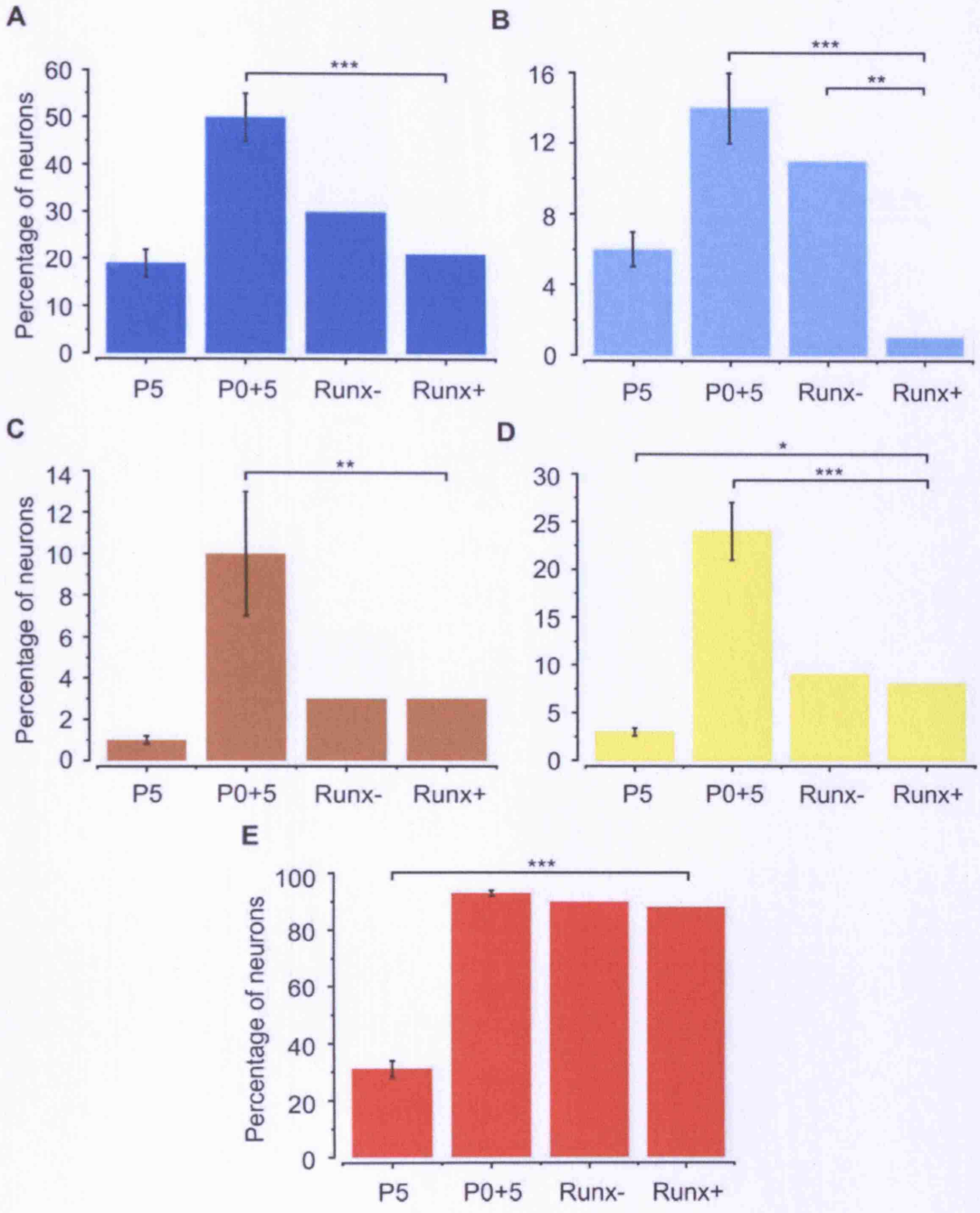

Figure 7.11. Neonatal DRG neurons transfected with Runx1d (Runx+) were assessed for functional sensitivity to cold (A), menthol (B), cinnamaldehyde (C), mustard oil (D) and capsaicin (E), and compared to Runx1d-negative neurons from the same coverslips (Runx-), acutely dissociated P5 DRG neurons, and non transfected DRG neurons maintained for five days in NGF (P0+5). P5: $n_{animals}$ = 4, n_{cells} = 705; P0+5: $n_{animals}$ = 5, n_{cells} = 693; Runx-: n_{cells} = 492; Runx+: n_{cells} = 107. Data are presented as mean percentage of responding neurons ± SEM (P5, P0+5), or as total percentage of responding neurons (Runx-, Runx+). * $P < 0.05$, ** $P < 0.01$, *** $P < 0.001$ (Yates' corrected Chi-squared test).

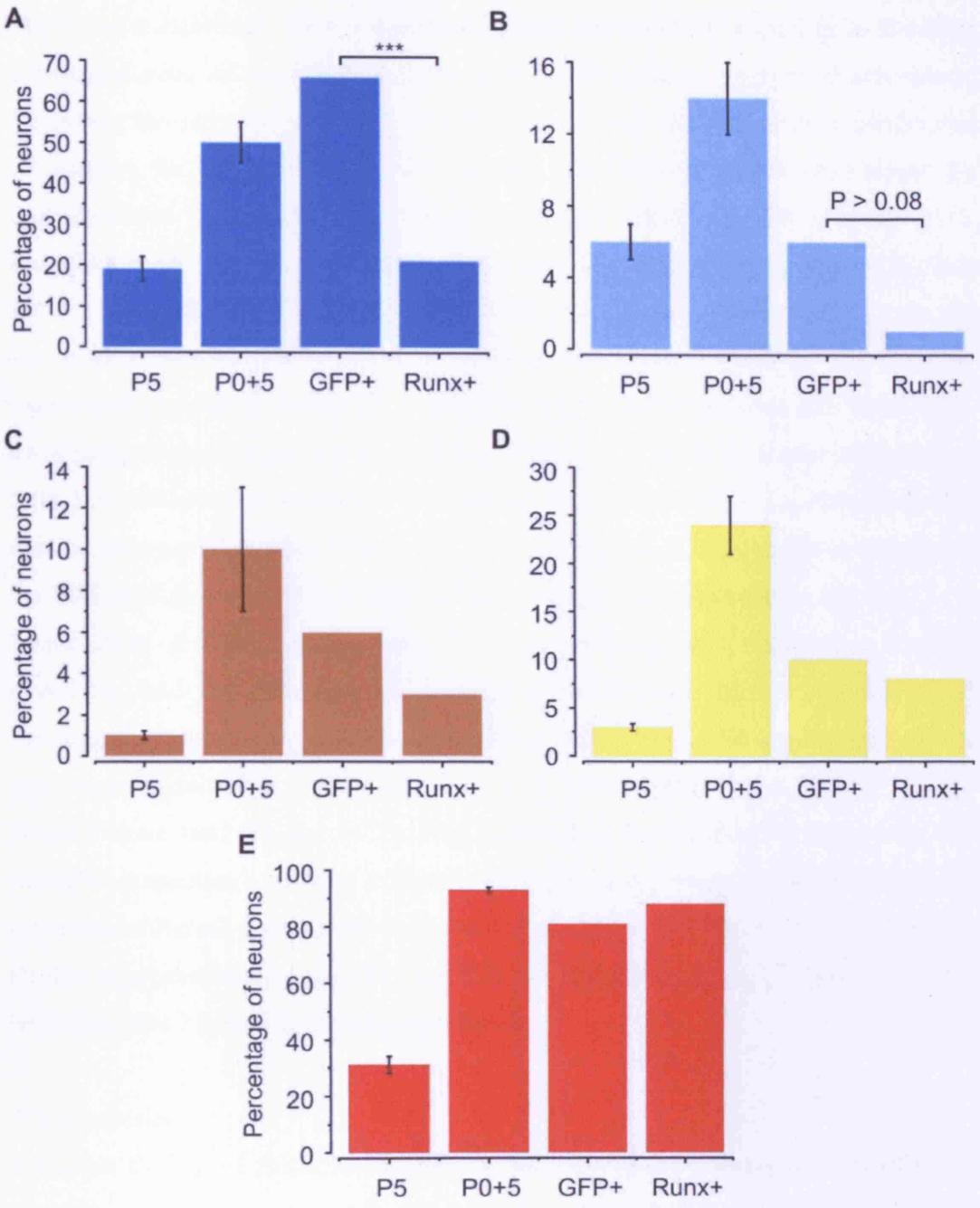

Figure 7.12. Neonatal DRG neurons transfected with GFP (GFP+) or Runx1d (Runx+) were assessed for functional sensitivity to cold (A), menthol (B), cinnamaldehyde (C), mustard oil (D) and capsaicin (E), and compared to acutely dissociated P5 DRG neurons, and non-transfected DRG neurons maintained for five days in NGF (P0+5). P5: $n_{animals} = 4$, $n_{cells} = 705$; P0+5: $n_{animals} = 5$, $n_{cells} = 693$; GFP+: $n_{cells} = 70$; Runx+: $n_{cells} = 107$. Data are presented as mean percentage of responding neurons ± SEM (P5, P0+5), or as total percentage of responding neurons (GFP+, Runx+). *** $P < 0.001$ (Yates' corrected Chi-squared test).

There was a significant down-regulation in cold and menthol sensitivity in Runx1d-transfected cells compared to NGF-treated non-transfected neurons. Furthermore, comparing the responses of Runx1d-positive cells with those of acutely dissociated P5 neurons, the knockdown of Runx1 activity was found to completely prevent the NGF-mediated up-regulation in responsiveness to either stimulus (Figure 7.11). Transfection of GFP alone did not lead to a down-regulation in cold sensitivity, thus demonstrating the specificity of the effects induced by the inhibition of Runx1, and the number of cold responses was therefore significantly lower in the Runx1d-transfected population compared to the GFP-transfected population (66 % of GFP-transfected neurons were cold-sensitive, compared to 21 % of Runx1d-transfected cells, $P < 0.001$, Yates' corrected Chi-squared test) (Figure 7.12). Together these data provide strong evidence that Runx1 is a critical component of the pathway underlying the NGF-mediated up-regulation of cold sensitivity in neonatal sensory neurons.

Transfection of DRG neurons with GFP alone did lead to a decrease in menthol sensitivity, and the difference in responsiveness between the two populations of transfected neurons was not statistically significant (6 % of GFP-transfected neurons were menthol-sensitive, compared to 1 % of Runx1d-transfected cells, $P > 0.08$, Fisher's exact test) (Figure 7.12). The down-regulation in menthol sensitivity was strongly exacerbated by the presence of Runx1d however, suggesting that the inhibition of Runx1 was nevertheless producing a specific effect on TRPM8 function. Further experiments are required to confirm this hypothesis, but it is highly likely that NGF regulates TRPM8 expression via Runx1.

7.5. Discussion

The main finding of this study is that the NGF-mediated up-regulation in cold and menthol sensitivity is regulated via the Runx1 transcription factor. Expression of TRPA1 and TRPV1 however is regulated by other mechanisms. Furthermore, the presence of NGF has contrasting influences on the expression of the growth factor receptors TrkA and Ret, and the transcription factor Runx1.

7.5.1. NGF promotes an immature phenotype in neonatal sensory neurons

The early postnatal period represents a time of ongoing change and development in sensory neurons, at the end of which the adult phenotype is established. Perhaps the most recognised of these changes is the switch from NGF to GDNF dependence in a

subpopulation of small-diameter C-fibre neurons. At P0, more than 80 % of cells in the DRG express the NGF receptor TrkA, while approximately 45 % also express the GDNF co-receptor Ret. Between P1 and P21, the simultaneous down-regulation of TrkA and up-regulation of Ret signal the formation of the non-peptidergic subpopulation of C-fibres (Molliver et al., 1997;Molliver and Snider, 1997). Neurons maintaining expression of TrkA constitute the adult peptidergic population. At the same time, there is a down-regulation in the expression of the nociceptor-specific transcription factor Runx1 in TrkA-positive neurons, so that in mature cells Runx1 expression is restricted to the Ret-expressing population (Chen et al., 2006b).

Recent studies have attempted to elucidate the signalling pathways controlling these postnatal developments. Expression of Runx1 is sufficient to induce the expression of TrkA soon after the completion of neurogenesis, suggesting that embryonically the NGF receptor is under the control of the Runx transcription factor (Marmigere et al., 2006). Postnatally, however, the situation appears to reverse, since in the NGF knockout mouse at P0, Runx1 expression is substantially reduced (Luo et al., 2007). These data would imply that while NGF is not required for the onset of Runx1, it is critical for the maintenance of expression at later stages. Loss of Runx1 was found to result in an impairment of the transition from TrkA to Ret dependence, and it was concluded that postnatally the transcription factor acts to suppress TrkA and promote Ret expression (Chen et al., 2006b). Subsequent studies of neurons from Ret knockout animals demonstrated no deficit in Runx1 expression, supporting the hypothesis that Runx1 lies upstream of Ret. In addition, Ret was found to be partially responsible for signalling the postnatal down-regulation in TrkA expression, reflecting the changes previously recorded in the Runx1 knockout mouse (Luo et al., 2007) (Figure 7.1).

Exposure of P0 sensory neurons to a high concentration of NGF for up to five days was found to induce a large up-regulation in Runx1 expression. Runx proteins are expressed in a number of cell types besides neurons. In particular, Runx1 is required for hematopoiesis, and defects in the activity of the transcription factor have been associated with the onset of leukaemia and autoimmune disease. For this reason, a number of investigations have concentrated on dissecting the regulatory mechanisms controlling Runx activity in the affected tissues (Bae and Lee, 2006). Runx1 possesses a number of sites within its transactivation domain that can be phosphorylated by members of the mitogen-activated protein kinase (MAPK) family.

MAPK-mediated phosphorylation disrupts the interaction between Runx1 and transcriptional corepressor proteins, thus potentiating the transactivating capacity of Runx1. It should be noted that in the cell types studied, phosphorylation of Runx1 was also found to destabilise the protein and increase its degradation via the ubiquitin-proteasome pathway, essentially down-regulating expression levels. Another member of the Runx family, Runx2, which is expressed in osteoblasts, is also subject to phosphorylation by MAPK, however in this case the protein is not degraded but up-regulated. This raises the possibility that Runx proteins are differentially regulated depending on the tissue type and/or interacting proteins present. There is currently no information available on the modulation of Runx1 activity in neuronal cells, although the findings from this study may provide some clues. When considered in context of the data described above, it can be hypothesised that the binding of NGF to TrkA and initiation of the MAPK signalling pathway results in the phosphorylation of Runx1 and increased activity. Rather than marking the protein for degradation, however, the phosphorylation induces an up-regulation in expression, similar to the effect mediated by the fibroblast growth factor on Runx2 in osteoblasts (Bae and Lee, 2006).

The data presented here suggest that the NGF-mediated up-regulation in Runx1 expression in sensory neurons is not dose-dependent. This may not be the case however, since E19 TG neurons cultured in 1 ng/ml NGF (the lowest concentration used in this study) show almost maximal survival (Davies et al., 1993). To fully determine whether NGF could regulate Runx1 expression in a dose-dependent fashion therefore, lower concentrations (within the picogram range) would need to be assessed.

NGF was found to down-regulate expression of both its own receptor, TrkA, and the GDNF co-receptor, Ret in neonatal sensory neurons. Between the ages of P0 and P7, Ret is up-regulated in IB4-positive non-peptidergic neurons, with levels increasing by approximately 50 % (Molliver et al., 1997). This was reflected in these experiments by the two-fold increase in Ret mRNA expression recorded in TG neurons between P2 and P5. The NGF-mediated down-regulation effectively reversed the naturally occurring increase in transcript levels. Runx1 has been shown to be necessary for the transition of TrkA to Ret dependence in small-diameter sensory neurons, and is believed to mediate the postnatal up-regulation of Ret (Chen et al., 2006b). It could be expected therefore that the large up-regulation in Runx1 expression observed in

the sensory neurons examined here would also lead to a similar up-regulation in Ret. This was not the case however, suggesting that other factors are involved in modulating Ret expression. One such factor could be the ligand for the Ret receptor, GDNF, which was not added to the culture medium for these experiments. A previous study of the survival of TrkA- and IB4-positive (Ret-expressing) neurons *in vitro* demonstrated a significantly reduced number of IB4-binding cells in the presence of NGF compared to neurons maintained in GDNF (Molliver et al., 1997). Ret signalling is required for the maintenance of expression of the ligand-binding alpha subunit of the GDNF receptor, and Ret itself may also be subject to the same autoregulatory mechanisms (Luo et al., 2007).

Few studies have investigated the influence of NGF on TrkA expression. *In vivo* injection of either NGF or anti-NGF between the ages of P2 and P14 had no apparent effect on the down-regulation of TrkA, although the cells were only analysed at P21, and therefore any alterations that occurred earlier in this time frame would have been missed (Molliver and Snider, 1997). Indeed data from the *in vitro* experiments performed for this study demonstrated that NGF applied between P0 and P5 resulted in an acceleration of the process, with a two-fold decrease in TrkA transcript levels, normally observed between P2 and P5 in DRG neurons, already present after just two days in NGF. *In vivo* the down-regulation of TrkA is mediated, at least in part, by signalling through the Ret receptor (Luo et al., 2007), although given that Ret is also down-regulated following treatment with NGF, it is unlikely that the GDNF receptor was responsible for the concomitant decrease in TrkA levels recorded in these cells. It should be noted that knockdown of Ret expression does not completely inhibit the down-regulation of TrkA, implying the involvement of a second NGF-initiated signalling pathway in the control of Trk receptor expression. It has been postulated that Runx1 suppresses TrkA during the early postnatal period (Chen et al., 2006b). While some of this effect is probably mediated via Ret signalling, Runx1 itself could also exert a direct control over TrkA expression, as is the case during embryonic development, via its interaction with a consensus sequence within the TrkA promoter (Marmigere et al., 2006). One potential caveat to this theory is the fact that NGF-mediated phosphorylation of Runx1 has been shown to increase transactivation and reduce repressor activity within the protein (Bae and Lee, 2006), and for this reason, involvement of a further transcriptional regulator cannot be ruled out (Figure 7.13).

The actions of NGF appear to promote the maintenance of an immature phenotype in neonatal sensory neurons, whereby Runx1 expression is maintained and up-regulated, while the increase in Ret expression is prevented and even reversed. This would imply that the transition from TrkA to Ret dependency, and the formation of the recognised peptidergic and non-peptidergic populations, is impaired in the presence of excess NGF. The postnatal down-regulation of TrkA is clearly mediated by NGF, both *in vitro* and *in vivo*, via activation of Runx1, Ret or other signalling intermediates. By this mechanism, the growth factor can influence the phenotype of C-fibre populations, and even render a subpopulation of sensory neurons insensitive to its effects. Unfortunately during this study the severe down-regulation in IB4 staining in the cultured neurons precluded an identification of the neuronal populations that were affected by the NGF-mediated changes in phenotype (see Chapter 6). Within neonatal neurons, the IB4-positive subpopulation appears to be particularly sensitive to axotomy: transection of the infraorbital nerve was found to result in a specific decrease in the number of trigeminal neurons binding the plant lectin *Bandierea simplicifolia*-I (White et al., 1990). These cells were small-diameter, negative for substance P and positive for fluoride-resistant acid phosphatase, properties characteristic of IB4-binding neurons. The reasons behind the observed down-regulation were not investigated, although it was postulated that the nerve injury-induced reduction in the availability of growth factors could have affected cell survival, or that the cells could have undergone alterations in phenotype.

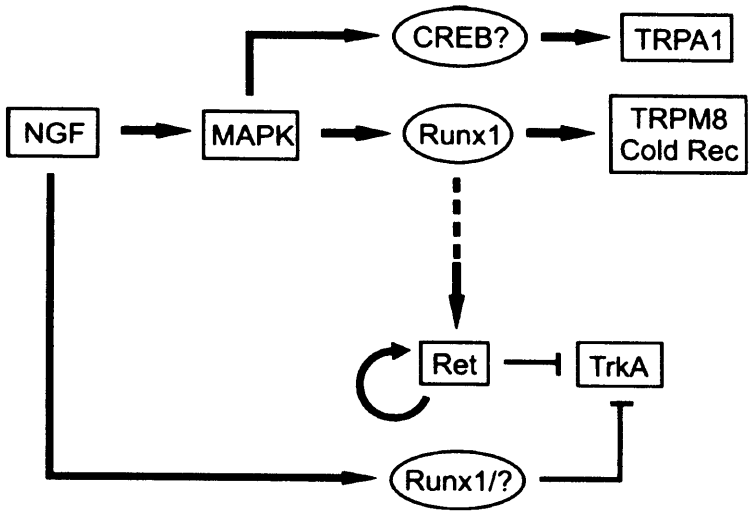

Figure 7.13. Schematic of the proposed relationship between NGF, Runx1, Ret and the TRP channels, TRPM8 and TRPA1, in neonatal sensory neurons cultured in NGF. The NGF-mediated phosphorylation of Runx1 increases its activity, resulting in an up-regulation in the expression of TRPM8 and a further, as yet unidentified, cold receptor. The expression of TRPA1 is not Runx1-dependent, and is likely controlled via another transcription factor activated downstream of MAPK, such as CREB. The recorded down-regulation in Ret expression in the cultured neurons may be due to a lack of autostimulation in the absence of GDNF. NGF mediates the down-regulation of its own receptor, TrkA, possibly via Runx1 or another transcriptional regulator.

7.5.2. NGF regulates TRPM8 expression via the nociceptor-specific transcription factor, Runx1

The previous chapter investigated the influence of NGF on functional cold sensitivity and TRP channel expression in neonatal sensory neurons. While sensitivity to all stimuli (cold, menthol, cinnamaldehyde, mustard oil and capsaicin) was significantly increased in neurons cultured for five days in NGF compared to acutely dissociated, age-matched controls, the regulation of TRPV1 expression was subsequently found to be NGF-independent. The observed down-regulation of TRPV1 *in vivo* between the ages of E14.5 and P7 (Hjerling-Leffler et al., 2007) led to the hypothesis that an intrinsic repressor mechanism was disrupted in cultured neurons, resulting in an uncontrolled increase in TRPV1 expression (see Chapter 6). Runx1 is known to operate as both a transactivator and a repressor, with its activity depending on the

isoform expressed, the binding partners present in a certain cell type, or signalling-mediated protein phosphorylation and acetylation (Bae and Lee, 2006;Marmigere and Ernfors, 2007). It could be reasoned that Runx1 is involved in the neonatal repression of TRPV1, and the fact that knockdown of Runx activity in transfected neurons had no effect on the up-regulation in capsaicin sensitivity would not exclude this possibility. There are however, several lines of evidence to suggest that neither NGF nor Runx1 regulate TRPV1 expression during postnatal development. Knockout of the Runx1 gene produced little effect on TRPV1, with a small decrease recorded only in the number of neurons displaying high levels of channel expression. The greater proportion of cells with an intermediate level of staining was unaffected (Chen et al., 2006b). Likewise, abolition of Ret expression did not alter TRPV1, and the NGF knockout mouse showed only a small reduction in the number of TRPV1-positive DRG neurons (Luo et al., 2007), suggesting limited influence of any of these factors on TRPV1 expression in neonatal neurons. Furthermore, if Runx1 were acting as a transcriptional repressor of TRPV1, one might expect to see an up-regulation in channel expression in the knockout animal, as opposed to a down-regulation. It may be the case that the up-regulation in TRPV1 expression recorded in cultured sensory neurons is due to the activity of a transcriptional activator, rather than the inhibition of a repressor mechanism. However, the lack of effect of the Runx1d isoform on capsaicin sensitivity eliminates a role for Runx1 in this regard also. It can be concluded therefore that TRPV1 expression is not regulated by NGF or Runx1 during development.

Unlike TRPV1, the up-regulation in TRPM8 and TRPA1 function was NGF-dependent, and it was hypothesised that these effects could be mediated via Runx1. Experiments in which Runx1d was used to knockdown Runx activity in NGF-treated neurons did show a decrease in functional sensitivity to TRPA1 agonists, however other observations preclude a role for Runx1 in the regulation of TRPA1 expression. Firstly, the Runx1d-mediated inhibition of NGF-induced cinnamaldehyde or mustard oil sensitivity was only partial, and did not reach baseline levels as recorded in acutely dissociated neurons. Secondly, the decrease in functional sensitivity in the Runx1d-transfected population was matched by a reduction in responsiveness in Runx1d-negative cells, as well as in the GFP-transfected control cultures, suggesting that the transfection procedure itself was interfering with TRP channel function. Thirdly, unlike TRPM8, the extent of the inhibition of channel activity was not

exacerbated by the presence of Runx1d compared to GFP alone. These findings point to a scenario in which Runx1 does not mediate the NGF-induced increase in TRPA1 expression in neonatal sensory neurons. Genetic ablation of both Runx1 and Ret have been shown to eliminate TRPA1 expression, and given that Ret lies downstream of Runx1, it appears that the GDNF receptor controls expression of the TRPA1 channel (Chen et al., 2006b;Luo et al., 2007). It is probable that Ret initiated the expression of TRPA1 prior to dissociation of the neurons at P0, but once in culture, Ret expression was down-regulated and in the absence of GDNF, any signalling via the receptor was minimal. It is therefore also highly unlikely that NGF was mediating its effects on TRPA1 via Ret. The up-regulation of NGF in adult sensory neurons, following nerve injury or inflammation, has been shown to lead to an increase in TRPA1 expression via a MAPK signalling cascade (Obata et al., 2005;Obata et al., 2006). In addition to Runx1, a number of transcription factors are known to be modulated via MAPK phosphorylation, one of which, the cyclic AMP response element binding protein (CREB) has previously been implicated in the regulation of TRPV1 expression (Bron et al., 2003). It remains to be seen whether the activation of CREB could also underlie the NGF-mediated up-regulation of TRPA1.

Previous studies have implicated Runx1, but not Ret, in the regulation of TRPM8 expression in sensory neurons (Chen et al., 2006b;Luo et al., 2007), and the data from this study concur with this finding. Thus, in the presence of Runx1d, menthol sensitivity was significantly lower than in non-transfected neurons, and although transfection with GFP alone did reduce responsiveness to menthol, the effect was greatly exacerbated with the additional knockdown of Runx activity. It has been proposed that postnatally Runx1 acts to suppress or promote the peptidergic or non-peptidergic phenotypes, respectively (Chen et al., 2006b). Accordingly, TRPM8 is not normally expressed in IB4-positive cells, although the non-peptidergic population does maintain the capacity to express TRPM8, as demonstrated by the up-regulation of menthol sensitivity in IB4-binding adult DRG neurons in culture (see Chapter 3). These observations enforce the idea that Runx1 functions initially as a transactivator to initiate receptor expression, and later switches to a repressor, by which means ion channels, including TRPM8, are segregated to a specific neuronal subpopulation. Moreover, the regulation of TRPM8 expression by Runx1 supports the previous suggestion that NGF-mediated phosphorylation of the transcription factor inhibits its repressor activity in favour of transactivation. It could equally be hypothesised that

the observed up-regulation in TRPM8 function would arise particularly within the non-peptidergic, Ret-expressing population.

Knockdown of Runx activity was found to completely inhibit the NGF-mediated up-regulation in functional sensitivity to cold. It was previously hypothesised that the increased cold sensitivity was due to an up-regulation in the function or expression of TRPM8 and TRPA1, respectively, with both channels contributing to cold transduction in the presence of NGF (see Chapter 6). While data from this study do support a role for TRPM8, they firmly rule out a contribution by TRPA1, following the discovery that expression of the latter was not mediated via Runx1. The suggestion that TRPA1 could be involved in the up-regulation of cold responsiveness came from studies in adult neurons, in which the ion channel was demonstrated to play a critical role in the NGF-induced development of cold hypersensitivity following nerve injury and inflammation (Obata et al., 2005;Katsura et al., 2006;Obata et al., 2006). In particular, administration of an antisense oligodeoxynucleotide targeted against TRPA1 was found to reduce injury-induced cold hyperalgesia. However the cold hypersensitivity was not completely abolished with the knockdown of this channel, implicating the presence of additional factors mediating the heightened cold sensation recorded in these animals. These findings provide further evidence for the presence of a TRP-independent mechanism of cold transduction in sensory neurons. The identity of the cold receptor is currently unknown, but like TRPM8 appears to be under the control of Runx1 during development.

In conclusion, the principal finding of this study is that the NGF-mediated up-regulation of cold and menthol sensitivity in neonatal sensory neurons is mediated by signalling via the nociceptor-specific transcription factor Runx1. Furthermore, NGF has the capacity to regulate the expression of Runx1 and growth factor receptors in neurons during the early postnatal period.

8. Discussion

8.1. The role of TRP channels in cold transduction

With the discovery that the capsaicin receptor TRPV1 could respond to thermal as well as chemical stimuli, and the subsequent characterisation of a number of other temperature-sensitive TRP channels, these ion channels have become recognised as the principal transducers of thermal stimuli in peripheral neurons (Caterina, 2007). When they were first identified, TRPM8 and TRPA1 were described as the innocuous cool and noxious cold receptors, respectively, expressed in thermoreceptive and nociceptive subpopulations of sensory neurons (McKemy et al., 2002;Peier et al., 2002a;Story et al., 2003). Since then, the role of TRPA1 in cold sensation has been brought into question on several occasions, primarily due to a lack of cold sensitivity within the cloned channel (Jordt et al., 2004) and the ability of TRPA1 knockout mice to respond to cold challenges as well as their wild type littermates (Bautista et al., 2006). It should be noted that a second group did report deficits in cold sensation with the knockdown of TRPA1 activity, although these deficits were greater in female compared to male animals, and these studies were therefore unable to fully resolve the question of whether TRPA1 does contribute to cold transduction in sensory neurons (Kwan et al., 2006). Furthermore, cold-sensitive cells from the SCG were found to express TRPA1, implicating this channel in the mediation of cold responses in these neurons also (Smith et al., 2004). More recently, two separate investigations have demonstrated that TRPA1 can be directly activated by calcium ions, leading to the postulation that the TRPA1-mediated cold responses observed in neurons are in fact caused by cold-induced increases in basal calcium levels (Zurborg et al., 2007;Doerner et al., 2007).

Unlike TRPA1, the role of TRPM8 in cold transduction is not disputed. There is a significant overlap between cold and menthol sensitivity in sensory neurons (Reid et al., 2002;Nealen et al., 2003;Babes et al., 2004;Jordt et al., 2004;Okazawa et al., 2004), and genetic ablation of the channel resulted in clear deficits in the detection of cold stimuli (Dhaka et al., 2007;Colburn et al., 2007;Bautista et al., 2007). Moreover, the expression of TRPM8 can render thermally-insensitive cells responsive to cold (de la Pena et al., 2005). There is however some discussion as to whether TRPM8 could contribute to the transduction of noxious as well as innocuous cold stimuli. Several groups have reported a significant overlap between the expression of TRPM8

and markers typical of nociceptive C-fibres in functional and molecular studies (McKemy et al., 2002;Babes et al., 2004;Okazawa et al., 2004;Xing et al., 2006;Hjerling-Leffler et al., 2007;Takashima et al., 2007), topical application of menthol was sufficient to induce pain (Wasner et al., 2004;Namer et al., 2005), and knockdown of TRPM8 activity resulted in deficits in noxious cold sensing (Dhaka et al., 2007;Colburn et al., 2007;Bautista et al., 2007).

This study was designed to assess the contribution of TRP channels to cold transduction in peripheral sensory and sympathetic neurons. Data from functional calcium imaging experiments supported a role for TRPM8, but not TRPA1, in the transduction of cold stimuli in sensory neurons. In particular, whereas more than 90 % of menthol-sensitive neurons were also cold-responsive, only a minority of the mustard oil- or cinnamaldehyde-sensitive population responded to a decrease in temperature. These findings concur with recent speculation that TRPA1 is not involved in the immediate detection of cold stimuli. It has been suggested that the ion channel may react to extreme or prolonged decreases in temperature (Reid, 2005), and may be important in the development of cold hypersensitivity following nerve injury or inflammation (Obata et al., 2005;Katsura et al., 2006;Obata et al., 2006), however the design of this particular study precluded any conclusions on the function of TRPA1 in relation to these latter theories.

With the exclusion of TRPA1 as the noxious cold receptor, one potential candidate for the role is TRPM8. The application of capsaicin with increasing concentrations of menthol demonstrated that neurons with a high sensitivity to the cooling compound were as likely to respond to capsaicin as those that only responded to saturating concentrations of menthol. These data clearly show that not only is TRPM8 expressed on nociceptive sensory afferents, but also rule out the possibility that very high concentrations of menthol are required to elicit a response in nociceptors. While this and other studies provide strong evidence that TRPM8 is involved in noxious cold transduction, it is certainly not the only receptor mediating this sensation in sensory neurons. A comparison between menthol-sensitive and -insensitive populations identified in this study found that the latter had a significantly colder threshold for activation, and deficits in responsiveness to noxious cold were only partially reduced following the knockout of TRPM8 (Dhaka et al., 2007;Colburn et al., 2007;Bautista et al., 2007).

The most important finding from this study was the discovery that a large proportion of sensory neurons and sympathetic neurons responded to cold in the absence of TRPM8 and TRPA1. Thus, 54 % of cold-sensitive sensory neurons, and more than 96 % of sympathetic neurons, were insensitive to menthol and mustard oil. Contrary to previous reports, the use of quantitative rt-PCR showed that the level of TRPA1 expression in the sympathetic ganglion was extremely low, and not sufficient to account for the high functional cold sensitivity recorded in dissociated SCG neurons. These data provide unequivocal evidence for the presence of alternative mechanisms for cold transduction in peripheral neurons.

8.1.1. The role of TRP channels in cold transduction – future perspectives

The next step for this project will be the identification of the mechanisms by which TRPM8-negative peripheral neurons transduce cold stimuli. One question to be answered is whether the receptor is common to both sensory afferent and sympathetic efferent fibres. Certainly the cold responses in dissociated DRG and SCG neurons have similar properties. Aside from being mediated via TRPM8-independent mechanisms, cold responses were abolished with the removal of calcium from the extracellular solution, and both menthol-insensitive sensory neurons and sympathetic cells had activation thresholds in the noxious cold range. Electrophysiological studies would provide further information on the biophysical characteristics of the cold response in sensory and sympathetic neurons, and may highlight additional similarities or differences in mechanisms of cold transduction between the two neuronal populations.

Data from this study showed that sympathetic neurons do not express TRP channels, although as potential candidates for the cold-sensitive receptor in sensory neurons, TRP channels cannot be ruled out on the basis of current evidence. One simple experiment that was not performed here, but which could provide some clues as to the contribution of other TRP channels to cold transduction, would be the use of a non-specific antagonist such as ruthenium red: inhibition of the cold response would implicate additional TRP channels in the mediation of cold sensitivity. Aside from TRP channels, the cold-induced blockade of potassium channels, or activation of sodium channels, has been associated with cold transduction in sensory neurons. As will be discussed in later sections however, while these ion channels may regulate the

onset of cold sensitivity, it is highly unlikely they contribute directly to the transduction of thermal stimuli.

In the past, putative cold-sensitive receptors have been identified on the basis of sequence similarity to known TRP channels (Peier et al., 2002a;Story et al., 2003), or their sensitivity to cooling compounds (McKemy et al., 2002). TRPM8 itself can be activated by many common chemicals with cooling properties, suggesting that the use of such compounds would not be beneficial in the identification of any additional mechanisms for cold transduction in sensory neurons. The expression of a noxious thermal receptor with apparent insensitivity to chemical stimuli is not without precedence, as demonstrated by the noxious heat receptor, TRPV2. Several studies have made use of cDNA expression libraries constructed from sensory neurons to identify clones susceptible to chemical activation (Caterina et al., 1997;McKemy et al., 2002). A similar strategy could prove useful in isolating clones from sensory and sympathetic neurons capable of conferring cold sensitivity to transfected cells. Much information could also be garnered from studies of the remaining cold-responsive neurons in the TRPM8 knockout mouse. In particular, electrophysiological investigation of the properties of the residual cold response would shed light on the type of ion channel involved in the mediation of noxious cold.

8.2. The role of voltage-gated potassium channels in cold transduction

The potential importance of voltage-gated potassium channels in the regulation of cold sensitivity was highlighted by two separate studies in sensory neurons. The first demonstrated that decreases in temperature resulted in the inhibition of a background potassium conductance, leading to an increase in input resistance and cell excitability (Reid and Flonta, 2001). The second study found that not only was the cold-sensitive background potassium current greater in cold-sensitive neurons, but conversely that cold-insensitive cells expressed higher levels of a transient potassium current, sensitive to the broad spectrum potassium channel blocker 4-AP (Viana et al., 2002). It was postulated that the transient current was acting as an excitability brake in the cold-insensitive population, preventing the cells from firing when a cold stimulus was applied.

Of particular interest was the discovery that blockade of the transient potassium conductance with 4-AP and another broad spectrum antagonist TEA could induce novel cold sensitivity in 30-60 % of previously unresponsive sensory neurons, both in

dissociated cultures and in the intact trigeminal ganglion (Viana et al., 2002;Cabanes et al., 2003).

The aim of this study was to further investigate the influence of potassium channel activity on cold transduction in sensory and sympathetic neurons. Pharmacological blockade of transient or delayed rectifier potassium currents with 4-AP or TEA, respectively, induced a novel cold sensitivity in a significant proportion of previously insensitive sensory neurons, in agreement with previous findings. Furthermore, the use of blockers specific to members of the Kv1 and Kv3 subfamilies demonstrated that these channels contribute to the regulation of cold sensitivity in sensory cells. The percentage of neurons displaying an induced cold response following the inhibition of either the Kv1 or Kv3 subfamily was much lower than that recorded in the presence of 4-AP or TEA, suggesting that other potassium channels may also be involved.

Prior to this study, there was no information on the role of potassium channels in cold transduction in sympathetic neurons, but like sensory neurons, broad spectrum potassium channel antagonists were found to induce novel cold sensitivity in a large percentage of cells. In spite of the obvious similarity in mechanism between the two neuronal populations, the use of different blockers highlighted distinct differences in the spectrum of channels involved. Specifically, delayed rectifier channels were found to play a more prominent role in the regulation of cold sensitivity in sympathetic neurons, and unlike the sensory population, inhibition of Kv1 and Kv3 channels had no influence on sympathetic cold transduction. This latter finding could be explained in part by the fact that neurons of the SCG were found to express lower levels of Kv1 and Kv3 channels compared to cells of the DRG.

Two observations from this and a parallel study carried out on the skin-nerve preparation discount a role for potassium channels themselves in the transduction of cold stimuli. Firstly, there was no correlation between the induction of cold sensitivity and responsiveness to the potassium channel antagonist, demonstrating that cells that were open to potassium channel blockade did not necessarily possess the capacity to respond to a change in temperature. Secondly, pharmacological inhibition of voltage-gated potassium channels did not alter sensitivity to heat or mechanical stimuli, implicating the presence of a cold-specific transduction mechanism (Vastani and Koltzenburg, 2007).

In the context of previous findings, data from this study support a scenario in which many, if not all, neurons constitutively express the ability to respond to a cold stimulus, but that under normal conditions the response is dampened by the activity of voltage-gated potassium channels. Inhibition or even down-regulation of potassium channel expression would effectively unmask the cold response and allow the neuron to reach firing threshold. It should be noted that neurons displaying a novel cold sensitivity following the blockade of potassium channels were menthol-insensitive, thus excluding a role for TRPM8 in the mediation of cold sensitivity in these cells.

8.2.1. The role of voltage-gated potassium channels in cold transduction – future perspectives

This study has raised several questions that require further consideration. Firstly, it will be important to identify which potassium channels are specifically required to regulate cold sensitivity in both sensory and sympathetic neurons. As already mentioned, there are significant differences between the two neuronal populations in terms of the complement of potassium channels involved in this regulatory mechanism, with delayed rectifiers playing a crucial role in sympathetic neurons in particular. Functional studies, such as those performed throughout this investigation, provide a reliable and rapid means of screening the effects of different potassium channel antagonists, although these studies could be hampered by the current lack of availability of specific channel blockers. This problem could be circumvented however with the use of antisense RNA technologies to block protein expression. During this investigation, data from quantitative rt-PCR experiments demonstrated clear differences in the expression of Kv1 and Kv3 potassium channels within the same cell type. It can be surmised that channels with higher levels of expression will be more important to the regulation of neuronal function. Consequently, it may prove beneficial to screen sensory and sympathetic ganglia for potassium channel expression prior to the design of functional experiments.

The next stage will be the identification of the cold-sensitive receptor mediating the responses unmasked by the blockade of potassium channel function. There is the possibility that the receptor may be the same as that mediating constitutive TRPM8-independent cold transduction in sensory and sympathetic neurons. The constitutive and induced responses do have properties in common, such as inhibition by the removal of extracellular calcium and a colder threshold for activation than the

menthol-sensitive population. Electrophysiological studies would provide biophysical information on the nature of the induced cold response, and could demonstrate whether the receptor is indeed common to sensory and sympathetic neurons, or even to induced and constitutive cold sensitivity. That one receptor could mediate both types of response is borne out by the previous observation that the potassium currents regulating neuronal excitability are differentially expressed in cold-sensitive versus cold-insensitive cells (Viana et al., 2002).

The discovery that the inhibition of potassium currents can induce a novel cold sensitivity is likely to be clinically relevant. The expression of voltage-gated potassium channels has been shown to be down-regulated in sensory neurons following nerve injury (Rasband et al., 2001;Ishikawa et al., 1999;Yang et al., 2004), and may therefore contribute to the development of cold hypersensitivity, a common symptom of neuropathic pain (Scadding and Koltzenburg, 2005). Furthermore, the expression of cold sensitivity in sympathetic neurons is postulated to contribute to the cold hypersensitivity manifest in cases of sympathetically maintained pain (Jänig and Baron, 2003). Consequently, it will be critical to translate the *in vitro* findings from this study to an *in vivo* context. A recent investigation demonstrated that antisense knockdown of Kv3 and Kv4 channels *in vivo* contributed to the development of mechanical and thermal hyperalgesia in DRG neurons (Chien et al., 2007), and a similar strategy could be used to define the role of potassium channel down-regulation in the onset of cold hypersensitivity.

8.3. The role of voltage-gated sodium channels in cold transduction

The platinum-based chemotherapeutic drug oxaliplatin is currently used in the treatment of colorectal, ovarian, breast and lung cancers. Like all platinum derivatives, cumulative doses can result in an accumulation of biotransformation products in the DRG and peripheral nerves, leading to a chronic peripheral sensory neuorotoxicity (Luo et al., 1999;Cavaletti et al., 2001). Specific to oxaliplatin however, is the onset of an acute neuropathy which is induced or exacerbated by exposure to cold, and is characterised by paraesthesias and muscle tightness in the jaw and limbs (Cersosimo, 2005;Pasetto et al., 2006).

Recent *in vitro* studies have implicated voltage-gated sodium channels in the development of this acute neurotoxicity. The application of oxaliplatin to nerve fibres or dissociated sensory neurons has been shown to result in an increased refractory

period, a reduction in sodium conductance, a shift in peak activation and inactivation to hyperpolarised potentials, and a slowing of the inactivation kinetics of sodium channels (Adelsberger et al., 2000;Grolleau et al., 2001;Webster et al., 2005;Benoit et al., 2006).

Behavioural studies have shown that rats administered with a single injection of oxaliplatin develop a cold hyperalgesia that can last up to a week after the injection (Ling et al., 2007), mirroring symptoms recorded in human patients (Binder et al., 2007). Furthermore, single unit recordings from the rat saphenous nerve have demonstrated an induction of cold sensitivity in previously unresponsive A-fibres (Vastani and Koltzenburg, 2007). One of the aims of this study therefore was to investigate whether application of oxaliplatin could modulate the cold sensitivity of dissociated sensory neurons. Despite trying a number of different experimental protocols and drug concentrations, neither acute nor chronic application of oxaliplatin induced a novel cold sensitivity in acutely dissociated neurons. Chronic exposure to the drug did however alter the quality of the cold response in a small population of cells, placing neurons in a state of repetitive firing reminiscent of the neuromyotonic discharge recorded in the motor nerves of patients displaying symptoms of acute oxaliplatin-induced neurotoxicity (Wilson et al., 2002;Lehky et al., 2004).

Since oxaliplatin is believed to exert its effects via the modulation of sodium current, experiments were also designed to investigate whether the activation of voltage-gated sodium channels was sufficient to alter cold sensing in neurons. Unlike potassium channels however, sodium channels were found to have no influence over cold transduction mechanisms. Moreover the effects of oxaliplatin could not be enhanced by the additional activation of sodium channels using the chemical agonist veratridine.

8.3.1. The role of voltage-gated sodium channels in cold transduction – future perspectives

There are obvious discrepancies between the effects of oxaliplatin recorded at the soma and those observed at the nerve terminal. In particular, the induction of cold sensitivity appears to be specific to the nerve terminal, as demonstrated by the lack of effect following the application of oxaliplatin to both the dissociated soma (this study) and the nerve branch (Vastani and Koltzenburg, 2007). Furthermore, whereas examination of myelinated axons treated with the chemotherapeutic drug reported

alterations in potassium, as well as sodium, conductance (Benoit et al., 2006), investigations using whole cell patch clamp techniques in DRG neurons failed to record any deficits in potassium channel function (Adelsberger et al., 2000). This may reflect vital differences in ion channel expression between the soma and nerve terminal, and an appreciation of such differences may lead to an understanding of how oxaliplatin is able to exert its effects in specific cellular regions. Functional studies on neurons maintained in culture over a period of days and/or in the presence of supporting cells such as Schwann cells may provide further clues as to the factors required for oxaliplatin-induced cold sensitivity.

It is possible that the underlying mechanism of cold transduction induced by oxaliplatin is similar to that induced via the blockade of voltage-gated potassium channels, and indeed may even result from drug-induced modification of potassium channel function. Certainly, the activation of sodium channels alone was insufficient to induce a novel cold sensitivity in sensory neurons, raising the possibility that additional factors are involved. It should be noted that in both dissociated cultures and the skin-nerve preparation, inhibition of voltage-gated potassium channels induced a novel cold sensitivity in a significant proportion of C-fibre neurons, whereas the effects of oxaliplatin are restricted to A-fibres. Nevertheless, an oxaliplatin-evoked alteration to ion channel function (be they potassium or sodium channels) may unmask a normally hidden cold response and enable cells to reach firing threshold. In this case, the receptor mediating cold sensation is likely to be the same as that responsible for the transduction of the novel cold response observed following the inhibition of potassium current.

One hypothesis for the oxaliplatin-induced neuropathy suggests that deficits in sodium channel inactivation caused by the presence of the drug are amplified by decreases in temperature, leading to a state of neuronal hyperexcitability. Consequently, whole cell electrophysiological recordings will be critical to understanding the precise actions of oxaliplatin on sodium channel function, in both ambient and cold environments. Despite the observed lack of novel cold sensitivity in dissociated neurons, chronic exposure to oxaliplatin did induce qualitative changes in the response to a cold stimulus, suggesting that neuronal cultures may nevertheless prove useful for gaining some understanding of how the drug mediates its effects. At the same time, it will be important to define the sodium channel isoforms subject to modulation by oxaliplatin, and based on current evidence, the most likely candidate

for this role is Nav1.6. Heterologous expression systems would provide a suitable means for assessing the effects of the chemotherapeutic drug on the activity of wild type and mutant sodium channel isoforms.

8.4. Modulation of cold sensitivity and TRP channel function by NGF

A recent study demonstrated that the onset of TRP channel expression and functional cold sensitivity in sensory neurons is regulated throughout embryonic and postnatal development (Hjerling-Leffler et al., 2007). TRPV1, TRPM8 and cold sensitivity are all expressed in embryonic DRG neurons, while TRPA1 is only detected from P0 onwards. Moreover, during the first two postnatal weeks, sensory neurons continue to undergo a number of developmental changes that subsequently contribute to the adult phenotype. In particular, a subpopulation of C-fibre nociceptors down-regulate the TrkA receptor and up-regulate expression of Ret, thus switching their growth factor dependency from NGF to GDNF (Molliver et al., 1997;Molliver and Snider, 1997). At the same time, the nociceptor-specific transcription factor Runx1, which is highly co-expressed with TrkA in embryonic ganglia, is also down-regulated and becomes restricted to the Ret-expressing population in mature neurons (Chen et al., 2006b).

The mechanisms by which TRP channel expression is regulated *in vivo* and *in vitro* are not fully understood. *In vivo*, the genetic knockdown of NGF or Runx1 was found to abolish expression of TRPM8 and TRPA1, and lead to a slight reduction in TRPV1 expression (Chen et al., 2006b;Luo et al., 2007), whereas the absence of Ret, while not altering expression of either TRPM8 or TRPV1, did eliminate expression of TRPA1 (Luo et al., 2007). *In vitro* studies looking at TRPA1 in neonatal sensory neurons have reported high functional expression in cells isolated at P0 and cultured for 2-3 days (Jordt et al., 2004;Bautista et al., 2006), which appears to contradict the finding that the TRPA1 transcript is only expressed postnatally (Hjerling-Leffler et al., 2007). Since neonatal neurons cannot survive in culture without NGF, it was hypothesised that the presence of the growth factor was influencing TRP channel expression in these cells.

Consequently, exposure of cultured neonatal sensory neurons to NGF for up to five days was found to result in an increase in functional sensitivity to cold, as well as chemical agonists of TRPM8 (menthol) and TRPA1 (cinnamaldehyde and mustard oil). Moreover, the presence of excess growth factor induced a significant up-regulation in expression of the TRPA1 transcript. These data support the theory that

NGF has the ability to regulate TRP channel expression *in vitro*, and this effect can therefore explain the discrepancies in TRPA1 expression reported from previous studies on neonatal sensory neurons. The same cannot be said for TRPV1 however, since functional capsaicin sensitivity was up-regulated to a similar extent in neurons cultured with or without NGF.

Further experiments were designed to investigate whether the observed changes in cold sensitivity and TRP channel expression induced by NGF were mediated via the transcription factor Runx1. Indeed, the expression of Runx1 itself was greatly up-regulated in the presence of NGF, in contrast to the expression of receptors for NGF and GDNF, which were down-regulated. Inhibition of Runx activity through the introduction of a dominant-negative isoform of the transcription factor into neonatal neurons was found to abolish the NGF-evoked increase in cold and menthol sensitivity, but have no influence over responsiveness to cinnamaldehyde, mustard oil or capsaicin. These data therefore demonstrated that NGF is capable of controlling protein expression in cultured sensory neurons via a number of different signalling pathways.

8.4.1. Modulation of cold sensitivity and TRP channel expression by NGF – future perspectives

There are a number of questions arising from this study that could be answered by future investigation. NGF is clearly able to alter the phenotype of cultured neonatal neurons, through its ability to regulate the expression of growth factor receptors, transcription factors and TRP channels. The administration of NGF or anti-NGF *in vivo* has previously been shown capable of altering the phenotype of Aδ- and C-fibre mechanoreceptors, but only if applied within a defined time frame in the early postnatal period (Lewin and Mendell, 1993). It would therefore be interesting to see whether neurons in culture are subject to the same constraints. Likewise, the phenotypic alterations induced *in vivo* are permanent, and long-term examination of cultured neurons could demonstrate whether the observed changes in protein expression *in vitro* can return to normal levels following the removal of NGF from the culture medium.

One crucial result from this study was the finding that NGF can regulate protein expression via a number of different signalling pathways. Thus, whereas changes in the expression of TRPM8 could be attributed to NGF-evoked modulation of the

activity of Runx1, this same transcription factor was not involved in the regulation of TRPA1. Current methods for elucidating intracellular signalling pathways include the use of pharmacological blockers targeted against activating or inactivating enzymes, or the measurement of the phosphorylation state of signalling intermediates, and such techniques could provide clues to the specific pathways involved in the regulation of TRP channel expression. Likewise, it is unclear from the data collected during this particular study how NGF mediates the down-regulation of the growth factor receptors, TrkA and Ret. With regards to the latter, addition of GDNF to the culture medium may provide support for the theory that Ret, like its co-receptors, is under autoregulatory control (Luo et al., 2007).

The expression of TRPV1 appears to be differentially regulated in adult versus neonatal neurons, both *in vitro* and *in vivo*. Thus, cells cultured from neonatal, but not adult, ganglia show a significant increase in functional capsaicin sensitivity when maintained for longer than a few hours, while the administration of NGF *in vivo* can induce thermal hypersensitivity (attributed to alterations in TRPV1 function) in adult rats, but not in neonates (Lewin et al., 1993). The observed up-regulation in TRPV1 expression in cultured neonatal neurons was not dependent on the presence of NGF, and the processes underlying these alterations in channel function require further investigation. It was hypothesised that when the neurons were dissociated for culturing, an intrinsic repressor mechanism was disrupted, leading to an uncontrolled up-regulation in TRPV1 expression. Alternatively, the channel could be under the control of an as yet unidentified transcriptional activator. Data from this investigation excludes a role for Runx1 in the regulation of TRPV1 expression, and results of a previous study suggest that the channel could be under the control of the CREB transcription factor, that can be activated by a number of signalling mediators via MAPK phosphorylation (Bron et al., 2003).

This particular study has concentrated on the effects mediated by NGF, however a significant percentage of neonatal sensory cells express Ret and are responsive to the GDNF family of growth factors. Overexpression of one member of this family, artemin, has already been shown to evoke an increase in TRPA1 and TRPV1 mRNA expression in adult DRG neurons (Elitt et al., 2006). Incidentally, there was also an increase in TrkA expression, providing further evidence for a complex interplay between growth factor availability and receptor expression. It would therefore be of great interest to investigate whether GDNF-related growth factors could have similar

effects to NGF on TRP channel expression and cold sensitivity during postnatal development.

Finally, it will be important to understand how the exposure of sensory neurons to excess concentrations of NGF, or even other growth factors, could alter neuronal function *in vivo*. In particular, it would be necessary to see whether cold sensitivity and TRP channel expression could be regulated in a similar fashion to that recorded *in vitro*. It has previously been shown that administration of NGF to neonatal rats can evoke a profound and long-lasting mechanical hyperalgesia (Lewin et al., 1993), and furthermore, that the occurrence of nerve injury or inflammation during the first postnatal week, both of which result in the synthesis and release of NGF, can sensitise neurons to subsequent challenges (Lidow, 2002;Gold and Flake, 2005). The influence of NGF on cold sensitivity and TRP channel expression during development may therefore determine the phenotype and function of adult sensory neurons, and their subsequent response to injury.

In summary, this project has demonstrated that the mediation of cold sensitivity in peripheral neurons is highly complex. While TRP channels currently remain the principal transducers of thermal stimuli in sensory neurons, this study has shown that TRP-independent mechanisms may play a significant role in the detection of cold in a large proportion of peripheral sensory and sympathetic neurons. Cold sensation is subject to regulation by voltage-gated potassium channels and growth factors, and defects in either of these regulatory mechanisms could contribute to the development of cold hypersensitivity following nerve injury. It is clear that many questions still need to be answered in order to reach a full understanding of how cold sensation, both in the normal and pathologic states, is mediated.

Reference List

Abdulla FA, Smith PA (2001) Axotomy- and autotomy-induced changes in Ca2+ and K+ channel currents of rat dorsal root ganglion neurons. J Neurophysiol 85:644-658.

Abe J, Hosokawa H, Sawada Y, Matsumura K, Kobayashi S (2006) Ca2+-dependent PKC activation mediates menthol-induced desensitization of transient receptor potential M8. Neurosci Lett 397:140-144.

Adelsberger H, Quasthoff S, Grosskreutz J, Lepier A, Eckel F, Lersch C (2000) The chemotherapeutic oxaliplatin alters voltage-gated Na+ channel kinetics on rat sensory neurons. Eur J Pharmacol 406:25-32.

AlQatari M, Munns C, Mair L, Crossley J, Koltzenburg M, Mendell LM (2007) Regulation of menthol sensitivity in non-peptidergic sensory neurons. Abstract Viewer/Itinerary Planner San Diego:SfN 2007 Online: 400.14.

Anand U, Otto WR, Casula MA, Day NC, Davis JB, Bountra C, Birch R, Anand P (2006) The effect of neurotrophic factors on morphology, TRPV1 expression and capsaicin responses of cultured human DRG sensory neurons. Neurosci Lett 399:51-56.

Andersson DA, Chase HW, Bevan S (2004) TRPM8 activation by menthol, icilin, and cold is differentially modulated by intracellular pH. J Neurosci 24:5364-5369.

Andersson DA, Nash M, Bevan S (2007) Modulation of the cold-activated channel TRPM8 by lysophospholipids and polyunsaturated fatty acids. J Neurosci 27:3347-3355.

Askwith C, Benson C, Welsh M, Snyder P (2001) DEG/ENaC ion channels involved in sensory transduction are modulated by cold temperature. Proc Nat Acad Sci 98:6459-6463.

Babes A, Zorzon D, Reid G (2004) Two populations of cold-sensitive neurons in rat dorsal root ganglia and their modulation by nerve growth factor. Eur J Neurosci 20:2276-2282.

Babes A, Zorzon D, Reid G (2006) A novel type of cold-sensitive neuron in rat dorsal root ganglia with rapid adaptation to cooling stimuli. Eur J Neurosci 24:691-698.

Baccaglini PI, Hogan PG (1983) Some rat sensory neurons in culture express characteristics of differentiated pain sensory cells. Proc Natl Acad Sci U S A 80:594-598.

Bae SC, Lee YH (2006) Phosphorylation, acetylation and ubiquitination: the molecular basis of RUNX regulation. Gene 366:58-66.

Bandell M, Dubin AE, Petrus MJ, Orth A, Mathur J, Hwang SW, Patapoutian A (2006) High-throughput random mutagenesis screen reveals TRPM8 residues specifically required for activation by menthol. Nat Neurosci 9:493-500.

Bandell M, Story GM, Hwang SW, Viswanath V, Eid SR, Petrus MJ, Earley TJ, Patapoutian A (2004) Noxious cold ion channel TRPA1 is activated by pungent compounds and bradykinin. Neuron 41:849-857.

Bautista DM, Jordt SE, Nikai T, Tsuruda PR, Read AJ, Poblete J, Yamoah EN, Basbaum AI, Julius D (2006) TRPA1 mediates the inflammatory actions of environmental irritants and proalgesic agents. Cell 124:1269-1282.

Bautista DM, Movahed P, Hinman A, Axelsson HE, Sterner O, Hogestatt ED, Julius D, Jordt SE, Zygmunt PM (2005) Pungent products from garlic activate the sensory ion channel TRPA1. Proc Natl Acad Sci U S A 102:12248-12252.

Bautista DM, Siemens J, Glazer JM, Tsuruda PR, Basbaum AI, Stucky CL, Jordt SE, Julius D (2007) The menthol receptor TRPM8 is the principal detector of environmental cold. Nature 448:204-208.

Beise RD, Carstens E, Kohllöffel LUE (1998) Psychophysical study of stinging pain evoked by brief freezing of superficial skin and ensuing short-lasting changes in sensations of cool and cold pain. Pain 74:275-286.

Benarroch EE (2007) Sodium channels and pain. Neurology 68:233-236.

Benoit E, Brienza S, Dubois J-M (2006) Oxaliplatin, an anticancer agent that affects both Na+ and K+ channels in frog peripheral myelinated axons. Gen Physiol Biophys 25:263-276.

Binder A, Stengel M, Maag R, Wasner G, Schoch R, Moosig F, Schommer B, Baron R (2007) Pain in oxaliplatin-induced neuropathy - Sensitisation in the peripheral and central nociceptive system. Eur J Cancer 43:2658-2663.

Black JA, Liu S, Tanaka M, Cummins TR, Waxman SG (2004) Changes in the expression of tetrodotoxin-sensitive sodium channels within dorsal root ganglia neurons in inflammatory pain. Pain 108:237-247.

Bonnington JK, McNaughton PA (2003) Signalling pathways involved in the sensitisation of mouse nociceptive neurones by nerve growth factor. J Physiol 551:433-446.

Bouhours M, Luce S, Sternberg D, Willer JC, Fontaine B, Tabti N (2005) A1152D mutation of the Na+ channel causes paramyotonia congenita and emphasizes the role of DIII/S4-S5 linker in fast inactivation. J Physiol 565:415-427.

Bouhours M, Sternberg D, Davoine C-S, Ferrer X, Willer JC, Fontaine B, Tabti N (2003) Functional characterization and cold sensitivity of T1313A, a new mutation of the skeletal muscle sodium channel causing paramyotonia congenita in humans. J Physiol 554:635-647.

Brauchi S, Orta G, Salazar M, Rosenmann E, Latorre R (2006) A hot-sensing cold receptor: C-terminal domain determines thermosensation in transient receptor potential channels. J Neurosci 26:4835-4840.

Bron R, Klesse LJ, Shah K, Parada LF, Winter J (2003) Activation of Ras is necessary and sufficient for upregulation of vanilloid receptor type 1 in sensory neurons by neurotrophic factors. Mol Cell Neurosci 22:118-132.

Cabanes C, Viana F, Belmonte C (2003) Differential thermosensitivity of sensory neurons in the guinea pig trigeminal ganglion. J Neurophysiol 90:2219-2231.

Campbell JN, Meyer RA (2006) Mechanisms of neuropathic pain. Neuron 52:77-92.

Campero M, Serra J, Bostock H, Ochoa JL (2001) Slowly conducting afferents activated by innocuous low temperature in human skin. J Physiol 535:855-865.

Caterina MJ (2007) Transient receptor potential ion channels as participants in thermosensation and thermoregulation. Am J Physiol Regul Integr Comp Physiol 292:R64-R76.

Caterina MJ, Rosen TA, Tominaga M, Brake AJ, Julius D (1999) A capsaicin-receptor homologue with a high threshold for noxious heat. Nature 398:436-441.

Caterina M, Leffler A, Malmberg A, Martin W, Trafton J, Petersen-Zeitz K, Koltzenburg M, Basbaum A, Julius D (2000) Impaired nociception and pain sensation in mice lacking the capsaicin receptor. Science 288:306-313.

Caterina M, Schumacher M, Tominaga M, Rosen T, Levine J, Julius D (1997) The capsaicin receptor: a heat-activated ion channel in the pain pathway. Nature 389:816-824.

Cattaneo L, Chierici E, Cucurachi L, Cobelli R, Pavesi G (2007) Posterior insular stroke causing selective loss of contralateral nonpainful thermal sensation. Neurology 68:237.

Cavaletti G, Tredici G, Petruccioli MG, Donde E, Tredici P, Marmiroli P, Minoia C, Ronchi A, Bayssas M, Etienne GG (2001) Effects of different schedules of oxaliplatin treatment on the peripheral nervous system of the rat. Eur J Cancer 37:2457-2463.

Cersosimo RJ (2005) Oxaliplatin-associated neuropathy: a review. Ann Pharmacother 39:128-135.

Chen AI, de Nooij JC, Jessell TM (2006a) Graded activity of transcription factor Runx3 specifies the laminar termination pattern of sensory axons in the developing spinal cord. Neuron 49:395-408.

Chen CL, Broom DC, Liu Y, de Nooij JC, Li Z, Cen C, Samad OA, Jessell TM, Woolf CJ, Ma Q (2006b) Runx1 determines nociceptive sensory neuron phenotype and is required for thermal and neuropathic pain. Neuron 49:365-377.

Chien LY, Cheng JK, Chu D, Cheng CF, Tsaur ML (2007) Reduced expression of A-type potassium channels in primary sensory neurons induces mechanical hypersensitivity. J Neurosci 27:9855-9865.

Chraïbi A, Horisberger J-D (2003) Dual effect of temperature on the human epithelial Na+ channel. Eur J Physiol 447:316-320.

Chuang H, Prescott ED, Kong H, Shields S, Jordt S-E, Basbaum AI, Chao MV, Julius D (2001) Bradykinin and nerve growth factor release the capsaicin receptor from PtdIns(4,5)P2-mediated inhibition. Nature 411:957-962.

Chuang HH, Neuhausser WM, Julius D (2004) The super-cooling agent icilin reveals a mechanism of coincidence detection by a temperature-sensitive TRP channel. Neuron 43:859-869.

Colburn RW, Lubin ML, Stone DJ, Jr., Wang Y, Lawrence D, D'Andrea MR, Brandt MR, Liu Y, Flores CM, Qin N (2007) Attenuated cold sensitivity in TRPM8 null mice. Neuron 54:379-386.

Craig A (2003) Pain mechanisms: labeled lines versus convergence in central processing. Annu Rev Neurosci 26:1-30.

Craig A, Bushnell M (1994) The thermal grill illusion: unmasking the burn of cold pain. Science 265:252-255.

Cummins TR, Dib-Hajj SD, Waxman SG (2004) Electrophysiological properties of mutant Nav1.7 sodium channels in a painful inherited neuropathy. J Neurosci 24:8232-8236.

Cummins TR, Waxman SG (1997) Downregulation of tetrodotoxin-resistant sodium currents and upregulation of a rapidly repriming tetrodotoxin-sensitive sodium current in small spinal sensory neurons after nerve injury. J Neurosci 17:3503-3514.

Dai Y, Wang S, Tominaga M, Yamamoto S, Fukuoka T, Higashi T, Kobayashi K, Obata K, Yamanaka H, Noguchi K (2007) Sensitization of TRPA1 by PAR2 contributes to the sensation of inflammatory pain. J Clin Invest 117:1979-1987.

Davies AM, Lee K-F, Jaenisch R (1993) p75-deficient trigeminal sensory neurons have an altered response to NGF but not to other neurotrophins. Neuron 11:565-574.

Davis KD (1998) Cold-induced pain and prickle in the glabrous and hairy skin. Pain 75:47-57.

Davis KD, Pope GE (2002) Noxious cold evokes multiple sensations with distinct time courses. Pain 98:179-185.

de la Pena E, Malkia A, Cabedo H, Belmonte C, Viana F (2005) The contribution of TRPM8 channels to cold sensing in mammalian neurones. J Physiol 567:415-426.

De Petrocellis L, Starowicz K, Moriello AS, Vivese M, Orlando P, Di M, V (2007) Regulation of transient receptor potential channels of melastatin type 8 (TRPM8): effect of cAMP, cannabinoid CB(1) receptors and endovanilloids. Exp Cell Res 313:1911-1920.

Desoize B, Madoulet C (2002) Particular aspects of platinum compounds used at present in cancer treatment. Crit Rev Oncol Hematol 42:317-325.

Dhaka A, Earley TJ, Watson J, Patapoutian A (2008) Visualising cold spots: TRPM8-expressing sensory neurons and their projections. J Neurosci 28:566-575.

Dhaka A, Murray AN, Mathur J, Earley TJ, Petrus MJ, Patapoutian A (2007) TRPM8 is required for cold sensation in mice. Neuron 54:371-378.

Dib-Hajj SD, Fjell J, Cummins TR, Zheng Z, Fried K, LaMotte R, Black JA, Waxman SG (1999) Plasticity of sodium channel expression in DRG neurons in the chronic constriction injury model of neuropathic pain. Pain 83:591-600.

Dib-Hajj SD, Rush AM, Cummins TR, Hisama FM, Novella S, Tyrrell L, Marshall L, Waxman SG (2005) Gain-of-function mutation in Nav1.7 in familial erythromelalgia induces bursting of sensory neurons. Brain 128:1847-1854.

Diochot S, Schweitz H, Beress L, Lazdunski M (1998) Sea anemone peptides with a specific blocking activity against the fast inactivating potassium channel Kv3.4. J Biol Chem 273:6744-6749.

Diogenes A, Akopian AN, Hargreaves KM (2007) NGF up-regulates TRPA1: implications for orofacial pain. J Dent Res 86:550-555.

Dittert I, Benedikt J, Vyklicky L, Zimmermann K, Reeh PW, Vlachova V (2006) Improved superfusion technique for rapid cooling or heating of cultured cells under patch-clamp conditions. J Neurosci Methods 151:178-185.

Dixon JE, McKinnon D (1996) Potassium channel mRNA expression in prevertebral and paravertebral sympathetic neurons. Eur J Neurosci 8:183-191.

Djouhri L, Wrigley D, Thut PD, Gold MS (2004) Spinal nerve injury increases the percentage of cold-responsive DRG neurons. Neuroreport 15:457-460.

Doerner JF, Gisselmann G, Hatt H, Wetzel CH (2007) Transient receptor potential channel A1 is directly gated by calcium ions. J Biol Chem 282:13180-13189.

Dostrovsky J, Craig A (2005) Ascending projection systems. In: Wall and Melzack's Textbook of Pain (McMahon S, Koltzenburg M, eds), pp 187-203. Philadelphia: Elsevier.

Elitt CM, McIlwrath SL, Lawson JJ, Malin SA, Molliver DC, Cornuet PK, Koerber HR, Davis BM, Albers KM (2006) Artemin overexpression in skin enhances expression of TRPV1 and TRPA1 in cutaneous sensory neurons and leads to behavioral sensitivity to heat and cold. J Neurosci 26:8578-8587.

Ernfors P (2001) Local and target-derived actions of neurotrophins during peripheral nervous system development. Cell Mol Life Sci 58:1036-1044.

Everill B, Kocsis JD (2000) Nerve growth factor maintains potassium conductance after nerve injury in adult cutaneous afferent dorsal root ganglion neurons. Neurosci 100:417-422.

Everill B, Kocsis JD (1999) Reduction in potassium currents in identified cutaneous afferent dorsal root ganglion neurons after axotomy. J Neurophysiol 82:700-708.

Fertleman CR, Baker MD, Parker KA, Moffatt S, Elmslie FV, Abrahamsen B, Ostman J, Klugbauer N, Wood JN, Gardiner RM, Rees M (2006) SCN9A mutations

in paroxysmal extreme pain disorder: allelic variants underlie distinct channel defects and phenotypes. Neuron 52:767-774.

Fleige S, Pfaffl MW (2006) RNA integrity and the effect on the real-time qRT-PCR performance. Mol Aspects Med 27:126-139.

Fleischhauer R, Mitrovic N, Deymeer F, Lehmann-Horn F, Lerche H (1998) Effects of temperature and mexiletine on the F1473S Na+ channel mutation causing paramyotonia congenita. Eur J Physiol 436:757-765.

Frederick J, Buck ME, Matson DJ, Cortright DN (2007) Increased TRPA1, TRPM8, and TRPV2 expression in dorsal root ganglia by nerve injury. Biochem Biophys Res Commun 358:1058-1064.

George L, Chaverra M, Todd V, Lansford R, Lefcort F (2007) Nociceptive sensory neurons derive from contralaterally migrating, fate-restricted neural crest cells. Nat Neurosci 10:1287-1293.

Gold MS, Flake NM (2005) Inflammation-mediated hyperexcitability of sensory neurons. Neurosignals 14:147-157.

Green BG, Schoen KL (2007) Thermal and nociceptive sensations from menthol and their suppression by dynamic contact. Behav Brain Res 176:284-291.

Grolleau F, Gamelin L, Boisdron-Celle M, Lapied B, Pelhate M, Gamelin E (2001) A possible explanation for a neurotoxic effect of the anticancer agent oxaliplatin on neuronal voltage-gated sodium channels. J Neurophysiol 85:2293-2297.

Guler AD, Lee H, Iida T, Shimizu I, Tominaga M, Caterina M (2002) Heat-evoked activation of the ion channel, TRPV4. J Neurosci 22:6408-6414.

Hadley JK, Passmore GM, Tatulian L, Al-Qatari M, Ye F, Wickenden AD, Brown DA (2003) Stoichiometry of expressed KCNQ2/KCNQ3 potassium channels and subunit composition of native ganglionic M channels deduced from block by tetraethylammonium. J Neurosci 23:5012-5019.

Han C, Lampert A, Rush AM, Dib-Hajj SD, Wang X, Yang Y, Waxman SG (2007) Temperature dependence of erythromelalgia mutation L858F in sodium channel Nav1.7. Mol Pain 3:3.

Han C, Rush AM, Dib-Hajj SD, Li S, Xu Z, Wang Y, Tyrrell L, Wang X, Yang Y, Waxman SG (2006) Sporadic onset of erythermalgia: a gain-of-function mutation in Nav1.7. Ann Neurol 59:553-558.

Harrison JLK, Davis KD (1999) Cold-evoked pain varies with skin type and cooling rate: a psychophysical study in humans. Pain 83:123-135.

Harty TP, Dib-Hajj SD, Tyrrell L, Blackman R, Hisama FM, Rose JB, Waxman SG (2006) Na(V)1.7 mutant A863P in erythromelalgia: effects of altered activation and steady-state inactivation on excitability of nociceptive dorsal root ganglion neurons. J Neurosci 26:12566-12575.

Heppenstall PA, Lewin GR (2000) Neurotrophins, nociceptors and pain. Curr Opin Anaesthesiol 13:573-576.

Hille B (2001) Ion Channels of Excitable Membranes. Sinauer Associates.

Hinman A, Chuang HH, Bautista DM, Julius D (2006) TRP channel activation by reversible covalent modification. Proc Natl Acad Sci U S A 103:19564-19568.

Hjerling-Leffler J, Alqatari M, Ernfors P, Koltzenburg M (2007) Emergence of functional sensory subtypes as defined by transient receptor potential channel expression. J Neurosci 27:2435-2443.

Hjerling-Leffler J, Marmigere F, Heglind M, Cederberg A, Koltzenburg M, Enerback S, Ernfors P (2005) The boundary cap: a source of neural crest stem cells that generate multiple sensory neuron subtypes. Development 132:2623-2632.

Huang EJ, Reichardt LF (2003) Trk receptors: roles in neuronal signal transduction. Annu Rev Biochem 72:609-642.

Huang J, Zhang X, McNaughton PA (2006) Modulation of temperature-sensitive TRP channels. Semin Cell Dev Biol 17:638-645.

Huang SM, Bisogno T, Trevisani M, Al-Hayani A, De Petrocellis L, Fezza F, Tognetto M, Petros TJ, Krey JF, Chu CJ, Miller JD, Davies SN, Geppetti P, Walker JM, Di Marzo V (2002) An endogenous capsaicin-like substance with high potency at recombinant and native vanilloid VR1 receptors. Proc Nat Acad Sci 99:8400-8405.

Inoue K, Ozaki S, Shiga T, Ito K, Masuda T, Okado N, Iseda T, Kawaguchi S, Ogawa M, Bae SC, Yamashita N, Itohara S, Kudo N, Ito Y (2002) *Runx3* controls the axonal projection of proprioceptive dorsal root ganglion neurons. Nat Neurosci 5:946-954.

Ishikawa K, Tanaka M, Black JA, Waxman SG (1999) Changes in expression of voltage-gated potassium channels in dorsal root ganglion neurons following axotomy. Muscle Nerve 22:502-507.

Jamieson SM, Liu J, Connor B, McKeage MJ (2005) Oxaliplatin causes selective atrophy of a subpopulation of dorsal root ganglion neurons without inducing cell loss. Cancer Chemother Pharmacol 56:391-399.

Jänig W, Baron R (2003) Complex regional pain syndrome: mystery explained? Lancet Neurol 2:687-697.

Jänig W, Levine JD (2005) Autonomic-endocrine-immune interactions in acute and chronic pain. In: Wall and Melzack's Textbook of Pain (McMahon SB, Koltzenburg M, eds), pp 205-218. Philadelphia: Elsevier.

Ji G, Zhou S, Kochukov MY, Westlund KN, Carlton SM (2007) Plasticity in intact Adelta- and C-fibers contributes to cold hypersensitivity in neuropathic rats. Neurosci 150:182-193.

Ji RR, Samad TA, Jin SX, Schmoll R, Woolf CJ (2002) p38 MAPK activation by NGF in primary sensory neurons after inflammation increases TRPV1 levels and maintains heat hyperalgesia. Neuron 36:57-68.

Johnson EM, Jr., Gorin PD, Brandeis LD, Pearson J (1980) Dorsal root ganglion neurons are destroyed by exposure in utero to maternal antibody to nerve growth factor. Science 210:916-918.

Jordt SE, Bautista DM, Chuang HH, McKemy DD, Zygmunt PM, Hogestatt ED, Meng ID, Julius D (2004) Mustard oils and cannabinoids excite sensory nerve fibres through the TRP channel ANKTM1. Nature 427:260-265.

Jordt SE, McKemy DD, Julius D (2003) Lessons from peppers and peppermint: the molecular logic of thermosensation. Curr Opin Neurobiol 13:487-492.

Julius D, Basbaum AI (2001) Molecular mechanisms of nociception. Nature 413:203-210.

Kang D, Choe C, Kim D (2005) Thermosensitivity of the two-pore domain K^+ channels TREK-2 and TRAAK. J Physiol 564:103-116.

Kang D, Kim D (2006) TREK-2 (K2P10.1) and TRESK (K2P18.1) are major background K+ channels in dorsal root ganglion neurons. Am J Physiol Cell Physiol 291:C138-C146.

Katsura H, Obata K, Mizushima T, Yamanaka H, Kobayashi K, Dai Y, Fukuoka T, Tokunaga A, Sakagami M, Noguchi K (2006) Antisense knock down of TRPA1, but not TRPM8, alleviates cold hyperalgesia after spinal nerve ligation in rats. Exp Neurol 200:112-123.

Kiernan MC, Krishnan AV (2006) The pathophysiology of oxaliplatin-induced neurotoxicity. Curr Med Chem 13:2901-2907.

Kim CH, Oh Y, Chung JM, Chung K (2002) Changes in three subtypes of tetrodotoxin sensitive sodium channel expression in the axotomized dorsal root ganglion in the rat. Neurosci Lett 323:125-128.

Kim D, Cavanaugh EJ (2007) Requirement of a soluble intracellular factor for activation of transient receptor potential A1 by pungent chemicals: role of inorganic polyphosphates. J Neurosci 27:6500-6509.

Kobayashi K, Fukuoka T, Obata K, Yamanaka H, Dai Y, Tokunaga A, Noguchi K (2005) Distinct expression of TRPM8, TRPA1, and TRPV1 mRNAs in rat primary afferent neurons with adelta/c-fibers and colocalization with trk receptors. J Comp Neurol 493:596-606.

Koltzenburg M (2004) Thermal sensitivity of sensory neurons. In: The pain system in normal and pathological states: a primer for clinicians (Villanueva L, Dickenson A, Ollat H, eds), Seattle: IASP Press.

Koltzenburg M, Bennett DLH, Shelton DL, McMahon SB (1999) Neutralization of endogenous NGF prevents the sensitization of nociceptors supplying inflamed skin. Eur J Neurosci 11:1698-1704.

Kramer I, Sigrist M, de Nooij JC, Taniuchi I, Jessell TM, Arber S (2006) A role for Runx transcription factor signaling in dorsal root ganglion sensory neuron diversification. Neuron 49:379-393.

Kress M, Koltzenburg M, Reeh PW, Handwerker HO (1992) Responsiveness and functional attributes of electrically localised terminals of cutaneous C-fibers in vivo and in vitro. J Neurophysiol 68:581-595.

Kwan KY, Allchorne AJ, Vollrath MA, Christensen AP, Zhang DS, Woolf CJ, Corey DP (2006) TRPA1 contributes to cold, mechanical, and chemical nociception but is not essential for hair-cell transduction. Neuron 50:277-289.

Lai J, Porreca F, Hunter JC, Gold MS (2004) Voltage-gated sodium channels and hyperalgesia. Annu Rev Pharmacol Toxicol 44:371-397.

LaMotte RH, Thalhammer JG (1982) Response properties of high-threshold cutaneous cold receptors in the primate. Brain Res 244:279-287.

Lampert A, Dib-Hajj SD, Tyrrell L, Waxman SG (2006) Size matters: Erythromelalgia mutation S241T in Nav1.7 alters channel gating. J Biol Chem 281:36029-36035.

Lehky TJ, Leonard GD, Wilson RH, Grem JL, Floeter MK (2004) Oxaliplatin-induced neurotoxicity: acute hyperexcitability and chronic neuropathy. Muscle Nerve 29:387-392.

Levanon D, Bettoun D, Harris-Cerruti C, Woolf E, Negreanu V, Eilam R, Bernstein Y, Goldenberg D, Xiao C, Fliegauf M, Kremer E, Otto F, Brenner O, Lev-Tov A, Groner Y (2002) The Runx3 transcription factor regulates development and survival of TrkC dorsal root ganglia neurons. EMBO J 21:3454-3463.

Lewin GR, Mendell LM (1993) Nerve growth factor and nociception. Trends Neurosci 16:353-359.

Lewin GR, Ritter AM, Mendell LM (1993) Nerve growth factor-induced hyperalgesia in the neonatal and adult rat. J Neurosci 13:2136-2148.

Lidow MS (2002) Long-term effects of neonatal pain on nociceptive systems. Pain 99:377-383.

Ling B, Coudore-Civiale MA, Balayssac D, Eschalier A, Coudore F, Authier N (2007) Behavioral and immunohistological assessment of painful neuropathy induced by a single oxaliplatin injection in the rat. Toxicology 234:176-184.

Linte RM, Ciobanu C, Reid G, Babes A (2007) Desensitization of cold- and menthol-sensitive rat dorsal root ganglion neurones by inflammatory mediators. Exp Brain Res 178:89-98.

Liu B, Qin F (2005) Functional control of cold- and menthol-sensitive TRPM8 ion channels by phosphatidylinositol 4,5-bisphosphate. J Neurosci 25:1674-1681.

Low PA (1993) Clinical Autonomic Disorders. Boston: Little, Brown and Co.

Luo FR, Wyrick SD, Chaney SG (1999) Comparative neurotoxicity of oxaliplatin, ormaplatin, and their biotransformation products utilizing a rat dorsal root ganglia in vitro explant culture model. Cancer Chemother Pharmacol 44:29-38.

Luo W, Wickramasinghe SR, Savitt JM, Griffin JW, Dawson TM, Ginty DD (2007) A hierarchical NGF signaling cascade controls Ret-dependent and Ret-independent events during development of nonpeptidergic DRG neurons. Neuron 54:739-754.

Macpherson LJ, Dubin AE, Evans MJ, Marr F, Schultz PG, Cravatt BF, Patapoutian A (2007a) Noxious compounds activate TRPA1 ion channels through covalent modification of cysteines. Nature 445:541-545.

Macpherson LJ, Geierstanger BH, Viswanath V, Bandell M, Eid SR, Hwang S, Patapoutian A (2005) The pungency of garlic: activation of TRPA1 and TRPV1 in response to allicin. Curr Biol 15:929-934.

Macpherson LJ, Xiao B, Kwan KY, Petrus MJ, Dubin AE, Hwang SW, Cravatt B, Corey DP, Patapoutian A (2007b) An ion channel essential for sensing chemical damage. J Neurosci 27:11412-11415.

Madrid R, Donovan-Rodriguez T, Meseguer V, Acosta MC, Belmonte C, Viana F (2006) Contribution of TRPM8 channels to cold transduction in primary sensory neurons and peripheral nerve terminals. J Neurosci 26:12512-12525.

Maingret F, Lauritzen I, Patel A, Heurteaux C, Reyes R, Lesage F, Lazdunski M, Honoré E (2000) TREK-1 is a heat-activated background K^+ channel. EMBO 19:2483-2491.

Malin SA, Nerbonne JM (2000) Elimination of the fast transient in superior cervical ganglion neurons with expression of KV4.2W362F: molecular dissection of IA. J Neurosci 20:5191-5199.

Malin SA, Nerbonne JM (2001) Molecular heterogeneity of the voltage-gated fast transient outward K+ current, I(Af), in mammalian neurons. J Neurosci 21:8004-8014.

Malin SA, Nerbonne JM (2002) Delayed rectifier K+ currents, IK, are encoded by Kv2 alpha-subunits and regulate tonic firing in mammalian sympathetic neurons. J Neurosci 22:10094-10105.

Malkia A, Madrid R, Meseguer V, de la PE, Valero M, Belmonte C, Viana F (2007) Bidirectional shifts of TRPM8 channel gating by temperature and chemical agents modulate the cold sensitivity of mammalian thermoreceptors. J Physiol 581:155-174.

Marmigere F, Ernfors P (2007) Specification and connectivity of neuronal subtypes in the sensory lineage. Nat Rev Neurosci 8:114-127.

Marmigere F, Montelius A, Wegner M, Groner Y, Reichardt LF, Ernfors P (2006) The Runx1/AML1 transcription factor selectively regulates development and survival of TrkA nociceptive sensory neurons. Nat Neurosci 9:180-187.

Maro GS, Vermeren M, Voiculescu O, Melton L, Cohen J, Charnay P, Topilko P (2004) Neural crest boundary cap cells constitute a source of neuronal and glial cells of the PNS. Nat Neurosci 7:930-938.

Martyn C, Hughes R (1998) Peripheral neuropathies. In: The epidemiology of neurological disorders (Martyn C, Hughes R, eds), pp 96-117. London: BMJ Books.

Matteson DR, Armstrong CM (1982) Evidence for a population of sleepy sodium channels in squid axon at low temperature. J Gen Physiol 79:739-758.

McKemy DD, Neuhausser WM, Julius D (2002) Identification of a cold receptor reveals a general role for TRP channels in thermosensation. Nature 416:52-58.

McNamara CR, Mandel-Brehm J, Bautista DM, Siemens J, Deranian KL, Zhao M, Hayward NJ, Chong JA, Julius D, Moran MM, Fanger CM (2007) TRPA1 mediates formalin-induced pain. Proc Natl Acad Sci U S A 104:13525-13530.

Meyer R, Ringkamp M, Campbell J, Raja S (2005) Peripheral mechanisms of cutaneous nociception. In: Wall and Melzack's Textbook of Pain (McMahon S, Koltzenburg M, eds), pp 3-34. Philadelphia: Elsevier.

Mohammadi B, Mitrovic N, Lehmann-Horn F, Dengler R, Bufler J (2003) Mechanisms of cold sensitivity of paramyotonia congenita mutation R1448H and overlap syndrome mutation M1360V. J Physiol 547:691-698.

Molliver DC, Snider WD (1997) Nerve growth factor receptor TrkA is down-regulated during postnatal development by a subset of dorsal root ganglion neurons. J Comp Neurol 381:428-438.

Molliver DC, Wright DE, Leitner ML, Parsadanian AS, Doster K, Wen D, Yan Q, Snider WD (1997) IB4-binding DRG neurons switch from NGF to GDNF dependence in early postnatal life. Neuron 19:849-861.

Montell C (2005) The TRP superfamily of cation channels. Sci STKE 2005:re3.

Nagata K, Duggan A, Kumar G, Garcia-Anoveros J (2005) Nociceptor and hair cell transducer properties of TRPA1, a channel for pain and hearing. J Neurosci 25:4052-4061.

Namer B, Seifert F, Handwerker HO, Maihofner C (2005) TRPA1 and TRPM8 activation in humans: effects of cinnamaldehyde and menthol. Neuroreport 16:955-959.

Nealen ML, Gold MS, Thut PD, Caterina MJ (2003) TRPM8 mRNA is expressed in a subset of cold-responsive trigeminal neurons from rat. J Neurophysiol 90:515-520.

Nicol GD, Vasko MR (2007) Unraveling the story of NGF-mediated sensitization of nociceptive sensory neurons: ON or OFF the Trks? Mol Interv 7:26-41.

Obata K, Katsura H, Mizushima T, Yamanaka H, Kobayashi K, Dai Y, Fukuoka T, Tokunaga A, Tominaga M, Noguchi K (2005) TRPA1 induced in sensory neurons contributes to cold hyperalgesia after inflammation and nerve injury. J Clin Invest 115:2393-2401.

Obata K, Katsura H, Sakurai J, Kobayashi K, Yamanaka H, Dai Y, Fukuoka T, Noguchi K (2006) Suppression of the p75 neurotrophin receptor in uninjured sensory neurons reduces neuropathic pain after nerve injury. J Neurosci 26:11974-11986.

Ochoa J, Yarnitsky D (1994) The triple cold syndrome: Cold hyperalgesia, cold hypoaesthesia and cold skin in peripheral nerve disease. Brain 117:185-197.

Okazawa M, Inoue W, Hori A, Hosokawa H, Matsumura K, Kobayashi S (2004) Noxious heat receptors present in cold-sensory cells in rats. Neurosci Lett 359:33-36.

Oliver AE, Baker GA, Fugate RD, Tablin F, Crowe JH (2000) Effects of temperature on calcium-sensitive fluorescent probes. Biophys J 78:2116-2126.

Pasetto LM, D'Andrea MR, Rossi E, Monfardini S (2006) Oxaliplatin-related neurotoxicity: how and why? Crit Rev Oncol Hematol 59:159-168.

Passmore GM, Selyanko AA, Mistry M, Al-Qatari M, Marsh SJ, Matthews EA, Dickenson AH, Brown TA, Burbidge SA, Main M, Brown DA (2003) KCNQ/M currents in sensory neurons: significance for pain therapy. J Neurosci 23:7227-7236.

Peier AM, Moqrich A, Hergarden AC, Reeve AJ, Andersson DA, Story GM, Earley TJ, Dragoni I, McIntyre P, Bevan S, Patapoutian A (2002a) A TRP channel that senses cold stimuli and menthol. Cell 108:705-715.

Peier AM, Reeve AJ, Andersson DA, Moqrich A, Earley TJ, Hergarden AC, Story GM, Colley S, Hogenesch JB, McIntyre P, Bevan S, Patapoutian A (2002b) A heat-sensitive TRP channel expressed in keratinocytes. Science 296:2046-2049.

Petruska JC, Mendell LM (2004) The many functions of nerve growth factor: multiple actions on nociceptors. Neurosci Lett 361:168-171.

Pfaffl MW, Horgan GW, Dempfle L (2002) Relative expression software tool (REST) for group-wise comparison and statistical analysis of relative expression results in real-time PCR. Nucleic Acids Res 30:e36.

Pierau F, Torrey P, Carpenter D (1974) Mammalian cold receptor afferents: role of an electrogenic sodium pump in sensory transduction. Brain Res 73:156-160.

Premkumar LS, Raisinghani M, Pingle SC, Long C, Pimentel F (2005) Downregulation of transient receptor potential melastatin 8 by protein kinase C-mediated dephosphorylation. J Neurosci 25:11322-11329.

Proudfoot CJ, Garry EM, Cottrell DF, Rosie R, Anderson H, Robertson DC, Fleetwood-Walker SM, Mitchell R (2006) Analgesia mediated by the TRPM8 cold receptor in chronic neuropathic pain. Curr Biol 16:1591-1605.

Ramsey IS, Delling M, Clapham DE (2006) An introduction to TRP channels. Annu Rev Physiol 68:619-647.

Rasband MN, Park EW, Vanderah TW, Lai J, Porreca F, Trimmer JS (2001) Distinct potassium channels on pain-sensing neurons. Proc Natl Acad Sci U S A 98:13373-13378.

Reid G (2005) ThermoTRP channels and cold sensing: what are they really up to? Pflugers Arch 451:250-263.

Reid G, Babes A, Pluteanu F (2002) A cold- and menthol-activated current in rat dorsal root ganglion neurones: properties and role in cold transduction. J Physiol 545:595-614.

Reid G, Flonta M (2001) Cold transduction by inhibition of a background potassium conductance in rat primary sensory neurones. Neurosci Lett 297:171-174.

Ritter AM, Lewin GR, Kremer NE, Mendell LM (1991) Requirement for nerve growth factor in the development of myelinated nociceptors in vivo. Nature 350:500-502.

Rohacs T, Lopes CM, Michailidis I, Logothetis DE (2005) PI(4,5)P2 regulates the activation and desensitization of TRPM8 channels through the TRP domain. Nat Neurosci 8:626-634.

Rush AM, Dib-Hajj SD, Liu S, Cummins TR, Black JA, Waxman SG (2006) A single sodium channel mutation produces hyper- or hypoexcitability in different types of neurons. Proc Natl Acad Sci U S A 103:8245-8250.

Scadding J, Koltzenburg M (2005) Painful peripheral neuropathies. In: Wall and Melzack's Textbook of Pain (McMahon S, Koltzenburg M, eds), pp 973-999. Philadelphia: Elsevier.

Schwarz JR (1986) The effect of temperature on Na currents in rat myelinated nerve fibres. Pflugers Arch 406:397-404.

Schwarz JR, Glassmeier G, Cooper EC, Kao T-C, Nodera H, Tabuena D, Kaji R, Bostock H (2006) KCNQ channels mediate IKS, a slow K+ current regulating excitability in the rat node of Ranvier. J Physiol 573:17-34.

Simone DA, Kajander KC (1996) Excitation of rat cutaneous nociceptors by noxious cold. Neurosci Lett 213:53-56.

Simone DA, Kajander KC (1997) Responses of cutaneous A-fiber nociceptors to noxious cold. J Neurophysiol 77:2049-2060.

Simonetti M, Fabbro A, D'Arco M, Zweyer M, Nistri A, Giniatullin R, Fabbretti E (2006) Comparison of P2X and TRPV1 receptors in ganglia or primary culture of trigeminal neurons and their modulation by NGF or serotonin. Mol Pain 2:11.

Smith GD, Gunthorpe MJ, Kelsell RE, Hayes PD, Reilly P, Facer P, Wright JE, Jerman JC, Walhin JP, Ooi L, Egerton J, Charles KJ, Smart D, Randall AD, Anand P, Davis JB (2002) TRPV3 is a temperature-sensitive vanilloid receptor-like protein. Nature 418:186-190.

Smith MP, Beacham D, Ensor E, Koltzenburg M (2004) Cold-sensitive, menthol-insensitive neurons in the murine sympathetic nervous system. Neuroreport 15:1399-1403.

Story GM, Peier AM, Reeve AJ, Eid SR, Mosbacher J, Hricik TR, Earley TJ, Hergarden AC, Andersson DA, Hwang SW, McIntyre P, Jegla T, Bevan S, Patapoutian A (2003) ANKTM1, a TRP-like channel expressed in nociceptive neurons, is activated by cold temperatures. Cell 112:819-829.

Sugiura Y, Makita N, Li L, Noble PJ, Kimura J, Kumagai Y, Soeda T, Yamamoto T (2003) Cold induces shifts of voltage dependence in mutant SCN4A, causing hypokalemic periodic paralysis. Neurology 61:914-918.

Takashima Y, Daniels RL, Knowlton W, Teng J, Liman ER, McKemy DD (2007) Diversity in the neural circuitry of cold sensing revealed by genetic axonal labeling of transient receptor potential melastatin 8 neurons. J Neurosci 27:14147-14157.

Tan ZY, Donnelly DF, LaMotte RH (2006) Effects of a chronic compression of the dorsal root ganglion on voltage-gated Na+ and K+ currents in cutaneous afferent neurons. J Neurophysiol 95:1115-1123.

Taylor-Clark TE, Undem BJ, Macglashan DW, Jr., Ghatta S, Carr MJ, McAlexander MA (2008) Prostaglandin-induced activation of nociceptive neurons via direct interaction with transient receptor potential A1 (TRPA1). Mol Pharmacol 73:274-281.

Thut PD, Wrigley D, Gold MS (2003) Cold transduction in rat trigeminal ganglia neurons in vitro. Neuroscience 119:1071-1083.

Torebjörk E, Wahren L, Wallin G, Hallin R, Koltzenburg M (1995) Noradrenaline-evoked pain in neuralgia. Pain 63:11-20.

Trevisani M, Siemens J, Materazzi S, Bautista DM, Nassini R, Campi B, Imamachi N, Andre E, Patacchini R, Cottrell GS, Gatti R, Basbaum AI, Bunnett NW, Julius D, Geppetti P (2007) 4-Hydroxynonenal, an endogenous aldehyde, causes pain and neurogenic inflammation through activation of the irritant receptor TRPA1. Proc Natl Acad Sci U S A 104:13519-13524.

Tsuruda PR, Julius D, Minor DL, Jr. (2006) Coiled coils direct assembly of a cold-activated TRP channel. Neuron 51:201-212.

Vastani N, Koltzenburg M (2007) Novel cold sensitivity of cutaneous sensory neurons induced by oxaliplatin and potassium channel blockers. Abstract Viewer/Itinerary Planner San Diego:SfN 2007 Online:185.5.

Vastani N, Maurer K, Koltzenburg M (2005) Sensitivity of primary afferent fibres innervating rat hairy skin to cold stimuli and transient receptor potential (TRP) channel agonists. Abstracts of the 11th World Congress on pain 1573.

Viana F, de la Pena E, Belmonte C (2002) Specificity of cold thermotransduction is determined by differential ionic channel expression. Nature Neurosci 5:254-260.

Vlachova V, Lyfenko A, Orkand RK, Vyklicky L (2001) The effects of capsaicin and acidity on currents generated by noxious heat in cultured neonatal rat dorsal root ganglion neurones. J Physiol 533:717-728.

Voets T, Droogmans G, Wissenbach U, Janssens A, Flockerzi V, Nilius B (2004) The principle of temperature-dependent gating in cold- and heat-sensitive TRP channels. Nature 430:748-754.

Voets T, Owsianik G, Janssens A, Talavera K, Nilius B (2007) TRPM8 voltage sensor mutants reveal a mechanism for integrating thermal and chemical stimuli. Nat Chem Biol 3:174-182.

Vydyanathan A, Wu ZZ, Chen SR, Pan HL (2005) A-type voltage-gated K+ currents influence firing properties of isolectin B4-positive but not isolectin B4-negative primary sensory neurons. J Neurophysiol 93:3401-3409.

Wasner G, Schattschneider J, Binder A, Baron R (2004) Topical menthol - a human model for cold pain by activation and sensitization of C nociceptors. Brain 127:1159-1171.

Webster RG, Brain KL, Wilson RH, Grem JL, Vincent A (2005) Oxaliplatin induces hyperexcitability at motor and autonomic neuromuscular junctions through effects on voltage-gated sodium channels. Br J Pharmacol 146:1027-1039.

White FA, Bennett-Clarke CA, Macdonald GJ, Enfiejian HL, Chiaia NL, Rhoades RW (1990) Neonatal infraorbital nerve transection in the rat: comparison of effects on substance P immunoreactive primary afferents and those recognised by the lectin Bandierea simplicifolia-I. J Comp Neurol 300:249-262.

Wilson RH, Lehky T, Thomas RR, Quinn MG, Floeter MK, Grem JL (2002) Acute oxaliplatin-induced peripheral nerve hyperexcitability. J Clin Oncol 20:1767-1774.

Wu F-F, Gordon E, Hoffman EP, Cannon SC (2005) A C-terminal skeletal muscle sodium channel mutation associated with myotonia disrupts fast inactivation. J Physiol 565:371-380.

Wu F-F, Takahashi MP, Pegoraro E, Angelini C, Colleselli P, Cannon SC, Hoffman EP (2001) A new mutation in a family with cold-aggravated myotonia disrupts Na+ channel inactivation. Neurology 56:878-884.

Xing H, Chen M, Ling J, Tan W, Gu JG (2007) TRPM8 mechanism of cold allodynia after chronic nerve injury. J Neurosci 27:13680-13690.

Xing H, Ling J, Chen M, Gu JG (2006) Chemical and cold sensitivity of two distinct populations of TRPM8-expressing somatosensory neurons. J Neurophysiol 95:1221-1230.

Xu H, Blair NT, Clapham DE (2005) Camphor activates and strongly desensitizes the transient receptor potential vanilloid subtype 1 channel in a vanilloid-independent mechanism. J Neurosci 25:8924-8937.

Xu H, Ramsey IS, Kotecha SA, Moran MM, Chong JA, Lawson D, Ge P, Lilly J, Silos-Santiago I, Xie Y, DiStefano PS, Curtis R, Clapham DE (2002) TRPV3 is a calcium-permeable temperature-sensitive cation channel. Nature 418:181-186.

Yang EK, Takimoto K, Hayashi Y, de Groat WC, Yoshimura N (2004) Altered expression of potassium channel subunit mRNA and alpha-dendrotoxin sensitivity of potassium currents in rat dorsal root ganglion neurons after axotomy. Neuroscience 123:867-874.

Yeung SY, Thompson D, Wang Z, Fedida D, Robertson B (2005) Modulation of Kv3 subfamily potassium currents by the sea anemone toxin BDS: significance for CNS and biophysical studies. J Neurosci 25:8735-8745.

Young KA, Ivester C, West J, Carr M, Rodman DM (2006) BMP signaling controls PASMC KV channel expression in vitro and in vivo. Am J Physiol Lung Cell Mol Physiol 290:L841-L848.

Zhang X, Huang J, McNaughton PA (2005) NGF rapidly increases membrane expression of TRPV1 heat-gated ion channels. EMBO J 24:4211-4223.

Zhu W, Oxford GS (2007) Phosphoinositide-3-kinase and mitogen activated protein kinase signaling pathways mediate acute NGF sensitization of TRPV1. Mol Cell Neurosci 34:689-700.

Zimmermann K, Leffler A, Babes A, Cendan CM, Carr RW, Kobayashi J, Nau C, Wood JN, Reeh PW (2007) Sensory neuron sodium channel Nav1.8 is essential for pain at low temperatures. Nature 447:855-858.

Zurborg S, Yurgionas B, Jira JA, Caspani O, Heppenstall PA (2007) Direct activation of the ion channel TRPA1 by Ca2+. Nat Neurosci 10:277-279.

Zygmunt PM, Petersson J, Andersson DA, Chuang HH, Sørgård M, Di Marzo V, Julius D, Högestätt E (1999) Vanilloid receptors on sensory nerves mediate the vasodilator action of anandamide. Nature 400:452-457.